

THREE-DIMENSIONAL SURFACE
MORPHOLOGY AND
ANTHROPOMETRY OF THE
PAEDIATRIC FOOT

MATYAS VARGA

A thesis submitted in partial fulfilment of the
requirements of the University of Brighton
for the degree of Doctor of Philosophy

May 2021

Abstract

The trajectory of the paediatric foot size and shape is poorly understood despite existing data. Furthermore, the two-dimensional (2D) foot anthropometrics typically captured using manual methods tell us very little about the multi-planar three-dimensional (3D) morphology of the foot. Finally, although 3D scanning allows for a quick, accurate and high resolution foot assessment, most paediatric foot studies to date use 2D methods. Therefore, this thesis aims to (1) investigate the reliability of a novel hand-held 3D scanning method to assess static paediatric foot shape, (2) establish 3D variables to evaluate foot surface morphology and (3) describe the development of children's 2D foot anthropometry and 3D surface morphology between the ages of 2 and 7 years. In the pilot study good reliability of hand-held 3D scanning of the paediatric foot was demonstrated in bipedal stance from the age of 3 years. The ability of curvedness and shape-index to evaluate surface morphology was also established, highlighting their capability to describe novel aspects of foot surface morphology development. In the main study, 148 children were recruited to participate for 3D hand-held scanning in bipedal stance. Thirteen 2D measures in three foot regions (rear-, mid- and fore-foot) were analysed using one-way ANOVA, and post-hoc multiple comparisons, to explore differences in foot size and proportions among the age-groups of 3, 4, 5, 6 and 7 years. Curvedness and shape-index were also investigated among the same age-groups, to explore differences in 3D surface morphology using statistical parametric mapping. Finally, simple linear regression was used to explore if age or normalized 2D measures can predict the 3D surface morphology changes identified. The key foot anthropometric findings revealed, for the first time, that foot regions have distinct developmental trajectories, indicating that the rear-foot grows differently compared to the mid- and fore-foot in height, width, and proportions. These results imply that the development of foot shape and size should not be described based on a few selected measures, instead, a comprehensive characterization of all three regions should be considered. The analysis of 3D foot surface morphology demonstrated (1) an increase in local 3D slenderness, (2) increasing prominence of anatomical landmarks, (3) a reduction in rear-foot eversion and (4) a novel trajectory in the development of the medial longitudinal arch (MLA). Most differences occurred between the ages of 4 and 6 years, with a distal to proximal development of the MLA until the age of 5 years, after which it was proximal to distal. The simple linear regressions of normalized 2D measures with 3D shape-descriptors showed that in the absence of 3D scanning technology, normalized rear-foot height, normalized mid- and fore-foot width can predict aspects of 3D foot surface morphology development. This analysis, for the first time, has also revealed that the changes of rear-foot and MLA surface morphology are less dependent on age, but can be predicted using normalized 2D anthropometric foot measures such as normalized rear-foot height, normalized mid- and fore-foot width.

This thesis presents a novel protocol and a comprehensive dataset for a higher resolution understanding of paediatric foot anthropometry and 3D surface morphology. These contributions will help inform approaches to research, footwear design, clinical assessment, and monitoring the impact of surgical and non-surgical interventions.

Table of Contents

Abstract	2
Table of Contents	3
List of tables	7
List of illustrations	12
Table of equations	16
Acknowledgements	17
Author's declaration	18
1. Thesis Introduction	19
1.1. Thesis Aims	21
1.1.1. Measuring the paediatric foot using a hand-held 3D scanner.....	22
1.1.2. The 2D anthropometry of the paediatric foot	24
1.1.3. The 3D surface morphology of the paediatric foot.....	25
1.2. Thesis Structure	27
2. Literature review	29
2.1. Paediatric foot development and growth	29
2.1.1. Postural development of the lower limb	32
2.1.2. The arches of the foot	34
2.1.3. Paediatric Gait development.....	38
2.1.4. Paediatric foot anthropometric development data sets	40
2.1.5. Summary	65
2.2. 3D scanning of the foot, an overview of technology and application	68
2.2.1. 3D scanning technology	69
2.2.2. 3D scanner types	69
2.2.3. Selecting the appropriate 3D foot scanning technology	72
2.2.4. Post-processing of 3D scans	75
2.2.5. Outcome measures of 3D foot scanning	76
2.2.6. The reliability of 3D scanners.....	78
2.2.7. 3D scanning of the paediatric foot.....	83
2.2.8. Quantifying 3D foot surface morphology.....	87
2.2.9. Summary	95
2.3. Summary of the literature review	97

3. Measuring the paediatric foot using a hand-held 3D scanner.....	99
3.1. Aims	102
3.2. Methods	103
3.2.1. Ethical approval	103
3.2.2. Participants	103
3.2.3. Scanner choice	104
3.2.4. Data capture	107
3.2.5. Post-processing	110
3.2.6. 2D foot anthropometric measures.....	113
3.2.7. 3D shape descriptors.....	114
3.2.8. Statistical analysis.....	117
3.3. Phase (a) results	120
3.3.1. Reliability of the 2D foot anthropometric measures.....	120
3.3.2. Reliability of the 3D surface morphology measures	123
3.4. Phase (a) discussion.....	129
3.4.1. Reliability of the 2D foot anthropometric measures.....	129
3.4.2. Validity of the 2D foot anthropometric measures	131
3.4.3. Reliability of the 3D foot surface morphology measures	135
3.5. Phase (a) conclusion	137
3.6. Phase (b) results.....	139
3.6.1. 3D surface morphology of the dorsal aspect of the paediatric foot.....	139
3.6.2. 3D surface morphology of the medial aspect of the paediatric foot.....	140
3.6.3. 3D surface morphology of the lateral aspect of the paediatric foot.....	141
3.6.4. 3D surface morphology of the plantar aspect of the paediatric foot.....	142
3.7. Phase (b) discussion.....	143
3.7.1. 3D surface morphology of the dorsal, medial, and lateral aspects of the paediatric foot.....	143
3.7.2. 3D surface morphology of the plantar aspect of the paediatric foot.....	144
3.8. Phase (b) conclusions	145
3.9. Summary and limitations of the pilot study.....	146
4. The 2D anthropometry of the paediatric foot	150
4.1. Aims.....	152
4.2. Methods	153
4.2.1. Participants	153
4.2.2. Data capture	154
4.2.3. Post-processing of scans	155
4.2.4. 2D measurements.....	157
4.2.5. Statistical analysis.....	162
4.3. Results	166
4.3.1. Whole body anthropometric characteristics of the participants	167
4.3.2. 2D foot anthropometric results	168
4.4. Discussion of the 2D anthropometric measure results	193
4.4.1. Foot length	194
4.4.2. The size development of paediatric foot regions	196
4.4.3. The proportional development of paediatric foot regions	204
4.5. Summary and contributions.....	210
4.5.1. Growth trajectory	210

4.5.2.	Contributions to clinical practice.....	212
4.5.3.	Contributions to footwear design.....	214
4.5.4.	Contributions to research.....	216
4.6.	Limitations.....	217
4.7.	Conclusions.....	218
5.	The 3D surface morphology of the paediatric foot.....	221
5.1.	Introduction to statistical parametric mapping.....	224
5.2.	Aims.....	228
5.3.	Methods.....	229
5.3.1.	Post-processing of scans.....	229
5.3.2.	Calculating 3D shape descriptors.....	231
5.3.3.	3D registration of foot scans.....	231
5.3.4.	Statistical analysis.....	232
5.4.	Results: The 3D surface morphology development of the paediatric foot.....	237
5.4.1.	The 3D surface morphology development of the dorsolateral aspect ...	237
5.4.2.	The 3D surface morphology development of the medial aspect.....	246
5.4.3.	The 3D surface morphology development of the plantar aspect.....	256
5.5.	Discussion of the 3D surface morphology development of the paediatric foot	266
5.5.1.	The 3D surface morphology development of the dorsolateral aspect ...	266
5.5.2.	The 3D surface morphology development of the medial aspect.....	270
5.5.3.	The 3D surface morphology development of the plantar aspect.....	273
5.6.	Results: Predictors of paediatric 3D foot surface morphology.....	277
5.6.1.	Predictors of decreasing rear-foot eversion.....	278
5.6.2.	Predictors of increasing arch height.....	280
5.6.3.	Predictors of 3D Slenderness.....	282
5.7.	Discussion of the paediatric 3D foot surface morphology predictors.....	286
5.7.1.	Predictors of decreasing rear-foot eversion.....	286
5.7.2.	Predictors of increasing arch height.....	288
5.7.3.	Predictors of 3D slenderness.....	292
5.8.	Summary.....	294
5.8.1.	The 3D surface morphology development of the paediatric foot.....	294
5.8.2.	Predictors of paediatric 3D foot surface morphology.....	297
5.9.	Contributions.....	300
5.9.1.	Contributions to footwear design.....	300
5.9.2.	Contributions to research.....	302
5.9.3.	Contributions to clinical practice.....	304
6.	Thesis summary.....	306
6.1.	Summary of the findings.....	308
6.1.1.	Measuring the paediatric foot using a hand-held 3D scanner.....	308
6.1.3.	The 2D anthropometry of the paediatric foot.....	310
6.1.4.	The 3D surface morphology of the paediatric foot.....	311
6.1.5.	Predictors of paediatric 3D foot surface morphology.....	313
6.2.	Contributions.....	314
6.2.1.	Contributions to footwear industry.....	314
6.2.2.	Contributions to research.....	316
6.2.3.	Contributions to clinical practice.....	317

6.3. Limitations	318
6.3.1. Measuring the paediatric foot using a hand-held 3D scanner	318
6.3.2. The 2D anthropometry of the paediatric foot	320
6.3.3. The 3D surface morphology of the paediatric foot.....	321
6.3.4. Predictors of 3D surface morphology of the paediatric foot	322
6.4. Future directions	323
7. References	326
8. Appendices	353
Appendix 1. Main study information sheets	353
Appendix 2. Informed consent forms and demographic data collection sheet	363
Appendix 3. Shapiro-Wilk tests of normality for 2D anthropometric measures per age- group.....	365
Appendix 4. Curvedness and shape-index regressions with normalized 2D anthropometric measures.....	368

List of tables

Table 1.: Ossification timetable (Evans, 2010).....	31
Table 2.: Studies examining foot dimensions and the MLA. N: total number of participants	41
Table 3.: Definition of foot length and width measures.....	43
Table 4.: Studies with foot length and/or foot width data. Mean (standard deviation) foot length, fore-foot width and rear-foot width in cm between the ages of two and seven years.	44
Table 5.: The definitions of MLA measures.	49
Table 6.: Datasets using MLA measures in children from the age of 3 years	52
Table 7.: Definition of foot posture measures.....	58
Table 8.: Studies assessing foot posture development in the children between the ages of 2 and 7 years with mean foot posture for the whole sample indicated.	60
Table 9.: The five selected 3D scanners and corresponding technical details. NA: not available.	105
Table 10.: The description and definition of the 2D anthropometric foot measures calculated by Foot3D.	113
Table 11.: Shape-index ranges for each shape for 3D shape descriptors adapted from Koenderink and van Doorn (1992)	116
Table 12.: Mean and root mean square error (RMSE) for each linear measure by group. Group 1: two years old, Group 2: five years old, Group 3: seven years old.	121
Table 13.: Percentage of mesh deviation under 0.5 and 1mm for each group.....	123
Table 14.: Comparative table of the mean (standard deviation) of the current study results and existing literature for foot length, foot width and rear-foot width in cm.	132
Table 15.: 2D measures derived from the 3D foot scans.	160
Table 16.: Mean (standard deviation) of foot measures from Muller et al. (2012) in cm and % between the ages of three and seven years.	162
Table 17.: Sample size (n) estimates for ANOVA and t-tests estimated using data from Muller et al. (2012). ANOVA sample sizes are total sizes, including all five groups, while t-test sample sizes are per group.	163

Table 18.: Anthropometric characteristics of the sample. Age is in years.....	167
Table 19.: ANOVA table of Kruskal-Wallis test for foot length comparing the age groups. SS: The sum of squares due to each source.	169
Table 20.: Foot length Dunn’s post-hoc pairwise comparison tests and effect size. Significance values have been adjusted by the Bonferroni correction for multiple tests, divided by two to result in 1-sided significance. Significantly different pairs of groups are highlighted in grey.	169
Table 21.: ANOVA table of Kruskal-Wallis test of rear-foot width comparing the age groups. SS: The sum of squares due to each source.	171
Table 22.: Dunn’s post-hoc pairwise comparison tests and effect size for rear-foot width. Significance values have been adjusted by the Bonferroni correction for multiple tests, divided by two to result in 1-sided significance. Significantly different pairs of groups are highlighted in grey.	171
Table 23.: ANOVA table of Kruskal-Wallis test of normalized rear-foot width comparing the age groups. SS: The sum of squares due to each source.	173
Table 24.: Dunn’s post-hoc pairwise comparison tests and effect size for normalized rear- foot width. Significance values have been adjusted by the Bonferroni correction for multiple tests, divided by two to result in 1-sided significance. Significantly different pairs of groups are highlighted in grey.	173
Table 25.: ANOVA table of one-way ANOVA test for rear-foot height comparing the age groups. *: $p < 0.05$, **: $p < 0.005$, ***: $p < 0.0005$	174
Table 26.: Rear-foot height Tukey-Kramer post-hoc tests. Significance values have been adjusted by the Bonferroni correction for multiple tests, divided by two to result in 1-sided significance. The mean difference is in mm. significantly different pairs are highlighted grey. *: $p < 0.05$, **: $p < 0.005$, ***: $p < 0.0005$	175
Table 27.: ANOVA table of one-way ANOVA test for normalized rear-foot height comparing the age groups. *: $p < 0.05$, **: $p < 0.005$, ***: $p < 0.0005$	176
Table 28.: ANOVA table of one-way ANOVA test for mid-foot width comparing the age groups. *: $p < 0.05$, **: $p < 0.005$, ***: $p < 0.0005$	177
Table 29.: Mid-foot width Tukey-Kramer post-hoc tests. Significance values have been adjusted by the Bonferroni correction for multiple tests, divided by two to result in 1-sided significance. The mean difference is in mm. significantly different pairs are highlighted grey. *: $p < 0.05$, **: $p < 0.005$, ***: $p < 0.0005$	178
Table 30.: ANOVA table of Kruskal-Wallis test for normalized mid-foot width comparing the age groups. *: $p < 0.05$, **: $p < 0.005$, ***: $p < 0.0005$	180
Table 31.: Normalized mid-foot width Dunn’s post-hoc pairwise comparison tests and effect size. Significance values have been adjusted by the Bonferroni correction for	

multiple tests, divided by two to result in 1-sided significance. Significantly different pairs of groups are highlighted in grey.	180
Table 32.: ANOVA table of one-way ANOVA test for mid-foot height comparing the age groups. *: $p < 0.05$, **: $p < 0.005$, ***: $p < 0.0005$	181
Table 33.: Mid-foot height Tukey-Kramer post-hoc tests. Significance values have been adjusted by the Bonferroni correction for multiple tests, divided by two to result in 1-sided significance. The mean difference is in mm. significantly different pairs are highlighted grey. *: $p < 0.05$, **: $p < 0.005$, ***: $p < 0.0005$	182
Table 34.: ANOVA table of one-way ANOVA test for normalized mid-foot height comparing the age groups. *: $p < 0.05$, **: $p < 0.005$, ***: $p < 0.0005$	183
Table 35.: Normalized mid-foot height Tukey-Kramer post-hoc tests. Significance values have been adjusted by the Bonferroni correction for multiple tests, divided by two to result in 1-sided significance. The mean difference is in mm. significantly different pairs are highlighted grey. *: $p < 0.05$, **: $p < 0.005$, ***: $p < 0.0005$	184
Table 36.: ANOVA table of one-way ANOVA test for fore-foot width comparing the age groups. *: $p < 0.05$, **: $p < 0.005$, ***: $p < 0.0005$	185
Table 37.: Fore-foot width Tukey-Kramer post-hoc tests. Significance values have been adjusted by the Bonferroni correction for multiple tests, divided by two to result in 1-sided significance. The mean difference is in mm. significantly different pairs are highlighted grey. *: $p < 0.05$, **: $p < 0.005$, ***: $p < 0.0005$	186
Table 38.: ANOVA table of Kruskal-Wallis test for normalized fore-foot width comparing the age groups. SS: The sum of squares due to each source.	188
Table 39.: Normalized fore-foot width Dunn's post-hoc pairwise comparison tests and effect size. Significance values have been adjusted by the Bonferroni correction for multiple tests, divided by two to result in 1-sided significance. Significantly different pairs of groups are highlighted in grey.	188
Table 40.: ANOVA table of one-way ANOVA test for fore-foot height comparing the age groups. *: $p < 0.05$, **: $p < 0.005$, ***: $p < 0.0005$	189
Table 41.: Fore-foot height Tukey-Kramer post-hoc tests. Significance values have been adjusted by the Bonferroni correction for multiple tests, divided by two to result in 1-sided significance. The mean difference is in mm. significantly different pairs are highlighted grey. *: $p < 0.05$, **: $p < 0.005$, ***: $p < 0.0005$	190
Table 42.: ANOVA table of Kruskal-Wallis test for normalized fore-foot height comparing the age groups. SS: The sum of squares due to each source.	192
Table 43.: Normalized fore-foot height Dunn's post-hoc pairwise comparison tests and effect size. Significance values have been adjusted by the Bonferroni correction for multiple tests, divided by two to result in 1-sided significance. Significantly different pairs of groups are highlighted in grey.	192

Table 44.: Post-hoc SPM1D two-tailed independent t-test results of curvedness projected onto heatmaps. The colour bars represent the t statistics, with the t threshold at each end. White points mark significant differences between age-groups. Dark to light blue colours indicates decreasing curvedness, while red, orange, and yellow colours indicate increasing curvedness from the younger to the older age-groups.	242
Table 45.: Post-hoc SPM1D two-tailed independent t-test results of shape-index projected onto heatmaps. The colour bars represent the t statistics, with the t threshold at each end. White points mark significant differences between age-groups. Dark to light blue colours indicates decreasing curvedness, while red, orange, and yellow colours indicate increasing curvedness from the younger to the older age-groups.	245
Table 46.: Post-hoc SPM1D two-tailed independent t-test results of curvedness projected onto heatmaps. The colour bars represent the t statistics, with the t threshold at each end. White points mark significant differences between age-groups. Dark to light blue colours indicates decreasing curvedness, while red, orange, and yellow colours indicate increasing curvedness from the younger to the older age-groups.	252
Table 47.: Post-hoc SPM1D two-tailed independent t-test results of shape-index projected onto heatmaps. The colour bars represent the t statistics, with the t threshold at each end. White points mark significant differences between age-groups. Dark to light blue colours indicates decreasing curvedness, while red, orange, and yellow colours indicate increasing curvedness from the younger to the older age-groups.	255
Table 48.: Post-hoc SPM1D two-tailed independent t-test results of curvedness projected onto heatmaps. The colour bars represent the t statistics, with the t threshold at each end. White points mark significant differences between age-groups. Dark to light blue colours indicates decreasing curvedness, while red, orange, and yellow colours indicate increasing curvedness from the younger to the older age-groups.	262
Table 49.: Post-hoc SPM1D two-tailed independent t-test results of curvedness projected onto heatmaps. The colour bars represent the t statistics, with the t threshold at each end. White points mark significant differences between age-groups. Dark to light blue colours indicates decreasing curvedness, while red, orange, and yellow colours indicate increasing curvedness from the younger to the older age-groups.	265
Table 50.: SPM1D simple linear regressions: Each cell contains a heat map with regression results between the variable at the beginning of the row and the 3D shape descriptor at the top of the column. Markings are referred to in the text.	279
Table 51.: SPM1D simple linear regressions: Each cell contains a heat map with regression results between the variable at the beginning of the row and the 3D shape descriptor at the top of the column. Markings are referred to in the text.	281
Table 52.: SPM1D simple linear regressions: Each cell contains a heat map with regression results between the variable at the beginning of the row and the 3D shape descriptor at the top of the column, with two views per regression where appropriate. Markings are referred to in the text.	284
Table 53.: Predictors of the identified structural and postural differences.	285

Table 54.: Normality test for foot length for each age-group. Sig.: significance, df.: degrees of freedom. *: $p < 0.05$, ***: $p < 0.001$	365
Table 55.: Normality tests for rear-foot width for each age-group. Sig.: significance, df.: degrees of freedom. *: $p < 0.05$, ***: $p < 0.001$	365
Table 56.: Normality tests for normalized rear-foot width for each age-group. Sig.: significance, df.: degrees of freedom. *: $p < 0.05$, ***: $p < 0.001$	365
Table 57.: Normality tests for rear-foot height for each age-group. Sig.: significance, df.: degrees of freedom. *: $p < 0.05$, ***: $p < 0.001$	365
Table 58.: Normality tests for normalized rear-foot height for each age-group. Sig.: significance, df.: degrees of freedom. *: $p < 0.05$, ***: $p < 0.001$	366
Table 59.: Normality tests for mid-foot width for each age-group. Sig.: significance, df.: degrees of freedom. *: $p < 0.05$, ***: $p < 0.001$	366
Table 60.: Normality tests for normalized mid-foot width for each age-group. Sig.: significance, df.: degrees of freedom. *: $p < 0.05$, ***: $p < 0.001$	366
Table 61.: Normality tests for mid-foot height for each age-group. Sig.: significance, df.: degrees of freedom. *: $p < 0.05$, ***: $p < 0.001$	366
Table 62.: Normality tests for normalized mid-foot height for each age-group. Sig.: significance, df.: degrees of freedom. *: $p < 0.05$, ***: $p < 0.001$	366
Table 63.: Normality tests for fore-foot width for each age-group. Sig.: significance, df.: degrees of freedom. *: $p < 0.05$, ***: $p < 0.001$	367
Table 64.: Normality tests for normalized fore-foot width for each age-group. Sig.: significance, df.: degrees of freedom. *: $p < 0.05$, ***: $p < 0.001$	367
Table 65.: Normality tests for fore-foot height for each age-group. Sig.: significance, df.: degrees of freedom. *: $p < 0.05$, ***: $p < 0.001$	367
Table 66.: Normality tests for normalized fore-foot height for each age-group. Sig.: significance, df.: degrees of freedom. *: $p < 0.05$, ***: $p < 0.001$	367

List of illustrations

Figure 1.: Nine representative shapes on the shape-index scale with permission from Koenderink and van Doorn (1992)	91
Figure 2.: 3D heat maps of Koenderink shape-index of the foot. Red: convex; green saddle-shaped; blue concave; and white: transition between these three different shapes. With permission from Liu et al. (2004).	92
Figure 3.: Example of a hand-held scanner being used on a five-year-old participant.....	107
Figure 4.: The Perspex platform on the custom-built stand with the Artec Eva scanner and battery pack.	109
Figure 5.: Post-processing steps in Artec Studio 12.	110
Figure 6.: Mean values for linear measures across age-groups (MTH1: metatarsal head 1, MTH5: metatarsal head 5, M. mall.: medial malleolus, L. mall.: lateral malleolus.	120
Figure 7.: Mean RMSE values for linear measures across age-groups. The red horizontal line represents the 2mm benchmark defined by Mauch et al. (2008). Abbreviations: MTH1: metatarsal head 1, MTH5: metatarsal head 5, M. mall.: medial malleolus, L. mall.: lateral	122
Figure 8.: Cumulative percentage of vertex deviations. Thick line with diamond markers: means of each group, thin lines: each participant. Red: seven-year-old group, black: five-year-old group, blue: two-year-old group. Vertical red dashed lines mark the 0.5 and 1 mm vertex deviations.	124
Figure 9.: Vertex deviation heat maps for one participant's foot from each group. Medial, lateral, and plantar view from top to bottom.....	125
Figure 10.: Mean shape-index (left) and curvedness (right) RMSE boxplot for each group. Group 1: two years old group, Group 2: five years old group, Group 3: seven years old group.	125
Figure 11.: Curvedness RMSE heat maps for an example foot from each group (Group 1 (two years old): Participant 3, Group 2 (five years old): Participant 4, Group 3 (seven years old): Participant 5). Medial, lateral, and plantar view from top to bottom.	127
Figure 12.: Shape-index RMSE heat maps for an example foot from each group (Group 1 (two years old): Participant 3, Group 2 (five years old): Participant 4, Group 3 (seven years old): Participant 5. Medial, lateral, and plantar view from top to bottom.....	128
Figure 13.: Dorsal aspect: Relative probability histograms: (A) curvedness (C) shape-index; Heat maps: (B) curvedness (D) shape-index.....	139

Figure 14.: Medial aspect: Relative probability histograms: (A) curvedness (C) shape-index; Heat maps: (B) curvedness (D) shape-index.....	140
Figure 15.: Lateral aspect: Relative probability histograms: (A) curvedness (C) shape-index; Heat maps: (B) curvedness (D) shape-index.....	141
Figure 16.: Plantar aspect: Relative probability histograms: (A) curvedness (C) shape-index; Heat maps: (B) curvedness (D) shape-index.....	142
Figure 17.: Post processing steps in Artec Studio 12, to calculate 2D measures using the markers on the foot, after the small object filter and hole filling step.	156
Figure 18.: Search area (darker green) for lateral malleolus on a point cloud of a 5-year-old child's foot. Black marks are the markers drawn on the foot and texture noise.	157
Figure 19.: Search area (darker green) and identified vertices (red stars) with marker colour for lateral malleolus on a point cloud of a 5-year-old child's foot. Black marks are the markers drawn on the foot and texture noise.	158
Figure 20.: Search area (darker green) and filtered vertices (red stars) with marker colour for lateral malleolus on a point cloud of a 5-year-old child's foot. Black marks are the markers drawn on the foot	158
Figure 21.: Search area (darker green) and the located lateral malleolus (red star) on a point cloud of a 5-year-old child's foot. Black marks are the markers drawn on the foot.....	159
Figure 22.: Scatter plot and error-bars for foot length for each age-group. Error-bar dots represent the median; caps represent the median ± 1 interquartile range.	168
Figure 23.: Scatter plot and error-bars for rear-foot width for each age-group. Error-bar dots represent the mean; caps represent the mean ± 1 standard deviation.....	170
Figure 24.: Normalized rear-foot width scatter plot and error-bars for each age-group. Error-bar dots represent the median; caps represent the median ± 1 interquartile range....	172
Figure 25.: Rear-foot height scatter plot and error-bars for all age-groups. Error-bar red dots represent the mean and caps represent the mean ± 1 standard deviation.	174
Figure 26.: Normalized rear-foot height scatter plot and error-bars for all age-groups. Error-bar red dots represent the mean and caps represent the mean ± 1 standard deviation.	176
Figure 27.: Mid-foot width (mm) scatter plot and error-bars for all age-groups. Error-bar red dots represent the mean and caps represent the mean ± 1 standard deviation.	177
Figure 28.: Normalized mid-foot width scatter plot and error-bars for all age-groups. Error-bar red dots represent the median and caps represent the median ± 1 interquartile range (IQR).	179

Figure 29.: Mid-foot height scatter plot and error-bars for each age-group. Error-bars' red dot represents the mean of each age-group, caps represent the mean ± 1 standard deviation.	181
Figure 30.: Normalized mid-foot height scatter plot and error-bars for all age-groups. Error-bar red dots represent the mean and caps represent the mean ± 1 standard deviation.	183
Figure 31.: Fore-foot width scatter plot and error-bars for all age-groups. Error-bar red dots represent the mean and caps represent the mean ± 1 standard deviation.	185
Figure 32.: Normalized fore-foot width scatter plot and error-bars for all age-groups. Error-bar red dots represent the median and caps represent the median ± 1 interquartile range (IQR).	187
Figure 33.: Fore-foot height scatter plot and error-bars for all age-groups. Error-bar red dots represent the mean and caps represent the mean ± 1 standard deviation.	189
Figure 34.: Normalized fore-foot height scatter plot and error-bars for all age-groups. Error-bar red dots represent the median and caps represent the median ± 1 interquartile range.	191
Figure 35.: Post-processing steps in Artec Studio 12.	230
Figure 36.: Mean curvedness maps for each age-group, dorsolateral view: A: 3-year-old mean, B: 4-year-old mean, C: 5-year-old mean, D: 6-year-old mean and E: 7-year-old mean curvedness map.	238
Figure 37.: Mean shape-index maps for each age-group, dorsolateral view: A: 3-year-old mean, B: 4-year-old mean, C: 5-year-old mean, D: 6-year-old mean and E: 7-year-old mean shape-index map.	239
Figure 38.: SPM1D ANOVA test results of curvedness among age-groups from the dorsolateral view. The colour bar represents the F statistics, with the threshold marked by red. Red points mark significant (at the $\alpha=0.05$ level) differences among age-groups. Dark to light grey colours indicate increasing F statistics, hence increasing differences among groups. The direction of change is not specified.	240
Figure 39.: SPM1D ANOVA test results of shape-index among age-groups from the dorsolateral view. The colour bar represents the F statistics, with the threshold marked by red. Red points mark significant (at the $\alpha=0.05$ level) differences among age-groups. Dark to light grey colours indicate increasing F statistics, hence increasing differences among groups. The direction of differences is not specified.	243
Figure 40.: Mean curvedness maps for each age-group, medial view: A: 3-year-old mean, B: 4-year-old mean, C: 5-year-old mean, D: 6-year-old mean and E: 7-year-old mean curvedness map.	247
Figure 41.: Mean shape-index maps for each age-group, medial view: A: 3-year-old mean, B: 4-year-old mean, C: 5-year-old mean, D: 6-year-old mean and E: 7-year-old mean shape-index map.	249

Figure 42.: SPM1D ANOVA test results of curvedness among age-groups from the medial view.	250
Figure 43.: SPM1D ANOVA test results of shape-index among age-groups from the medial view.	253
Figure 44.: Mean curvedness heat-maps for each age-group, plantar view: A: 3-year-old mean, B: 4-year-old mean, C: 5-year-old mean, D: 6-year-old mean and E: 7-year-old mean curvedness map.	257
Figure 45.: Mean shape-index maps for each age-group, plantar view A: 3-year-old mean, B: 4-year-old mean, C: 5-year-old mean, D: 6-year-old mean and E: 7-year-old mean curvedness map.	259
Figure 46.: SPM1D ANOVA test results of curvedness among age-groups from the plantar view.	260
Figure 47.: SPM1D ANOVA test results of shape-index among age-groups from the plantar view.	263
Figure 48.: Normalized rear-foot height in ascending order and curvedness heat maps of the first, 37 th , middle (74 th), 111 th and last (148 th) participant in this order. Red lines indicate the first, middle and last participants.	289
Figure 49.: SPM1D regression of curvedness with normalized 2D measures, dorsolateral view. The colour bar represents the t statistics, with the threshold at each end (alpha level of 0.05). White points mark significant correlation. Dark to light blue colours indicate increasing negative correlation, red, orange, and yellow colours indicate increasing positive correlation.	368
Figure 50.: SPM1D regression of shape-index with normalized 2D measures, dorsolateral view. The colour bar represents the t statistics, with the threshold at each end (alpha level of 0.05). White points mark significant correlation. Dark to light blue colours indicate increasing negative correlation, red, orange, and yellow colours indicate increasing positive correlation.	369
Figure 51.: SPM1D regression of curvedness with normalized 2D measures, medial view. The colour bar represents the t statistics, with the threshold at each end (alpha level of 0.05). White points mark significant correlation. Dark to light blue colours indicate increasing negative correlation, red, orange, and yellow colours indicate increasing positive correlation.	370
Figure 52.: SPM1D regression of shape-index with normalized 2D measures, medial view. The colour bar represents the t statistics, with the threshold at each end (alpha level of 0.05). White points mark significant correlation. Dark to light blue colours indicate increasing negative correlation, red, orange, and yellow colours indicate increasing positive correlation.	371
Figure 53.: SPM1D regression of curvedness with normalized 2D measures, plantar view. The colour bar represents the t statistics, with the threshold at each end (alpha level of	

0.05). White points mark significant correlation. Dark to light blue colours indicate increasing negative correlation, red, orange, and yellow colours indicate increasing positive correlation.....372

Figure 54.: SPM1D regression of shape-index with normalized 2D measures, plantar view. The colour bar represents the t statistics, with the threshold at each end (alpha level of 0.05). White points mark significant correlation. Dark to light blue colours indicate increasing negative correlation, red, orange, and yellow colours indicate increasing positive correlation.....373

Table of equations

Equation 1.: Equation for RMSE117

Equation 2.: Equation for transforming the r distribution into t distribution.....235

Acknowledgements

I would like to thank my supervisors, Dr Stewart Morrison and Dr Carina Price for their relentless support and guidance, which helped me achieve this fantastic milestone in my life.

I would also like to express my gratitude to Dr Nicholas Smeeton, who motivated and supported me along the way.

Furthermore, I am very grateful to the late Dr Tibor Szilagyi and the late Dr Peter Molnar for introducing me to the world of research, championing and motivating me to always strive for more.

I would also like to express my sincere gratitude to Eleonora Montagnani who encouraged and inspired me on this challenging journey, especially during the most difficult lockdowns.

The most important thanks are going to my parents who supported and loved me no matter what and pushed me to finally finish what I started.

Last but not least I would like to thank my girlfriend and my son who, against all odds supported me during these trying times and provided the much needed emotional background.

Author's declaration

I declare that the research contained in this thesis, unless otherwise formally indicated within the text, is the original work of the author. The thesis has not been previously submitted to this or any other university for a degree and does not incorporate any material already submitted for a degree.

Signed: Matyas Varga

Dated: 28.05.2021

Chapter 1

1. Thesis Introduction

The advancement of bipedal locomotive behaviour in children is accompanied by the progressive development of the paediatric foot, and its role in the child's overall health is undebated. Understanding this developmental trajectory underpins research that aims to clarify the relationship between anthropometric and structural changes in the foot. Such detailed knowledge could also inform decisions in clinical practice and footwear last design. Despite its undoubted importance, the development of the healthy paediatric foot is poorly understood. Although data describing this development throughout childhood has existed for many years (Morrison et al., 2017, Muller et al., 2012, Cheng et al., 1997a, Gould et al., 1990, Anderson et al., 1956b, Morrison et al., 2018), the range of measures used across studies is inconsistent. Similarly, foot posture and the development of the medial longitudinal arch (MLA) have also been investigated. These studies used various 2D parameters, such as rear-foot angle or resting stance calcaneal position (RSCT) (Žukauskas et al., 2021, Cho et al., 2019), navicular height (Chang et al., 2012, Gilmour and Burns, 2001) or footprint measures (Muller et al., 2012, Gilmour and Burns, 2001, Forriol et al., 1990, Sacco et al., 2015, Bosch et al., 2010b). Additionally, although a dataset of 2D measures may describe size, proportional and postural changes in the foot, they fall short of characterising the multiplanar 3D development of the paediatric foot (Chang et al., 2012,

Uden et al., 2017, Banwell et al., 2018, Lee et al., 2014, Gill et al., 2016). The literature readily demonstrates this in the context of medial longitudinal arch development, where at least 16 2D measures have been used to describe changes in a 3D structure (Uden et al., 2017, Banwell et al., 2018).

The methods to assess children's feet have also changed throughout the years. In contrast with the widely used manual methods, technology advancement at the turn of the century allowed for more effective and accurate foot measurement, using 3D scanning (Telfer and Woodburn, 2010, Witana et al., 2006). However, this technology has mostly been used to offer more precision in 2D measures than traditional methods (Delgado-Abellán et al., 2014, Jimenez-Ormeno et al., 2013, Mauch et al., 2009, Mauch et al., 2008, Waseda et al., 2014), as opposed to utilising more relevant 3D measures of the foot. Furthermore, the number of studies using 3D scanning and examining younger children's feet across a wide range of ages (i.e. two to seven years of age) is also limited. These gaps in the literature lead to challenges with understanding development, which impacts clinical theory and practice. Therefore, robust, contemporary, combined 2D and 3D data is needed to understand the foot's typical trajectory throughout the complex and variable stages of growth and development. Such data can provide reference values that characterise the development of foot shape and can be used in research and applied environments. Moreover, understanding more about the anthropometric and 3D surface morphology changes throughout childhood is essential to advance the prevailing arguments about the typical growth trajectory of children's feet (Uden et al., 2017) and inform the development of appropriate clinical and footwear last measures.

For these reasons, the lack of contemporary foot developmental datasets using 3D scanners and relevant 3D foot measures motivated this research.

1.1. Thesis Aims

The aim of this thesis was to provide a deeper understanding of the trajectory of foot shape and size development. It also aimed to derive a method for capturing 2D anthropometric and 3D foot surface morphology measures using a hand-held 3D scanner and to demonstrate the application of these novel 3D measures in characterizing foot development. Furthermore, to describe the trajectory of foot size and shape development in childhood with 2D and 3D measures using a hand-held 3D scanner. The specific aims and objectives related to the experimental chapters of the research are outlined in the next sections.

1.1.1. Measuring the paediatric foot using a hand-held 3D scanner

This chapter aims to establish protocols and 3D measures for describing 2D and 3D foot development trajectory in two phases with specific objectives. These two phases of work will underpin the methods used in the following chapters and offer novel insights into measuring the paediatric 3D foot surface morphology. Both phases will utilise the same data collected using a custom set-up to scan the foot, including the plantar aspect, using a hand-held 3D scanner. The rationale for choosing the particular scanner is also detailed in this chapter.

First, in phase (a), the objective was to examine the reliability of capturing 2D and 3D foot measures in children aged 2 to 7 years using a hand-held 3D scanner. This phase will establish the reliability of the custom set-up used to provide the 2D and 3D measurements of the paediatric foot.

Second, in phase (b), the objective was to investigate whether 3D shape descriptors can help characterise and quantify differences in 3D foot surface morphology between the age groups of 2, 5 and 7 years.

The novelty and contribution of this pilot study are two-fold. First, a methodology will be established to capture children's feet using a custom set-up and a hand-held 3D scanner allowing the scanning of the whole foot, including the plantar aspect. Although this method requires longer scanning time than conventional step-in laser scanners, it is less expensive, and the portability of the system allows the scanning to take place in the children's environment (school, nursery). Furthermore, the contribution and novelty of phase (b) lie in applying 3D surface shape descriptors to characterize paediatric foot development, which – to the author's knowledge – has never been done before. These novel 3D surface morphology

measures may complement the existing 2D measures in describing and quantifying the multiplanar 3D development of the paediatric foot. This approach will provide morphological maps (3D surface shape descriptors mapped onto 3D foot scans) for research, clinical and footwear last design applications.

1.1.2. The 2D anthropometry of the paediatric foot

This chapter aims to offer an understanding of 2D anthropometric foot development between the ages of 2 and 7 years, and to provide a contemporary dataset of 2D anthropometric paediatric foot measures. This study will employ the chosen hand-held 3D scanner and the methods established in phase (a) of the pilot study. To achieve this, the objectives were twofold. First, characterize the size development of foot regions (rear-, mid- and fore-foot) in children aged 2-7 years. The research questions are:

- How do the dimensions of foot regions change during development?
- Is there a difference in the development of width among the three foot regions between the ages of 3 and 7 years?
- Is there a difference in height development among the three foot regions between the ages of 3 and 7 years?

The second objective was to characterize the proportional development of foot regions in children aged 2-7 years. The research questions are:

- How do the proportions of foot regions change during development?
- Is there a difference in the development of width proportions among foot regions?
- Is there a difference in the development of height proportions among foot regions?

This chapter's novelty and contribution is the current, detailed, and accurate 2D foot anthropometric dataset on the development of foot size and proportions in children in three foot regions. To the author's knowledge, the development of separate foot regions has never been compared before. This will provide crucial information for establishing the developmental trajectory of the paediatric foot and for clinical and footwear last design applications.

1.1.3. The 3D surface morphology of the paediatric foot

This chapter aims to advance the understanding of 3D foot surface morphology development between the ages of 2 and 7 years.

To achieve the aim above the first objective was to determine and locate 3D surface morphology differences between age-groups on the dorsolateral, medial, and plantar aspects of the foot between the ages of 2 and 7 years. The specific research questions related to the objective are:

- What is the average 3D surface morphology of the foot in each age-group?
- What are the differences between age-groups in 3D surface morphology, and how do these relate to differences in foot posture and underlying structure?

The second objective was to determine 2D predictors of 3D surface morphology changes across age-groups and the research questions was:

- What are the best 2D foot anthropometric predictors of the identified 3D surface morphology changes?

The value, novelty and originality of this chapter are threefold. The first one is applying statistical parametric mapping to 3D shape descriptors to support the identification and localization of surface morphology changes during foot development. While this method has been used in brain imaging and foot pressure analysis, this is the first time it is used to assess 3D paediatric foot surface morphology. This method allows the statistical comparison of the 3D scans of different age-groups or pre- and post-surgery or treatment, providing exact locations of the differences on the foot.

The second contribution is the contemporary, high resolution, and accurate 3D dataset on the development of foot surface morphology in children. This allows the characterization of

age-group foot surface shapes and the quantitative and qualitative comparison of these age-group characteristics. This type of data will complement the 2D dataset in the previous chapter, and for the first time, it will describe the multiplanar 3D development of the paediatric foot.

Finally, identifying 2D anthropometric predictors of 3D surface morphology changes will provide crucial information for practitioners without 3D scanners to still benefit from the previous findings in this chapter and use 2D foot measures to predict 3D foot surface shape.

1.2. Thesis Structure

The first part (2.1. Paediatric foot development and growth) of the literature review will summarize the development occurring in the lower limb and the foot during childhood and will also overview the development of gait. Next, the limited number of datasets (2.1.5. Paediatric foot anthropometric datasets) on children's foot size and posture will be evaluated and the need for an up to date dataset created using 3D scanning technology, 2D size and 3D morphological foot measures will be highlighted. The second part of the literature review (2.2. 3D scanning of the foot, an overview of technology and application) will consider the use of 3D scanning in foot measurement. An understanding of the available 3D scanning technology will be first introduced followed by discussing the reliability of this technology. Next, studies employing 3D scanners to measure the paediatric foot will be critically evaluated to argue the need for acquiring 3D foot shape information during paediatric foot development, rather than relying on 2D measures only. Following this, more analytical studies looking at the assessment of foot morphology will be critically evaluated, suggesting a 3D approach to foot morphology measurement: differential geometry.

Chapter 3.(3. Measuring the paediatric foot using a hand-held 3D scanner) will first investigate the reliability of capturing 2D anthropometric and 3D surface morphology measures using a hand-held 3D scanner. The results of this Phase (a) will inform the protocols used in the main study for capturing 2D foot size and 3D foot surface morphology measurements of children using a hand-held 3D scanner. Phase(b) will look into how 3D shape descriptors can be used to characterize the 3D surface morphology development of the paediatric foot. Chapter 4. (4. The 2D anthropometry of the paediatric foot) will explore the trajectory of 2D anthropometric foot development between the ages of two and seven years using the experimental protocols defined in earlier chapters. Chapter 5 will employ the

protocols and 3D shape descriptors established in chapter 3. to investigate the development of 3D foot surface morphology in children aged 2 to 7 years. For videos to visualize 3D results please refer to https://www.youtube.com/channel/UCF8_OmPMWbZjo_s4oY5wiTQ. Finally, the thesis summary (6. Thesis summary) will provide an overview of each chapter, will discuss the contributions of this thesis to footwear design, research and clinical practice, limitations, and future directions.

Chapter 2

2. Literature review

The following chapter will first describe foot, lower limb, and gait development. This is followed by a critical evaluation of the existing literature relating to the development of children's foot shape and size. The datasets on paediatric foot morphology will be examined with particular attention to their resolution and relevance to practical applications. The aims of the chapter are (1) to critically evaluate existing literature relating to children's foot shape, size, and posture and potential measurement technologies, (2) to critically evaluate the measures used in the literature in terms of relevancy and resolution and (3) to define the need to establish an up to date foot development dataset that includes 2D and 3D measures, using 3D scanning technology.

2.1. Paediatric foot development and growth

The thigh, leg and foot on the embryo become recognisable by the 9th week of intrauterine life, and by the completion of the embryonic stage, the neural, vascular, and muscular components of the limb are present and closely resemble those of an adult. On the other hand, the child's foot is not a replica of the adult foot. The child's foot appears fat, relatively shorter and wider, narrowing towards the rear-foot, as this part is less fully developed. The

foot also seems flat at birth due to the adipose padding on the MLA, although this is gradually absorbed during the first year (Frowen et al., 2010).

It was argued by Bertsch et al. (2004) that the foot reaches 50% of its final length by the age of 12-18 months. Furthermore, Tax (1985 pp. 95) suggested that the rate of growth "drops rapidly from a high in infancy to 4 or 5 years of age, when a plateau is reached with a yearly increase in size of about 0.9cm/year. " On the other hand, Gould et al. (1990) suggested that the foot grows in spurts, and these occur at different ages in children. In terms of posture, the new born foot is reported to be very elastic (Bernhardt, 1988) and will adopt an adult-like appearance by the age of 6 years (Hennig and Rosenbaum, 1991)

The development of the foot is considered completed when the full ossification of the foot's skeletal structure is finished. The times of ossification are reported in Table 1. The ossification starts in the longer, larger bones and extends gradually to the smaller bones. The predominantly cartilaginous bones begin to strengthen when the ossification centres appear in the epiphyses in the lower limb.

Table 1.: Ossification timetable (Evans, 2010)

Bone	Primary centres	Secondary centres
Tibia – diaphysis	7 th week	
Tibia – upper epiphysis	At birth	20 th year
Tibia – lower epiphysis	2 nd year	18 th year
Fibula – diaphysis	8 th week	
Fibula – upper epiphysis	4 th year	25 th year
Fibula – lower epiphysis	2 nd year	20 th year
Calcaneum – body	6 th month	
Calcaneum – epiphysis	6 th -10 th month	13 th -15 th year
Talus	7 th month	
Cuboid	At birth	
Lateral cuneiform	1 st year	
Medial cuneiform	3 rd year	
Intermediate cuneiform	4 th year	
Navicular	4 th year	
First metatarsal shaft	8 th -9 th week	
First metatarsal base	3 rd year	17 th -20 th year
Other metatarsal shafts	8 th -9 th week	
Proximal phalanx shafts	12 th -14 th week	
Proximal phalanx bases	3 rd -6 th year	17 th -18 th year
Intermediate phalanx shafts	4 th -9 th month	
<i>Intermediate phalanx bases</i>		
Distal phalanx of hallux	3 rd -6 th year	17 th -18 th year
Distal phalanx shafts	8 th week	
Distal phalanx bases	6 th year	17 th -18 th year

2.1.1. Postural development of the lower limb

The posture of the hips and lower limb in utero in the last trimester is characterized by flexion and abduction of the hips, knee flexion, medial tibial position, ankle dorsiflexion and relative adduction of the feet. This posture is partly required due to the increasing body size, hence reducing space. Post-birth, there is a reduction in this flexed and tightly packed posture and the musculoskeletal development leads to an extended and bipedal appearance of the child in 10-16 months (Evans, 2010). Although the flexion in the hip gradually decreases from its original 30°, typical hip extension is still only around 0° at the age of 3 years, which partly explains the short stride length in children under 3 years. The abduction of the hip reduces from the original 75° to around 45° by the age of 2 years, which is an adult-like appearance. The 30° flexion in the knee found in neonates (due to intrauterine positioning and the maturation of the nervous system – flexor muscle activity) reduces by the age of 6 months. This process is aided by the “mouthing” of the feet in infants, which helps hamstrings elongation that is further continued by standing and later bipedal locomotion (Evans, 2010).

The most important changes in lower limb posture between the ages of 2 and 7 years occur in the frontal plane. Prior to this age, infants present with genu varum or bow legs, when the shafts of the tibia and the femur are bowed laterally (Beeson, 1999). This posture is physiological and aids early ambulation, which is characterized by lack of balance, forward pelvic tilt, increased lumbar lordosis (hence protruding abdomen), flexed legs and flexed and abducted arms used for balancing (Asher, 1975). This bow leg (varus) appearance is considered normal up to the age of 2 years, although normally the knee is straightened by 18 months of age (Salenius and Vankka, 1975, Cheng et al., 1991). Due to the continuous external rotation of the tibia resulting in an internal rotation of the femur, the femoral condyles are brought closer together (Asher, 1975). This leads to a valgus or knock knee

(genu valgum) position, which peaks around the age of 3 years (Engel and Staheli, 1974). This genu valgum is thought to last until the age of 6 years (Salenius and Vankka, 1975), when the tibia and the femur reaches a straight alignment (Tax, 1985).

The degree of bow leg can be assessed radiographically or on photographs using the tibiofemoral angle. This angle is around 15-17° varus at birth and decreases to around 11° valgus by the age of 3 years. After this age, the genu valgum decreases to 6° valgus by the age of 9 years (Salenius and Vankka, 1975). Other studies suggested that children reach 7° valgus between the ages of 5 and 7 years (Cohen-Sobel and Levitz, 1991), or 5° by the age of 8-10 years, which is considered a mature value (Heath and Staheli, 1993).

Considering the ankle, ankle dorsiflexion is 40° in a new born, but only 5-10° remains for normal gait. In the rear-foot, the subtalar joint is in a varus position at birth compared to the leg (10°) and the calcaneus will be at 10° eversion at 12 months of age. This resting calcaneal stance position reduces during the first 6-8 years of life (McCarthy and Drennan, 2009, Tachdjian, 1985). When the fore-foot is considered, it is 10-15° inverted on the rear-foot at birth (embryonic “praying”). The non-weight-bearing fore-foot varus in post-natal development is maintained by shortened medial soft tissues and possibly talar torsion (Evans, 2010).

2.1.2. The arches of the foot

2.1.2.1. The structure and function of foot arches

The two longitudinal and a single transverse arch are made up of the tarsal and metatarsal bones. The calcaneus, talus, navicular, the three cuneiforms, and the first, second and third metatarsals form the MLA, while the lateral longitudinal arch (LLA) is much flatter than the MLA and is formed by the calcaneus, cuboid, and the fourth and fifth metatarsals. These two arches create a single structure between the calcaneus and the metatarsal heads. The anterior five tarsals and the bases of the metatarsals together form the transverse arch, which runs across the foot from lateral to medial. The arches of the foot are supported by passive and active elements. Passive elements are the ligaments that are sufficiently elastic to allow the arches to flatten on foot-ground contact and then recoil, enabling the arches to function as springs to dampen impacts with the ground. The ligaments provide passive support as a beam and as a true arch, and this function is assisted by the muscles (active support) of the lower leg and the foot.

Based on the muscles (active elements) ability to plantar or dorsiflex the intertarsal, tarsometatarsal and metatarsophalangeal joints and increase or decrease the ankle joint reaction force (shift the bodyweight forward or backwards, respectively) they are classified into four groups. These are (1) direct arch raisers (plantarflexion tendency), (2) indirect arch raisers (shift the bodyweight backwards), (3) direct arch flattener (dorsiflexion tendency) and (4) indirect arch flatteners (shift the bodyweight forward) (Frowen et al., 2010).

Making use of the above structures the MLA plays a crucial role in gait. The two main functions of the MLA during gait are shock absorption and propulsion. Shock absorption occurs after heel strike in mid-stance when the MLA is lengthened and flattened as a result of pronation after the initial supination at heel strike. Mechanical energy is also stored due

to the stretching of the elastic tendons and ligaments. After reaching its maximum length the MLA starts to shorten. As a result of supination during rollover and due to the stored energy released back, the arch becomes shorter and higher until toe-off. This shortening and heightening releases the mechanical energy stored to provide power for the propulsion of the foot and the medial three metatarsal heads (the anterior pillar of the MLA) will act as a springboard in take-off.

2.1.2.2. Medial longitudinal arch development

Typically developing children are born with flexible flat feet, and the arch progressively develops during the first ten years of life (Uden et al., 2017). The low appearance of the MLA is argued to be partly due to increased joint laxity in this age-group, making the arch vulnerable to collapse in the presence of load (Kirby and Green, 1992). Another cause is the underdeveloped bony structures; hence the structure of the MLA would not be evident (Hennig and Rosenbaum, 1991). Finally, it is also suggested that a protective fat pad underneath the MLA is present, increasing the loaded area, reducing the pressures and shear forces, but also occluding the MLA. This fat pad is argued to be gradually absorbed during the first 4 or 5 years of life; however, the MLA is thought to develop until the age of 6 years (Bertsch et al., 2004). Additionally, Bernhardt (1988) suggested that the load of the body mass falls medially to the hallux in early walkers increasing pronation, and hence further emphasising the low appearance of the MLA.

The literature has shown a decreasing trend of low arched feet with increasing age (Pfeiffer et al., 2006, Muller et al., 2012). Flat foot type has been reported for 3-4-year-old children and “normal foot” posture has been shown to be achieved by the age of 8 years (Sacco et al., 2015, Forriol et al., 1990), although Nikolaidou and Boudolos (2006) reported “normal foot” posture by the age of 7 years. While there is a certain degree of agreement in the literature

about the increasing height of the MLA, there are still ongoing debates about the definition of the paediatric physiological flat foot. This is because there is currently no consensus on typical foot posture in children and how this posture should change with increasing age. Furthermore, it is also unclear when the development of the arch or the foot itself is complete. In terms of establishing when the foot posture should be considered mature, there are three methods reported in the literature. (1) The cessation of growth, (2) closure of growth plates and (3) stabilisation of posture (Uden et al., 2017). According to the first two methods, mature foot is argued to be reached by 13-16 years of age (Liu et al., 1998, Leung et al., 2005, Tax, 1985). However, based on foot posture, it is reported to be reached by 6-10 years of age (Onodera et al., 2008).

The lack of consensus over the MLA development is partly due to the missing definition of “typical” foot posture. Furthermore, currently, there is no gold standard approach to measure foot posture or the MLA (Uden et al., 2017). The measures and the datasets using different approaches will be detailed in section 2.2.3. While there is an absence of MLA in most 3-7-year-old children’s feet, this is part of a developmental process; hence it is considered “normal” due to the laxity of bones and ligaments, increased adipose tissue and immature neuromuscular control (Banwell et al., 2018). Although the percentage of feet with low arch decreases with increasing age, this does not mean a change towards “normal”, as low arched foot is considered typical at these ages. (Morrison et al., 2017)

The development of the MLA has also been considered in cross-sectional and longitudinal studies using pressure platforms (Bosch et al., 2010a, Bosch et al., 2007, Phethean et al., 2014, Chang et al., 2014b, Muller et al., 2012). Most of these studies revealed increasing peak pressures in the heel and fore-foot, however peak pressures slightly decreased in the mid-foot (Muller et al., 2012, Bosch et al., 2010a, Bosch et al., 2007) between the ages of 3

and 7 years. Furthermore, Alvarez et al. (2008) have shown that the timing of foot area loadings changes with increasing age and the developing arch. While the initial contact in all three age groups (<2 years, 2-5 years and >6 years) was with the heel, the youngest groups proceeded to load the medial and lateral mid-foot followed by the lateral and medial fore-foot. On the contrary, both older age-groups loaded the fore-foot after the heel indicating the development of the MLA. Additionally, as maximum % force increased in the heel, it decreased in the medial mid-foot from the youngest to the oldest age-group. Finally, there was a decrease in the % of time spent on the medial mid-foot: 77.6%, 37.6% and 11.9% in the youngest, middle, and oldest age-group respectively. These changes in loading variables suggest the development of the initial heel contact and a more dynamic roll-over process (Bosch et al., 2007).

2.1.3. Paediatric Gait development

The infant goes through a series of stages in locomotor development before starts to walk independently, and these stages show high variability among children. Some infants attend all stages, while others skip or remain in a particular stage longer than others. These stages include: sitting, creeping, propping and bear standing, kneeling, pulling up to standing, cruising, climbing, squatting, standing and finally supported and independent walking (Evans, 2010). The final stage is usually reached between the ages of 9 and 17 months (Payne and Isaacs, 2016) with large variations. After this stage, as their strength, motor coordination and balance improves, their gait will become more effective and stable, and they develop further advanced gait patterns such as running, jumping or hopping (Evans, 2010).

In the early stages of independent walking, the infant's gait is robotic with short and fast steps, and a wide base of support, which helps them to balance. As gait improves, the base of support gradually reduces in width and reaches the width of the trunk after 4-5 months of independent walking (Payne and Isaacs, 2016). A characteristic of early walkers is the "high guard" position of the arms to provide more stability. At this stage, the arms swing is absent and will appear later once balance has improved sufficiently. In terms of foot contact, the child shows flat footed ground strike and develops heel strike between 18-24 months of age.

At the age of one year, the rear-foot is in an eversion of 5-10 ° relaxed calcaneal stance angle. By the age of 2 years, the arms are lowered to their sides and there is a narrower base of gait with faster and longer steps. This is due to the increased strength and developing propulsion. The first signs of mature gait appear around the age of 3 years (Tachdjian, 1985, Shepherd, 1995), however there are variations with a range between 2 and 6 years (Payne and Isaacs, 2016). The typical posture at this stage consists of hyperextension at the knee, lumbar

lordosis, genu valgum, calcaneal eversion in weight-bearing and diminished medial plantar fat pad.

Between the ages of 4 and 7 years the maximal genu valgum resolves (Heath and Staheli, 1993), but there is an increased lumbar lordosis due to anterior pelvic tilt. At this stage both the rear- and fore-foot varus reduces, the eversion of the calcaneus decreased and the fore-foot plane aligns with that of the rear-foot to almost parallel (Tachdjian, 1985).

The difference between the gait of an under 3-year-old and that of an older child is fourfold. The younger child has (1) shorter steps, (2) higher cadence, (3) slower speed and (4) limited single leg support. To achieve the mature gait patterns seen in most over 4 year olds, leg length needs to increase and single leg stability needs to improve. Furthermore, as Gill et al. (2016) suggested that the development of the MLA may also support the increase of step length. This is due to the increased ability of the MLA structures to store elastic energy as they stretch from a shorter and higher into a longer and lower position in mid-stance. On the other hand, the stability is supported by the low transverse arch, which develops later (Gill et al., 2016).

2.1.4. Paediatric foot anthropometric development data sets

Providing robust size and shape data quantifying the paediatric foot development has numerous applications such as the ergonomic design of footwear and clinical assessments (Telfer and Woodburn, 2010). As stated before in the Thesis Introduction, such data would also help clinicians understand the foot's typical trajectory, help inform understanding of how the paediatric foot develops and offers a baseline for informing work exploring foot deformity and/or orthopaedic issues. These data can also provide expected values at each age, supporting paediatric foot assessment and footwear last design.

Although there have been attempts to create tools to track children's foot development and create anthropometric datasets (see Table 2. for a list of studies with related data), several factors should be considered when assessing the foot or enabling proper fit of shoes.

Examples of the factors that are associated with foot size and morphology are ethnicity (Kouchi, 1998), BMI (Mauch et al., 2008), sex (Delgado-Abellán et al., 2014), and socioeconomic status (Sacco et al., 2015). Partly due to the several contributing factors, the literature on paediatric foot size and shape development is inconsistent. However, the main concern is that the measures are 2D and hence cannot capture and quantify the multi-planar and 3D changes occurring in the paediatric foot. Several 2D measures exist to characterize the changes occurring in different parts of the foot, or specific measures are used to describe the whole foot. To establish basic dimensions of the foot, foot length and forefoot width are used in research, footwear sizing, and by clinicians. While foot length and forefoot width are the most consistent measures used, width and height in other parts (mid-foot or rear-foot width from footprints and dorsum or instep height) of the foot are also used for different purposes.

Table 2.: Studies examining foot dimensions and the MLA. N: total number of participants

First author (year)	Measurement device	Age range (N)	Measures captured
Anderson et al. (1956b)	Wooden calliper	1-18 (512)	foot length
Forriol et al. (1990)	footprint	3-17 (1676)	footprint angle, Chippaux-Smirak index
Kouchi (1998)	scriber, tape	3-88 (3272)	foot length, instep length, toe length, foot girth, foot breadth, heel breadth, ball angle, toe angle, indices
Gilmour and Burns (2001)	Footprint with paint, Vernier height gauge	5-10 (272)	AI, navicular height
Chen et al. (2009)	3D coordinate measurement system, digital tape, Harris mat	5-13 (1024)	foot length, foot length (sitting), foot breadth, foot breadth (sitting), heel breadth, heel breadth (sitting), navicular height, navicular height (sitting), medial malleolus height, lateral malleolus height, ball girth, waist girth, instep girth, long heel girth, short heel girth
Mauch et al. (2009)	3D scanner	2-14 (2867)	cluster analysis of foot length, ball-of-foot length, ball-of-foot width, rear-foot width, ball angle, dorsal arch height
Chang et al. (2012)	3D scanner	2-6 (44)	navicular height, arch volume, arch volume index
Muller et al. (2012)	foot measuring device, plantar pressure	1-13 (7788)	foot length, foot width, AI
Jimenez-Ormeno et al. (2013)	INESCOP 3D foot digitiser	6-12 (1032)	foot length, heel-fifth metatarsal, heel-first metatarsal, metatarsal width, forefoot width, heel width, ball height, instep height, arch height
Delgado-Abellán et al. (2014)	INESCOP 3D foot digitiser	6-12 (1031)	foot length, heel-fifth metatarsal, heel-first metatarsal, instep distance, rear-foot width, ball width ball height, arch height, instep height, heel girth, ball girth.
Waseda et al. (2014)	3D scanner	6-18 (10155)	foot length, navicular height, arch height ratio
Sacco et al. (2015)	Harris mat	3-10 (94+391)	rear-, mid- and fore-foot width, Chippaux-Smirak index, Staheli indices

Additionally, quantifying foot posture and medial longitudinal arch development is a constant debate (Banwell et al., 2018, Uden et al., 2017). Authors use different methods such as footprint or pressure platform to estimate the development of the MLA, with inconsistent results and debatable validity.

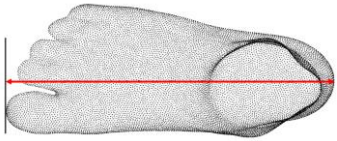
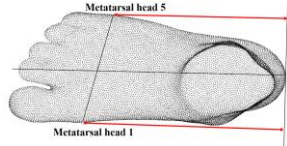
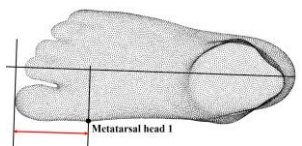
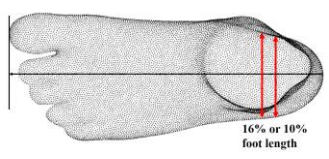
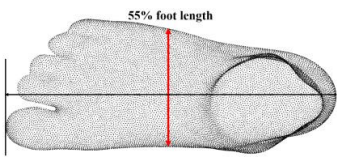
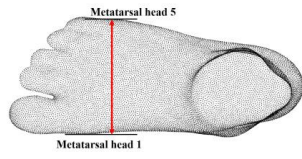
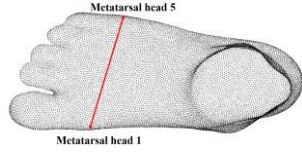
Although there is still a lack of a comprehensive and up to date 2D dataset on the development of children's foot shape and size, there have been attempts to provide such information. In the next sections, these datasets will be further evaluated, which will estimate the current state of knowledge and understanding of paediatric foot anthropometry development. This will be in the order of (1) length and width measures, (2) measures of the MLA and (3) foot posture measures.

2.1.4.1. The length and width of the paediatric foot

Foot length and width provide the most basic characterisation of the paediatric foot. They allow the assessment of the foot's developmental state and are the starting point for shoe last design and sizing. The definition of foot length and width measures are presented in Table 3.

The earliest attempt to establish a dataset on children's foot development was carried out by Anderson et al. (1956b) who, using wooden calliper, measured the foot length of 227 girls and 285 boys, between the ages of one and 18 years. The authors presented the data in a growth chart for each sex, marking the 3rd, 25th, 50th, 75th and 97th percentiles. The data distribution provided a "norm" to which the individual's foot could be compared to between the ages of one and 18 years. It was reported that half of the final foot length is reached by the age of 1-1.5 years and in boys, it continues to grow up to the age of 15 years, while in girls there is very little change after the age of 13 years.

Table 3.: Definition of foot length and width measures

2D measure	Description	
Foot length	Distance between the most posterior point of the heel and the end of the longest toe, projected onto the longitudinal axes	
First or fifth metatarsal length	Distance from the heel to the first/fifth metatarsal	
Toe length	The distance between the most medial point of the first metatarsal head and the end of the longest toe parallel to the foot axis (Kouchi, 1998).	
Heel width	The distance between the most lateral and most medial point of the heel at 16% (Kouchi, 1998) or 10% foot length (Jurca et al., 2019).	
Mid-foot width	The distance between the most lateral and most medial point of the foot at 55% of foot length (Jurca et al., 2019).	
Fore-foot width	Distance between the first and fifth metatarsal heads projected onto the foot's medio-lateral axis.	
Foot breadth	The distance between the most medial point of the first metatarsal head and the most lateral point of the fifth metatarsal head (Kouchi, 1998).	

Based on studies by Anderson et al. (1956b), Gould et al. (1990) and Cheng et al. (1997b) children's foot length increases by 2 cm per year until the age of three years (foot length at the age of three between 13.2 and 16.8cm), then 1cm per year until the age of five years (foot length at the age of five between 15 and 19.2cm) and 0.8 to 1cm per year up to the age of 12 years (foot length at the age of 12 between 20.06 and 25.9cm). Table 4. summarizes the studies that assessed children's feet between the ages of 3 and 7 years.

Table 4.: Studies with foot length and/or foot width data. Mean (standard deviation) foot length, fore-foot width and rear-foot width in cm between the ages of two and seven years. ¹

Kouchi (1998)						
Age (years)	3 (n=71)	4 (n=84)	5 (n=89)	6 (n=111)	7 (n=112)	
FL [cm]	15.31 (0.76)	16.28 (0.76)	16.97 (0.99)	18.04 (1.01)	19.16 (0.92)	
FW [cm]	6.40 (0.38)	6.78 (0.34)	7.07 (0.42)	7.35 (0.40)	7.71 (0.46)	
HW [cm]	4.17 (0.29)	4.3 (0.28)	4.47 (0.27)	4.66 (0.31)	4.88 (0.41)	
Muller et al. (2012)						
Age (years)	2 (n=455)	3 (n=676)	4 (n=834)	5 (n=938)	6 (n=931)	7 (n=787)
FL [cm]	14.58 (1.82)	15.71 (2.00)	16.74 (1.95)	17.71 (2.04)	18.69 (2.17)	19.74 (2.35)
FW [cm]	6.1 (0.84)	6.41 (0.83)	6.69 (0.84)	6.94 (0.84)	7.21 (0.93)	7.46 (0.90)
Jimenez-Ormeno et al. (2013)						
Age (years)				6 (n=41)	7 (n=103)	
FL [cm]				18.79 (1.16)	19.78 (0.99)	
FW [cm]				6.99 (0.43)	7.17 (0.43)	
HW [cm]				4.38 (0.38)	4.44 (0.35)	
Waseda et al. (2014)						
Age (years)				6 (n=428)	7 (n=1140)	
FL [cm]				18.44 (0.97)	19.14 (0.1)	
Brazil Sacco et al. (2015)						
Age (years)	3 (n=32)	4 (n=73)	5 (n=62)	6 (n=74)	7, 8 (n=32)	
FW [cm]	5.69 (0.47)	6.04 (0.60)	6.15 (0.65)	6.52 (0.48)	6.84 (0.52)	
HW [cm]	3.31 (0.36)	3.52 (0.33)	3.50 (0.39)	3.62 (0.35)	3.84 (0.31)	
Germany Sacco et al. (2015)						
Age (years)	3 (n=94)	4 (n=92)	5 (n=92)	6 (n=88)	7,8 (n=85)	
FW [cm]	5.80 (0.37)	6.23 (0.40)	6.69 (0.40)	6.98 (0.46)	7.34 (0.44)	
HW [cm]	3.25 (0.28)	3.35 (0.32)	3.63 (0.29)	3.78 (0.30)	3.92 (0.30)	

¹ FL: foot length, FW: foot width, HW: rear-foot width

Although some of the authors provided charts for normative foot growth, the relevance of this data in the modern context is debatable due to changes in lifestyle and environmental factors. As an example, these changes over generations and decades have caused the increase in the prevalence of overweight and obese children (Jackson-Leach and Lobstein, 2006) and the increase in BMI or percentage\kg body fatness in children over the generations on most continents (Lobstein et al., 2004, Horvat et al., 2009, Lobstein et al., 2003). These BMI and body composition trends could cause changes in foot structure and hence foot morphology altering the trajectory of foot development (Mauch et al., 2008).

Foot width and length measures were reported by Kouchi (1998) who found that until 11 years of age normalized fore-foot width measures decrease along with normalized rear-foot width and normalized ball girth (normalized =foot measure/foot length). The authors used a scribe to record the foot's outline and a tape to measure the foot of 1559 children between the ages of 3 and 18 years; however, the results are now over 20 years old and were captured using manual techniques. Another manual technique, footprint and Harris mat was used to measure foot shape (foot length, midfoot width, and foot form defined as midfoot width divided by length without toes, as a percentage) by Bosch et al. (2007). The authors reported their data in percentiles between 0 and 48 months of walking experience, starting at a mean age of 15.3 months in 90 healthy German children. They used the 3rd and 97th percentiles to describe the distribution of their data and suggested that any child presenting a foot measure outside of this distribution may warrant further investigation along with medical examinations (Bosch et al., 2007). Although the authors attempted to characterize changes in foot form (proportions), they only used mid-foot width (measured on a Harris mat as the minimal foot width of the mid-foot area on the footprint) to quantify the whole foot's form, which could result in misleading information as other regions of the foot (rear- or fore-foot) might develop differently. Furthermore, the width of the mid-foot on a footprint may

represent more than changes in slenderness as it is related to the development of the MLA. Although the authors provided a dataset presented similar to growth charts, the sample size is small to generalize and establish clear outcomes related to clinical decisions. The dataset is also limited to a small number of 2D measures, which, without further 2D measures and the investigation of the 3D foot surface morphology, has limited applicability. Based on a larger sample size (7788 children between the ages of one and 13 years), but still using a manual device (WMS1 foot measurement system, with an attached millimetre scale; DSI, Offenbach, Germany), Muller et al. (2012) suggested that the growth of the foot is predominantly in length rather than width between the ages of two and seven years. This argument is also based on the width of one region, the fore-foot; hence implications to the whole foot might be incorrect. The authors also presented foot geometry (foot width/foot length) and plantar pressure (force-time integral, peak pressures, and AI) data in reference charts. This study resulted in age-specific data from the cohort to define a normal range for static and dynamic foot parameters, with the intention of practical application in clinical settings and supporting suitable shoe development. They reported an increase of approximately 1cm in foot length each year and less than 3mm increase in foot width. Regarding foot geometry, the study results showed a decrease of 0.03 arbitrary unit (a.u.) between the ages of 3 (0.41 a.u.) and 7 years (0.38 a.u.). The authors argued that these results suggest a relative narrowing of the foot and reaching a foot shape more similar to those of adults by the age of 8 with a foot geometry value of 0.37. Although these results are essential in describing the fore-foot, applying this information to characterize the whole foot shape might be misleading and could cause footwear last design and fitting issues.

To capture the shape of the foot at different regions, Sacco et al. (2015) measured – using footprints - the width of the forefoot, midfoot, and rearfoot and used Chippaux-Smirak and Staheli indices to characterize the medial longitudinal arch. The study's purpose was to

compare the foot shape of Brazilian and German children in a mixed cross-sectional (391 Brazilian children) and longitudinal (94 German children) study. They have identified significant differences in the width and MLA measurements. The feet of Brazilian children were consistently narrower at the fore-foot, with an increasing difference with age. The authors suggested that the cause of the difference is the lower BMI among the Brazilian children, due to socioeconomic differences between the countries. Despite providing width measures in three foot regions, these regions' height was not measured. The method used (footprints) also limited the application of data, as footprints only measure the part of the foot in contact with the ground. For this reason, the actual width of the fore-foot (distance between the most medial and lateral point of first and fifth metatarsal heads respectively), mid-foot (the largest distance between the most lateral and most medial point of the mid-foot) and the heel (the largest distance between the most lateral and most medial point of the heel) might be larger. The authors argue that the results show that the European shoe lasts would not provide a good fit for specific age-groups in the Brazilian population. Although they used a German sample of children, this sample was limited to a particular region in Germany, making generalization to European children's feet questionable. As an example, Muller et al. (2012) from 61 different cities across Germany reported wider fore-foot width in all age groups than Sacco et al. (2015), although this difference could also be the result of the methods used. As explained before, Sacco et al. (2015) used foot-prints, which possibly underestimates width measures, whereas Muller et al. (2012) used a foot measuring device with a separator and a slider, which captures foot width at the correct anatomical location. Although the study captured the foot width at three different points on the foot, differences in the height of foot regions or changes in the foot's 3D surface morphology would not have been included. This could mean that two children with equal mid-foot width parameters, could have different mid-foot height and/or dorsal, lateral, or medial aspect morphology and

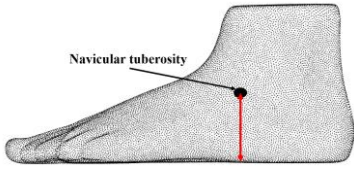
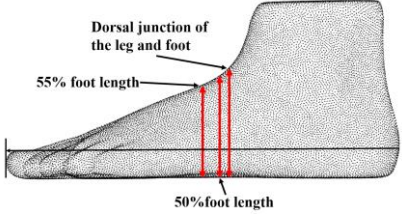
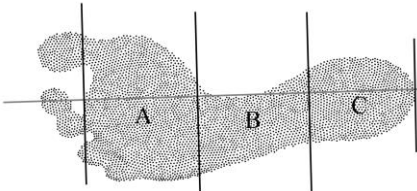
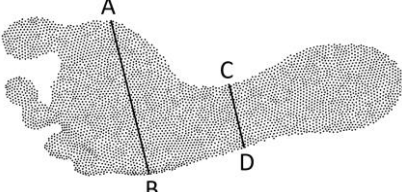
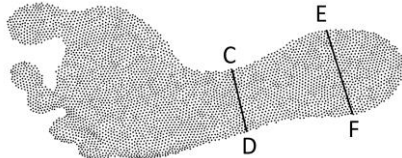
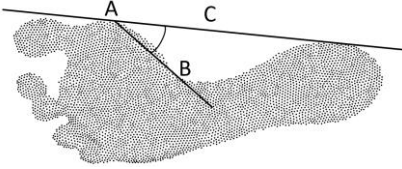
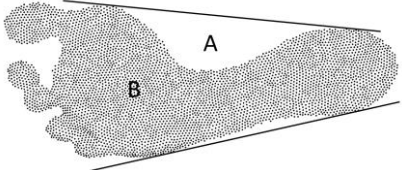
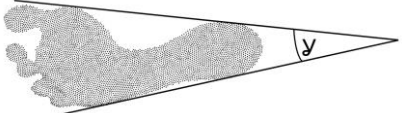
the same size shoe would not fit both well, due to the possibly differing proportions and 3D surface characteristics of the foot.

In summary, although foot length and width measures provide a general description of the foot or foot regions, they lack resolution and are limited to 2D. While these are important in assessing the development of the foot and in practical applications, they are limited in what they can tell us about the 3D multi-planar development of the paediatric foot. As an example, although mid-foot width captured from a footprint may quantify the width of the MLA, it cannot quantify its height or 3D surface morphology. It also lacks resolution, as it only captures the width at the thinnest point of the mid-foot ignoring the shape of the MLA. Furthermore, there is a variation of foot dimension definitions and measurement methods resulting in the inability to integrate and compare results from different studies. While this is an issue in integration of findings, the different mid-foot width measures may also capture different aspects of foot development, such as slenderness as opposed to foot posture, depending on their definition. These inconsistencies may result in misinterpretation of findings and an incorrect understanding of foot shape and size development.

2.1.4.2. The medial longitudinal arch of the paediatric foot

Researchers and clinicians have used various 2D parameters to (1) measure the development of the MLA, (2) measure the relationship between MLA measures and other parameters such as BMI in children or (3) diagnose flat foot in children. Despite the range of parameters and measurement methods available, the most used clinical measurements are footprint measures (Uden et al., 2017), due to their simplicity. These parameters are thought to represent the height and development of the MLA, and hence they are used to describe and quantify the "normal" MLA height in healthy children and to aid diagnosis of pathological flat foot. The definitions of commonly used MLA measures are listed and defined in Table 5.

Table 5.: The definitions of MLA measures.

Measure	Definition	Diagram
Navicular height	The height of the navicular tuberosity from the ground	
Instep\dorsum height	The height of the foot dorsum at 50% (Williams and McClay, 2000, Witana et al., 2006) or 55% (Jurca et al., 2019) of foot length or at the dorsal junction of the leg and the foot from the ground (Mauch et al., 2009).	
Arch index	Area of the midfoot divided by the area of the whole footprint without the toes. $AI=B/(A+B+C)$ (Cavanagh and Rodgers, 1987)	
Chippaux-Smirak Index	The width of the narrowest part of the mid-foot divided by the fore-foot width: $CD/AB*100$ (Chen et al., 2011)	
Staheli Arch Index	The width of the narrowest part of the mid-foot divided by the heel width: $CD/EF*100$ (Chen et al., 2011)	
Clarke's angle	The angle between a medial tangential line connecting the medial edges of the first metatarsal head and the heel, and a line connecting the first metatarsal head and the acme of the MLA (Chen et al., 2011).	
Keimig index	the missing area of a footprint relative to the size of the toeless footprint: A/B (Gill et al., 2016)	
Gamma angle	The angle between the medial and lateral tangent of the foot edges (Jankowicz-Szymanska and Mikolajczyk, 2015).	

Some of the above measures (arch index, Chippaux-Smirak Index and Staheli Arch Index) have also been used to establish a classification of flatfoot by frequency distribution characteristics in footprint measures (Chang et al., 2014a), the bimodality of this distribution suggesting a leap between flat and non-flat foot rather than a continuous distribution. Furthermore, CSI has also been used to investigate whether motor-developmentally delayed children between the ages of 3 and 6 years have flatter feet than normally developing children (Chen et al., 2014). Chen et al. (2014) found that children with delayed development had higher prevalence of flat feet than normally developing children. Additionally, the prevalence of flat foot was also higher in overweight children or children with excessive joint laxity. The authors suggested that their results may serve as a reference for clinicians in dealing with children with delayed motor development.

Although these measures are simple and easy to acquire, questions remain about their validity in measuring the MLA (Banwell et al., 2018), and most certainly in describing the shape of this 3D multi-planar structure (Lee et al., 2014). There have been attempts to use footprint and other 2D measures in creating datasets on the development of the MLA in childhood, and these will be discussed next (see Table 6. on the next page for studies employing MLA measures).

One of the earliest attempts to assess the development of the medial longitudinal arch using footprint measures was by Forriol et al. (1990). The authors in this study investigated the Clark's angle and CSI of 1676 children aged between 3 and 17 years using plantograms. The age-groups important regarding this thesis were the first (3-4-year-old) and second (5-8-year-old). The study demonstrated significant differences between these age-groups both in Clark's angle and CSI ($p < 0.01$ in all tests). The Clark's angle has increased (mean of boys and girls, left and right feet; first age group: 24.5° , second age-group: 38.41°), while

the CSI decreased (mean of boys and girls, left and right feet; first age-group: 48.54%, second age-group: 34.12%), and the authors argued that these results indicated the raising of the MLA in both sexes and feet. Although these measures may represent a ratio or an angle of foot regions in contact with the ground, they cannot quantify the height or the shape of the MLA. A child may have a high Clark's angle or a low CSI, but their MLA may still be low, leading to misinterpretation of the results and possibly misdiagnosis. Another limitation of the study is the wide range of ages in the second age-group, 5 to 8 years. This is a time of rapid changes in foot posture, size, and shape; hence a higher resolution grouping could have provided a more detailed understanding of MLA development.

Table 6.: Datasets using MLA measures in children from the age of 3 years

First author (year)	Measurement device	Age range in years (N)	MLA measures
Forriol et al. (1990)	footprint	3-17 (1676)	footprint angle, Chippaux-Smirak index
Gilmour and Burns (2001)	Footprint with paint, Vernier height gauge	5-10 (272)	arch index, navicular height
El et al. (2006)	Harris and Beath footprint mat	6-12 (579)	Staheli arch index
Bosch et al. (2008)	capacitive pressure distribution platforms	1 and 7 (52)	arch index
Bosch et al. (2010a)	Harris mat, pressure platform	1-10 (36)	arch index
Chen et al. (2011)	Harris mat	3-6 (1319)	Clark's angle, Chippaux-Smirak index, Staheli arch index
Chang et al. (2012)	3D scanner	2-6 (44)	navicular height, arch volume, arch volume index
Muller et al. (2012)	foot measuring device, plantar pressure pad	1-13 (7788)	arch index
Chen et al. (2013a)	Harris mat	3-6 (1319)	Clark's angle, Chippaux-Smirak index, Staheli arch index
Waseda et al. (2014)	3D scanner	6-18 (10155)	navicular height, arch height ratio
Jankowicz- Szymanska and Mikolajczyk (2015)	computer- aided podoscope	4-6 (207)	Clarke's angle
Sacco et al. (2015)	Harris mat	3-10 (94+391)	Chippaux-Smirak index, Staheli arch index

This rapid development was demonstrated by a longitudinal study of 156 normal weight children (based on Cole et al. (2000)) by Jankowicz-Szymanska and Mikolajczyk (2015)

using computer aided podoscope. Clarke's and gamma angle (suggested to be used to measure the height of the transverse arch) was measured at the age of 4 years and two years later. Clarke's angle was shown to increase significantly (left foot: $p=0.010$, right foot: $p=0.001$), by approximately 4° (left foot: from 33.04° to 37.37° , right foot: from 34.35° to 38.76°), which - according to the authors - suggests the increase in arch height. On the other hand, gamma angle only decreased (left foot: $p=0.704$, right foot: $p=0.475$) by less than one degree (left foot: from 15.35° to 15.26° , right foot: from 14.99° to 14.86°), indicating a much lower magnitude of development in the transverse arch.

Arch index (AI) and navicular tuberosity height (NH) were used by Gilmour and Burns (2001b) to assess the MLA in 272 children between the ages of five and ten years. The AI is thought to be related to the MLA height, and it is suggested that it decreases as MLA height increases. The study aimed to examine the relationship between NH and AI and how gender, limb preference, and body weight affect these measures. The results showed that the NH increased from 27 mm in the six-year-old group through 31 mm in the eight-year-old group to 34 mm in the ten-year-old group. The direct height measure of the navicular tuberosity was not affected by gender, body weight, and no differences between the left and right feet were found. In comparison, the AI reduced from 0.22 in the six years old group to 0.21 in the eight years old group but did not decrease further in the ten years old group and it was influenced by gender (males had higher AI values by 0.01) and body weight (obese children had higher AI values by 0.04). Based on their results of moderate correlation between the AI and navicular tuberosity height ($r = - 0.46$; $p = 0.0001$) they argued that the AI reflects the height of the MLA just as well as the NH. This is questionable since they also found that navicular height could differentiate between all age-groups (six, eight and ten years old), whereas AI could only differentiate between the six and eight-year-old groups. The AI's

inability to differentiate between age groups might partly be because this measure (as it is a ratio of foot areas) is inherently normalized to foot size, whereas NH is not. Another cause might be that AI measures a ratio of areas under specific parts of the foot rather than the actual height of the MLA. This could mean that two children with the same AI can have different navicular tuberosity height. The anatomical significance of their results (statistically significant difference in the AI between the six- and eight-year-old groups: AI difference 0.01) is also questionable, as the inter-limb comparison within participants showed the same difference (0.01), with the same means and similar standard deviations. This means that the change in AI between the two age groups is the same as the difference between the participants' two feet. Although the navicular height data may confirm that the development of the MLA is continued past the age of eight years, it might also be affected by the foot and lower limb's general growth. Therefore, normalized (to foot length) navicular height may have been a more appropriate representation of the increase in MLA height. This measure was shown not to increase between the ages of 6 and 7 years (values between 13.8% and 14%) but to significantly increase between the ages of 10 and 12 years in Japanese girls and between the ages of 11 and 13 years in Japanese boys (Waseda et al., 2014). This study – confirming the results of Gilmour and Burns (2001b) - has also demonstrated a continuous significant increase in NH from the age of 6 (25.5mm) until the age of 13 (37.9mm) in boys and from the age of 8 (26.8mm) to 13 (35.1mm) years in girls. The discrepancy between the absolute and normalized NH indicate that they represent a different developmental process. While NH may be a representation of general growth, increasing normalized NH may represent the development of the MLA height suggesting that NH increases faster than foot length.

Similar to Gilmour and Burns (2001b), the AI has also been reported to decrease with age in childhood by Bosch et al. (2010a) in 36 children in a 9-year longitudinal study. The first foot measurements took place when the children were approximately two years old. Although the researchers found that with increasing age, the 50th percentile AI decreased by 44% (from 0.36 at the first measurement to 0.20 at the last measurement), these methods may not fully capture the arch development due to their limited ability to describe the changes in the actual height and shape of the MLA.

In a much larger dataset, Muller et al. (2012) also used AI to characterize changes in the MLA in 10,382 children aged between one and 13-year-old using a pressure measurement platform and the contact area of the relevant foot areas. They found that the AI decreased from 0.32 in the one-year-old group to 0.19 in the 7-year-old group and remained constant afterwards. These findings agree with the results of Bosch et al. (2008) who, using capacitive pressure distribution platforms, recorded the AI of 26 toddlers (mean age: 1.3 years) – mean AI 0.36 - and 26 seven years olds – mean AI 0.18. Interesting to note, both German studies (Bosch et al., 2010, Muller et al., 2012b) show a lower AI value than the American sample (Gilmour and Burns, 2001b), which may be due to ethnic differences.

Another set of footprint measures were employed by Chen et al. (2011) and in a follow-up study by the same authors (Chen et al., 2013a) using digital images in 1319 children aged between 36 and 82 months. The authors aimed to identify footprint measures that can be used for measuring MLA height and hence the classification of flat foot in preschool children. The authors also compared footprint measure results with clinical diagnosis based on Pfeiffer et al. (2006). The measures they used were: Staheli AI (SAI), Clarke's angle (CA) and Chippaux-Smirak index (CSI). The authors suggested that all three measures were suitable for assessing flatfoot in children of this age-group, and recommended CSI as the

primary screening tool for preschool children, as it had superior performance over the other two measures based on likelihood ratio calculations. The Staheli arch index was also shown to differentiate ($p=0.000$) between groups of children with normal or mild flatfoot ($N=456$, Staheli arch index= 0.67 ± 0.19) and children with moderate or severe flat foot ($N=95$, Staheli arch index= 1.12 ± 0.17) between the ages of 6 and 12 years (El et al., 2006). The same study has also shown a significant negative correlation ($r = -0.104$, $p < 0.05$) of the Staheli arch index with age, suggesting that with increasing age, the Staheli arch index decreases, indicating a narrowing plantar mid-foot. German and Brazilian children of the same age (6 to 10 years of age) have been shown to have similar Staheli index values by Sacco et al. (2015), between 0.66 at the age of 6 years and 0.46 at the age of 10. This study has shown a continuous decrease in this index as well as in CSI in the Brazil sample, while the German sample has shown an increase in the 9-year-old group before reducing again. Additionally, this study has demonstrated a continuous decrease in Staheli (Brazil: 0.83 to 0.68 and German: 0.84 to 0.72) and CSI index (Brazil: 48.8 to 39.2 and German: 46.4 to 38.0) between the ages of 3 and 5 years too in both samples indicating no differences in arch development between the two populations. The CSI has also further decreased in both population until the age of 10 (Brazil: 26.0, German: 29.2). While the above studies suggest the decrease in plantar mid-foot width with increasing age in different populations from the age of 3 to 12 years, they cannot quantify the height or the morphology of the MLA, which is possibly more relevant to function.

Although footprint measures are easy to use in the clinics, they are ratios of areas or width of plantar aspects in contact with the ground. This implies that they cannot account for changes in the actual height of the MLA and 3D morphology of its surface. This may cause misrepresentation of the MLA, as the plantar aspect in contact with the ground might be

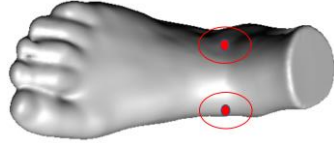
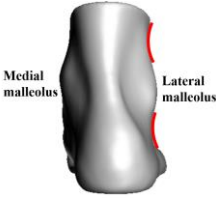
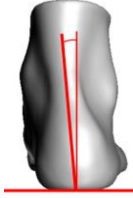

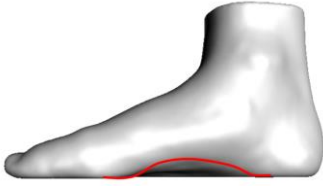

changing differently to the arch's height or shape. Despite being feasible to capture quickly in clinical practice, with minimal equipment and technical expertise, footprint measures might provide misleading information about the foot structure and lead to inaccurate diagnosis. A more relevant measure, the normalized navicular height may be an appropriate parameter to capture the development of the MLA height as it represents the relative increase in NH accounting for changes in foot length. However, locating the navicular tuberosity may pose problems in children due to local soft tissue (Waseda et al., 2014), affecting the reliability of this measure (Williams and McClay, 2000). Although dorsal arch height at 50% of foot length normalized to truncated foot length has been suggested as a reliable and valid method to capture MLA height (Williams and McClay, 2000), Waseda et al. (2014) argued that the 50% foot length may not be at the same anatomical location in different participants. Furthermore, although the normalized measures provide a more direct representation of the MLA height, they only capture the vertical component of the MLA, ignoring its 3D surface morphology or shifts in its location.

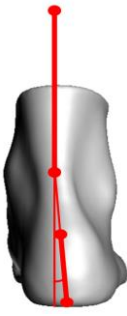
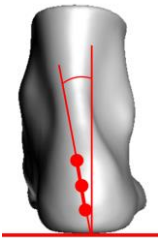
In summary, one of the most debated characteristics of the paediatric foot is the height, shape, and development of the MLA as there is no gold standard measurement method for this in a clinical setting or research (Uden et al., 2017, Banwell et al., 2018). Studies to date have used at least 16 different arch measures with ten footprint measures and navicular height included (Uden et al., 2017). These measures are two dimensional, either capturing the vertical or the horizontal component of the MLA, and hence are not suitable to characterize MLA development, which is three dimensional. By using a single footprint or height based method, the arch is treated as a uni-planar structure ignoring the complexity and multi-planar nature of the foot and the significant differences in foot posture (Gill et al., 2016, Uden et al., 2017).

2.1.4.3. The foot posture of the paediatric foot

Measures of foot posture have been used to assess the development of the paediatric foot (Gijon-Nogueron et al., 2019, Martínez-Nova et al., 2018), for identifying foot types (Razeghi and Batt, 2002) or for the comparison of different populations (Gijon-Nogueron et al., 2017). The definitions of foot posture measures are in Table 7.

Table 7.: Definition of foot posture measures.

Measure	Definition	Diagram
	Talar head palpation	
	Supra and infra lateral malleolus curvature	
	Calcaneal frontal plane position	
Foot posture index 6 (Redmond et al., 2006b)	Prominence in region of talonavicular joint (TNJ)	
	Congruence of medial longitudinal arch	
	Abduction/adduction of forefoot on rearfoot	

Measure	Definition	Diagram
Rear-foot angle	The acute angle between two lines: (1) connecting the base of calcaneus and the Achilles-tendon attachment and (2) connecting the centre of the Achilles-tendon at the level of the medial malleolus and the centre of the posterior aspect of the shank 15cm above the previous marker (Langley et al., 2016).	
Resting calcaneal stance position (RCSP)	The angle (in full weightbearing bipedal stance) between the line perpendicular to the ground and a line connecting the upper, middle, and lower parts of the posterior calcaneus marked in prone position. (Ahn et al., 2017, Root et al., 1971, Cho et al., 2019)	

The most commonly used foot posture measure is the FPI-6 which provides a comprehensive assessment of foot posture including rear-, mid- and fore-foot (Gijon-Nogueron et al., 2019), while other measures only consider the rear-foot (such as rear-foot angle or RCSP).

Studies related to the age range between 2 and 7 years are presented in Table 8.

RCSP is suggested to measure calcaneal eversion, which is assumed to reduce with increasing age and decreasing pronation. For this reason, assuming a relationship between calcaneal eversion and flat foot, RCSP has been suggested to be used as an assessment of paediatric or adult flat foot. It was found that RCSP decreased from 11 degrees valgus to 6 degrees varus when orthosis was worn (Jay et al., 1995). Furthermore, the success of operation to correct flatfoot was decided based on RCSP in a study of 49 8-year-old patients, with the RCSP decreasing from 9.6 degrees valgus to 2.7 degrees valgus

postoperatively (Lundeen, 1985). The reliability of the RCSP was assessed by Sobel et al. (1999) in 14 volunteers (age was not provided) by having three examiners measuring the RCSP on two separate occasions. The authors found moderate to high intratester reliability with intraclass correlation coefficients ranging from 0.61-0.90 for the three examiners when using manual goniometer. They also found no significant differences between the measurements of examiners using electric goniometers indicating acceptable intertester reliability. Normal values of 88 adults aged 21 to 36 years (mean RCSP=6.07° valgus) and 124 children aged 5 to 17 years (mean RCSP=5.6° valgus) were also established and no significant difference was found between the two groups.

Table 8.: Studies assessing foot posture development in the children between the ages of 2 and 7 years with mean foot posture for the whole sample indicated.

First author (year)	Age range (N)	Foot posture measure
Sobel et al. (1999)	6-12 (150)	Mean RCSP=5.6°
Redmond et al. (2008)	3-17 (397)	Mean FPI-6=3.7
Sadeghi-Demneh et al. (2015)	7-14 (667)	Mean rear-foot angle: 9°
Gijon-Nogueron et al. (2016b)	6-11 (1762)	Mean FPI-6=3.82
Gijon-Nogueron et al. (2017)	6-12 (1798)	Mean FPI-6=3.8
Martínez-Nova et al. (2018)	5-11, 8-14 (1032)	FPI-6: 3.6 and 3.3
Gijon-Nogueron et al. (2019)	3-15 (3217)	Mean FPI-6=4.15

Children's RCSP ranged between 6° varus and 12° valgus, while that of the adults ranged between 1° varus and 14° valgus. The result also showed that RCSP did not decrease with age which is contrary to the suggestion of Root et al. (1971) that it decreases with age to a 0°±2° by adulthood. Sobel et al. (1999) also indicated that 80% of children had RCSP outside of the range of theoretical "ideal" suggested by Root et al. (1971). The authors argued that

the 5.6° average RCSP in children, the range of the measurements and the lack of correlation between age and RCSP suggest that the “ideal“ $0^\circ \pm 2^\circ$ RCSP defined by Root et al. (1971) is invalid. They also indicated that RCSP should not be used as an indicator of pathology. More than 3° higher hind-foot valgus ($9^\circ \pm 5.7^\circ$) was observed by Sadeghi-Demneh et al. (2015) in a group of 7-14-year-old children using rear-foot angle, although this measure captures the angle between the Achilles-tendon and the bisection of the calcaneus. The authors used this measure in conjunction with arch index, arch angle, and the appearance of the MLA to define flat foot in their participants and found a decreasing trend in its prevalence from the age of 7 (26%) to 14 years (14%). While these studies provided a reliable measure of rear-foot posture, they could not capture the changes occurring in the mid- or fore-foot, hence their ability to describe foot posture development is limited. However, the main concern is that RCSP and rear-foot angle only measure changes of the subtalar joint (which is a tri-planar joint) in the frontal plane, and for this reason they cannot capture the multi-planar variations and development of the paediatric foot posture (Menz, 1998, Uden et al., 2017).

While RCSP only considers the rear-foot, FPI-6 incorporates all three regions of the foot: rear-, mid- and fore-foot. This measure was developed to assess foot posture in multiple planes and anatomical segments, and while it is a static measure, it had a higher ability to predict ankle joint complex kinematics than any other clinical measures at the time of its development (Redmond et al., 2006b). Although it was originally used only in adult populations, it has also been validated in children aged 6-18 years to diagnose paediatric flexible flat foot (Hegazy et al., 2020), and its reliability was also confirmed in children aged 5-16 years (Morrison and Ferrari, 2009), and 6-12 years (Lee et al., 2015). Furthermore, the study of Žukauskas et al. (2021) has shown a significant correlation of FPI-6 with other clinical parameters of foot posture in 5-8 year-old children with flatfoot and no flatfoot.

Finally, FPI-6 was in the first three most used assessment methods for paediatric pes planus among UK podiatrists (Morrison et al., 2020) along with joint range of motion and standing tip-toe (joint range of motion: 68.8%, FPI-6: 62.5% and standing tip-toe: 62.5%).

The first study to provide normative data on a comprehensive foot posture measure, namely the FPI-6 (Redmond et al., 2006b), was completed by Redmond et al. (2008). FPI-6 is a composite foot posture measure comprised of six items (see Table 7.). Each item can be scored from -2 to +2, and the six scores are added up to provide a full score. Higher scores suggest a pronated foot posture while lower scores indicate a supinated foot posture. Redmond et al. (2008) found that children aged 3-18 years had a mean FPI-6 score of 3.7, which is a pronated foot posture, and was reported to be significantly more pronated than the feet of the adult (18-59-year-old) population of the same study. The authors suggested that the more pronated foot posture is a consequence of the developmental process of the MLA as indicated by Staheli et al. (1987). Unfortunately, the child population was not divided into age-groups, hence the changes in FPI-6 during growth could not be established. A more detailed analysis was performed by Gijon-Nogueron et al. (2016b), who measured the feet of 1762 children between the ages of 6 and 11 years using FPI-6. They found that the average FPI-6 for the whole sample was 3.77 and 3.87 for the right and left foot, respectively (mean=3.82). Based on the percentile presentation the 50th percentile was at FPI=4 for 6 year-old children and fell to FPI=3 by the age of 11 years, while the 85th percentile was approximately at FPI=6 (between 6 and 9 the foot posture is considered pronated), hence they suggested it as a cut-off point between normal and pronated foot. Although FPI-6 decreased from 6 to 11 years of age, the only significant decrease occurred from the age of 9 years.

Gijon-Nogueron et al. (2017) have also shown a decreasing tendency in FPI-6 among 1798 schoolchildren aged 6 to 12 years from 4.52 at the age of 6 years to 3.3 at the age of 9. The average FPI-6 of the whole sample was 3.8 which coincides with previous findings of Redmond et al. (2008) and Gijon-Nogueron et al. (2016b). Furthermore, in this study, boys aged 6-7 years had more pronated feet, while at ages 8, 9, 10 and 11 years, there were no differences. By the age of 12 years the earlier trend reversed, and girls had more pronated feet due to increased laxity in the female foot (Gijon-Nogueron et al., 2017). The study has also shown no relationship between BMI and FPI-6 contrary to previous findings using simpler foot measures. This may be because FPI-6 considers rear-, mid- and fore-foot in three spatial planes while the measures used previously do not. Furthermore, FPI-6 is independent of the possible influence of the volume of fat on the plantar surface compared to footprint measures.

While the previous studies provided a cross sectional view of the FPI-6 changes in late childhood, Martínez-Nova et al. (2018) performed a follow-up study. The researchers measured anthropometric characteristics and FPI-6 of children aged 5-11 years and re-assessed them three years later. They found that FPI-6 reduced (although not significantly) from 3.6 ± 2.8 (range, from -4 to +12) at the first measurement to 3.3 ± 2.7 (range, from -3 to +12) at the follow-up. Only two items showed significant reduction after three years, talar head palpation ($p < 0.001$) and the curves around the lateral malleolus ($p = 0.038$). The authors also observed a reduced frequency of pronated (reduction of -2.2%, FPI-6 between 8 and 10) and highly pronated (reduction of -2.0%, FPI-6 between 11 and 12) foot posture and an increase of 3.5% in the neutral (FPI-6 between 1 and 7) foot posture category after three years. The authors, based on their results suggested that the average foot posture in childhood is $FPI = 4 \pm 3$, which indicates that 68% of children would fall in the neutral category between

FPI=1 and 7 and 95% would fall in the supinated, normal, and pronated categories between -2 and +10. As the authors relate pronated foot to flat foot, they highlight that their study confirms the natural development of childhood flatfoot morphology which decreases with age. Based on the findings they also argue that a child in the first decade of their life with pronated or even highly pronated foot should be considered “normal”, if painless. A yearly or bi-annual follow up could have increased the resolution and the value of the dataset.

Gijon-Nogueron et al. (2019) have showed similar but slightly higher (left foot: 4.11, right foot: 4.20, range: -4 to 12) average FPI-6 for a group of 3217 children aged 3-15 years. They also showed that the prevalence of pronated foot posture declined with age with FPI-6 being +6 at the age of 3 years and +3 at the age of 14 years. At the age of 7 years, the average FPI-6 was +4.32. The authors also highlight the broad range of values: -1 to +11 at the age of 3 years, and +3 to +9 at the age of 14 years. The range at the age of 7 years was -4 to +12. Gijon-Nogueron et al. (2019) emphasised that FPI-6 is a more appropriate measure of foot posture compared to footprint measures, which might not capture the anatomical foot morphology. The authors also suggest that the mean and ± 1 , $\pm 2SD$ values enable clinicians to provide parents with information about their children foot posture compared to the normal population (e.g. within 68 or 95% of the normal range).

In summary, while rear-foot posture measures such as RCSP and rear-foot angle provided a frontal plane assessment of the rear-foot, FPI-6 allowed a more complex, multi-planar measurement of rear-, mid- and fore-foot posture. Both studies employing rear-foot posture measures found that the posture of the rear-foot in childhood is everted, and this pronation decreases with age, although no studies examined children before the age of 5 years. Despite the reduction of the RCSP angle, Sobel et al. (1999) found that rear-foot posture does not reach neutral (RCSP angle: $0^{\circ} \pm 2^{\circ}$) as suggested by Root et al. (1971). As these measures are

limited to a single plane (frontal) and the rear-foot, a composite measure, the FPI-6 was developed (Redmond et al., 2006b) to assess the foot in all three planes. FPI-6 has been employed to measure the foot posture of children between the ages of 3 and 18 years. Whole sample means ranged between 3.3 and 4.2 valgus suggesting a mostly pronated foot posture at all ages and significantly more pronated compared to adults (Redmond et al., 2008). The studies also found that the pronation decreased with age, although the range of FPI-6 suggests a wide variation of foot posture. A cut-off value of FPI=6 (85th percentile) for pronated foot posture was suggested by Gijon-Nogueron et al. (2016b). Although FPI-6 is a useful clinical measure, caution must be applied when interpreting the current literature, as a wide spread of ages were included in each study, not accounting for the predicted changes each year (Uden et al., 2017). A further limitation of FPI-6 may be its low predictive power of mid-foot dynamics during walking as was shown in a study by Nielsen et al. (2008) in adults.

2.1.5. Summary

In this section of the literature review, the development of the paediatric foot, and lower limb posture was first described, followed by an overview of gait development. The next part of this section examined the current literature on foot morphology development detailing three types of measures: (1) length and width, (2) MLA measures and (3) foot posture. This review exposed a clear need for further research into the investigation of paediatric foot morphology development.

Firstly, existing datasets captured how the 2D foot anthropometry changes as independent walking matures. Width of foot regions, foot length, and ratios have been used to track and describe foot size and slenderness changes. Although provided important size information, these datasets were limited in accuracy due to the methods used (footprints or foot measuring

device). They also did not provide a complete characterization of each foot region (rear-, mid- and fore-foot) at standardized anatomical locations. Using standardized width, height and proportion parameters of each foot region could contribute towards a more consistent knowledge and understanding of paediatric foot shape development. To evaluate the foot's structural development, researchers and clinicians often measure foot posture and the medial longitudinal arch. The MLA is a highly debated characteristic with inconclusive results, partly due to the high inter-individual, ethnic, and environmental differences. However, the main concern is that 2D anthropometric MLA measures cannot optimally quantify the complex 3D shape changes related to the developing paediatric foot posture. Of particular importance is the wide variety of measures used (Table 5.) and their validity (or lack thereof) to the actual height and structure of the MLA. The measures used are two dimensional, considering height, width, length, or area in contact with the ground, and hence are not appropriate to describe the 3D multi-planar complexity of the MLA. Although FPI-6 does capture the multi-planar posture of the foot, it is subjective, and no normative dataset has been established with yearly data. Furthermore, these measures cannot provide information on the shape of the rear-foot or the plantar aspect that is not touching the ground - its shape, e.g., flat, convex, concave, or curved -, and how that surface is changing over time. This information could be relevant and valuable to quantify changes in the MLA and foot posture.

The second issue is that to capture more accurate and higher resolution 2D and 3D foot measures, 3D scanning is required. If the children's feet in the above studies had been captured using a 3D scanner, a comprehensive list of more accurate, higher resolution measurements could have been developed. Such measurements would support the development of benchmarks for 2D and 3D foot morphology, which would have high theoretical and practical value.

Finally, there is no up to date, high resolution data about the development of children's foot shape, captured using 3D scanning technology. Datasets are available in different age-groups using manual methods, and 3D scanning data in limited age ranges (these will be discussed in section 2.3.3.). However, to the authors' knowledge, no 3D scanning studies examined the 2D anthropometric and 3D surface morphology of children's feet between the ages of 2 and 7 years.

Such dataset, consisting of relevant, accurate and valid measures, combined with the latest measurement technology methods could provide a theoretical underpinning of health professionals' education and clinical practice. Moreover, the practical values could include reference data for parameters related to the development of the paediatric foot shape, follow up and evaluation of post-surgical outcomes for children with congenital foot deformities (Ganesan et al., 2017), direct information on age-group foot shape which could aid footwear last design.

In conclusion, this part of the literature review provided an overview of foot, lower limb and gait development and foot measurement methods and measures. It also demonstrated that there had been several studies measuring children's foot size, shape, and posture, using mostly manual or other 2D measurement techniques. Although these studies provided important information about the changes in foot size and shape, they could not describe the changes taking place in height, width, and proportions in the three main regions of the foot. In addition, there is still a lack of relevant data on the trajectory of 3D surface morphology changes occurring in the foot in childhood, using current 3D scanning technology and high resolution and accurate 3D measures. Such dataset integrated with 2D anthropometric parameters may establish an understanding of foot shape and size development for researchers, clinicians, and the footwear industry.

2.2. 3D scanning of the foot, an overview of technology and application

The literature review in the previous section (section 2.2.) outlined the importance of developing higher resolution and more accurate 3D foot assessment methods to complement 2D measures for assessing the paediatric foot. Current 3D scanning systems have the potential to capture children's foot shape and provide such measures, allowing for more accurate clinical decisions based upon robust, highly accurate measurement of foot dimensions. The first half of this chapter will provide an understanding of the use of 3D scanning technology in foot assessment, overview and describe the steps taken to process and analyse 3D scanning data and finally will look at the reliability of 3D scanners. The second half of this chapter will first review the studies employing 3D scanning that resulted in 2D measurements of the paediatric foot. This part of the literature review will demonstrate the importance of this technology in research and the roles and limitations of 2D measures in clinical practice and footwear design. Although most studies used 2D measures derived from 3D scanning, some researchers attempted to provide higher resolution or 3D information about the foot. These approaches will be evaluated briefly before introducing a novel approach to 3D foot surface analysis.

2.2.1. 3D scanning technology

3D scanning, as opposed to traditional anthropometric methods such as callipers or tape measure, allows the capturing and saving of human body surfaces in a digital form for future processing with this technology. The human error associated with manual measurements is reduced, the measurements can also be obtained later, and the experiment time could be shorter. Three-dimensional scan data also provide more information than traditional methods, e.g., surface area, volume, and 3D shape can also be calculated over and above the 2D measures. Using appropriate software, it is also possible to compare foot shape and size pre- and post-treatment, providing a quantitative approach for evaluating treatment effectiveness. Consequently, this technology is ideal for clinical research and practice, orthosis, or footwear last design.

The next section will describe (1) how this technology works, (2) what are the criteria for choosing the appropriate scanner, (3) how to process data resulting from 3D scanning, (4) what are the possible outcome measures and (5) how reliable this technology is in foot scanning?

2.2.2. 3D scanner types

The three main types of imaging technologies used in foot assessment are (1) stereophotogrammetry, (2), laser scanning and (3) white-light or structured light scanning. Stereophotogrammetry takes multiple photographic images from different positions and estimates an object's 3D coordinates. These images must be taken at the exact same time and from known distances from the captured object. This technique's advantages are the speed of capture and that they are relatively lightweight, hence easily portable. However, post-processing takes a long time; the accuracy of the measurements depends on the cameras'

quality, the distance between the object and the camera, and the camera's field of view (Goonetilleke, 2012).

In contrast, laser scanning is an active technology. In this technique, laser lines are projected onto the object, and they are scattered, which is then imaged by one or more cameras. Triangulation is then used to calculate the spatial coordinates of points along the laser line (Azernikov and Fischer, 2008). There are static and hand-held laser scanners available commercially in visible and infra-red ranges of the light spectrum. These scanners – because they rely on the laser line's scattering – depend on surface properties like roughness or reflectiveness, and certain colours may not be captured accurately. Most foot scanning laser systems are step-in scanners, that are bulky, mostly not portable, and expensive, although data capture is fast (1-5 seconds).

Due to their speed (produces 10-30 frames per second), white or patterned light scanners can also be used as hand-held scanners and make this technology more accessible for clinical use. Hand-held scanners have been used in different fields from scanning human skeletal remains for 3D printing for museums (Allard et al., 2005), through measurement of paediatric pectus excavatum (Hebal et al., 2019) to measuring the volume of residual limb models (Armitage et al., 2019). This type of scanner projects a fully structured light pattern onto the object being scanned, and a 3D image is calculated using the sensed deformed pattern. The accurate location of each point on the object's surface is determined by structured light triangulation. In this process, a picture of a point P is taken by both cameras, then identified in both pictures using the light patterns. The system then determines a plane from both cameras and point P. The intersection point on the two rays from the cameras is calculated to obtain the z-coordinate of point P (Daanen and Ter Haar, 2013). 3D scanning

captures the object's surface in the form of a point cloud or triangulated surface, from which discrete measurements can be drawn.

When considering foot scanning specifically, the most common type of scanner used is the step-in laser scanner, which provides fast scanning, but is expensive (e.g., Vitus Smart 3D whole-body scanner (Vitus\Smart, Vitronic GmbH, Wiesbaden, Germany), Pedus foot scanner (PEDUS, Vitronic GmbH, Wiesbaden, Germany)). Another disadvantage is that the cameras are fixed, and hence there will be areas of the object missed, which cannot be reliably filled, although the trade-off with high capture speed might worth the cost.

In contrast, hand-held 3D scanners (e.g., Handyscan, FastSCAN, Artec, Faro) are smaller in size, more cost-effective, and portable. They also allow the scanning of occluded surfaces by moving around the object, creating an almost perfect representation. This technology should enable the effective collection of 3D foot data. As these scanners use structured light, they can capture the texture and the geometry of the object in question. The downside of hand-held scanners is that they require experience using the scanner, and post-processing demands more time and expertise than step-in scanners. Other methodological challenges to consider may include scanning the plantar aspect in a static weight-bearing position, the participant's ability to remain static for the duration of the scanning, and software capabilities. Once 3D scanning data capture is completed, the outcome in most cases is a point cloud or triangulated mesh. This cloud of information then requires post-processing to represent the scanned object accurately, and this will be described in 2.3.2.3.

2.2.3. Selecting the appropriate 3D foot scanning technology

The different scanners mentioned in the previous section have their application in scanning feet or other body parts. They all have their advantages and disadvantages, so the critical question is, how does one choose the appropriate scanner for a specific application? An advisable approach is to create a prioritized list of shape measurement criteria and match them with the available 3D scanners (Goonetilleke, 2012). Here, a list of criteria is presented.

2.2.3.1. Speed of Data Capture

When considering the speed of data capture in 3D scanning, higher speed allows for a fast data collection, making it a more acceptable experience for both the participant and the researcher. Laser scanners usually offer faster data capture as opposed to structured-light scanners, although they have their disadvantages as described in the previous section. Faster data collection is especially crucial in populations that may not be able to stay still for prolonged periods of time, such as people with certain conditions, the elderly or young children. In their case, laser scanning may be the optimal option to avoid movement during scanning.

2.2.3.2. Speed of Data Reconstruction

Once the 3D scan is captured, fast data reconstruction allows the researcher to decide whether the data collected is sufficient or if the scanning needs to be repeated, which reduces the inconvenience of waiting after scanning, which is especially important in specific populations or in small children.

2.2.3.3. Accuracy

The accuracy of 3D scanners varies, affecting what applications they can be used for. It is suggested that for foot measurements, linear measures should be accurate within ± 1 mm, foot length should be accurate within ± 2 mm, and circumferences within ± 3 mm (Goonetilleke,

2012). Goonetilleke (2012) also argues that footwear design measures should be twice as accurate.

2.2.3.4. Surface Coverage

This criterion is very much dependent on the application of the data, for example, for shoe sizing applications capturing the whole 3D surface may not be needed. An important consideration is capturing the plantar aspect, which is especially difficult in a full weight-bearing position. Goonetilleke (2012) argues that most of the plantar aspect is flat in this case and suggests that a full scan of the foot might be needed in custom shoe applications. Although most of the plantar aspect is flat in a full weight-bearing position, the changes in the medial longitudinal arch with increasing age are important considerations from a developmental perspective. Hence, in a developmental study, capturing the plantar aspect is crucial and a technical challenge.

2.2.3.5. Usability

Usability refers to the feasibility of scanning technology for a particular application. It is essential, especially in retail settings, that the scanner is easy to use and provides quick results. Although some scanners can provide this, they may not be appropriate for research or shoe manufacturing purposes. These applications require more flexibility and accuracy and repeatable results (see section 2.3.2.5. for the reliability of 3D foot scanners). It is also advisable to consider the type and number of participants required for the application. Hand-held scanners make it possible to collect data in the field, in the participants' environment, which can be an essential factor, for example, in young children. However, hand-held scanners require experience from the researcher to move the scanner around the foot to capture a full 3D model. This part of the process is more convenient in step-in scanners.

2.2.3.6. Post-Processing

Once the scans are captured, it is crucial whether post-processing requires a long time, or a 3D model can be available quickly. Post-processing also depends on the application. In a retail environment (footwear store), quick and easy post-processing is required to provide fast results for the customer. Scanners, such as Volumental can provide post-processed results quickly and display these to a customer in a shoe shop (Jurca et al., 2019). However, if the aim is accuracy and a high precision 3D model, e.g., in research or shoe last design, longer post-processing (see details in section 2.3.2.3.) is necessary, which requires more knowledge and experience.

2.2.3.7. Publications

Another criterion that researchers want to consider is whether the 3D scanner has been used in peer-reviewed publications. These might be necessary for establishing the scanner's accuracy, reliability, and validity and might give the researcher more confidence in using that particular scanner, although new technologies arise constantly and hence studies without previous publications on the technology are also commonplace.

2.2.3.8. Summary

This section described criteria considered when choosing the 3D foot scanner for an application. As mentioned at the beginning of this section, this is not an exclusive list, and users should create their own list of relevant criteria and compare the available technologies before deciding. Although it has not been listed, the price of the 3D scanner can also be a criterion that supports prioritising the other criteria and the decision making. Although it is essential to consider as many criteria as possible, it is impossible to consider all of them; hence, it is crucial to be aware of the limitations of the technology and methods used.

2.2.4. Post-processing of 3D scans

After completing the scanning, the first step is to align the multiple scans captured from different cameras (laser step-in scanners) or different views (hand-held scanners). Alignment is achieved using a registration method, typically using the iterative closest point (ICP) method. Once alignment is complete, the overlap is removed. Which points are removed usually is dependent on their distance from the centre of the scans: points closer to the centre are more likely to be kept (Goonetilleke, 2012). After alignment, the point cloud or mesh will include noise from different sources, such as transitions between different textures or geometry. This noise has to be removed without interfering with the object's true model. Once the noise is removed, the point cloud is transformed into a mesh of triangles, that allows for more accurate computation of measurements. This mesh model of the scanned object will usually include holes (no data points in an area) due to inherent capabilities of laser scanning or inappropriate scanner movement in case of handheld scanning, or simply due to the shape of the captured object. These holes can be filled using the provided software, typically by automatic algorithms, although manual hole filling is also available. While manual hole filling is available, it is recommended to be used in small holes in relatively flat areas. The hole-filling operations completed the model, which is then turned into a watertight polygonal mesh. Although the mesh is complete, further operations might be needed to make the model ready for the specific measurements. Such an operation is the reduction of points\triangles in the mesh to reduce file size and, hence processing time. The reduction of points might be necessary for experiments including a high number of scans and high point cloud density. Specific algorithms in software are available for this task, making sure information is not lost while reducing the number of points\triangles in the model. Once the required point cloud density is achieved, the mesh needs to be regularized so that the mesh triangles are approximately the same size, and they are distributed evenly over the surface.

Further steps can include the smoothing of the mesh surface to even out rough edges or eliminate unwanted geometry, such as skin creases and folds. This step allows for accurate measurements and 3D shape calculations to reduce skin artefacts' effects. The complete model then can be saved in many different file types, such as stl or obj and exported into 3D measurement software.

2.2.5. Outcome measures of 3D foot scanning

Three-dimensional scans of the human body or body parts allow the collection of anthropometric measurements and surface area, volume, segmental representations, or 3D shape. Although there are inherent errors in this method, it is currently the most advanced technology to measure the human body. These errors may come from the human body's posture and involuntary motion during scanning and human sources. These human sources might include errors while locating specific anatomical landmarks, measuring, and handling data.

The types of data that can be extracted from 3D scans as identified by Goonetilleke (2012) include: (1) linear (2D) measurements, (2) surface curve measurement, (3) shape analysis, (4) overlay or superimposing and (5) mass properties. With the advancement of applied differential geometry, further shape descriptors can be calculated from the 3D scans, such as Gaussian curvature and its derivatives, e.g., minimum, and maximum curvature, curvedness, shape-index. These variables can describe the 3D surface in more relevant detail and higher resolution. These will be discussed in section 2.3.4.

The quantitative description of the human foot is important and used in many applied fields: ergonomic footwear design, orthotics and clinical assessment (Telfer and Woodburn, 2010). Proper fit is the most critical facet of shoe design, which will prevent the foot from moving

in the shoe (Krauss et al., 2010). Appropriate fit is achieved by matching the shape of the shoe's inside with that of the foot and supporting the foot in its function (Hawes et al., 1994). To enable properly fitting shoe design, the factors affecting foot shape (e.g. age, body mass, sex), should also be considered (Krauss et al., 2010).

Linear and cross-sectional measures have been used to characterize foot shape from 3D scanning (Hong et al., 2011, Jimenez-Ormeno et al., 2013, Krauss et al., 2008, Mauch et al., 2009, Xiong et al., 2009) in static positions, usually bipedal standing. Three-dimensional scanning technology also allowed the comparison of male and female foot shape (Hong et al., 2011, Robling and Turner, 2009), different loading conditions (Xiong et al., 2009), foot growth patterns and body weight (Jimenez-Ormeno et al., 2013). 3D scans of static feet have also been used to investigate if male shoe lasts would fit female feet (Krauss et al., 2010) and to attempt to classify adults' (Krauss et al., 2008) and children's feet (Mauch et al., 2009).

Although there are also studies using large cohorts and manual methods (see section 2.2.), the technology to measure paediatric foot morphology has also shifted to 3D scanning (step-in laser scanners) in the last two decades. The reliability of step-in scanners and the methods to identify anatomical landmarks (palpating and marking before scanning) has its limitations in children due to the adipose tissue covering these landmarks. Nevertheless, researchers used this technology to report foot measures in developing children and to classify children's feet by their shape. As a new and promising technology introduced into research, clinical and design applications, the reliability of 3D scanners and the associated protocols employed are essential to guide diagnosis, design decisions, assess treatment results, and be comparable to traditionally used methods. For this reason, the next section will overview the studies investigating the reliability of step-in and hand-held 3D scanners.

2.2.6. The reliability of 3D scanners

Hand-held scanners' reliability is often addressed in the 3D scanning literature, as researchers require reliable data when introducing new technology. For this purpose, Park et al. (2006) evaluated the reliability of 3D laser hand-held scanning and landmark localization for craniometry by comparing the results to sliding and spreading callipers measurements. They investigated distance and breadth measurements of 30 unidentified skulls and found that both the direct and 3D scanning methods showed excellent intra-examiner reliability (ICC values ranged from 0.9152 to 0.9982). Furthermore, the 3D scanning also presented excellent inter-examiner reliability (ICCs ranging from 0.8013 to 0.9969). Although the 3D scanning method tended to provide lower readings (mean difference of 33 craniometric variables averaged: -0.69mm), there was no significant difference between the direct and 3D scanning method highlighting the validity of this technology. The authors suggest that this technology could replace the direct measuring method and provide reliable data. Dessery and Pallari (2018) using the whole lower limb and circumference measures, investigated the reliability and validity of high (Artec Eva (Artec Group, Luxembourg, Luxembourg)) and low cost (iSense (3D Systems, Rock Hill, SC, USA) hand-held scanners against a manual (standard flexible tape measure with a sensitivity of 1mm) technique. They found that the hand-held 3D scanner, Artec Eva, provided limb circumference measurements similar in accuracy, but better in repeatability than the manual technique. They also argued that although the low-cost 3D scanner (I-sense) used in their study was able to scan nine times quicker than the Artec Eva, it overestimated the circumferences, especially in smaller sizes (mean biases for the sections ranged between -8.3mm and 3.4mm absolute difference and -2.3% and 1.0% relative difference).

While hand-held scanners have a multipurpose use, step-in scanners were explicitly designed for foot scanning, and their reliability was assessed in various age-groups. The validity and reliability of the Infoot 3D foot digitizer (I-Ware Laboratory Co., Ltd) were investigated (De Mits et al., 2010) and compared to those of X-rays and clinical foot measurements in a study of healthy adult participants (ages between 27 and 66 years old). ICC values for the linear and angular foot measurements were greater than 0.8, while the smallest detectable difference (SDD%) values were between 1.88 and 16.89%. The standard error of measurement (SEM) ranged between 0.3 and 2.7 mm (foot measures ranged from right height of the toe #5 joint: 19mm to foot length: 254mm). Considering the measures' validity, Pearson correlation coefficients were between 0.715 and 0.982 (all $p < .05$) between the foot digitizer data and the X-ray data. However, while this measure captures a relationship between the two datasets, the results from the two methods can change in the same way but with a consistent bias, meaning that the absolute values might be vastly different with a strong correlation result. For this reason, correlation is not a suitable method for assessing validity, as association and agreement are not the same. While association (correlation) quantifies the tendency for one variable to increase (or decrease) as another increase and by how close points lie to any straight line on a scatter plot, agreement (reliability) means that repeated results are equal and that points lie on the line of equality. Using correlation might show high validity, where the two datasets are very different. The software used for post-processing (I-Ware Laboratory Co., Ltd) uses landmarks attached to the foot at specific anatomical points to calculate the foot measures.

To compare the precision and accuracy of the Infoot USB (I-Ware Laboratory Co., Ltd) 3D scanner to three other types of clinical measures (digital calliper, Harris mat and digital footprint image), Lee et al. (2014) also used anatomical landmarks attached to the foot in

130 participants aged between 18 and 30 years old measuring foot length, ball of foot length, outside ball of foot length, foot breadth diagonal, foot breadth horizontal and heel breadth. Based on the mean absolute difference (MAD) between the repeated measurements, they found that the 3D scanner had better precision than the other three measurement types. The ICC calculated for six different foot parameters were similar to those found by De Mits et al. (2010) and ranged between 0.95 and 0.98 for the 3D scanner. The mean absolute differences (MAD) between the repeated measurements for the 3D scanner, which is considered a precision measure, ranged between 0.6 and 11.9mm (foot measures ranged from: mean heel breadth: 63.2mm, mean foot length: 249.3mm) for the six parameters.

The reliability of step-in 3D scanning in children was assessed in a study by Mauch et al. (2008), who investigated differences in foot morphology between normal, under- and overweight children. In this study, the Pedus 3D scanner (Pedus, Human Solutions Inc., Germany) was used to measure 12 foot parameters in 2887 children aged two to 14 years old. The intra-tester measurement error was established on five different children's feet, scanned four times by the same investigator. The researchers also calculated the root mean square error (RMSE) for the different foot measures (Bland and Altman, 1996). For metric measures, the RMSE results were between 0.5 mm and 2 mm, and for angular measures 1.31° and 1.41°. The anatomical landmarks used for measurements were located manually by the investigator, which unavoidably introduced subjectivity and, therefore, affected reliability; hence they reported RMSE.

Although studies investigating step-in 3D scanners have used various measures and age-groups, their results show that they are a valuable tool when comprehensive foot anthropometric measures are needed. The literature suggests that 3D scanners could provide the same or higher accuracy as conventional measurements. Although the calculation of foot

parameters relied on manually located anatomical landmarks, their reliability was the same or higher than traditional measurement methods. This method requires an experienced investigator and introduces error, however, automatic landmark detection in most software is based on adult foot data and hence using these can also increase the error when calculating measures of children's feet.

As the previous paragraphs show, although step-in scanners' reliability and validity are well documented to be high for adult populations, there is limited data available in children. The results from adult populations will need to be considered carefully as children's feet are considerably smaller in size: foot length: 130.7mm at the age of one (Muller et al., 2012), 184.4mm at the age of 6 and 254.9 at the age of 18 (Waseda et al., 2014). In addition to the small size, the adipose tissue present in small children makes palpating anatomical landmarks more complicated, and this age-group is also more prone to movement during scanning than adults. Furthermore, children are also more likely to stand in differing poses for subsequent scans therefore altering reliability. For these reasons, further investigations are needed to ascertain the reliability of measuring foot parameters using 3D scanning in children.

The studies above provide a justification for the use of both hand-held and step-in scanning in a wide variety of contexts. Unfortunately, step-in scanners' validity and reliability are not transferable to hand-held scanners, mainly due to the critical difference between stationary and mobile scanning. Hand-held scanners capture frames as they are moved around the object and align the frames using dynamic referencing or self-positioning (reference system is based on the object itself rather than an outside fixed reference). In contrast, step-in scanners capture multiple frames from the same position, calculate the average, use static referencing, or external positioning (reference system is based on an outside fixed reference).

Although determined in other fields, no studies have examined the reliability of hand-held 3D scanners for capturing paediatric foot shape.

Therefore, the reliability of hand-held scanners has to be determined to employ this technology in scanning a cohort of children's feet. Regarding the validity of hand-held scanning compared to laser scanning, this has been examined in previous research (Koban et al., 2020, Seminati et al., 2017). Koban et al. (2020) examined the Artec Eva scanner's reliability and validity against a non-portable reference scanner, the Vectra XT 3D Surface Imaging System (Canfield Scientific Inc., Parsippany, NJ, USA) in capturing faces. This system is widely used (Koban et al., 2020), employs passive stereophotogrammetry and was designed especially for the health care sector. The study found RMSE of under 1mm in the surface-to-surface deviation between the scans captured by Vectra XT and Artec Eva. This result suggests high validity in the case of face scanning of volunteers in an upright, non-excessive sitting position with eyes and mouth closed. Investigating the Artec Eva scanner's validity, Seminati et al. (2017) compared its performance to a reference scanner, the Romer (Romer scanner, CMS108, Hexagon, UK) laser scanner with a coordinate measuring arm, and an accuracy of 0.04mm. They found that the RMSE between the scans from the two scanners were under 1mm (between 0.23 and 0.65 mm). These results, although using limb models and not live participants, also suggest high validity of the Artec Eva scanner against a laser scanner.

2.2.7. 3D scanning of the paediatric foot

This section will overview studies using 3D scanners to analyse foot size and shape in children aged 3-7 years.

Using the INFOOT three-dimensional laser scanner (INFOOT, I-Ware Laboratory Co. Ltd., Osaka, Japan) Waseda et al. (2014) scanned the feet of 10155 Japanese children between the ages of 6 and 18 years. In this study a marker was placed on the navicular tuberosity, foot length (FL) and navicular height (NH) was measured to calculate arch height ratio (AHR% = $NH \times 100/FL$). The authors reported that FL increased significantly between the ages of 6 to 14 years in boys and 6 to 13 years in girls. In their sample, NH increased significantly in boys from 6 to 13 years and then gradually up to the age of 18 years. NH increased significantly in girls from the age of 8 to 13 years and then gradually up to the age of 16 years. The gradual increase after 13 years of age was slower in girls. The significant change in AHR was between 11 and 13 years in boys; and between 10 and 12 years in girls, although there was no change before, a gradual increase afterwards was present. This study provided a large dataset on Japanese children's 2D foot anthropometric measures and considered a combination of two measures (AHR) to characterize normalized changes in foot size and MLA height. However, the 2D characteristics of the measures limited the application of the results; hence, the study is constrained in how it describes the multiplanar MLA. To characterize the foot in more detail, Delgado-Abellán et al. (2014) used the INESCOP 3D foot scanner (ACN06/01 Model INESCOP, Elda, Spain) to capture 11 foot measures in a sample of 1031 Spanish children between the ages of 6 and 12 years. They found that most measures increased with age at an average of 3-5% per year, although changes between consecutive age-groups were mostly not significant except for foot length. They argue that the application of their results is in shoe last design for children, highlighting the importance

of considering age differences in footwear design. This study provided a large dataset of measures demonstrating the need to differentiate between age groups in footwear design. However, the measures (length, width, and girth) captured were 2D and hence restricted in their application to support a more appropriate shoe last design that also considers the 3D shape of the paediatric foot. To explore the foot morphology of 2887 normal, overweight and underweight children between the ages of two and 14 years, Mauch et al. (2008) used the Pedus 3D scanner. The authors captured 2D foot measures to classify children's feet using Factor and Cluster analysis. As a result, four principal components were identified from 11 normalized foot measures, which accounted for 88% of the variance. These were: *arch* (arch angle, CSI, and SI), *volume* (ball-of-foot width and circumference, heel width and dorsal arch height), *angle* (outside ball-of-foot length and ball angle) and *length* (ball-of-foot length and toe length). These four components were then used in a cluster analysis to obtain the greatest differences possible among groups. As the angle factor did not yield significant differences among the calculated clusters it was excluded. Based on the remaining three factors five different foot types were identified. *Flat feet*, characterized by flattened MLA, *slender feet* characterized by very small volume (narrow ball and heel width and low dorsal arch height), *robust feet* characterized by large volume, short toes, and average arch. The fourth type identified was *short feet* characterized by short rear-foot proportion and a long fore-foot, with relatively high arch and volume. The final type was *long feet* characterized by long ball of foot length and short toe length with average volume and arch. In the normal weight group, they found that children's feet changed from "robust" to "slender" with increasing age. This change in foot shape agrees with Muller et al. (2012) and Kouchi (1998) who used manual 2D measurements. It was also reported that with increasing age, the number of "flat" foot type children decreased, and there was an increase in the "long" foot type. The reduction in children with flat feet has also been reported in studies using manual

footprint measurements (Gilmour and Burns, 2001, Muller et al., 2012, Chen et al., 2011, Chen et al., 2013b, Bosch et al., 2008). Younger children also had larger relative forefoot length measurements and greater relative volumes than older children. Mauch et al. (2008) created average foot types across age-groups and shoe sizes, rather than creating a typical foot type for each age-group and identifying differences and similarities. The measures considered in this study were 2D measures, e.g., footprint measures and angles derived from a 3D scan of the foot. Although the foot types provided may be useful in shoe last design, they are low in resolution (the classification reduced the foot dimensions into whole foot shape) and cannot characterize the 3D surface morphology differences between age-groups.

To investigate the foot arch from a 3D perspective, Chang et al. (2012) intended to capture a 3D measure of the MLA by calculating the arch volume using “Peripher 3D Scanner”, in 44 children aged two to six years. Arch volume was calculated by creating an arch plane along the first metatarsal head, the centre of the midfoot and the medial point of the half of the heel. This plane projected to the ground supporting the foot formed the arch volume. The authors also measured the navicular tuberosity height to capture the MLA's height. Their findings confirm previous results that arch height increased with age, and they report typical values for age-groups (two to six years old). The authors also compared 3D scanning and manual measurements and found high correlations in foot length and width measurements, moderate to high correlations in navicular height from the manual measurements and the arch volume from the 3D scanner measures ($r = 0.642, 0.712; p < .01$). They argue that the volume measures capture the height of the MLA as well as the width and length, giving a more valuable measure of this structure. Although they provided typical values for age-groups, and a 3D measure (arch volume) to characterize the MLA, the sample size was limited. Furthermore, although the arch volume is a 3D measure and can give us an idea of

the arch's 3D size, it cannot characterize the actual 3D surface or shape of the MLA and numerous different shapes can have the same volume.

In summary, while the above studies have used 3D scanners to capture children's feet, with the exception of Chang et al. (2012) the resulting foot measures were 2D foot anthropometric measures. Although the technology allowed for more accurate and reliable measurements, the outcome measures did not provide more information than outcome measures of manual methods such as calliper or tape measure. As discussed in section 2.2.5. 2D measures are limited in what they can tell us about the 3D multiplanar development of the paediatric foot. Furthermore, the technology employed in the reviewed studies is capable of providing higher resolution and 3D outcome measures and such outcome measures will be discussed in the next sections.

2.2.8. Quantifying 3D foot surface morphology

The previous section (2.2.7.) looked at studies that captured 2D measures (e.g., foot length, foot width) of the paediatric foot using manual or 3D scanning methods. As it was explained in chapter 2.2. 2D measures are limited in resolution as they only capture the distance between two points on the foot. This line of distance may include many different landmarks and shapes; hence the simple length or width measures have restricted resolution and are limited in what they can tell us about foot shape or changes in foot shape. In a different approach to achieve a higher resolution description of the foot, Price and Nester (2016) used the INESCOP (INESCOP, Elda, Spain) 3D laser scanner to measure cross-sections of the foot to describe the differences between healthy (N=23), overweight (N=23) and obese (N=23) adults' foot dimensions and morphology. They found that obese adults had significantly larger foot dimensions (ball of foot, heel, foot height and widths and circumferences) than healthy and overweight adults. The cross-sectional measures (width, height, and circumference at 31 points along the foot) identified further significant differences at locations where traditional measures did not. Obese adults had significantly wider feet for 23-53% of the foot length and for 37-40% of foot length the obese adults' feet were also wider than that of overweight adults. The height of obese adults' feet was also larger in the midfoot compared to the healthy adults. Considering the circumferences, for 40-47% of foot length the obese feet were larger than the overweight or healthy feet, while at 50-57% they were larger than the healthy feet only, but not the overweight. The authors argue that although the usual anatomical measures capture some of the differences, cross-sectional measures can provide a higher resolution and more sensitive comparison of populations, especially when anatomical landmarks may be occluded due to adiposity, oedema, or foot deformity. Although this study provided a higher resolution analysis of foot shape differences between groups and the cross-sectional approach may inform about the

global shape of the foot or cross-sections, they fail to describe local shape characteristics such as concavity or the curvature of the foot surface. Therefore, a cross-section with the same circumference, width or height may have a different shape at different points on the measurement path. To allow for such analysis, geometric methods have been applied. These approaches can quantify not only the size, but the shape of the object too.

One of these approaches is geometric morphometrics (GM). In this framework, three types of corresponding landmarks (anatomical and geometric) are identified on the surface of the scanned objects (Bookstein, 1992). In most studies the objects are then scaled, translated, and rotated to align, eliminating non-shape variations from the landmark configurations (Hennessy and Moss, 2001). This is called Generalized Procrustes Analysis (GPA) (Dryden and Mardia, 1998). After aligning the objects, Principal Component Analysis (PCA) is applied to the landmark coordinates to capture areas of the object that account for most of the shape variations. The resulting uncorrelated principal components then can be correlated with other variables of interest. Researchers have used GM and GPA to analyse 2D footprints of adults, to identify the association of foot shape with sex, stature and body mass in a healthy population (Domjanic et al., 2015) and the effects of body mass index, shoe size, frequency of wearing high heels, age, and sports activities on a small sample of young women's footprint shape (Domjanic et al., 2013). The same method was extended to 3D by Stanković et al. (2018) in a proof of concept study to analyse the effects of sex, age, shoe size, frequency of sports activity, Body Mass Index (BMI), foot asymmetry, and foot loading on the 3D shape of 62 healthy adults between the ages of 18 and 60 years. Multivariate linear regression and correlation were also applied to the factors and selected PCA modes to find areas of the foot that were affected by that particular factor (Stanković et al., 2018). Although this study represented a 3D approach to foot shape analysis, the interpretation of the principal shape

components and their association with the subject characteristics is somewhat subjective and qualitative. This method provides localization of the principal shape components, however the interpretation of the differences between shapes with lower and higher scores within the PC remains subjective. An example of this is the second principal component (PC) found in the study: low PC2 scores represented narrow ball width with touching toes and high PC2 scores represented wide ball width with spread out toes. Moreover, the variations captured by the PCs such as PC1, high arched or flat feet, PC3, ankle width, and girths, or PC6, mid-foot width could have been measured using less sophisticated 2D methods. The same applies to the interpretation of the effects of subject characteristics on foot shape. The Euclidean distance maps allow for the localization of differences between the upper and lower limits, but the differences in shape are not defined objectively or quantitatively; hence are open to subjective interpretations. Furthermore, findings, such that low BMI was associated with narrow ankle, heel, or mid-foot; or that mid-foot width, ball, waist, and instep girth increase with BMI do not require such sophisticated statistical approach and can be achieved by using 2D measures.

While the above methods yielded similar results to traditional 2D measurement methods, another geometric approach, differential geometry aimed at capturing the shape of the surface of the scanned object or body part. This approach will be discussed in the next section.

2.2.8.1. Differential geometry

The geometrical 3D shape of the foot surface may be captured by employing an approach that describes the foot by its particular shape at any given point on the surface. These geometric surface morphology characteristics may be related to how flat or curved the surface is; or if a protrusion or depression is present. While this method may not describe the foot's global shape or size, it can provide local 3D surface information crucial in describing foot morphology changes. Furthermore, this approach allows for a more relevant and accurate representation of the foot surface shape with higher anatomical resolution, leading to a more applicable foot development description. In turn, this method allows for more appropriate shoe last design and higher accuracy in clinical decisions or treatment\surgical follow-up assessments. This approach is possible due to the high accuracy 3D surface data provided by 3D scanning, which allows the mathematical analysis of the surface using differential geometry, resulting in principal curvature (minimum and maximum) and Gaussian-curvature data for each surface point.

Gaussian-curvature is an invariant shape descriptor, meaning that it does not depend on the actual coordinate system or surface parameterization. On the other hand, principal curvature describes “*the rate at which the unit tangent changes directions as it moves along the curve*” (Liu et al., 2004, p. 226). The Gaussian-curvature and principal curvatures together can identify a range of geometric shapes: planar, parabolic, elliptic, or hyperbolic. While these would provide novel information about a surface, their interpretation and application are challenging. For this reason, the shape index was developed (Dorai and Jain, 1997, Koenderink and van Doorn, 1992) to describe more subtle changes in shape, to provide a continuous gradation between salient shapes and to compress all information into a single index. The shape index ranges from -1 to 1 (Figure 1.), and the opposing sides of zero

represent complementary types of shapes, e.g., -1 represents a shape of cup whereas 1 represents a shape of a cap (Koenderink and van Doorn, 1992, Dorai and Jain, 1997).

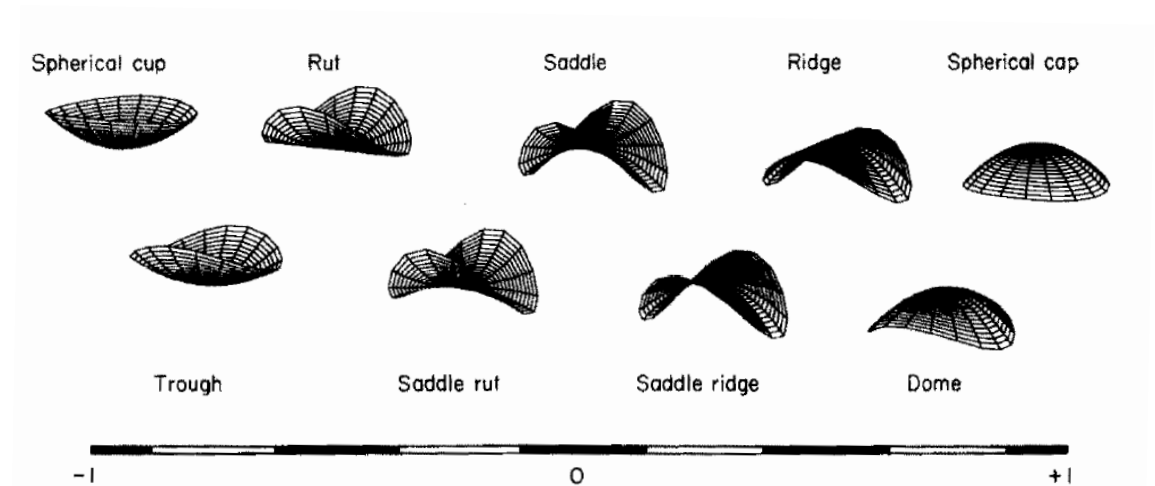


Figure 1.: Nine representative shapes on the shape-index scale with permission from Koenderink and van Doorn (1992)

In addition, Koenderink and van Doorn (1992) developed a measure called curvedness to complement the shape index and define the amount of the surface curvature at each point on the surface. Subsequently, the shape index is independent of scale, whereas curvedness is not. This characteristic provides two different types of 3D measurements, describing and quantifying foot shape changes. For a detailed calculation of both measures the reader is referred to Koenderink and van Doorn (1992) or Dorai and Jain (1997).

Gaussian-curvature and its derivatives (shape-index, curvedness) are frequently used in the literature to describe human body parts. They have been used to identify anatomical landmarks on the surface of the human back (Drerup and Hierholzer, 1985, Frobin and Hierholzer, 1982) or lower leg (Liu et al., 2005), to aid face description, measurement and recognition (Calignano and Vezzetti, 2011, Vezzetti and Marcolin, 2012, Vezzetti et al., 2014, Inan and Halici, 2012), to locate anatomical landmarks for precise measurements for specialized garment design (Markiewicz et al., 2017) or to automatically identify landmarks on CT scans of bones (Subburaj et al., 2009).

The only authors who applied curvature analysis to feet were Liu et al. (2004) who used shape-index to identify anatomical landmarks on the foot employing the FastSCAN laser scanner (Polhemus, Colchester, Vermont, USA). They argue that using the shape-index it is possible to capture the local shape and give a map (Figure 2.) of convex, concave, and hyperbolic areas and it will help in the automatic localization of anatomical landmarks. Subsequently, they located several landmarks on the lower leg and the foot including both malleoli, fibular head and the medial tibial condyle using the shape-index.



Figure 2.: 3D heat maps of Koenderink shape-index of the foot. Red: convex; green saddle-shaped; blue concave; and white: transition between these three different shapes. With permission from Liu et al. (2004).

While these 3D shape descriptors (shape-index, curvedness) can help in identifying anatomical landmarks, they can also describe the surface itself and identify differences in the shape of the surface between healthy and unhealthy groups or changes due to treatment or development. As the shape is represented by numbers for each point on the surface, these can be subject to statistical analysis hence they can be used to quantify the differences or

changes in the 3D morphology of the surface. Heat maps (Figure 2.) can be created using 3D shape descriptors which can help analyse 3D surface morphology changes at an individual level. However, the statistical analysis of large samples of this type of data requires an advanced method.

Recent advances in virtual surface and statistical analysis have seen the development of statistical parametric mapping (SPM) designed to characterise changes in 3D topological surfaces (such as a foot surface) and make statistical inferences of the whole surface. Using these methods, one can identify and localize changes in the developing foot shape in all three dimensions without being constrained to linear measurements. The SPM framework and associated theory were initially developed by Friston et al. (1994) to analyse functional brain imaging data incorporating the general linear model and Gaussian random field theory to analyse 2D or 3D data.

In a statistical parametric map, the value in each point of an image or surface expresses the evidence against the null hypothesis that there is no change in that point induced by the experiment (hence the values are distributed according to a probability density function such as the Student's T or F distributions). Statistical maps can be thought of as images or surfaces with change significance, instead of measurement magnitude. An alternative way to describe it is that they are designed to localise change for a given level of significance (Friston et al., 1991). Although SPM was developed to allow high resolution and spatially extended analysis in brain imaging research (Worsley et al., 1996, Worsley et al., 1992, Friston, 1997, Friston et al., 1991), it was also adapted to pedobarographic research (Pataky and Goulermas, 2008). In plantar pressure analysis, SPM as an alternative to masking (dividing the foot surface into smaller areas when considering foot pressure), allows the localization of differences in foot pressure data at a pixel (the smallest level of pressure measurement) level

(Pataky et al., 2008, Pataky and Goulermas, 2008). As statistical maps represent images of change significance rather than change magnitude, this method allows the comparison of regions or pixels based on relative significance (Friston et al., 1991). The application of SPM is valid on pedobarographic data (Phethean et al., 2014). It can also be valid on 3D shape data because there are (1) constant intra-subject geometry, (2) varying inter-subject geometry, (3) arbitrary postures and (4) pixel (vertex) intensity changes that represent organ function, in this case, morphological organ development (Pataky and Goulermas, 2008). This statistical approach will be discussed in more detail in section 5.2.

2.2.9. Summary

This section of the literature review looked at 3D scanning of the foot. First, a description of 3D scanning methods was conducted, followed by the review of the literature on the reliability of 3D foot scanning. Studies using step-in 3D scanners to measure the paediatric foot were then critically evaluated to give an overview of the role and limitations of the 2D measures used in these studies. The next section considered methods that attempted to measure the foot employing higher resolution or geometric approaches. Differential geometry was then evaluated, suggesting statistical parametric mapping as a statistical approach to present an alternative solution to 3D surface morphology analysis. The findings of this literature review chapter exposed the need for further investigation of paediatric foot morphology development using 3D scanning technology.

Firstly, the reliability of using hand-held 3D scanning in a paediatric population needs to be established. Although the studies using step-in scanners assessed their reliability and validity, they were conducted mostly in adults, and the reliability of step-in scanners cannot be transferred to hand-held scanners. The existing reliability studies using hand-held scanners looked at other body parts or objects; hence their result cannot be generalized to children's feet.

Secondly, although several studies used step-in 3D scanners, the reported results – with one exception (Chang et al., 2012) - were 2D measures. Even though the technology allows for a higher resolution 3D shape analysis, the existing literature only uses it to capture the foot's length, width, and area parameters more accurately and effectively than manual or other techniques. Although the geometric morphometric studies reviewed provided higher resolution results, they were still restricted to two dimensions and subjective interpretations when quantifying foot shape. Conversely, differential geometry can quantify the foot's 3D

surface morphology from a 3D scan at every vertex, providing a high resolution, relevant and accurate dataset. The high-resolution data derived from 3D scans and differential geometry is best analysed using a continuous, spatially extended statistical approach, namely statistical parametric mapping, which allows vertex level analysis of 3D shape descriptors (i.e., curvedness, shape-index) data.

In conclusion, this literature review chapter demonstrates that there have been several attempts to characterize foot shape development or foot shape of different populations using step-in 3D scanning reporting 2D measures. It has also been established, that the reliability of hand-held 3D foot scanning has not been examined in children, and the measures extracted from the 3D scans are still low in resolution and dimensionality.

2.3. Summary of the literature review

The period between 2 and 7 years of age is a time for significant foot shape, size, and functional changes. Independent gait places load on all tissues, changing the musculoskeletal structures and functions. As walking develops, the foot adapts to create a stable and flexible base for multiple functions. This adaptation will become visible in the changing shape and size of the paediatric foot, which can be measured, to capture its developmental trajectory. Accordingly, robust data is needed to understand the foot's typical trajectory throughout the complex and variable stages of growth and development. This data can provide reference values that characterise the development of the foot shape and can be used in research and applied environments. Moreover, understanding more about the morphological changes throughout childhood is essential to advance the prevailing arguments about the typical development of children's feet (Uden et al., 2017) and inform the development of appropriate clinical and footwear last measures. However, as mentioned in section 2.2., although there have been attempts to describe the changes in foot shape and size in childhood, existing data comprises a limited number of 2D foot anthropometric measures during this critical stage of foot development. Consequently, there is no detailed, high resolution and up to date information on how the paediatric 2D foot anthropometry and 3D foot surface morphology develops. This literature review demonstrates that the growth and development of the paediatric foot throughout childhood is poorly understood. Therefore, there is a clear need to revisit our understanding of how the foot develops to inform theory underpinning clinical practice. Additionally, the literature review has shown that the manual and other traditional foot measurements methods used to capture the existing foot parameters are also limited in resolution and accuracy. In light of these limitations, there is a potential for greater utilisation of 3D scanning technology and 3D surface morphology information in

foot development research and applied environments such as footwear industry and clinical practice. The findings of the literature review also reiterate previous suggestions from Telfer and Woodburn (2010) promoting the use of 3D scanners. Although step-in 3D scanners provide a reliable and valid solution to capture children's foot shape and size, they are expensive and not mobile. On the other hand, hand-held scanners have been used in different research fields, but their reliability has not been addressed in children's foot measurement. In this context, there are also various methodological challenges to consider, and as a consequence, further work is needed to understand the reliability of the measurement of children's feet with a hand-held 3D scanner.

As highlighted above, capturing 3D shape is essential to advance the prevailing arguments about the typical development of children's feet, while the relevance of 3D shape data in research and the clinical assessment of the foot shape has already been highlighted by Stanković et al. (2018) and Nelson et al. (2017). Furthermore, section 2.2.8.1. has shown that differential geometry (3D shape descriptors: shape-index and curvedness) offers an analytical and high-resolution approach to characterize the 3D foot surface. Accordingly, it may allow new insights into the changes in foot morphology and structure during development. This approach provides clinicians with a clear morphological map of the foot, which could be considered a translation of basic research into applicable measures that can be interpreted in an applied setting. The present thesis will establish the application of this method to the assessment of paediatric foot development constituting a foundation for understanding more about the morphological development of the foot, improving diagnosis techniques, tracking changes over time, orthotics, and footwear last design, or understanding disease process and its impact on foot development.

Chapter 3

3. Measuring the paediatric foot using a hand-held 3D scanner

Section 2.2.6. of the literature review outlined the studies that examined the reliability of 3D foot scanning by laser scanners and highlighted the need to assess the reliability of using hand-held 3D foot scanning in children. For this reason and to inform the main study methods, a pilot study was carried out, which was divided into two phases.

First, to quantify the trajectory of foot development in children using a hand-held 3D scanner, the reliability of the methods needed to be tested. Previous studies discussed in section 2.2.6. of the literature review, have quantified the reliability of step-in scanners in measuring children's (RMSE \leq 2mm for length and width measures (Mauch et al., 2008)) or adults' feet (MAD \leq 11.9mm (Lee et al., 2014) and SEM \leq 2.7mm (De Mits et al., 2010)). These results have shown that the step-in 3D scanners were equally or more reliable to capture foot size than traditional methods (e.g., ink or digital footprint). The literature review also highlighted that hand-held scanning is reliable and valid in capturing objects and different body parts except for feet, which have not been examined yet. Unfortunately, the reliability results found in hand-held scanning studies were specific to the scanner, sample, object, or body part, and could not be used to demonstrate reliability in the current thesis. In

addition, the adipose tissue typically present in the foot of the younger age-groups makes palpating or detecting anatomical landmarks more challenging. Furthermore, these age-groups are also more prone to movement during scanning than adults. As hand-held scanning requires longer time than step-in scanners, movement during scanning can cause problems. Automated foot measurement software has been developed (Foot3D) to avoid human error in identifying anatomical landmarks but have not been tested in young children. As a consequence, further work was needed to establish the reliability of anthropometric measurement in children's feet using hand-held scanning.

While 2D measurements have been examined for reliability from 3D scans using step-in scanners, 3D shape descriptors have only been investigated in their ability to reliably identify features on a surface (Ho and Gibbins, 2009), but not their repeatability. Although these measures do not depend on anatomical landmark locations, their reliability still had to be established as other sources of variability can affect them e.g. the exact posture of the foot or scanning movement pattern differences. Due to the lack of reliability data on shape-descriptors in the literature, carrying out such study was novel and necessary to inform the main study methods.

For these reasons, phase (a) of the pilot study was designed to test the reliability of 2D anthropometric and 3D surface morphology measures derived from a hand-held 3D scanner in children. Part of this chapter was presented at the 10th International Conference and Exhibition on 3D Body Scanning and Processing Technologies (Varga et al., 2019)

The findings from the literature review section 2.1.4. revealed that existing 2D foot measures fall short of optimally quantifying the 3D shape development in the paediatric foot. Although there have been attempts to investigate these changes (mostly in adulthood), most studies

used a combination of 2D, low resolution and inaccurate measures. While these results provided further information on foot morphology, they failed to describe and quantify the actual 3D shape of the paediatric foot surface. In section 2.3.4.2. of the literature review, an alternative method was introduced: differential geometry, which provides 3D shape descriptors to quantify 3D surface morphology. As mentioned in the literature review, although there was one study (Liu et al., 2004) looking at 3D shape descriptors to locate anatomical landmarks on adult feet, these measures have not been used to describe or quantify developmental shape changes in children's feet. To apply these methods in the main study, their ability to quantify and describe such changes needed to be tested. This was a novel, and necessary step before the main study could be completed.

For these reasons, phase (b) of the pilot study was designed to establish whether 3D shape descriptors can describe and quantify the surface morphology changes occurring during foot development in children. This section of the thesis was published in Varga et al. (2020).

3.1. Aims

The aim of this chapter was to establish protocols and 3D surface morphology measures for characterizing the 2D and 3D foot development trajectory. This chapter will underpin the methods used in the following chapters and offer novel insights into measuring the paediatric 3D foot surface morphology. The objectives of this chapter were

in phase (a) to:

- examine the reliability of capturing 2D measures of the foot in children using a hand-held scanner, and to
- examine the reliability of capturing 3D shape descriptors of the foot in children using a hand-held scanner
- examine the validity of capturing 2D measures through comparison with existing literature data

and in phase (b) to

- investigate whether 3D shape descriptors can help to characterise and to quantify differences in 3D foot surface morphology between age groups in a small cohort of children.

3.2. Methods

3.2.1. Ethical approval

The investigation was approved by the Life, Health and Physical Sciences College Research Ethics Committee at the University of Brighton. Written informed consent was obtained from all parents on behalf of their child.

3.2.2. Participants

The two phases of the pilot study used the same participants. Fifteen children aged between two and seven years of age from three sites (Willingdon Primary School, Happyjacks Soft Play Centre, and Brighton Sports Centre) were recruited in Eastbourne. Five children were recruited from each of the three age-groups: Group 1: two years of age (3 males and 2 females), Group 2: five years of age (3 females and 2 males) and Group 3: seven years of age (3 females and 2 males). This enabled the capturing of data across the age-range determined for the thesis. The exclusion criteria were skin disorders affecting the foot such as eczema, psoriasis, or any skin abrasions; and suffering from epilepsy or light-sensitive conditions.

3.2.3. Scanner choice

At the outset of the study, it was agreed that a critical review of existing hand-held scanning technologies was required to choose the most appropriate technology for this study. Ten hand-held scanners were identified and refined to five possible choices shown in Table 9.

The technical data included were chosen based on the requirements of the study:

- Resolution: due to the small size of the paediatric foot and the need to carry out high resolution statistics.
- Accuracy: higher accuracy helps capturing the actual morphology of the foot.
- Data acquisition: fast data acquisition is required due to the age-group (not being able to stand still for long) of the study.
- Peer reviewed papers: The breadth of studies help to gauge how well researchers accept the technology as a valid and reliable tool in different fields and considering different sized objects, and body parts.
- Price: the research budget was restricted to between £10,000-£15,000.

Table 9.: The five selected 3D scanners and corresponding technical details. NA: not available.

Scanner (company)	Resolution	Accuracy	Data acquisition speed	Peer reviewed papers	price
zSnapper (ViALUX)	NA	<0.3mm	NA	1	~£19,000
Fastscan II. (Polhemus, Canada, ARANZ Medical Limited)	0.01mm	0.18mm RMSE	NA	>10	~£17,000
EinScan- Pro (Shining 3D)	0.2-2mm	0.1mm	1,500,000 points/sec ond	3	~£11,000
BodyScan (TechMed 3D, Canada)	1mm	0.5mm	550,000 points/sec ond	0	~£9000
Artec Eva (Artec 3D)	0.5mm	0.1mm	2mln points/sec ond	>10	~£14,000

Due to their prices, the zSnapper and Fastscan II. was excluded. Furthermore, the BodyScan scanner was also excluded as its data acquisition speed, accuracy, and resolution (data acquisition speed: 550,000 points/second, accuracy: 0.5mm, resolution: 1mm), were below those of Artec Eva (data acquisition speed: 2mln points/second, accuracy: 0.1mm, resolution: 0.5mm) and EinScan-Pro (EinScan-Pro data acquisition speed: 1.5mln points/second, accuracy: 0.2-2mm, resolution: 0.1mm). While EinScan (Macron et al., 2018) had similar capabilities to Artec Eva, the breadth of studies on body measurements where Artec Eva was used (Modabber et al., 2016, Stewart et al., 2016, Stewart et al., 2015, Ozsoy

et al., 2015, Peters et al., 2016, Sawh-Martinez and Steinbacher, 2018, Yamamoto et al., 2016, Yan and Shah, 2017, Coltman et al., 2017, Ganapathi and Prakash, 2018) was much larger and Artec Eva had higher data acquisition speed. Furthermore, to assess its validity, (Seminati et al., 2017, Koban et al., 2020) compared the Artec Eva to a high precision laser scanner. Investigating residual limb models and faces of volunteers, it was found that the RMSE between the scanners was below 1mm, suggesting high validity of the Artec Eva scanner, which further supported the decision to choose Artec Eva.

Based on this information, the Artec Eva hand-held scanner was chosen. Manufacturers of the Artec Eva scanner (Artec 3D) report an accuracy of ± 0.1 mm, a resolution of 0.5mm and a data acquisition speed of 2 million points/second at a distance of 400mm to 1000mm. Stewart et al. (2015) report a percentage technical error of measurement for this scanner between 0.47 and 0.63 for intra-operator error and between 0.75 and 0.82 for inter-operator error for upper body size measurements. The scanned object is illuminated with patterns of visible light stripes by the scanner to acquire the 3D data, and three cameras capture these patterns. One of the cameras is located in the scanner's centre to obtain texture information and is surrounded by flash LEDs. The scanner takes up to 16 3D pictures per second, and these are used in the Artec Studio software to create the 3D surface of the object. The scanner uses structured light and causes no damage/irritation to the skin and is safe to use on children of any age.

3.2.4. Data capture

Both phases of the pilot study used the same data capture methods. The scanning of children's feet was undertaken at the three locations, using the Artec Eva scanner (Figure 3.).

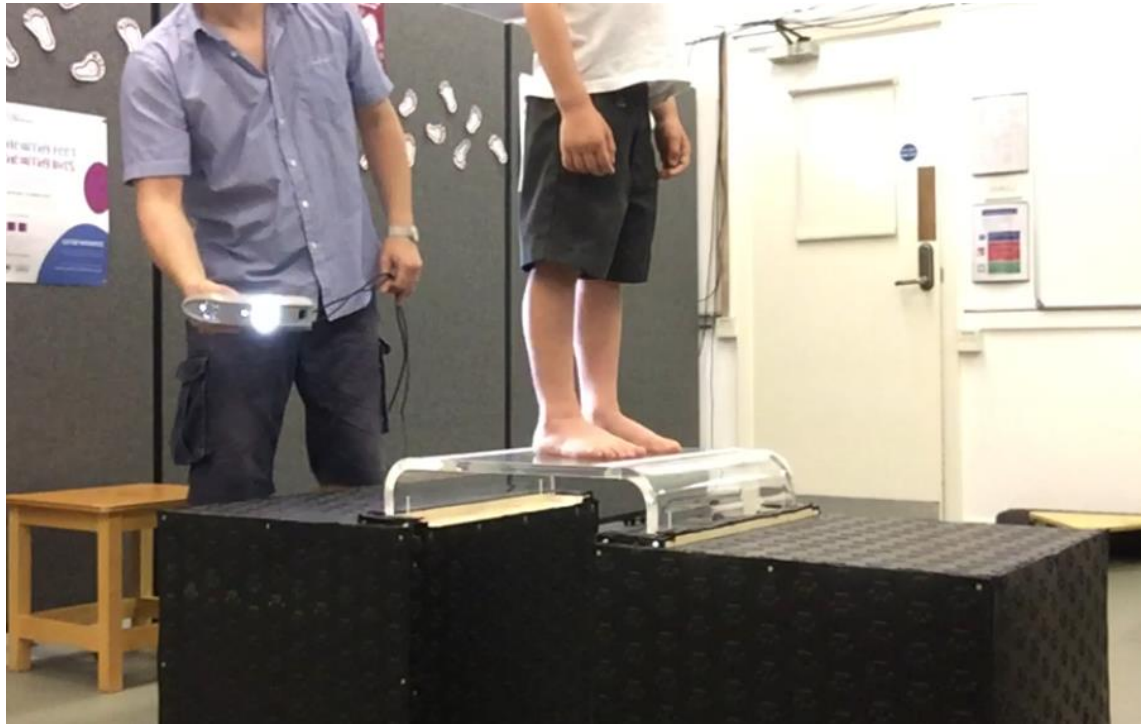


Figure 3.: Example of a hand-held scanner being used on a five-year-old participant.

Each participant's feet were scanned three times within the same session, although in phase (b) only the first scans were analysed. Furthermore, although both feet were scanned, only the right feet were considered for analysis to ensure statistical independence within the samples (Menz, 2004). The literature has also shown that there are no statistical differences between the right and left foot (Delgado-Abellán et al., 2014). A see-through Perspex platform (certified up to 150kg bodyweight) and a custom-built stand of 550mm height were used to allow the scanning of the plantar aspect. Two strips of white tapes were attached to the top side of the platform, one anterior and one posterior to the foot position to aid post-processing (alignment: see section 2.3.2.3.) of the scans (Figure 4.).

The scanning of the feet was conducted in the following manner. The child sat down and was asked to remove their shoes and socks. Following this, the parent or teacher was asked to clean the child's feet with a skin disinfecting wipe. The child was then asked to step up onto the platform (manual support was provided when needed by holding their hands), and to find a comfortable position for both feet on the platform. The child was asked to stand with their feet pointing anteriorly. All children were explained what the experimenter was going to do before scanning started.

Children were encouraged to look forward, level with their eyes at a screen, where age appropriate cartoons were shown. The management of the youngest children during scanning sometimes required the participant's parent to hold the child's hand. Furthermore, children were asked to keep their feet and toes as still as possible. At times, this was only possible by instructing the child to watch their feet to see if they are still. A further measure to keep the child still during scanning, was to constantly explain to them what the experimenter was doing and what they needed to do (e.g., do not follow the experimenter with their head and eyes as he is going around them while scanning).

Using the methods outline above, three separate sub-scans were performed to capture the whole foot, including the plantar aspect. (1) scanning of the dorsal aspect, with the scanner, scanning around both feet in an anticlockwise manner, starting and finishing at the toes, (2-3) scanning of the plantar aspect from either side of the platform (scanning stopped between sides), with the scanner moved from facing the edge of the platform downwards in an arch, until it faced the plantar aspect under the platform. According to the manufacturer's guidelines, all scanning (where possible) was performed from a distance of 0.4-0.6 meters. The scanning distance was displayed and checked during scanning on the Artec Studio software on the laptop screen. Scanning times were between 80 and 120 seconds.

During longer 3D scanning in young children, such as in the current study, it is recommended to have a screen or a parent\teacher in front of the participant, at eye level to ensure consistent posture. Furthermore, it is also recommended that the experimenter continuously communicates with the participant to keep them calm and to encourage stillness of the foot and the whole body. Some children may be extremely afraid of the scanner (noisy and flashing). This can be managed by the experimenter scanning their own hand prior to foot scanning and showing the outcome on the screen before data capture. This may help reduce the anxiety of the participant. In the case of a group of very young children, it may be beneficial to perform this at the beginning of data collection in front of the whole group by scanning a doll or a toy on the platform.

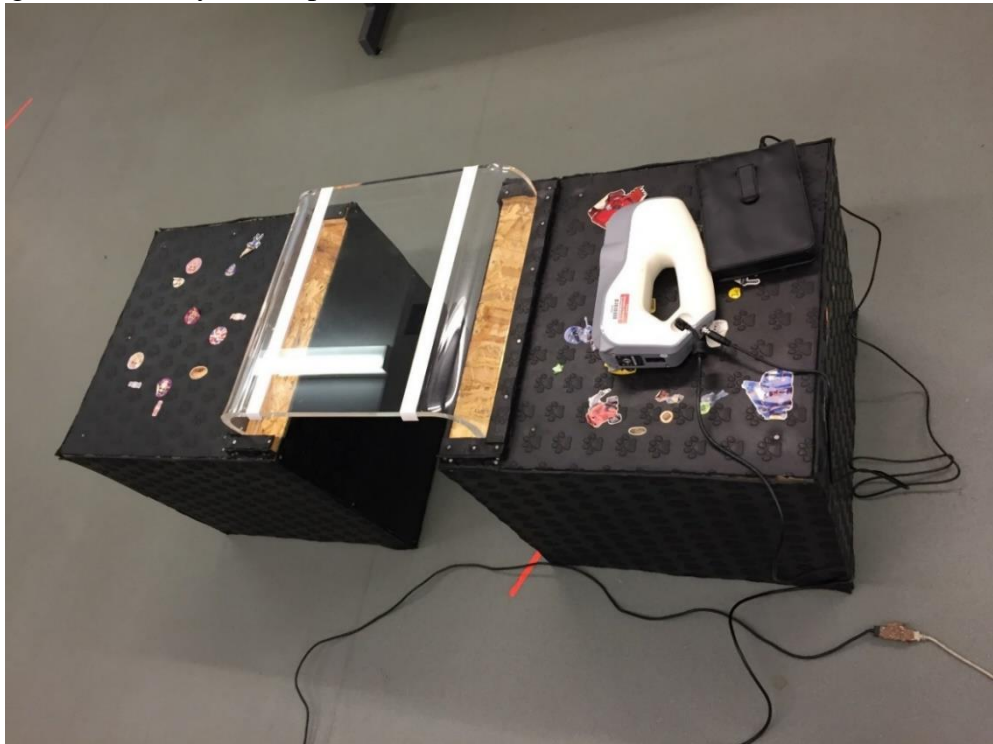


Figure 4.: The Perspex platform on the custom-built stand with the Artec Eva scanner and battery pack.

3.2.5. Post-processing

Artec Studio software (Artec Studio 12, Artec 3D) was utilized to post-process the scans and create a full 3D model of each foot. Post-scanning processing was performed, in phase (a) on the 3*15 raw scans (each consisting of three sub-scans) and in phase (b) on the 1*15 raw scans (each consisting of three sub-scans) collected during the field scanning in order to allow the extraction of 2D and 3D measurements. Post-processing included the following steps (Figure 5.) following manufacturers guidelines.

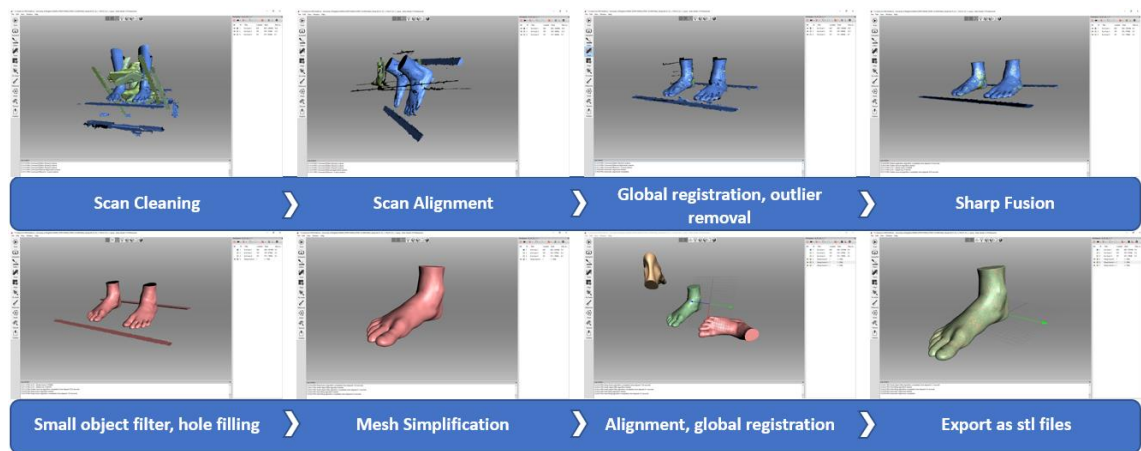


Figure 5.: Post-processing steps in Artec Studio 12.

1. **Scan cleaning (phase (a) and phase (b)):** The sub-scans included body parts and clothing above ankle level which were highly likely to move during scanning and parts of the platform, that were unnecessary to be processed. For this reason, before further processing, these parts of the three sub-scans were manually removed. The only features outside of the two feet, remaining in the sub-scans were the two lines (white tapes) on the platform. The cleaning and the two lines also improved the chances of automatic alignment in the next step.
2. **Data Alignment (phase (a) and phase (b)):** As each foot scan consisted of three sub-scans, these had to be aligned in Artec Studio 12 professional software. This alignment was attempted to be performed automatically, and if this failed manual

alignment was performed. The two lines at the posterior and anterior end of the feet were used as guides to aid manual alignment in each plane. This alignment is an initial approximation of the final registration to improve the chances of the next step to converge on the best possible registration of sub-scans.

3. **Global registration (phase (a) and phase (b)):** An automatic algorithmic registration of the three sub-scans was then performed following manufacturers guidelines in the software to match them in all three dimensions, using sub-scan geometry and/or texture information. The software provides information on registration quality for each sub-scan, and these were checked. The registration quality was aimed to be 0.5 or below based on manufacturers guidelines.
4. **Outlier removal/Noise elimination (phase (a) and phase (b)):** As the original sub-scans included noise which consisted of extra points outside of the feet, these had to be erased. This was done using the outlier removal option in Artec Studio 12 (outliers were defined as points outside of two standard deviations distance from the mean). If global registration was not satisfactory in the previous step, it was repeated after this noise elimination process.
5. **Sharp fusion (phase (a) and phase (b)):** Once sub-scans were cleaned and registered, the three sub-scans were fused into one 3D model using the sharp fusion option to allow precise measurements based on the manufacturers guidelines.
6. **Small object filter & hole filling (phase (a) and phase (b)):** The fused 3D model still contained holes (e.g., the top of the scan where the ankle joins the leg) and noise (extra points or fused parts outside of the foot model), which were repaired using the small object filter and hole filling options. The repaired model still

included both feet and the two lines, which were removed in this step, resulting in a model of the right foot only.

7. **Mesh simplification (phase (a) and phase (b)):** Once all three scans from the same participant have been processed using the above steps, the three models of the same foot were simplified (the number of vertices reduced) to the lowest number of vertices of the three models. This was to allow vertex-to-vertex comparison and the calculation of mesh deviations. Vertex numbers varied between 36000-37800 in the two-year-old groups, between 42100-53000 in the five-year-old group and between 50800-76200 in the seven-year-old group. The difference in the number of vertices between age groups is due to the size of the feet: larger feet had more vertices to have the same point density.
8. **Model alignment and global registration (phase (a) only):** The three models of the same foot were automatically aligned and then globally registered. All models were translated and rotated to approximately fit into the same coordinate system to reduce the amount of coding needed in MATLAB. The X-axis was set as the sagittal axis of the foot, the Y-axis represented the frontal axis of the foot, and the Z-axis was the vertical axis of the foot. The origin was placed on the most posterior and inferior point of the centre of the heel manually. Finally, the three models of the same foot for each participant were cut above the medial malleolus while being overlaid, to ensure they were cut at the same level, so both the medial and lateral ankle was still part of the models.
9. **Export as stl files (phase (a) and phase (b)):** The models were exported as stereolithography (stl) files into MATLAB and Foot 3D.

In phase (b) data processing was identical to that in phase (a), but only a single right foot model was created and exported as stl file from the first scan of each participant.

3.2.6. 2D foot anthropometric measures

In phase (a) the measurement of anthropometric parameters (Table 10.) was performed automatically in Foot3D software (INESCOP, Spain). The automated marker recognition and placement were checked and manually adjusted when needed.

Table 10.: The description and definition of the 2D anthropometric foot measures calculated by Foot3D.

Linear measure	Description
Foot length	Distance between the most posterior point of the heel and the end of the longest toe, projected onto the longitudinal axes
Forefoot Width	The distance across the widest points of the forefoot.
Metatarsal head one length	Distance between the rearmost point of the foot and the first metatarsal head.
Metatarsal head five length	Distance between the rearmost point of the foot and the fifth metatarsal head.
Ball width	Distance between points metatarsal head one and five.
Ball height	Height of ballpoint.
Rear-foot width	Distance obtained between the outermost points to intersect a plane perpendicular to the foot axis away 15 % of foot length and 1 cm high.
Instep height	Distance between the point of the instep and the ground plane.
Medial malleolus height	The distance between the supporting surface and the most medial point of the medial malleolus.
Lateral malleolus height	The distance between the supporting surface and the most lateral point of the lateral malleolus.
Ankle width	The distance between the most medial point of the medial malleolus and the most lateral point of the lateral malleolus.

3.2.7. 3D shape descriptors

In phase (a) the three models of the same foot had to be registered (transformed, so the three models optimally overlap) to extract reliability data. As the three models represent the same foot in approximately the same posture, these models' shape and size must remain the same throughout the registration process. MATLAB offers three types of point cloud registration: iterative closest point (ICP, MATLAB function: `pcregistericp`), the coherent point drift (CPD, MATLAB function: `pcregistercpd`) algorithm, and the normal-distributions transform (NDT MATLAB function: `pcregisterndt`). All three methods allow for rigid transformation which means that the shape and size of the registered clouds are preserved: the point clouds can undergo translations (“sliding” the point clouds along any of the three axes), rotations (“turning” the point clouds around any of the three axes), or both, and the same transformation is applied to all points. The NDT has a better performance with point clouds with different resolutions and densities (Magnusson, 2009), which is not the case in this pilot study, considering that the three models are of the same foot using the same scanner and scanning method. For these reasons, the NDT method was not used. Studies that compared the ICP and CPD methods (Cutter et al., 2016, Myronenko and Song, 2010) concluded that the CPD method is slower, and performs better when noise, missing points and outliers are present in the to be transformed point cloud. As the three foot models have been thoroughly post-processed in Artec Studio 12, they did not include noise, missing points, or outliers, and for these reasons, the ICP method was adopted. The rigid, iterative closest point (ICP) algorithm-based registration of point clouds (Besl and McKay, 1992, Chen and Medioni, 1992) is designed to find a 3D rigid body transformation in order to match and overlap 3D coordinates of the point clouds that might have been captured at different angles (He et al., 2017). This local registration method relies on an initial transformation estimate achieved in Artec Studio by performing model alignment and global registration of the three models.

After the initial transformations, the ICP algorithm will iterate by alternating in (1) finding the closest vertex in one point cloud for every vertex in the other point cloud; and (2) finding the best rigid transformation by solving the least-squares problem (Besl and McKay, 1992). As such, it works best if the initial pose of one point cloud is sufficiently close to the other. As He et al. (2017, p. 1) describes:

“In this method, the transformation parameters of two point sets are calculated through the relationship between the corresponding matching points of two point sets to satisfy the given convergence precision, and finally the translation and rotation parameters between the two points are obtained to complete the registration process.”

After registering the three models as point-clouds, a triangulation was performed to achieve higher accuracy in identifying nearest neighbours; and to be able to calculate curvature, which is needed to calculate 3D shape descriptors. The triangulation uses the 3D coordinates of the vertices and a connectivity list that defines which vertices form a triangle to create a triangulated surface. This information was available in the stl file imported from Artec Studio 12. Triangulation was an important step, as nearest neighbour calculations on point clouds could provide false results due to not having a defined surface through interconnected vertices. In a triangulation, nearest neighbour search is performed using the extra information from the connectivity list of vertices which creates so-called faces defined by the three vertices they connect. In phase (b), only one model was used from each participant for this processing. Principal (minimum and maximum) and Gaussian-curvature were calculated using a custom-written, open-source script by Gabriel Peyre (Peyre, 2007), based on Alliez et al. (2003) and Alliez et al. (2003). In both phases of the study, shape-index and curvedness were calculated for each vertex on the foot models, based on the equation used

in Koenderink and van Doorn (1992) in a custom-written code. Shape-index ranges from -1 to 1, with nine different shapes defined (Table 11.).

Table 11.: Shape-index ranges for each shape for 3D shape descriptors adapted from Koenderink and van Doorn (1992)

Shape	Shape-index range
Spherical cup	-1 to -0.875
Trough	-0.875 to -0.625
Rut	-0.625 to -0.375
Saddle rut	-0.375 to -0.125
Saddle	-0.125 to 0.125
Saddle ridge	0.125 to 0.375
Ridge	0.375 to 0.625
Dome	0.625 to 0.875
Spherical cap	0.875 to 1

3.2.8. Statistical analysis

3.2.8.1. Phase (a)

2D anthropometric measures

Root mean square error (RMSE) (O'Meara et al., 2010) was calculated to provide information on the absolute difference between the three repeated measures. The sum of squares was determined (Equation 1.) from the square root of the difference between the measurement (x_i) and the mean of three measurements (\bar{x}) to calculate RMSE.

Equation 1.: Equation for RMSE

$$RMSE = \sqrt{\frac{1}{n} \sum_{i=1}^n (x_i - \bar{x})^2}$$

Root mean square error is used to quantify the variance in the difference between observations and a model; in this case, the three measurements' mean. RMSE is particularly useful in this study as larger deviations (due to the squaring of the differences) from the model (mean) should be punished with more weight. The only RMSE findings of 2D foot measures reliability in children are from Mauch et al. (2008) and Mauch et al. (2009), who reported RMSE for distance measures between 0.5 and 2mm. This will be used in phase (a) as a benchmark, to aid decision making when considering 2D measure reliability from the current method. The validity of the methods will be assessed through the comparison of the current results with the existing literature, hence so statistics are employed.

3D shape descriptors

Vertex deviations (the distances between corresponding vertices of two foot models) were calculated using Euclidean-distances between the three models of the same foot for all participants to evaluate the reliability of the scanning method to replicate the same 3D foot

model. Corresponding vertices were identified using a built-in MATLAB function which finds nearest neighbours in a triangulation (a foot model) to a query point (in this case a vertex in another triangulation (model) of the same foot) based on Euclidean-distance. Cumulative statistics were calculated to identify the percentage of vertex deviations under 0.5mm and 1mm, which quantifies agreement between 3D models (Wan et al., 2017, Psikuta et al., 2015). The distances calculated between two pairs of models were averaged to have one set of data for each participant. The RMSE for shape-index and curvedness at the corresponding vertices of the three foot scans of the same foot was calculated (O'Meara et al., 2010) using the same equation as for the 2D measures, to quantify the absolute reliability of measuring 3D shape,

3.2.8.2. Phase (b)

Four foot surfaces were extracted from each foot model to compare the age groups: plantar, dorsal, medial, and lateral. These surfaces were defined in a custom-written MATLAB script using the orientation of normal vectors of vertices. The range of normal vector orientation for each surface and age group was chosen manually and applied to each foot model in a loop manner, but all extracted surfaces were checked manually and corrected when necessary. The distribution of shape-index and curvedness of each surface were used to compare the surfaces between age-groups. Relative probability histograms were created to visualize the differences between age-groups distributions in both shape-index and curvedness for each foot surface. Relative probability histograms were chosen to avoid the differences in the number of vertices between age-groups influencing the results. When considering the shape-index, each bar of the relative probability histogram represented the shape defined for that range in Table 10. Shapes below zero were considered concave, and shapes over zero were considered convex. Visual representation of example curvedness and

shape-index heat maps of foot surfaces from one representative participant from each of the three age-groups was also included. The heat maps show the vertices in the foot model with their colour representing either curvedness or shape-index values provided on the colour bar. The heat maps presented also contain the rest of the foot in black for reference purposes. When comparing the plantar aspects - because flat is not defined with a specific shape-index value - only the vertices with a curvedness value higher than 0.0015 were considered in the histograms and heat maps of the shape-index data.

3.3. Phase (a) results

3.3.1. Reliability of the 2D foot anthropometric measures

The magnitude of all linear measures increased with age as expected (Figure 6.), with the length measures increasing at a higher rate than any other measures.

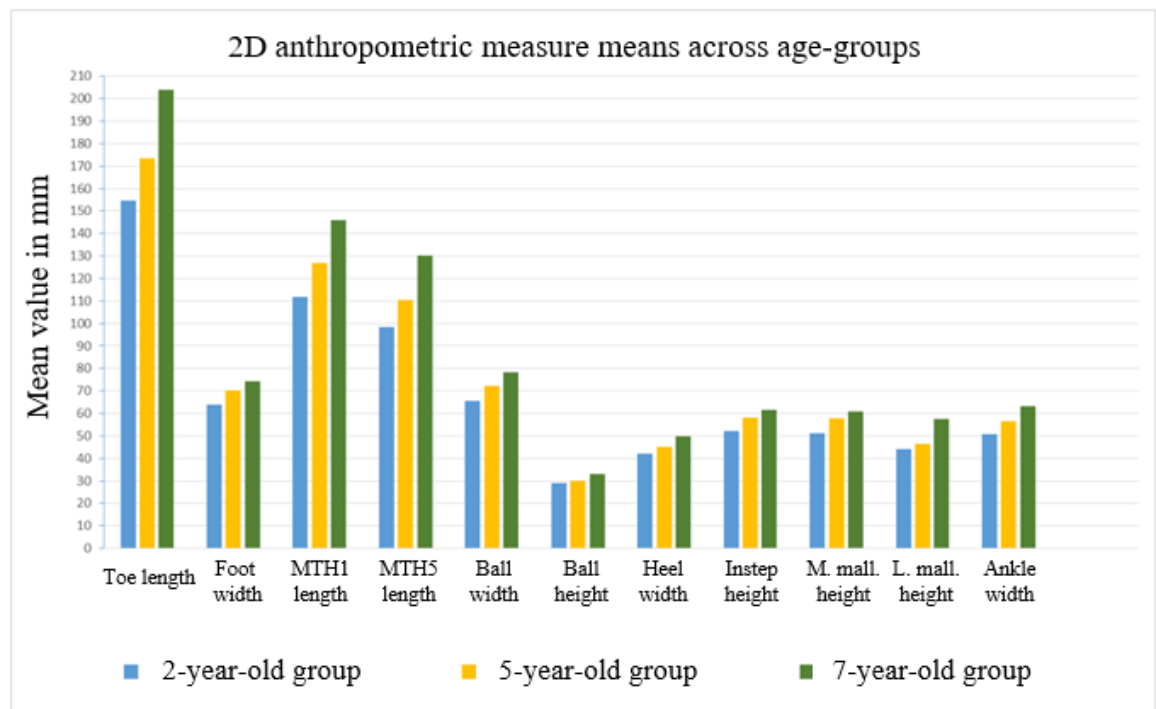


Figure 6.: Mean values for linear measures across age-groups (MTH1: metatarsal head 1, MTH5: metatarsal head 5, M. mall.: medial malleolus, L. mall.: lateral malleolus).

Data for all linear measures per Group and overall are presented in Table 12. The average absolute RMSE for all measures across groups did not exceed 2 mm (mean=1.14 mm, SD = 0.2), and the maximum RMSE was found in metatarsal head one (MTH1) length measurement: 3.73 mm in Group 1. Metatarsal head lengths were the only measures to exceed the RMSE of 2mm defined based on Mauch et al. (2009), Mauch et al. (2008).

Table 12.: Mean and root mean square error (RMSE) for each linear measure by group. Group 1: two years old, Group 2: five years old, Group 3: seven years old. ²

Variables	Group 1		Group 2		Group 3		Overall
	Mean (SD) (mm)	RMSE (mm)	Mean (SD) (mm)	RMSE (mm)	Mean (SD) (mm)	RMSE (mm)	Mean (SD) (mm)
Foot length	154.63 (4.82)	0.9	173.48 (5.05)	0.64	203.9 (17.03)	0.58	0.71 (0.17)
Foot Width	63.97 (3.43)	0.5	70.13 (5.18)	0.47	74.21 (8.86)	0.49	0.49 (0.02)
MTH1 length	111.72 (5.85)	3.73	126.93 (3.52)	1.13	145.88 (16.32)	3.29	2.72 (1.39)
MTH5 length	98.36 (7.61)	2.47	110.51 (2.42)	1.91	130.34 (15.49)	1.84	2.07 (0.35)
Ball width	65.66 (3.74)	0.69	72.12 (5.22)	0.59	78.17 (8.67)	1.4	0.89 (0.44)
Ball height	28.89 (1.31)	1.15	29.92 (1.66)	0.78	32.91 (4.85)	0.71	0.88 (0.24)
Rear-foot width	42.16 (1.46)	0.48	44.99 (3.12)	0.46	49.84 (3.77)	0.53	0.49 (0.04)
Instep height	52.17 (1.02)	1.39	58.29 (1.62)	0.68	61.4 (3.73)	0.76	0.94 (0.39)
M. mall. height	51.02 (1.16)	0.72	57.95 (2.29)	1.88	60.73 (6.05)	1.59	1.40 (0.60)
L. mall. height	43.99 (2.29)	1.79	46.34 (2.30)	0.95	57.34 (7.86)	0.98	1.24 (0.48)
Ankle width	50.84 (1.16)	0.72	56.46 (1.88)	0.7	63.33 (8.66)	0.69	0.70 (0.02)
MEAN (SD)		1.32 (1.00)		0.93 (0.52)		1.17 (0.84)	1.14 (0.2)

When investigating the RMSEs between the groups (Table 11. and Figure 7.), MTH1 and MTH5 length RMSE exceeded 2 mm in Group 1, while MTH1 length RMSE also exceeded

² Abbreviations: MTH1: metatarsal head 1, MTH5: metatarsal head 5, M. mall.: medial malleolus, L. mall.: lateral malleolus

2 mm in Group 3. For eight out of the 11 2D measures, the highest RMSE was found in Group 1. The exceptions are ball width and rear-foot width RMSE was the highest in Group 3, and medial malleolus height RMSE was the highest in Group 2.

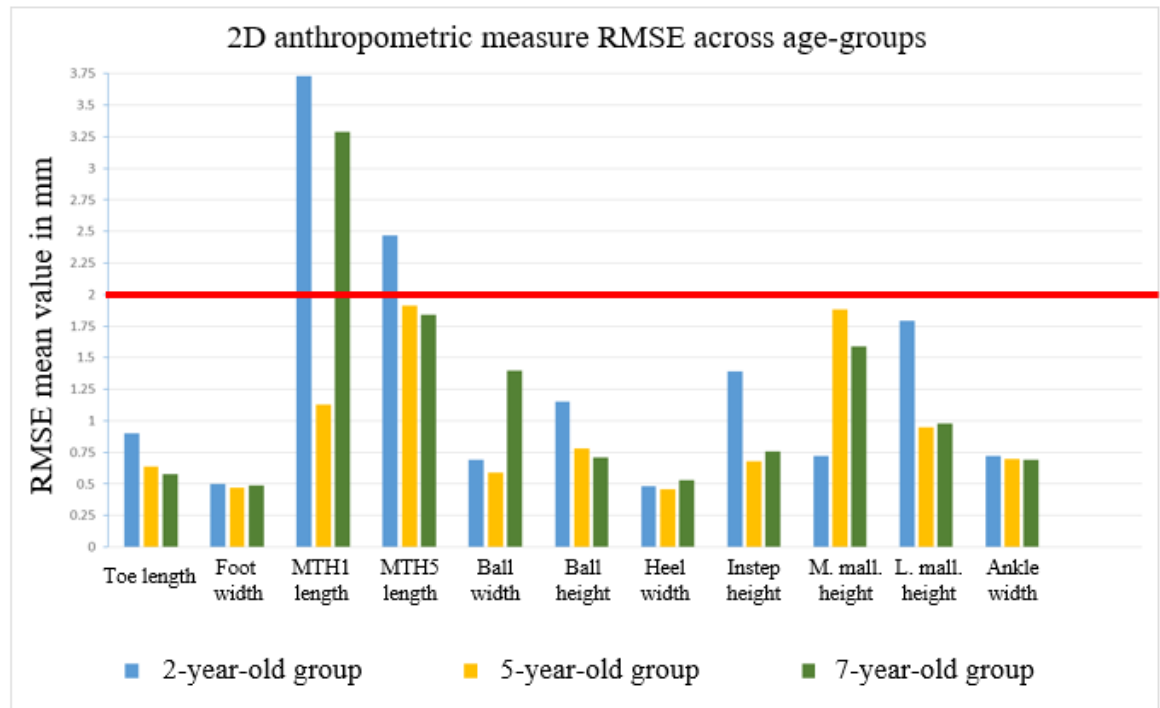


Figure 7.: Mean RMSE values for linear measures across age-groups. The red horizontal line represents the 2mm benchmark defined by Mauch et al. (2008). Abbreviations: MTH1: metatarsal head 1, MTH5: metatarsal head 5, M. mall.: medial malleolus, L. mall.: lateral

3.3.2. Reliability of the 3D surface morphology measures

The results of the vertex deviation calculations for each Group and participants can be seen in Table 13. The mean percentage of vertex deviations across participants and Groups under 0.5 mm was 63.42% (SD=8.65) and under 1 mm was 91.22%. (SD=5.60). The lowest reliability values were found in Group 1 both for under 0.5 and 1 mm. There was also an improvement in reliability with increasing age except for the deviations under 0.5 mm where Group 2 had a higher (higher reliability) result (73.03%) compared to Group 3 (68.82%).

Table 13.: Percentage of mesh deviation under 0.5 and 1mm for each group.

	Group 1 Mean (SD)	Group 2 Mean (SD)	Group 3 Mean (SD)
<i>% of mesh deviations under 0.5mm</i>	53.19% (16.18)	73.03% (21.16)	68.82% (11.47)
<i>% of mesh deviations under 1mm</i>	85.83% (14.76)	94.12% (7.97)	96.20% (3.49)

The graph in Figure 8. shows the cumulative statistics presenting each participants' cumulative vertex deviations curve and the mean for each age group (blue: two years old, black: five years old, red: seven years old group). This graph shows the increasing reliability as age increases, with the cumulative deviation curves becoming steeper and reaching 100% at smaller vertex distances.

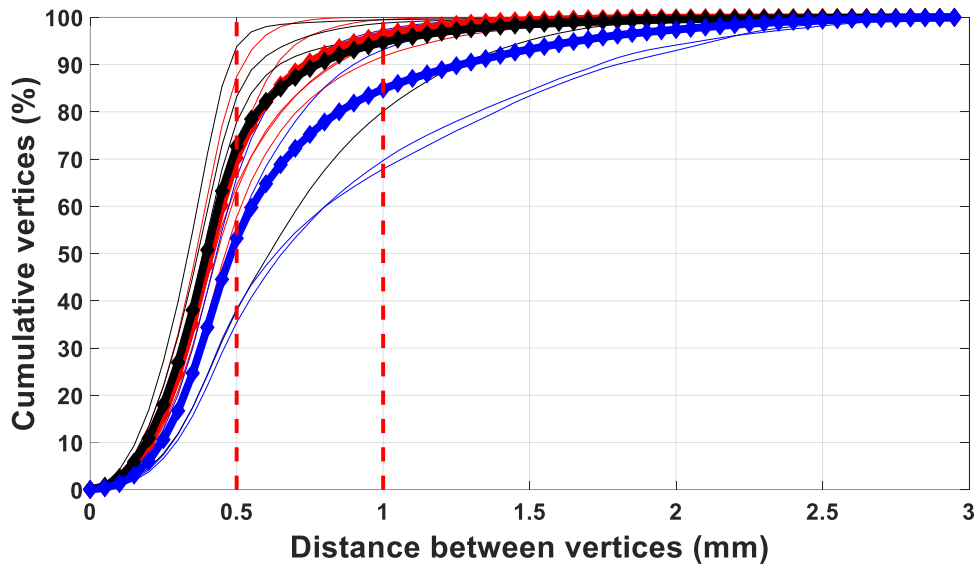


Figure 8: Cumulative percentage of vertex deviations. Thick line with diamond markers: means of each group, thin lines: each participant. Red: seven-year-old group, black: five-year-old group, blue: two-year-old group. Vertical red dashed lines mark the 0.5 and 1 mm vertex deviations.

Heat maps representing vertex deviations per-vertex have also been created to locate the vertex deviation differences on the foot. The heat maps in Figure 9. demonstrate the vertex deviations for one participant from each age-group from medial, lateral, and plantar view, and are included for illustrative purposes. The participants were chosen to be a representative example of the group. The percentage of deviations between 0.5 and 1mm and above 1mm were higher in Groups 1 and 2 in distinct areas marked by lighter blue, green-yellow and red colours respectively on one participant's foot from each group. These were the toes, ankle, dorsal aspect, lateral and medial edge of the foot, under the ball of the foot and the lateral part of the plantar aspect.

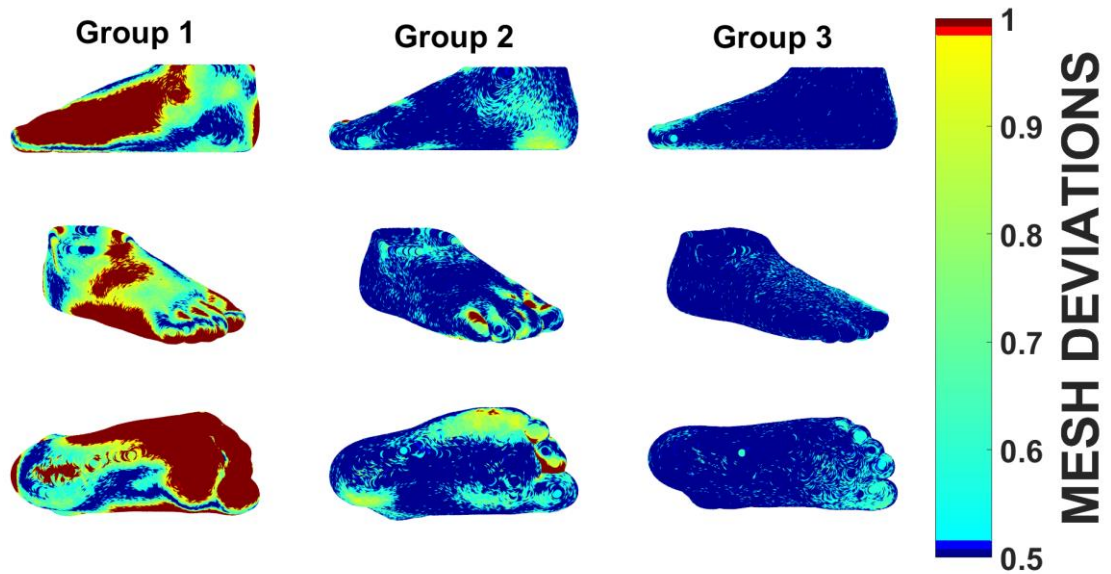


Figure 9.: Vertex deviation heat maps for one participant's foot from each group. Medial, lateral, and plantar view from top to bottom.

Curvedness and shape-index RMSE for each group are shown in Figure 10. Boxplot representation was chosen as the RMSE values are minimal, especially in curvedness, and they would be difficult to read in a table form.

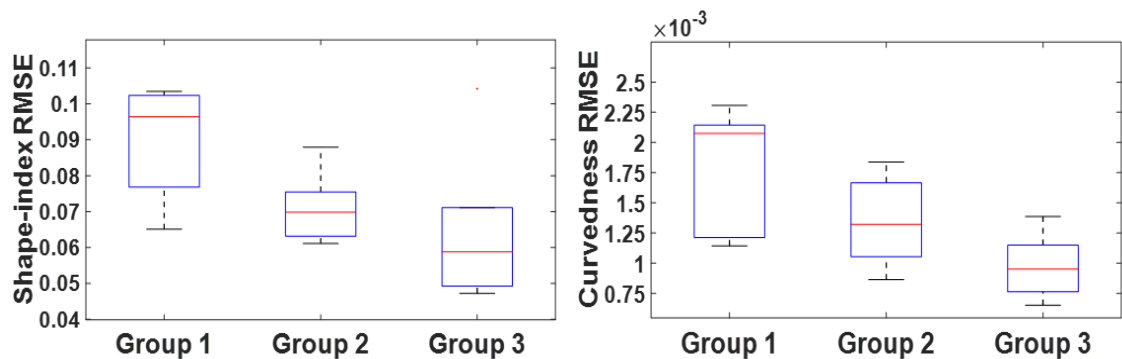


Figure 10.: Mean shape-index (left) and curvedness (right) RMSE boxplot for each group. Group 1: two years old group, Group 2: five years old group, Group 3: seven years old group.

The figure shows that both the curvedness and shape-index RMSE decreases with age. The range of curvedness was approximately 0.02; hence RMSEs as the percentage of the range were 10% in the 2-year-old group, 6.5% in the 5-year-old group and 4.5% in the 7-year-old group. The range for shape-index was two, and the RMSE percentages were approximately 4.75% for the 2-year-old group, 3.5% for the 5-year-old group and 3% for the 7-year-old group. The boxplots also show that the youngest age-group interquartile range for both

shape-descriptors is larger than in the other age-groups and positively skewed towards the higher RMSE values. The boxplots also highlight that, with 95% confidence:

- the median curvedness RMSE in Group 1 is different (higher) from Group 3 (the interquartile range boxes of the two groups do not overlap).
- The median shape-index RMSE in Group 1 is different (higher) from Group 2 and Group 3 (the interquartile range boxes of the groups do not overlap).
- The median curvedness RMSE of Group 2 is likely to be different (higher) from that of Group 3 (the median (red) line of Group 3 is outside of the interquartile range box of Group 2).
- The median shape-index RMSE of Group 2 is likely to be different (higher) from that of Group 3 (the median (red) line of Group 3 is outside of the interquartile range box of Group 2).

Figures 11. and 12. shows the RMSE heat maps of curvedness and shape-index respectively for one participant (same as for the vertex deviation heat maps in Figure 9.) from each group. Colours represent RMSE magnitude at each vertex, curvedness RMSE increasing from dark blue (RMSE~0) through light blue (RMSE~0.0015-0.002), green (RMSE~0.002-0.003), yellow\orange (RMSE~0.003-0.0035) and red (RMSE>~0.0035).

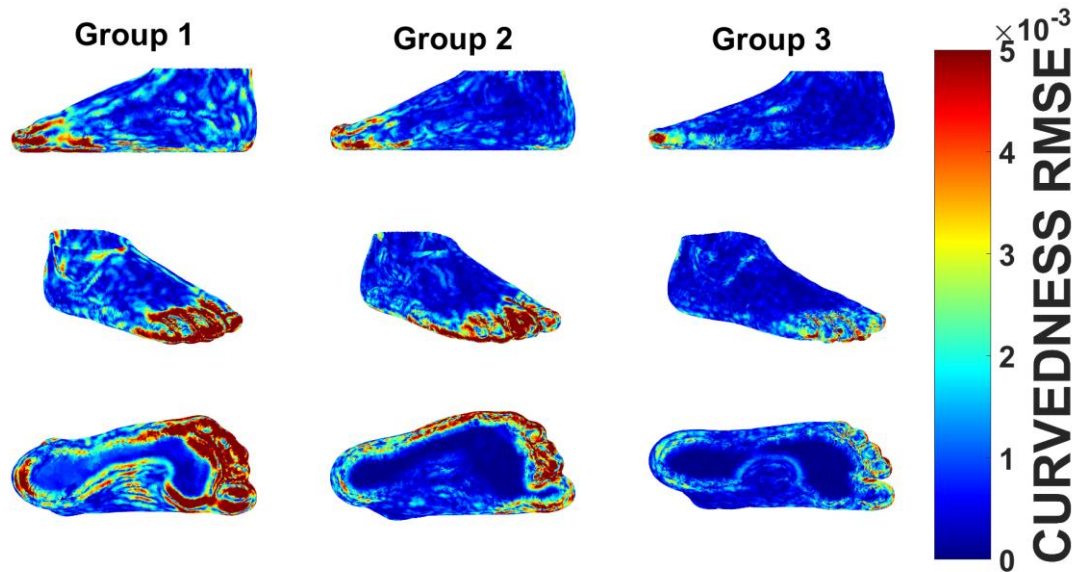


Figure 11.: Curvedness RMSE heat maps for an example foot from each group (Group 1 (two years old): Participant 3, Group 2 (five years old): Participant 4, Group 3 (seven years old): Participant 5). Medial, lateral, and plantar view from top to bottom.

Shape-index RMSE increases from dark blue (RMSE \sim 0) through light blue (RMSE \sim 0.06-0.08), green (RMSE \sim 0.08-0.12), yellow\orange (RMSE \sim 0.14-0.14) and to red (RMSE $>$ \sim 0.14). On the plantar view, the RMSE values corresponding to vertices with a curvedness value less than 0.0015 (flat against the ground) have been replaced with 0. The curvedness and shape-index RMSE heat maps show a similar tendency to the mesh deviations, but with fewer differences between the groups. Most differences in RMSE were found around the toes, the lateral and dorsal aspect, the medial longitudinal arch, under the medial malleolus and the heel.

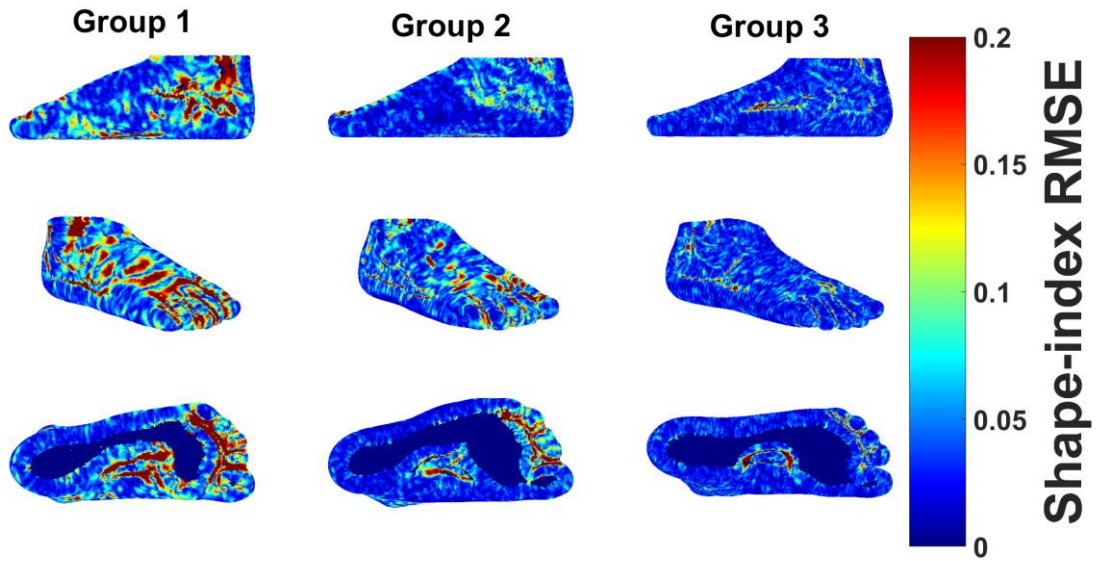


Figure 12.: Shape-index RMSE heat maps for an example foot from each group (Group 1 (two years old): Participant 3, Group 2 (five years old): Participant 4, Group 3 (seven years old): Participant 5. Medial, lateral, and plantar view from top to bottom.

3.4. Phase (a) discussion

The objectives of phase (a) of the pilot study were to (1) examine the reliability of capturing 2D measures of the foot in children using the Artec Eva hand-held scanner and, to (2) examine the reliability of capturing 3D surface shape measures of the foot in children, using the Artec Eva hand-held scanner. To achieve these objectives, the RMSE of 2D and 3D measures and 3D vertex deviations were captured from three models of the same foot were analysed in 15 children, five from each age group: two, five and seven years old.

3.4.1. Reliability of the 2D foot anthropometric measures

Although the linear measures RMSE results were mixed, they showed good reliability in Groups 2 and 3 for most measures, but Group 1 had lower reliability (higher RMSE) in eight out of the 11 measures. Compared to existing reliability data in children's feet (RMSE between 0.5 and 2mm) from the Pedus foot scanner (Mauch et al., 2008, Mauch et al., 2009), the overall average results across Groups, MTH1 and MTH5 length exceeded 2mm. When examining the Group results separately, the same measures from Group 1 and MTH1 length from Group 3 also demonstrated greater than 2mm values of RMSE. Although these two anatomical landmarks (MTH1 and MTH5) are relatively easy to locate, it seems that the location of these, relative to the most posterior aspect of the calcaneus changed between scans more than it did in the other groups. This could suggest variation in the angle of stance between scans resulting in changing foot shape for this group. The higher absolute RMSE in most of the other linear measures in Group 1 supports this argument (RMSE range: Group 1: 0.48-3.73, Group 2: 0.46-1.91, Group 3: 0.53-3.29). Another possible explanation for this finding is the software that was used to calculate the measures (Foot3D), as the algorithms were developed from adult feet, and hence there were discrepancies in the location of the anatomical landmarks. Due to these findings, the main study will utilise custom MATLAB

code using markers on the anatomical landmarks. Marking the anatomical landmarks has also been shown to result in more accurate and faster facial 3D scanning measurements, increasing the accuracy by 50%, from 2mm to 1mm, and reducing the measurement time from 4'18" without the marking points to 2'49" with marker points (Franco de Sá Gomes et al., 2019).

3.4.2. Validity of the 2D foot anthropometric measures

When considering existing literature investigating the validity of Artec Eva, (Seminati et al., 2017, Koban et al., 2020) compared this scanner to a high precision laser scanner.

Investigating residual limb models and faces of volunteers, it was found that the RMSE between the scanners was below 1mm, suggesting high criterion validity of the Artec Eva scanner. Although this is not related to the validity of the protocols used, it shows that the 3D scanner used in the current study is a valid alternative to high precision laser scanners.

Considering the validity of the protocols, comparing the current results to existing data from the literature can give an insight into the external validity of the methods used. Table 14. shows the comparison between the results of the current study (highlighted grey) and existing literature for foot length, fore-foot width and rear-foot width. The larger differences are discussed below the table.

Table 14.: Comparative table of the mean (standard deviation) of the current study results and existing literature for foot length, foot width and rear-foot width in cm.

	Age (years)	2	5	7
Foot length [cm]	Current thesis	15.46 (0.48)	17.35 (0.51)	20.39 (1.70)
	Kouchi (1998)		16.97 (0.99)	19.16 (0.92)
	Muller et al. (2012)	14.58 (1.82)	17.71 (2.04)	19.74 (2.35)
	Waseda et al. (2014)			19.06 (1.01)
	Delgado-Abellán et al. (2014)			20.02 (1.11)
	Jimenez-Ormeno et al. (2013)			19.78 (0.99)
	Foot Width [cm]	Current thesis	6.40 (0.34)	7.01 (0.52)
Kouchi (1998)			7.07 (0.42)	7.71 (0.46)
Muller et al. (2012)		6.10 (0.84)	6.94 (0.84)	7.46 (0.90)
Sacco et al. (2015) Brazil			6.15 (0.65)	6.84 (0.52)
Sacco et al. (2015) German			6.69 (0.40)	7.34 (0.44)
Delgado-Abellán et al. (2014)				7.68 (0.60)
Jimenez-Ormeno et al. (2013)				7.17 (0.43)
Rear-foot width [cm]	Current thesis	4.22 (0.15)	4.50 (0.31)	4.98 (0.38)
	Kouchi (1998)		4.47 (0.27)	4.88 (0.41)
	Sacco et al. (2015) Brazil		3.50 (0.39)	3.84 (0.31)
	Sacco et al. (2015) German		3.63 (0.29)	3.92 (0.30)
	Delgado-Abellán et al. (2014)			4.58 (0.83)
	Jimenez-Ormeno et al. (2013)			4.44 (0.35)

Foot length

Considering foot length, the data from the study of Kouchi (1998) and Waseda et al. (2014) showed that Japanese children had shorter feet. This discrepancy could be attributed to ethnic differences. Shorter feet of Asian populations (Jurca et al., 2019) and Japanese and Indonesian samples (Kouchi, 1998) have already been shown, although only in adults, and these differences might start to appear in childhood.

Fore-foot width

Although the data from Kouchi (1998) was also very similar to the current study, the fore-foot width of their sample increased faster – by 3mm - between the ages of 5 and 7 years resulting a 3mm wider fore-foot at the age of 7 years. Furthermore, the study of Waseda et al. (2014) have also shown shorter foot length at the age of 7 compared to the current study in the same ethnic group: Japanese children. Japanese male adults have already been reported to have wider fore-foot (Kouchi, 1998, Jurca et al., 2019), and the development of these differences might start to occur at this age. The fore-foot width of the Brazilian and German children in the study of Sacco et al., (2015) measured by footprints, was shown to be less compared to the current data by approximately 1 to 8mm. These results suggest that by measuring fore-foot width using footprints it may be underestimated. This is due to the fact that the widest part of the fore-foot is on the first and fifth metatarsal heads approximately at half ball height (between 14-17mm from the ground). This distance can be captured from a 3D scanner, but not from a footprint. Furthermore, Sacco et al. (2015) suggested that the cause of the narrower feet in the Brazilian sample is the lower BMI among the Brazilian children, due to socioeconomic differences between the countries.

Rear-foot width

The Brazilian and German children (Sacco et al., 2015) showed approximately 1cm less wide rear foot, which may be the result of the location of the measurement and the lower BMI and socioeconomic differences as suggested by the authors. In the current study, rear-foot width was measured at 15% foot length at 1cm height, while in Sacco et al., (2015) it was measured as the widest part of the rear-foot on a footprint. These results are similar to the results of fore-foot width as the footprint may not capture the widest part of the actual rear-foot, while the same measurement at 1cm height may do, which might have led to the 1cm difference in rear-foot width.

Summary

Although there are discrepancies between the current data and the literature, these differences are mostly not larger than one standard deviation of the larger literature sample. When the difference is larger than one standard deviation, the discrepancies are due to ethnic (Japanese sample) or socioeconomic (Brazilian sample) differences, different measurement locations, or techniques (such as footprint) used. Furthermore, unfortunately height and weight were not captured in the current study and hence the effects of these on foot dimensions could not be considered. As a result, the comparison with literature – although shows differences between the current data and the literature – indicates that the Artec Eva, using the current protocols, produces data comparable to the literature and hence captures externally valid 2D foot anthropometric measures in all three age-groups.

3.4.3. Reliability of the 3D foot surface morphology measures

The reliability of 3D foot shape measurement was evaluated using vertex deviations and calculating absolute RMSE of 3D shape descriptors. When considering the vertex deviations as a 3D model agreement measure, the results showed increased reliability as age increased. Consistent with this, the considerably higher proportion of corresponding vertex distances above 0.5 and 1mm in Group 1 suggests that the three models of the same foot were considerably more different in this age-group. More specifically, in Group 1 considerably different foot shapes between scans were indicated by the more extensive areas of mesh deviations over 1mm (red) around the ankle, on the sole's lateral aspect, under the metatarsals, and on the dorsal aspect. These differences in foot shape between scans may have resulted from and were consistent with the difficulties encountered during data collection: movement during scanning, and differences in stance between scans witnessed by the researcher.

The reliability of 3D shape descriptors was also investigated to examine how the 3D model vertex deviations translated into actual 3D surface shape differences. Although the boxplots showed the lowest reliability in the youngest group, the heat maps indicated much smaller areas of increased 3D shape descriptor RMSE than vertex deviations. Furthermore, the differences in the location of higher RMSE areas between the mesh deviation and 3D shape descriptor heat maps suggest that the vertex distances between models do not directly translate into shape differences. This highlights the discrepancies in the utility of the two reliability measures: while mesh deviations can indicate differences in vertex and surface location, 3D shape descriptor RMSE indicates differences in surface morphology. For this reason, although mesh deviation results suggest large areas of low reliability, this does not translate into low reliability in 3D shape descriptor RMSE. Additionally, the highest mean

shape-index RMSE value of ~ 0.11 in the youngest group is less than half of the difference between two shapes on the shape-index scale (0.25). Similarly, the highest curvedness RMSE is ~ 0.0024 , which is $\sim 10\%$ of the curvedness range within the foot. These findings suggest that the increased 3D shape descriptor RMSE in the 2-year-old group does not cause unreliable 3D surface shape identification.

3.5. Phase (a) conclusion

The aim of phase (a) was to investigate the reliability and validity of capturing 2D anthropometric and 3D surface morphology measures of the paediatric foot using the Artec Eva hand-held scanner and a custom-built stand and platform between the ages of two and seven years.

In conclusion, Group 1, the youngest children, had the lowest reliability considering

- eight out of 11 linear measures, two of which exceeded the benchmark value,
- spatial agreement (cumulative vertex deviation) between 3D models and
- both 3D shape descriptors.

Furthermore, the validity of the methods was assessed by a comparison to existing datasets in the literature. This assessment showed that the current data is valid, and the disparities compared to existing datasets are due to ethnical or methodological differences.

Based on the results, it can be concluded that the experimental set-up used was a reliable and valid way to capture these measures in the five and seven-year-old age-groups, but there were issues in the two-year-old group. It is suggested that the low 3D model agreement in the two years old group translated (although not directly) into lower reliability in 2D anthropometric measures but not in 3D shape descriptors. The results also suggest that although there are large areas of high mesh deviations in the youngest group, the differences in 3D surface morphology (although present) will not affect findings significantly. Therefore, as the reliability of the 3D shape descriptors in the youngest group was found to be adequate, these will be utilized in phase (b) of the pilot study.

The reliability issues regarding the 2D measures and mesh deviations were proposed to be due to specific behavioural, neuromuscular, and soft tissue properties of this particular age-group instead of the scanner's functional capacity or the setup. Furthermore, based on the researcher's experience when scanning the youngest age-group, children who were closer to the age of three, were more likely to stand still during scanning and had a more consistent stance throughout the scans. As the above properties cannot be controlled by the researcher, the two-year-old age-group was not included in the main study where 2D measures will also be used, and a higher number of scans are required. Therefore, the lowest age in the main study was increased to three years of age.

3.6. Phase (b) results

3.6.1. 3D surface morphology of the dorsal aspect of the paediatric foot

The curvedness histograms (Figure 13.A) for the foot's dorsal aspect show an increase in the lower curvedness values and a decrease in the higher values from Group 1 to Group 2 and 3. The second peak around 0.01 decreases from Group 1 to Group 2 and disappears in Group 3. The curvedness heat maps (Figure 13.B), show the increased area of lower curvedness (as identified by the dark blue) and a decrease in medium curvedness (light green) on the lateral side of the dorsal aspect with age, which agrees with the histogram and an increasing area of higher curvedness on the medial side. The shape-index histograms (Figure 13.C) indicate an increase in concave shapes, a decrease in the ridge shape and an increase in the saddle ridge shape from Group 1 to Group 2. The shape-index heat maps show that an alternating saddle-ridge-ridge pattern is developing with age on the medial side of the dorsal aspect. There is also a reduction of convex and an increase in saddle shape on the rest of the dorsal aspect.

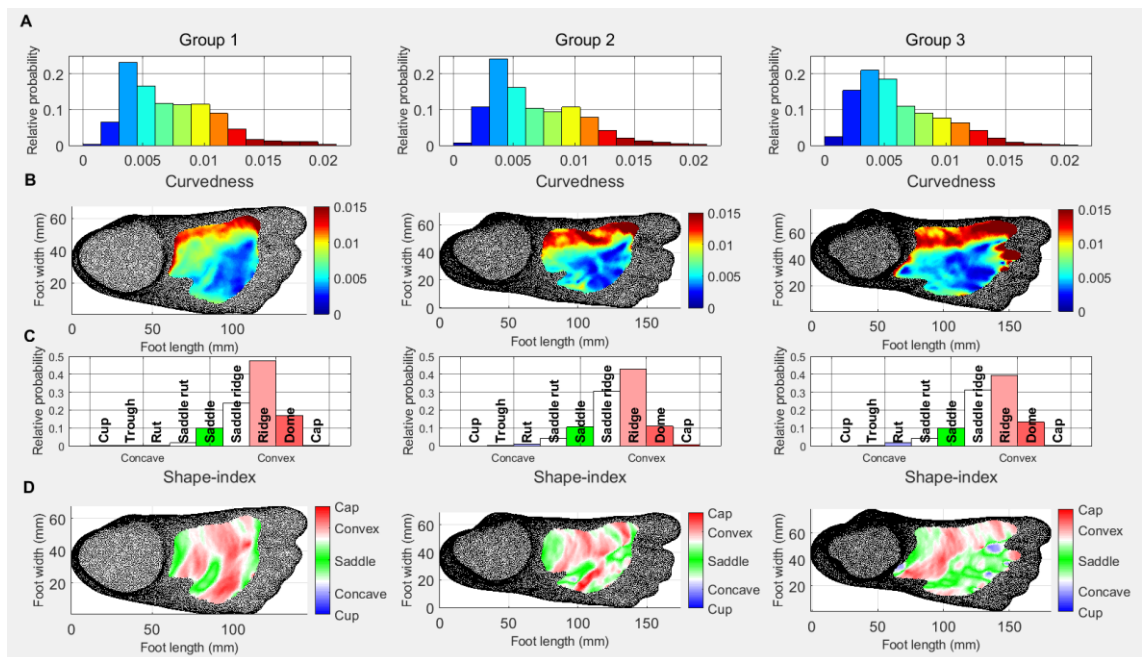


Figure 13.: Dorsal aspect: Relative probability histograms: (A) curvedness (C) shape-index; Heat maps: (B) curvedness (D) shape-index

3.6.2. 3D surface morphology of the medial aspect of the paediatric foot

Similar to the dorsal aspect, the medial one also shows a reduction in higher curvedness values and an increase in lower curvedness values as age increases (Figure 14.A.) Figure 14.B shows a decreased curvedness on the inferior medial aspect in the Group 3 participant and increased curvedness around anatomical landmarks like the medial malleolus and the navicular in the Group 2 and Group 3 participants. The maps also demonstrate that curvedness decreases with age on the superior boundary of the medial aspect. The shape-index data reveals an increase in concave shapes and a slight decrease in dome shape (Figure 14.C) from Group 1 to Group 2. The shape-index heat maps show the medial malleolus, the navicular and the first metatarsal head which are more prominent in the older children, along with concavity appearing posterior to the medial malleolus. Consistent with the dorsal aspect pattern, an alternating red, white, green pattern appears on the superior boundary of the medial aspect.

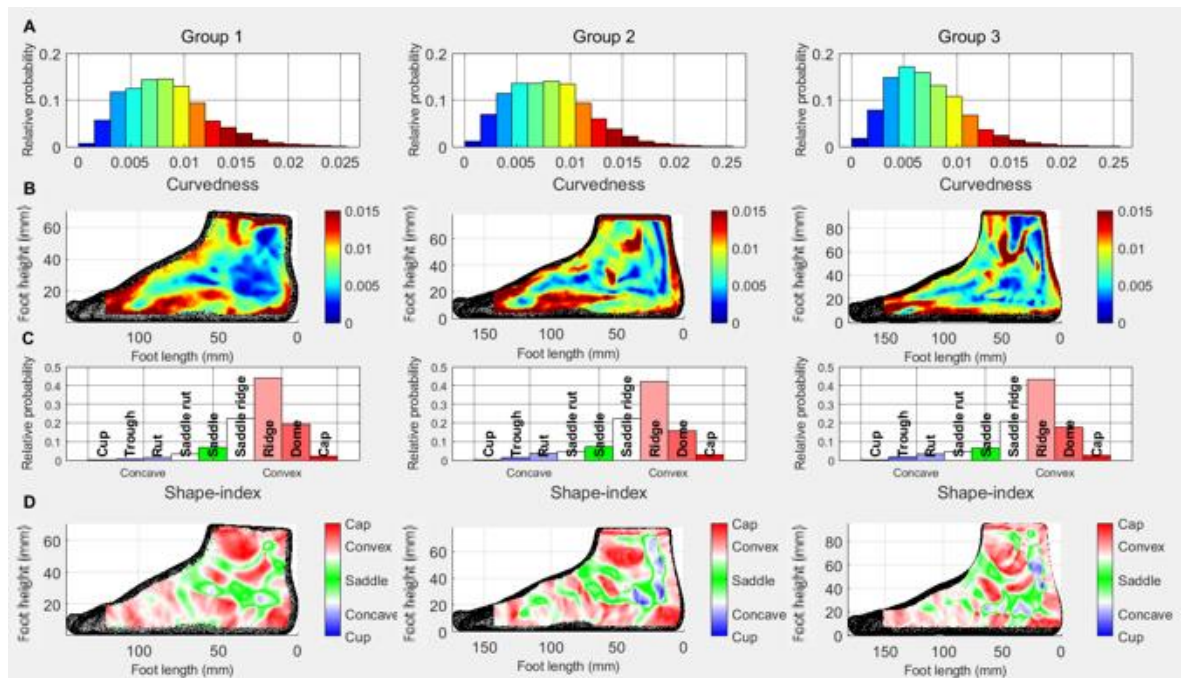


Figure 14.: Medial aspect: Relative probability histograms: (A) curvedness (C) shape-index; Heat maps: (B) curvedness (D) shape-index

3.6.3. 3D surface morphology of the lateral aspect of the paediatric foot

The curvedness histograms (Figure 15.A.) of the lateral aspects demonstrate a shift towards lower curvedness values with increasing age. The curvedness heat maps (Figure 15.B.) show a shift in the curvedness of the foot's lateral border and the increase in size and curvedness of the lateral malleolus with age. A higher curved structure inferior and anterior to the lateral malleolus is apparent in the Group 1 and Group 2 participants, which disappears or shifts more anteriorly in the Group 3 participant. The main differences between the Groups in shape-index are the increase in ridge shape (Figure 15.C.) and the reduction in saddle shape in Group 3 and increased concave shapes as age increases. The shape-index heat maps demonstrate the development of the lateral malleolus (see Figure 15.D.). The concave shape-index values for Groups 2 and 3, mainly appear posterior and anterior to the lateral malleolus.

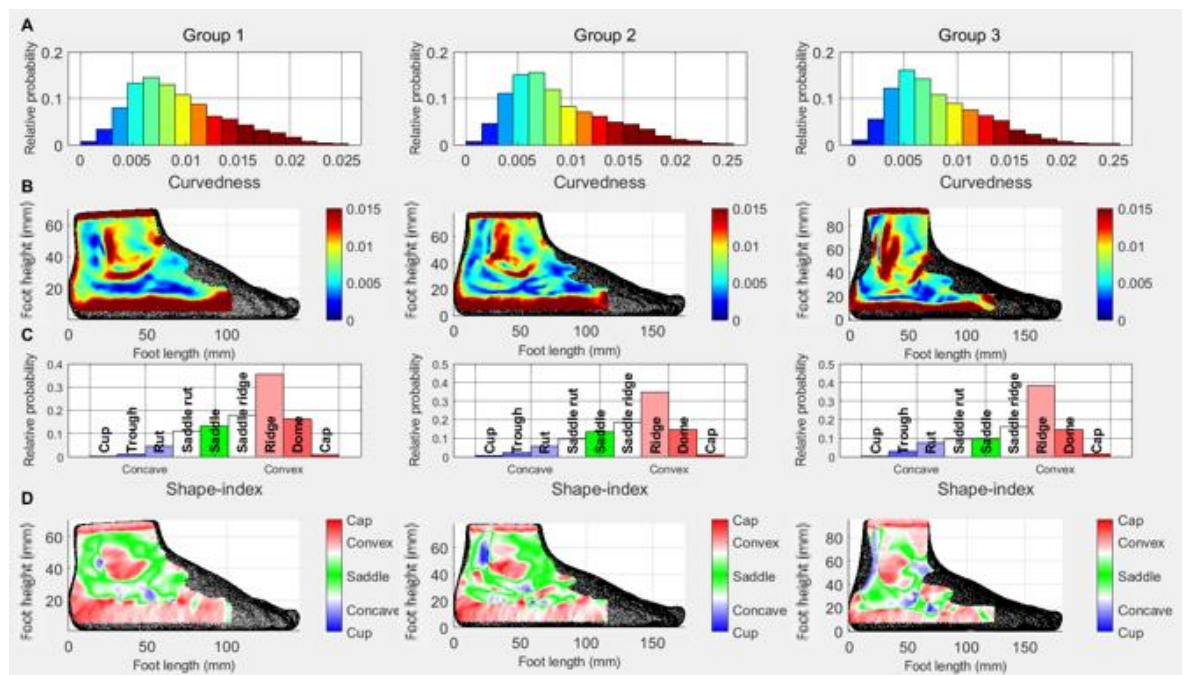


Figure 15.: Lateral aspect: Relative probability histograms: (A) curvedness (C) shape-index; Heat maps: (B) curvedness (D) shape-index

3.6.4. 3D surface morphology of the plantar aspect of the paediatric foot

Due to the plantar aspect being mostly flat, the shape descriptor histograms are very different from those of the other surfaces (Figure 16.A.). There is a slight increase in the lowest curvedness values in Group 3. The curvedness heat maps (Figure 16.B.) show the medial longitudinal arch's development across the age-groups. Medium curvedness values extend into the plantar aspect from the medial side and create an arch-shaped area with increasing age, incorporating lower curvedness values, and in Groups 2 and 3, some medium values too. The curvedness maps also show that with increasing age, the curvedness on the medial edge of the midfoot (red line on the Group 1 participant's foot) decreases or shifts medially. The shape-index data (Figure 16.C.) show a slight decrease in ridge shape in Group 3. The shape-index heat maps (Figure 16.D.) are consistent with those of the curvedness and show the development of a convex arch on the medial side extending into the plantar aspect, with an increasing area of concavity within it as age increases.

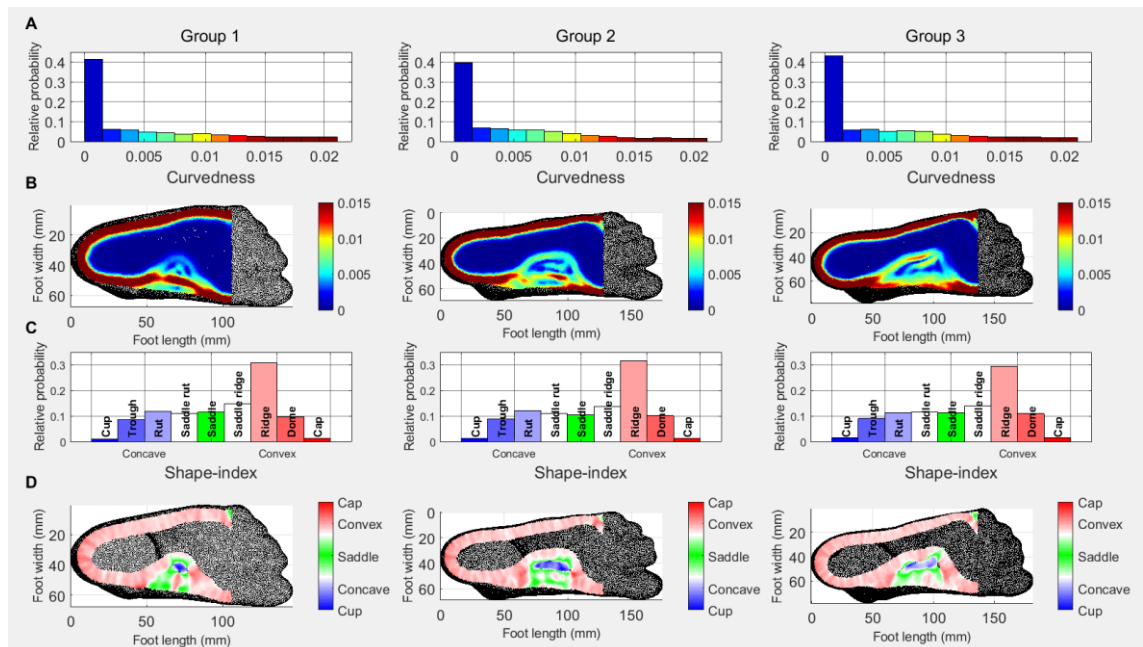


Figure 16.: Plantar aspect: Relative probability histograms: (A) curvedness (C) shape-index; Heat maps: (B) curvedness (D) shape-index

3.7. Phase (b) discussion

3.7.1. 3D surface morphology of the dorsal, medial, and lateral aspects of the paediatric foot

The changes in the curvedness data distribution in the dorsal, medial, and lateral aspects indicate that the overall surface morphology of the foot becomes less curved with age. This is likely to be related to the changing proportions of the foot as it becomes more slender with age (relatively smaller width and circumference measures along with larger length parameters), as suggested in previous reports (Muller et al., 2012, Mauch et al., 2009, Mauch et al., 2008). These changes are supported by the shape-index histograms of the same surfaces, showing increasing areas of concavity among the convex areas during development.

Visual inspection of the curvedness heat maps of the dorsal, medial, and lateral aspects demonstrates the increasing prominence of foot structures: bony landmarks are developing showing higher curvedness on these locations, with flatter areas surrounding them. The shape-index heat maps of the lateral and medial aspects show that the increase in concavity is also likely related to the emergence of bony landmarks creating “valleys” around them. The increase in concave and saddle ridge shapes on the dorsal aspect histograms and the changes on the shape-index heat maps suggest similar changes to the medial and lateral aspects: the changing proportions of the foot and an emergence of bony architecture exposing the developing cuneiform bones. These findings also confirm previous results, where younger children’s feet were found to be more robust (larger width and circumference measures and smaller length measures) based on 2D anthropometric parameters (Mauch et al., 2009). However, while the circumference and width measures only give us a measure

between two points, the heat maps and 3D shape descriptors used in this study can identify specific foot regions where the 3D shape changes (robust to slender) occur.

3.7.2. 3D surface morphology of the plantar aspect of the paediatric foot

When considering the plantar aspect, the increase in lower curvedness values (see Figure 16.A.) might suggest an increase in the flat (weight-bearing) areas of the plantar aspect. On the other hand, the MLA development with age is also visible on both the curvedness and shape-index heat maps of the plantar aspect. The increase in concavity shown on the shape-index histograms suggests the increase of the MLA size, consistent with previous reports suggesting an increase in the MLA area during development; however, these studies used footprint measures (see section 2.1.4.2. for these studies). These methods do not allow for the description and quantification of the surface morphology of the MLA, hence neglecting the 3D properties of a multi-planar structure (Banwell et al., 2018). Although a study by Chang et al. (2012) used an indirect 3D measure of the MLA, the arch volume (the volume under the MLA) and reported an increase with age, this method cannot characterize the changes in the 3D surface of the arch. In addition to the results of the cited studies, phase(b) of the pilot study using novel 3D scanning and shape descriptor analysis, for the first time, enabled the quantification of an increase in the MLA surface's concavity. This change in the shape of the MLA suggests the structural and functional development of the surrounding soft and bony tissues as a weight bearing, shock absorbing and propulsive unit.

3.8. Phase (b) conclusions

The aim of phase (b) was to test whether 3D shape descriptors derived from 3D scanning can characterise and quantify changes in foot shape between the ages of two and seven years. Previous literature using 3D scanners in foot development research adapted this technology to provide a time-efficient and accurate way of capturing 2D anthropometric foot measures. Phase (b) of the pilot study provided further justification for the use of 3D scanning in foot development research. Additionally, it served as proof that 3D shape descriptors derived from 3D foot scans can help identify, locate, and characterise changes in foot surface morphology during development. Furthermore, the results supported previous findings from the literature (e.g. the foot becomes slenderer with increasing age, the area of the MLA increases), as well as provided novel, high resolution, and relevant insights into how the 3D shape of the paediatric foot surface develops (e.g. the MLA becomes more concave with increasing age, the emergence of bony landmarks). While the relative probability histograms served as a quantitative approach to the analysis of 3D foot shape, the heat maps provided a qualitative approach: a clear morphological map of the foot and changes between age groups. The findings reported in this pilot study also demonstrate the potential for greater utilisation of technology in clinical practice, reiterating previous suggestions from Telfer and Woodburn (2010) promoting the use of 3D scanners in research on the foot, foot orthotics and customised footwear last design. Although there have been studies that investigated (Nelson et al., 2017) or suggested (Stanković et al., 2018) the use of 3D data in clinical assessment, this study is a novel attempt to translate 3D shape descriptor research into 3D foot surface morphology measures which can be interpreted in an applied clinical setting (Varga et al., 2020). Hence the parameters used in this study will be applied to the foot surface evaluation in the main study of the thesis.

3.9. Summary and limitations of the pilot study

The pilot study aimed to establish the reliability of the methods used in the main study and determine whether 3D shape descriptors can help characterise and quantify the morphological development of the paediatric foot.

As the literature review showed, step-in 3D foot scanners have been found to provide reliable and valid results in adults and children, but hand-held scanners have not been investigated for this purpose. Phase (a) of this study was the first to provide information on the reliability and validity of hand-held 3D scanning of the paediatric foot, while also examining the reliability of capturing novel and relevant 3D surface morphology information.

In summary, the results showed that while the 3D measures were reliable in all age groups, the linear measures were only reliable in the two older age groups, and validity was demonstrated through comparison to existing literature in all age-groups. In the youngest age-groups, the differences in the consequent models of the same foot led to considerable differences in 2D anthropometric measures. Although hand-held scanning has its advantages of being portable and less expensive, its limitation is due to the longer scanning time, which means that children below a certain age (who cannot stand still for one-one and half a minute) cannot be scanned reliably for 2D measures. Along with the experiences during scanning (two years old children moving during the process), the results of phase (a) of the pilot study have led to the decision of excluding the two years old age-group from the main study and setting the lower age limit to three years of age. This will ensure smooth and speedy data collection as well as high-quality foot models. Although the 2D measures in the youngest group were deemed unreliable, the increased RMSE of 3D shape descriptors is not a concern; hence phase (b) of the pilot study will use Group 1's curvedness and shape-index data.

One of the limitations of the study is the partly subjective approach to the RMSE cut-off limit. While two studies examined the reliability of laser scanners (Mauch et al., 2009, Mauch et al., 2008) demonstrating RMSE ranging between 0.5 and 2mm, there is currently no reliability data using structured light, hand-held scanner in children. For these reasons, the choice of 2mm as a limit is somewhat arbitrary, although still suggests high reliability for the older age-groups.

A further limitation of phase (a) is the lack of validity data, although Artec Eva's validity has already been examined (Seminati et al., 2017, Koban et al., 2020) looking at comparing it to a high precision laser scanner. Investigating residual limb models and faces of volunteers, it was found that the RMSE between the scanners was below 1mm, suggesting high validity of the Artec Eva scanner. Furthermore, the foot length, foot width and heel width data resulted from the current study aligns with data in the literature (table 14.) with minor differences, which also suggests validity of the current methods. In addition, while the plantar surface was scanned through the Perspex platform, which may affect accuracy regarding the data concerning the plantar surface, the upper part of the foot, where all 2D measures were measured from, was scanned similarly to other scanning techniques. While the 2D measures were captured above the platform, the 3D measures related to the plantar surface were captured through the Perspex platform. For this reason, a technical validation of the protocols may be necessary to eliminate or control the effects of light refraction of the Perspex platform. Although this has been done before using laser scanners (Chang et al., 2007, Li et al., 2008a, Li et al., 2008b) only one study looked at refraction correction using structured light scanner in underwater scanning (Anwer et al., 2017). The authors argued that depending on the thickness of the platform, the distance of each point measured in the scan from the scanner maybe different from the real distance. This could cause inaccuracies

in the 3D model. The validation may have to be done using a known sized object at a known distance from the scanner, that is scanned through the Perspex platform and without the Perspex platform and/or through refraction correction and adjusting time of flight values as detailed in Anwer et al. (2017).

As the 3D measures and the methods have been proved to be reliable, they were used in phase (b) to investigate if they can help identify, locate, and characterise changes in foot surface morphology during development.

This phase of the pilot study showed that 3D shape descriptors can identify changes in foot surface morphology found in previous studies and provide novel and relevant 3D morphological maps of the paediatric foot. With these high-resolution heat maps and the relative probability histograms, one can locate and characterize the 3D shape changes in the foot qualitatively and quantitatively. While the generalized results derived from 2D measures of previous studies (foot becomes slenderer, MLA area increases) can give an idea about the size and shape changes, the morphological 3D maps can also localize and optimally quantify the surface shape development. This data may also provide information about the changes in the underlying structures without using more expensive, invasive, and time-consuming imaging methods, and help clinicians in decision making or shoe manufacturers in footwear last design. Consequently, the results of phase (b) showed, that 3D shape descriptors can be used in the main study to optimally quantify and locate the 3D surface morphology changes taking place during development in the paediatric foot.

One of the limitations of phase (b) is the small sample size, which is due to the study's nature. This will be addressed in the main study, where the same measures will be examined in a larger sample. Another limitation, which is a consequence of the former, is the lack of statistics comparing the age groups. Although relative probability histograms were used,

these cannot provide the opportunity for relevant statistical evaluation. With the larger sample size, this issue will also be addressed in the main study, applying a method specifically designed to deal with such data: statistical parametric mapping. This approach allows the statistical comparison of 3D data in a vertex by vertex manner, thus providing a tool to localize statistically significant changes in 3D foot surface morphology. Finally, similarly to the 2D measure reliability study, the approach to the reliability of the 3D measures was also partly arbitrary as currently there is no available data in children or adults.

The following experimental chapter will present a cross-sectional study that utilised the methods investigated in the pilot study to examine the 2D anthropometric and 3D surface morphology changes occurring in the paediatric foot between the ages of three and seven years.

Chapter 4

4. The 2D anthropometry of the paediatric foot

As discussed in the Thesis Introduction, capturing foot development trajectory using 2D measures is critical for research, clinical practice, and footwear last design. Although there have been several studies on this topic, no consensus exists around which foot measures should be used for this purpose (Uden et al., 2017, Banwell et al., 2018). Existing datasets, although supported clinical decisions and footwear last design, are incomplete and outdated, hence using them may compromise the quality of practical applications. As an example, although relative\normalized fore-foot width can provide an estimate of the slenderness of the foot, it cannot describe how the rear- or mid-foot proportions change with age. Hence, if used to characterize the whole foot in practical applications, it can lead to an incorrect and oversimplified description of the foot.

While 2D measures of different foot regions have been investigated before, there is a lack of analysis of these regions' developmental trajectories compared to one another. Although Sacco et al. (2015) examined the width of three foot regions in 3 to 10-year-old Brazilian and German children, the only consideration was comparing the two populations and not the differences between regions. As these regions have distinctive underlying structures and particular but overlapping functions, their morphological development is possibly different.

Capturing these regions' varying developmental trajectories can offer a higher resolution assessment of the paediatric foot for clinicians and footwear last designers.

The technologies used to capture 2D measures of the foot in children are also inconsistent. They range from foot-prints (Gijon-Nogueron et al., 2019, Sacco et al., 2015, Gilmour and Burns, 2001) through tape measure and calliper (Anderson et al., 1956a, Anderson et al., 1956b, Kouchi, 1998), through manual foot measuring device (Muller et al., 2012) to 3D laser scanning (Waseda et al., 2014, Delgado-Abellán et al., 2014, Jimenez-Ormeno et al., 2013, Mauch et al., 2009, Mauch et al., 2008). While the reliability and validity of most of these methods have been established, 3D scanning has become widely used (see literature review section 2.2.3.) and accepted as the gold standard of foot measurement (Witana et al., 2006, Lee et al., 2014, Telfer and Woodburn, 2010). Despite this and the validation of 3D scanning technology in this field (see literature review section 2.3.2.5.), it has rarely been used to capture the changing dimensions of children's feet. Studies that have used 3D scanning for this purpose measured the feet of children over the age of six or seven years (Delgado-Abellán et al., 2014, Jimenez-Ormeno et al., 2013, Waseda et al., 2014, Mauch et al., 2008, Mauch et al., 2009) in Spanish, German, and Japanese populations. These studies provided accurate information on children's foot size and shape either using standalone measures or cluster analysis of multiple measures; however, there was no consideration of regional comparisons such as differences or similarities in development between rear-, mid- and fore-foot size and shape. While Mauch et al. (2008) described morphological changes with increasing age or BMI, in their approach measures of different foot regions were clustered together to create foot types; hence possible discrepancies between regions could not be considered.

For these reasons, an up to date dataset of 2D foot measures, including all three foot regions captured with current technology in this age-group is missing from the literature.

4.1. Aims

To address the gap identified in the literature, the purpose of this chapter was to offer an understanding of 2D anthropometric foot development between the ages of 3 and 7 years, and to provide a contemporary dataset of 2D anthropometric paediatric foot measures. This was achieved employing the Artec Eva hand-held 3D scanner, and the methods established in phase (a) of the pilot study (Chapter 3.).

Objective 1: Characterize the size development of foot regions in children aged 3-7 years.

Research questions

- How do the dimensions of foot regions change during development?
- Is there a difference in the development of width among the three foot regions between the ages of 3 and 7 years?
- Is there a difference in height development among the three foot regions between the ages of 3 and 7 years?

Objective 2: Characterize the proportional development of foot regions in children aged 3-7 years.

Research questions

- How do the proportions of foot regions change during development?
- Is there a difference in the development of width proportions among foot regions?
- Is there a difference in the development of height proportions among foot regions?

4.2. Methods

The investigation was approved by the Life, Health and Physical Sciences College Research Ethics Committee at the University of Brighton. Written informed consent was obtained from all parents on behalf of their child on an approved printed consent form. This form was either sent out to the parents by the school or handed to them by the investigator along with the information sheets.

4.2.1. Participants

Children between the ages of three and seven years old were recruited from local schools, nurseries, and sports centres, using convenience sampling.

The inclusion criteria for the study were (all self-reported by parents):

1. Typically developing
2. Able to stand barefoot for 5 minutes
3. Aged between 3 and 7 years

Exclusion criteria:

1. Skin disorders affecting the foot such as dermatitis, psoriasis, or any skin abrasions
2. Suffering from epilepsy or light-sensitive conditions
3. Foot deformity

4.2.2. Data capture

Data collection took place in the Human Motion Laboratory of the University of Brighton and in local schools, nurseries, and sports centres between January-2019 and March 2020. Two adults were present during scanning: MV and an assistant (university, school, nursery staff or a parent who was informed about the data collection procedure during a preparation visit) known to the child.

The equipment used was identical to the one in the pilot studies (section 3.3.4.): two bespoke wooden platforms, covered with rubber mat; a Perspex see-through platform (weight limit: 150kg), the Artec Eva hand-held scanner, tape-measure, and a digital scale. The child sat down and was asked to remove their shoes and socks, then the parent or teacher was asked to clean their feet with a skin disinfecting wipe. The child was then asked to step up onto the platform (manual support holding their hands was provided when needed) and find a comfortable position for both feet on the platform. Each child was asked to stand with their feet pointing anteriorly. Anatomical landmarks on the feet were palpated and marked (approximately 1mm) on the skin with a sterile surgical skin marking pen. The landmarks located were both malleoli, the most lateral and medial point on the fifth and first metatarsal heads, respectively. Each child was then asked to move their feet on the platform gently and find a position where they were comfortable. Feet were approximately shoulder-width apart—this technique allowed for each child to be comfortable throughout the scanning. The scanning procedure followed the protocol outlined in the pilot study (see section 3.3.4.). In this instance, one full scan of both feet was performed.

Following scanning, children's height (bare feet) and weight were measured using a tape measure and a digital scale, respectively, gender and ethnicity were self-identified by the child's parents on the consent form.

4.2.3. Post-processing of scans

From each scan, a 3D model (this included the texture captured by the scanner) was created to locate the marked anatomical landmarks and to calculate 2D measures (Figure 17.). This process followed the same steps as in the pilot study (section 3.2.5.), and further steps were added to support marker identification:

1. **Texturing:** The scans' texture was applied to the model and adjusted for a MATLAB script to locate the markers on the anatomical landmarks to function. Once texturing was completed, only the right foot model was carried over to the next stage for analysis to ensure statistical independence within the samples (Menz, 2004).
2. **Texture adjustment:** The foot surface colour was changed to green, making the purple markers black and stand out from their green surroundings. This was important for the identification of landmarks in MATLAB.
3. **Coordinate system alignment:** The Brannock axis was aligned with the x-axis of the software, the y-axis was aligned with the mediolateral direction, while the z-axis represented the vertical direction. The origin of the coordinate system was at the most posterior point of the heel.
4. **Export:** The 3D models were exported into MATLAB as .xyzrgb files, including the 3D locations and colour information in RGB (red, green, blue colours each represented by a number between 0 and 256, e.g. 0,256,0 means green) format for each vertex.

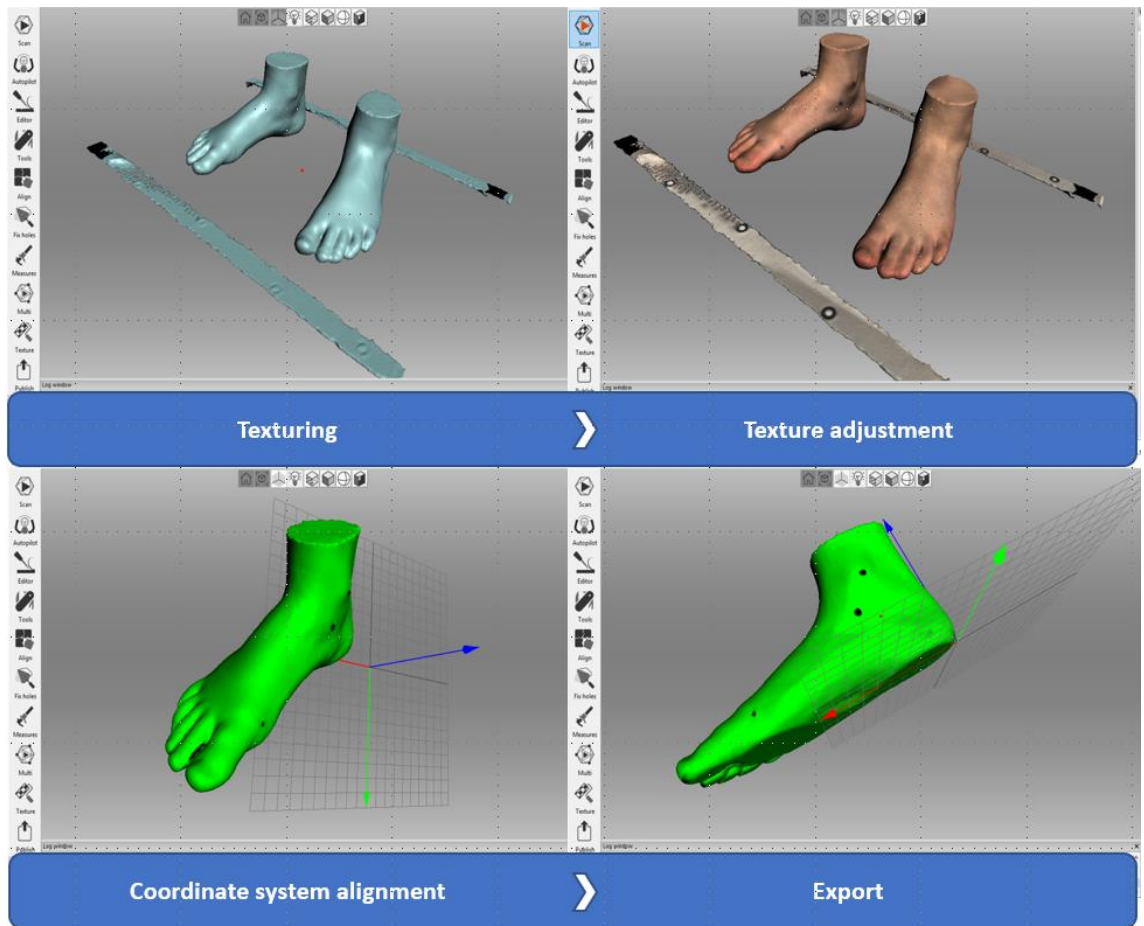


Figure 17.: Post processing steps in Artec Studio 12, to calculate 2D measures using the markers on the foot, after the small object filter and hole filling step.

4.2.4. 2D measurements

2D measures were calculated for the rear-, mid- and fore-foot regions. First, a custom-written script was used to identify and locate four anatomical landmarks: both malleoli and the most lateral and medial point on the fifth and first metatarsal heads, respectively. The technique to identify these marks is outlined below, demonstrating the localization of the lateral malleolus:

1. First, a search area was created on the foot surface where the particular anatomical landmark was located, and the mark would likely be found (Figure 18.). This was based on the foot's general anatomical proportions: between 10-70% of the ankle in the anterior-posterior direction, and between 40-70% of the scan height. As the zero in the mediolateral direction was at the most lateral point of the foot, only the first third of the scan was considered.

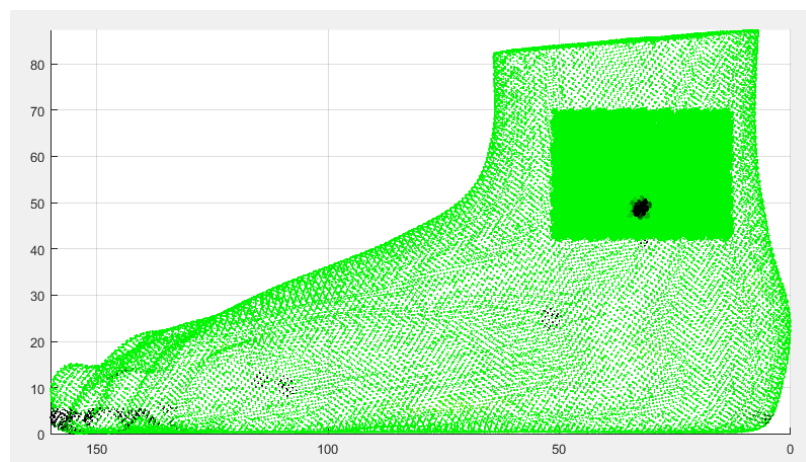


Figure 18.: Search area (darker green) for lateral malleolus on a point cloud of a 5-year-old child's foot. Black marks are the markers drawn on the foot and texture noise.

2. Within this search area, a custom-written algorithm identified the vertices with a specific combination of RGB values, to identify black vertices that were thought to represent the mark and hence the anatomical landmark. In the case of noise in the texture, this could have included points outside the marker (see Figure 19.).

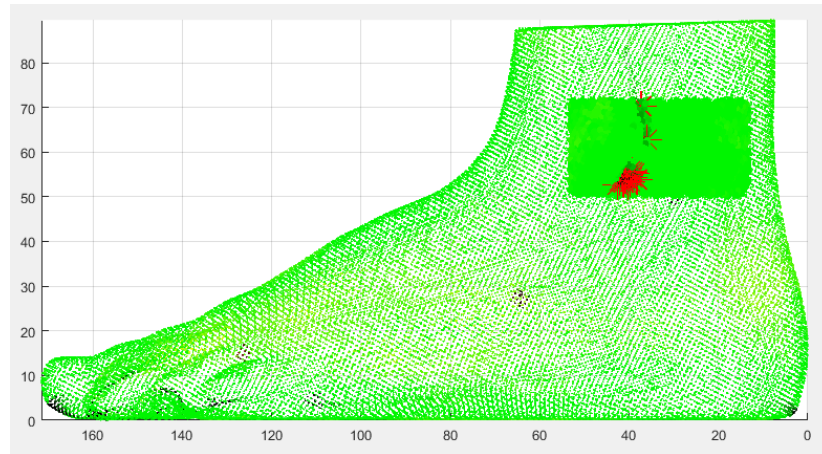


Figure 19.: Search area (darker green) and identified vertices (red stars) with marker colour for lateral malleolus on a point cloud of a 5-year-old child's foot. Black marks are the markers drawn on the foot and texture noise.

3. Any outliers (black vertices more than two standard deviations Euclidean distance away from the average location of the black vertices) that might have resulted from texture noise on the surface were filtered from the list (Figure 20.).

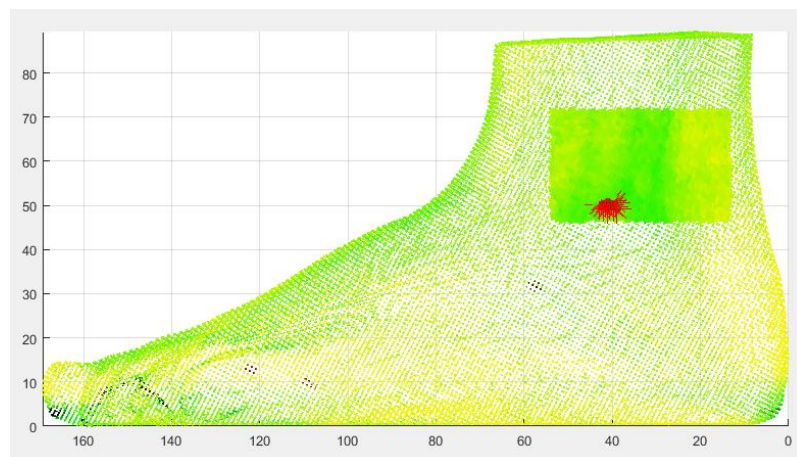


Figure 20.: Search area (darker green) and filtered vertices (red stars) with marker colour for lateral malleolus on a point cloud of a 5-year-old child's foot. Black marks are the markers drawn on the foot

4. The centre of the black vertices - and hence the anatomical landmark - was found by calculating the mean of the 3D locations of all remaining black vertices within the search area (Figure 21.).

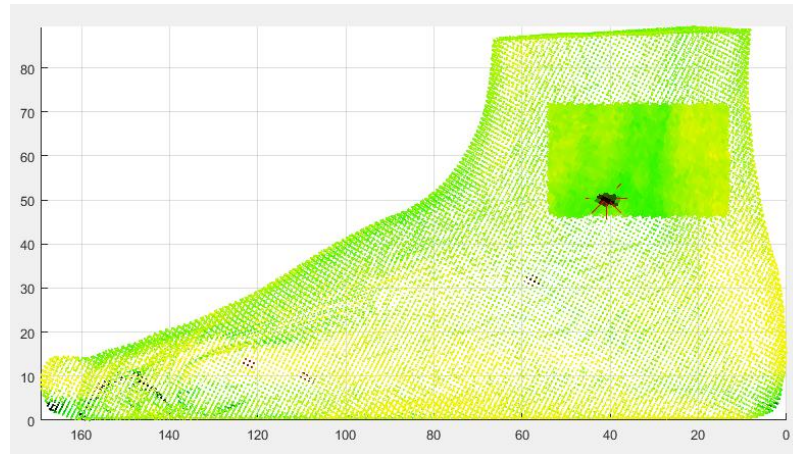
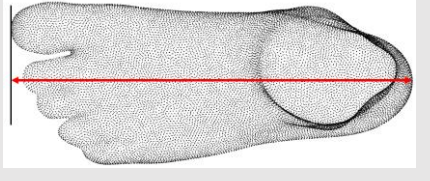
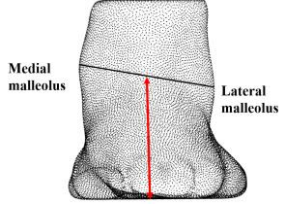
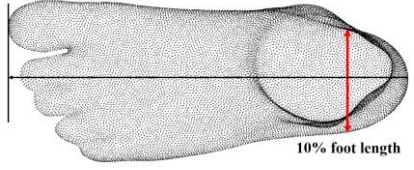
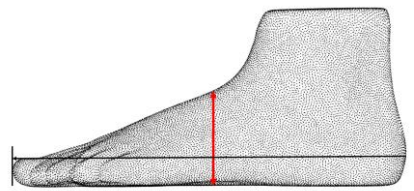
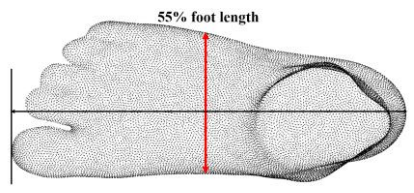
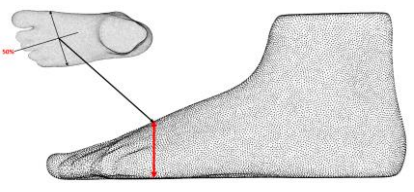
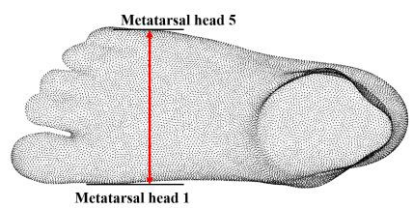


Figure 21.: Search area (darker green) and the located lateral malleolus (red star) on a point cloud of a 5-year-old child's foot. Black marks are the markers drawn on the foot.

From the four landmarks, two additional points were identified: fore-foot centre: the central point between metatarsal head one and five (calculated as the mean of the 3D coordinates of these two landmarks), and ankle centre: the midpoint between the medial and lateral malleolus (calculated as the mean of the 3D coordinates of these two landmarks). The following 2D measures were calculated in a custom-written script using these landmarks: foot length, rear-foot height, rear-foot width, mid-foot width, mid-foot height, fore-foot height and fore-foot width (Table 15.).

Table 15.: 2D measures derived from the 3D foot scans.

Linear measure	Description	
Foot length	Distance between the most posterior point of the heel and the end of the longest toe, projected onto the longitudinal axes	
Rear-foot height	The distance between the supporting surface and the 3D midpoint between the two malleoli.	
Rear-foot width	The distance between the most lateral and most medial point of the heel at 10% foot length (Jurca et al., 2019).	
Mid-foot height	The distance between the supporting surface and the foot's highest point at 55%-foot length (Jurca et al., 2019).	
Mid-foot width	The distance between the most lateral and most medial point of the foot at 55% of foot length.	
Fore-foot height	The distance between the supporting surface and the midpoint between the two metatarsal heads.	
Fore-foot width	Distance between the markers located on the first and fifth metatarsal heads projected onto the foot's medio-lateral axis.	

To compare the 2D measures between subjects with different foot sizes, and to appropriately track the static foot size and shape through development, all measures were also normalized

to foot length (Aboelnasr et al., 2018). This was calculated by dividing all dimensions by foot length and multiplying by 100. This approach created a percentage of foot length value for a better conceptualization of the normalized measures. Although it has been suggested that normalization to truncated foot length might be more appropriate to avoid bias caused by toe deformities, children of the age-groups of the present study rarely suffer from such deformities. Any related deformities would have been self-reported by the parents, and the child would have been excluded from the study.

4.2.5. Statistical analysis

All data were analysed using SPSS (version 16). A priory sample size calculations using data from Muller et al. (2012) were conducted for foot length, fore-foot width and normalized fore-foot width (fore-foot width divided by foot length) using G*Power (G*Power 3.1.9.7, Germany, Heinrich Heine University, Dusseldorf). The data used for the calculations can be seen in Table 16. This calculation provided sample size calculations for differences of 10mm, 2.6mm and 1% among age groups for foot length, fore-foot width and normalized fore-foot width, respectively.

Table 16.: Mean (standard deviation) of foot measures from Muller et al. (2012) in cm and % between the ages of three and seven years. ³

Age (years)	3 (n=676)	4 (n=834)	5 (n=938)	6 (n=931)	7 (n=787)
FL [cm]	15.71 (1.00)	16.74 (0.97)	17.71 (1.02)	18.69 (1.08)	19.74 (1.17)
FW [cm]	6.41 (0.41)	6.69 (0.42)	6.94 (0.42)	7.21 (0.46)	7.46 (0.45)
NFFW [%]	41 (2)	40 (2)	39 (2)	39 (2)	38 (2)

The sample size calculations were completed on the data from the age-groups 3 to 7 years, to estimate the total sample size needed for correctly rejecting the null hypothesis of no difference among age-groups at an alpha level of 0.05 with a power of 0.95. ANOVA sample size calculations yielded (1) for foot length a total sample size of 20 (effect size $f=1.29$), (2) for fore-foot width a total sample size of 35 (effect size $f=0.81$) and (3) for normalized fore-foot width a total sample size of 90 (effect size $f=0.48$). Sample size calculations were performed for each variable at a power level of 0.8, to estimate the sample sizes needed for each age-group to reject the null hypothesis of no difference correctly. This was set lower for the post-hoc tests than for the ANOVA because differences between subsequent age-

³ Abbreviations: FL: foot length, FW: foot width, NFFW normalized fore-foot width

groups have been reported to reach significance rarely. The two subsequent age-groups with the smallest absolute difference were chosen for each variable from Muller et al. (2012). The calculations for foot length between the 4 and 5-year-old groups (mean difference=0.97cm) yielded an estimated sample size of 14 per group (effect size $d=0.97$). The calculations for foot width between the 4 and 5-year-old groups (mean difference=0.25cm) yielded an estimated sample size of 36 per group (effect size $d=0.60$). The sample size calculations for normalized fore-foot width between the 4 and 5-year-old groups (mean difference=1%) estimated a sample size of 51 per group to correctly reject the null hypothesis of no difference (effect size $d=0.5$). The sample size needed to correctly reject the null hypothesis of no difference between non subsequent age-groups has also been calculated for fore-foot width and normalized fore-foot width, with a power of 0.95, as it was necessary to detect these differences correctly. For the fore-foot width, this calculation was based on the 3 and 5-year-old groups with a mean difference of 0.53cm and resulted in a required sample size of 15 per age-group (effect size $d=1.27$). For the normalized fore-foot width, the calculation was based on the largest difference between two age-groups of 2 years' difference: the 3 and 5-year-old age-groups (mean difference=2%). The calculations yielded a sample size of 23 per group (effect size $d=1$). Table 17. summarizes the required sample sizes for each test.

Table 17.: Sample size (n) estimates for ANOVA and t-tests estimated using data from Muller et al. (2012). ANOVA sample sizes are total sizes, including all five groups, while t-test sample sizes are per group.

Age (years)	ANOVA	t-test subsequent	t-test two years diff.
Foot length	20	15	
Fore-foot width	35	36	
Normalized fore-foot width	90	51	23

All 2D measures were tested for normality in each age-group, using the Shapiro-Wilks test as it is recommended to be used on small sample sizes and has been shown to have higher

power than other normality tests such as Kolmogorov-Smirnov (Razali and Wah, 2011, Ghasemi and Zahediasl, 2012). Only significant results are reported in the results section, all test results are presented in Appendix 3.

Scatter plots and error-bars within the same figures have been used to visualize changes in the 2D measures across ages. Red error-bar dots represent central tendency: either the mean or the median and variability: standard deviation or interquartile range (depending on the normality of the data).

In normally distributed data, to describe the trajectory of development, mean and standard deviation was used, and for statistical analysis, a one-way ANOVA was performed. This test allows the comparison of means of multiple groups and can ascertain whether there is a difference in the dependent variable among the groups. This test can also establish how much of the variance in a particular 2D measure can be accounted for by age-group membership, using the effect size eta squared. Once a significant result is ascertained, post-hoc tests can determine which pairs of groups have significantly different means, hence exploring differences between specific age groups. To compare all groups with unequal sample sizes, post-hoc Tukey-Kramer is suggested (Lee and Lee, 2018), and was used. The resulting p-value was divided by two to indicate a one-sided test as all absolute measures were expected to increase, while all normalized measures were expected to decrease.

The median and interquartile range was used to describe the data if the data was not normally distributed. The Kruskal-Wallis test was performed to explore the statistical differences between the groups as a non-parametric rank-based alternative to the parametric one-way ANOVA. Bonferroni corrected Dunn's post-hoc tests (Dinno, 2018) were performed to reveal which pairs of groups were significantly different. The resulting p-value was divided

by two to indicate a one-sided test as all absolute measures were expected to increase, while all normalized measures were expected to decrease.

Effect sizes as partial eta squared (Lakens, 2013) were calculated in SPSS using the data in the case of ANOVA. In Kruskal-Wallis tests, the eta squared were calculated based on Tomczak and Tomczak (2014). As the tests performed are one-way ANOVAs, the partial eta squared reported by SPSS is identical to eta squared (Lakens, 2013, Tomczak and Tomczak, 2014). This type of effect size measure assumes values from 0 to 1. When multiplied by 100, it indicates the percentage of variance in the dependent variable explained by the independent variable (Ialongo, 2016, Tomczak and Tomczak, 2014), or by group membership (Lakens, 2013), which in this case is age-group membership. The alpha level was set at 0.05 for all statistical tests. Effect size (Cohen's *d*) for the post-hoc tests were calculated by dividing the differences between the group means by the standard deviation.

4.3. Results

This section will first report the participant characteristics and age-group summaries. Next, foot length data will be considered, then the 2D measures in the following order: rear-foot measures, mid-foot measures and fore-foot measures. The measures within sections will be reported in the next order: (1) width, (2) normalized width, (3) height and (4) normalized height. The normality tests (Shapiro-Wilks) results are presented in Appendix 3., however significant results will also be included in the text. Next, the descriptive analysis will be presented using the appropriate central tendency and variability measures demonstrated in the mixed scatterplot and error bar figures. Following this, the omnibus (ANOVA or Kruskal-Wallis) test will be reported, and, if the omnibus test showed significance, post-hoc tests (parametric corrected Tukey-Kramer or non-parametric Bonferroni corrected Dunn's test) will be considered. Significant results in tables are highlighted grey, and levels of significance are marked by asterisk(s): *: $p < 0.05$, **: $p < 0.01$, ***: $p < 0.001$.

4.3.1. Whole body anthropometric characteristics of the participants

One hundred forty-eight children were recruited, 44 males and 104 females. The sample's anthropometric characteristics are reported in Table 18. Unfortunately, no further data collection could take place due to coronavirus restrictions. Although not all age-groups have reached the required sample size estimated by the a-priori sample size calculations for the post-hoc tests, the sample size needed for the ANOVA has been reached, even for the variable requiring the largest sample (normalized fore-foot width: 90). Except for the youngest group, all other age-groups have reached the estimated sample size 23 required for a group comparison between groups of two years' difference. Comparison of boys and girls has not been performed due to the low numbers in the age-groups and the extremely unbalanced ratios of girls and boys due to the convenience sampling method.

Table 18.: Anthropometric characteristics of the sample. Age is in years.

Age	N	Age (SD)	Height (cm) (SD)	Weight (kg) (SD)	BMI (SD)	Foot length (mm) (SD)
3	12	3.72 (0.32)	98 (4.5)	16.29 (2.19)	16.98 (2.09)	159.42 (10)
4	38	4.52 (0.47)	105 (6)	17.80 (2.15)	16.09 (1.51)	168.77 (10.15)
5	35	5.58 (0.57)	113 (5)	20.89 (2.63)	16.28 (1.88)	178.83 (10.07)
6	41	6.44 (0.46)	119 (6.25)	22.96 (3.48)	16.05 (2.54)	188.24 (11.24)
7	23	7.26 (0.35)	124 (6)	26.91 (4.07)	16.33 (2.01)	196.63 (11.43)
Total	148	5.67 (1.15)	113.25 (9.62)	21.22 (4.72)	16.38 (1.68)	180.38 (16.07)

4.3.2. 2D foot anthropometric results

4.3.2.1. Foot length

The Shapiro-Wilk tests showed that the foot length data of the 4-year-old group was not normally distributed (Shapiro-Wilk statistic=0.932, degrees of freedom (df)=38, p=0.023), hence the median and interquartile ranges were used to describe the data. Based on Figure 22., foot length increased continuously with age by 9-10mm each year. The youngest participants' median foot length was 159mm, while the median length for the oldest group was 197mm, indicating a 37mm growth in foot length across the five age groups. The interquartile ranges of the age groups were very similar (10-11mm), suggesting no substantial foot length variability changes.

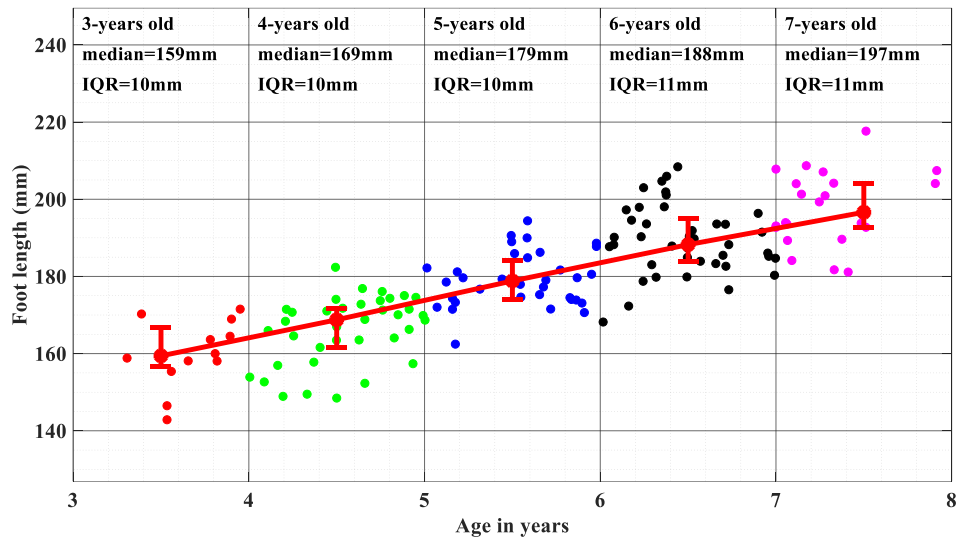


Figure 22.: Scatter plot and error-bars for foot length for each age-group. Error-bar dots represent the median; caps represent the median ±1 interquartile range.

Kruskal-Wallis H test was showed (Table 19.). a statistically significant difference between the foot length of different age groups ($\chi^2(2, N = 147) = 106.977, p = 0.000$). The proportion of variance in the ranked foot length accounted for by the age group variable was 73%.

Table 19.: ANOVA table of Kruskal-Wallis test for foot length comparing the age groups. SS: The sum of squares due to each source. ⁴

Source	SS	df	MS	Chi-sq.	Prob>Chi-sq.	Effect size
Groups	196587.360	4	49146.840	106.977	0.000***	
Error	73549.640	143	514.333	[]	[]	0.73
Total	270137	147	[]	[]	[]	

The pairwise Dunn's test results with Bonferroni correction showed a significant difference between the foot length of all groups except between the 3 and 4 and 6- and 7-years old groups (Table 20).

Table 20.: Foot length Dunn's post-hoc pairwise comparison tests and effect size. Significance values have been adjusted by the Bonferroni correction for multiple tests, divided by two to result in 1-sided significance. Significantly different pairs of groups are highlighted in grey. ⁵

Group 1 Group 2	Test Statistic	Std. Error	Std. Test Statistic	Sig.	Adj. Sig.	Effect size d
3-year-old group- 4-year-old group	-13.588	14.195	-.957	.169	1.000	0.73
3-year-old group- 5-year-old group	-53.767	14.340	-3.749	.000	.001**	2.44
3-year-old group- 6-year-old group	-85.825	14.070	-6.100	.000	.000***	3.34
3-year-old group- 7-year-old group	-105.530	15.384	-6.860	.000	.000***	4.11
4-year-old group- 5-year-old group	-40.179	10.043	-4.001	.000	.000**	1.68
4-year-old group- 6-year-old group	-72.237	9.653	-7.483	.000	.000***	2.66
4-year-old group- 7-year-old group	-91.943	11.484	-8.006	.000	.000***	3.47
5-year-old group- 6-year-old group	-32.059	9.865	-3.250	.000	.006**	1.30
5-year-old group- 7-year-old group	-51.764	11.663	-4.438	.000	.000***	2.26
6-year-old group- 7-year-old group	-19.705	11.329	-1.739	.041	.410	0.88

⁴ Df: Degrees of freedom. MS: The mean squares for each source, which is the ratio SS/df. Chi-sq.: Chi-square statistic. Prob> Chi-sq.: The p-value is the probability that the Chi-square statistic can take a value larger than the computed test-statistic value, derived from the cdf of Chi-square-distribution. *: p<0.05, **: p<0.005, ***: p<0.0005

⁵ Sig.: significance. Adj.Sig.: adjusted significance, *: p<0.05, **: p<0.005, ***: p<0.0005

4.3.2.2. Rear-foot

Rear-foot width

The Shapiro-Wilk tests showed that the rear-foot width values of the 7-year-old groups were not normally distributed (Shapiro-Wilk statistic=0.904, df=522, p=0.035); hence median and interquartile range was used to describe the data. Rear-foot width (Figure 23.) increased from 36mm in the youngest group to 44mm in the oldest group. The largest increase, 3mm, was between the two youngest age-groups. Variability was similar throughout the age-groups as demonstrated by the standard deviation: 3mm in the 3, 5 and 6-year-old groups, and 4mm in the 4 and 7-years old groups.

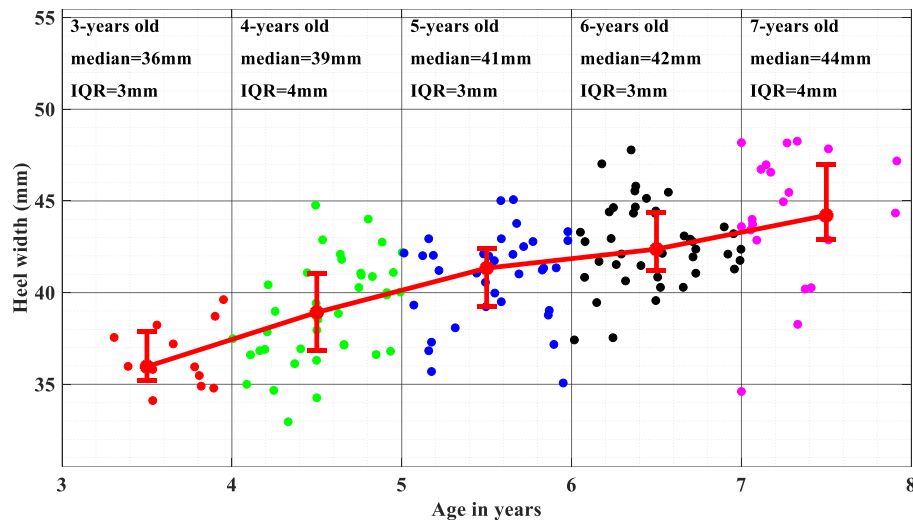


Figure 23.: Scatter plot and error-bars for rear-foot width for each age-group. Error-bar dots represent the mean; caps represent the mean ±1 standard deviation.

The Kruskal-Wallis H test (Table 21.) indicated a statistically significant difference between the rear-foot width of different age groups ($\chi^2(2, N = 147) = 61.88, p = 0.000$). The proportion of variance in the ranked rear-foot width accounted for by the age group variable was ~42%.

Table 21.: ANOVA table of Kruskal-Wallis test of rear-foot width comparing the age groups. SS: The sum of squares due to each source. ⁶

Source	SS	Df	MS	Chi-sq.	Prob>Chi-sq.	Eta squared
Groups	113712.51254	4	28428.13	61.88	0.000***	
Error	156424.49	143	1093.88	□	□	0.42
Total	270137	147	□	□	□	

The pairwise Dunn's test results with Bonferroni correction showed a significant difference between all groups' rear-foot width except between all subsequent age-groups (Table 22.).

Table 22.: Dunn's post-hoc pairwise comparison tests and effect size for rear-foot width. Significance values have been adjusted by the Bonferroni correction for multiple tests, divided by two to result in 1-sided significance. Significantly different pairs of groups are highlighted in grey.⁷

Sample 1 Sample 2	Test Statistic	Std. Error	Std. Test Statistic	Sig.	Adj. Sig.	Cohen's d
3-year-old group- 4-year-old group	-27.307	14.195	-1.924	.027	.272	1.06
3-year-old group- 5-year-old group	-51.562	14.340	-3.596	.000	.001**	2.06
3-year-old group- 6-year-old group	-75.285	14.070	-5.351	.000	.000***	3.05
3-year-old group- 7-year-old group	-92.652	15.384	-6.023	.000	.000***	2.95
4-year-old group- 5-year-old group	-24.255	10.043	-2.415	.008	.079	0.72
4-year-old group- 6-year-old group	-47.978	9.653	-4.970	.000	.000***	1.45
4-year-old group- 7-year-old group	-65.344	11.484	-5.690	.000	.000***	1.67
5-year-old group- 6-year-old group	-23.723	9.865	-2.405	.008	.081	0.75
5-year-old group- 7-year-old group	-41.090	11.663	-3.523	.000	.004**	1.14
6-year-old group- 7-year-old group	-17.367	11.329	-1.533	.063	0.626	0.56

⁶ Df: Degrees of freedom. MS: The mean squares for each source, which is the ratio SS/df. Chi-sq.: Chi-square statistic. Prob> Chi-sq.: The p-value is the probability that the Chi-square statistic can take a value larger than the computed test-statistic value, derived from the cdf of Chi-square-distribution. *: p<0.05, **: p<0.005, ***: p<0.0005

⁷ Sig.: significance. Adj.Sig.: adjusted significance, *: p<0.05, **: p<0.005, ***: p<0.0005

Normalized rear-foot width

The Shapiro-Wilk tests showed that the normalized rear-foot width data of the 7-years old group was not normally distributed (Shapiro-Wilk statistic=0.743, df=22, p=0.000), hence the median and interquartile range were used to describe the data. Normalized rear-foot width (Figure 24.) decreased from 24% in the 4-year-old group to 22% in the 6-year-old group and increased to 23% in the oldest group. The interquartile range (variability) was between 1-2% in all age-groups.

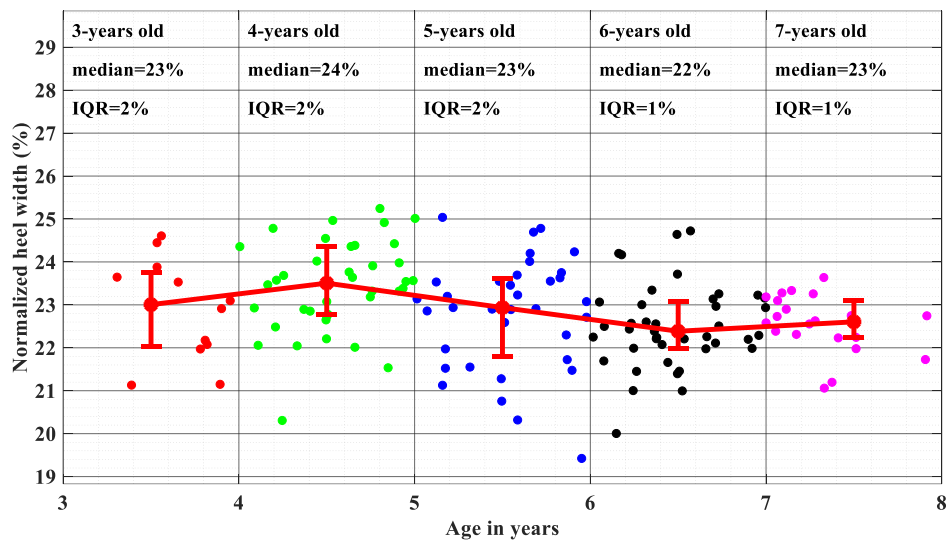


Figure 24.: Normalized rear-foot width scatter plot and error-bars for each age-group. Error-bar dots represent the median; caps represent the median ±1 interquartile range.

The Kruskal-Wallis H test (Table 23.) showed a statistically significant difference between the normalized rear-foot width of different age groups ($\chi^2(2, N = 147) = 18.40, p = 0.000$). The proportion of variance in the ranked normalized rear-foot width accounted for by the age group variable was 10%.

Table 23.: ANOVA table of Kruskal-Wallis test of normalized rear-foot width comparing the age groups. SS: The sum of squares due to each source. ⁸

Source	SS	df	MS	Chi-sq.	Prob>Chi-sq.	Effect size
Groups	33817.98	4	8454.49	18.40	0.001	
Error	236319.0233	143	1652.58	□	□	0.10
Total	270137	147	□	□	□	

The results of the pairwise Dunn's test with Bonferroni correction showed a significant difference between the normalized rear-foot width of the 4-6 and 4-7-year-old group pairs (Table 24.).

Table 24.: Dunn's post-hoc pairwise comparison tests and effect size for normalized rear-foot width. Significance values have been adjusted by the Bonferroni correction for multiple tests, divided by two to result in 1-sided significance. Significantly different pairs of groups are highlighted in grey. ⁹

Sample 1 Sample 2	Test Statistic	Std. Error	Std. Test Statistic	Sig.	Adj. Sig.	Effect size d
3-year-old group- 4-year-old group	-21.487	14.195	-1.514	.065	0.650	0.47
3-year-old group- 5-year-old group	-.507	14.340	-.035	.486	1.000	0.07
3-year-old group- 6-year-old group	-16.409	14.070	-1.166	.122	1.000	0.36
3-year-old group- 7-year-old group	-15.750	15.384	-1.024	.153	1.000	0.45
4-year-old group- 5-year-old group	-20.980	10.043	-2.089	.018	.184	0.52
4-year-old group- 6-year-old group	-37.895	9.653	-3.926	.000	.000***	0.90
4-year-old group- 7-year-old group	-37.237	11.484	-3.242	.000	.006**	0.95
5-year-old group- 6-year-old group	-16.916	9.865	-1.715	.043	.432	0.26
5-year-old group- 7-year-old group	16.257	11.663	1.394	.082	0.817	0.36
6-year-old group- 7-year-old group	-.659	11.329	-.058	.477	1.000	0.14

⁸ Df: Degrees of freedom. MS: The mean squares for each source, which is the ratio SS/df. Chi-sq.: Chi-square statistic. Prob> Chi-sq.: The p-value is the probability that the Chi-square statistic can take a value larger than the computed test-statistic value, derived from the cdf of Chi-square-distribution. *: p<0.05, **: p<0.005, ***: p<0.0005

⁹ Sig.: significance. Adj.Sig.: adjusted significance, *: p<0.05, **: p<0.005, ***: p<0.0005

Rear-foot height

All age-groups' rear-foot height data were normally distributed; hence mean and standard deviation were used to describe the data. Rear-foot height (Figure 25.), continuously increased with age from 46mm to 58mm. The differences between age groups varied between 2 and 5 mm. The largest, 5mm increase occurred between the 4 and 5-year-old groups. The variability represented by the standard deviation was between 3 and 4mm, with no substantial differences among the age-groups.

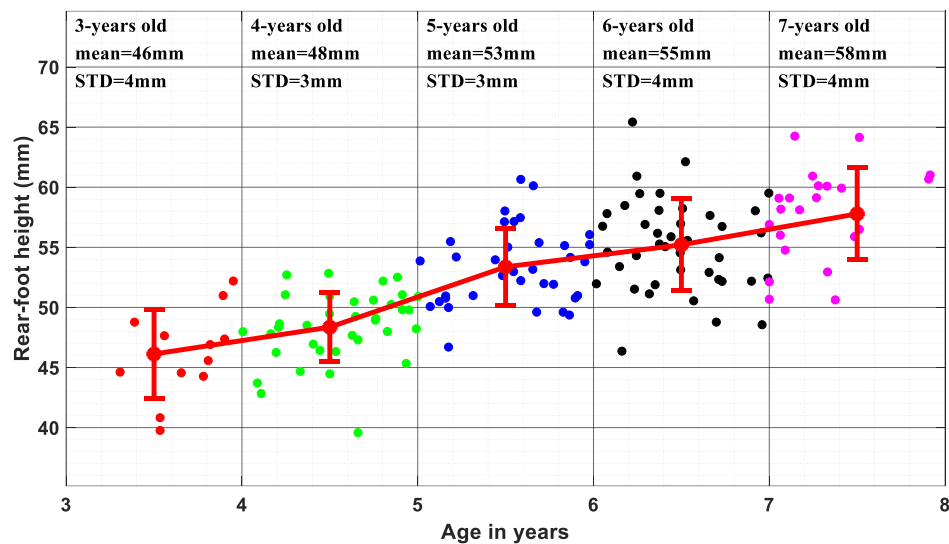


Figure 25.: Rear-foot height scatter plot and error-bars for all age-groups. Error-bar red dots represent the mean and caps represent the mean ± 1 standard deviation.

The one-way ANOVA (Table 25.) showed differences in the mean of rear-foot height among the age-groups, and the proportion of variance accounted for by the age group variable was 55%.

Table 25.: ANOVA table of one-way ANOVA test for rear-foot height comparing the age groups. *: $p < 0.05$, **: $p < 0.005$, ***: $p < 0.0005$

	Sum of Squares	degrees of freedom	Mean Square	F statistics	Sig.	Eta squared
Between Groups	2077.171	4	519.293	43.780	.000***	
Within Groups	1696.164	143	11.861			0.55
Total	3773.335	147				

The pairwise Tukey-Kramer test results (Table 26.) demonstrated that the rear-foot height means of all pairs of age-groups were significantly different except for the pairs of 3 and 4, and 5 and 6-years old groups.

Table 26.: Rear-foot height Tukey-Kramer post-hoc tests. Significance values have been adjusted by the Bonferroni correction for multiple tests, divided by two to result in 1-sided significance. The mean difference is in mm. significantly different pairs are highlighted grey. *: $p < 0.05$, **: $p < 0.005$, ***: $p < 0.0005$.

(I) Group (J) Group	Mean Difference (I-J)	Std. Error	Sig.	95% Confidence Interval		Effect size d
				Lower Bound	Upper Bound	
3-year-old group- 4-year-old group	-2.234	1.140	.145	-5.3852	.9166	0.68
3-year-old group- 5-year-old group	-7.249	1.152	.000***	-10.432	-4.066	2.11
3-year-old group- 6-year-old group	-9.086	1.130	.000***	-12.209	-5.962	2.42
3-year-old group- 7-year-old group	-11.658	1.236	.000***	-15.072	-8.243	3.11
4-year-old group- 5-year-old group	-5.014	.807	.000***	-7.244	-2.785	1.54
4-year-old group- 6-year-old group	-6.851	.776	.000***	-8.994	-4.708	2.05
4-year-old group- 7-year-old group	-9.423	.923	.000***	-11.972	-6.874	2.84
5-year-old group- 6-year-old group	-1.837	.793	.073	-4.027	.3530	0.52
5-year-old group- 7-year-old group	-4.409	.937	.000***	-6.998	-1.820	1.26
6-year-old group- 7-year-old group	-2.572	.910	.021*	-5.087	-.057	0.67

Normalized rear-foot height

All age-group data of normalized rear-foot height were normally distributed according to the Shapiro-Wilks tests; hence means and standard deviations were employed to describe the data. The mean of normalized rear-foot height, was 29-30% throughout the age-groups. The variability represented by the standard deviation was 1-2% across all age groups (Figure 26.).

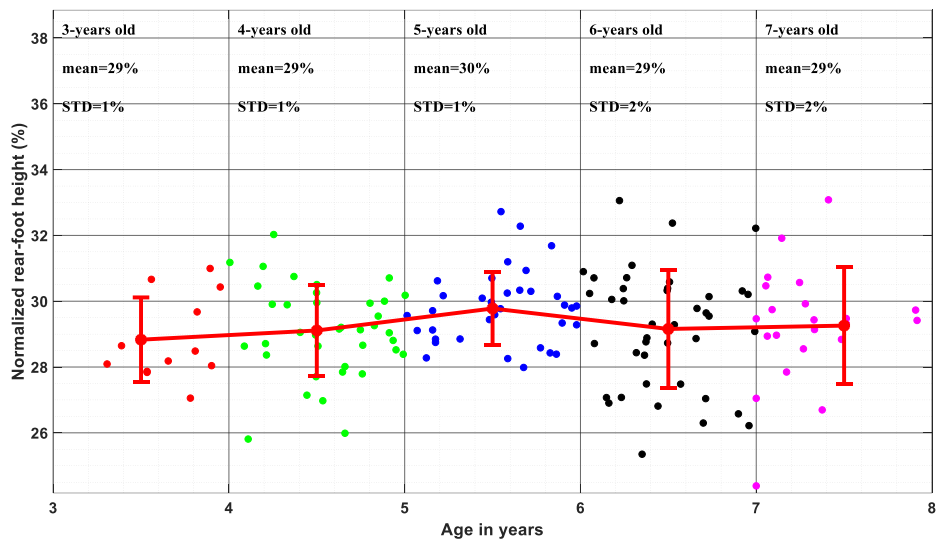


Figure 26.: Normalized rear-foot height scatter plot and error-bars for all age-groups. Error-bar red dots represent the mean and caps represent the mean ±1 standard deviation.

The one-way ANOVA (Table 27.) showed no differences in the mean of normalized rear-foot height among the age-groups, and the proportion of variance accounted for by the age group variable was only 4%.

Table 27.: ANOVA table of one-way ANOVA test for normalized rear-foot height comparing the age groups. *: p<0.05, **: p<0.005, ***: p<0.0005.

	Sum of Squares	° of freedom	Mean Square	F statistics	Sig.	Eta squared
Between Groups	12.835	4	3.209	1.412	.233	
Within Groups	324.891	143	2.272			0.04
Total	337.726	147				

4.3.2.3. Mid-foot

Mid-foot width

All age-group mid-foot width data were normally distributed; hence, the mean and standard deviation were used to describe the data. Mid-foot width means (Figure 27.) increased gradually from 59mm in the youngest group up to 67mm in the two oldest age groups by 2-3mm each year. The variability represented by the standard deviation was 4mm in most age-groups except for the 4-year-old group where it was 3mm.

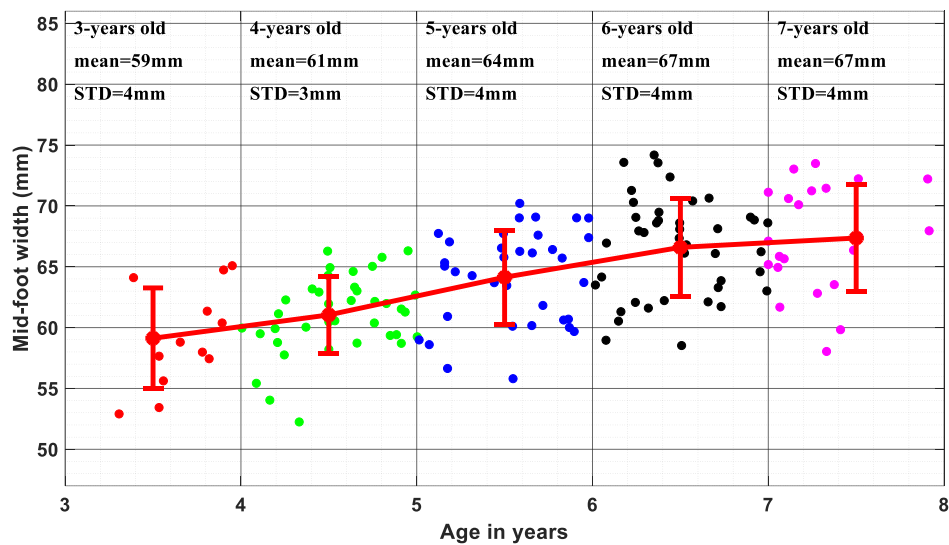


Figure 27.: Mid-foot width (mm) scatter plot and error-bars for all age-groups. Error-bar red dots represent the mean and caps represent the mean ±1 standard deviation.

The one-way ANOVA (Table 28.) showed differences in the mean of mid-foot width among the age-groups, and the proportion of variance accounted for by the age group variable was ~35%.

Table 28.: ANOVA table of one-way ANOVA test for mid-foot width comparing the age groups. *: p<0.05, **: p<0.005, ***: p<0.0005.

	Sum of Squares	degrees of freedom	Mean Square	F statistics	Sig.	Eta squared
Between Groups	1141.042	4	285.261	19.186	.000***	
Within Groups	2126.139	143	14.868			0.35
Total	3267.182	147				

The pairwise Tukey-Kramer results (Table 29.) demonstrated that the mid-foot width means of all pairs of age-groups were significantly different except for the pairs of 3 and 4; and 6- and 7-years old groups.

Table 29.: Mid-foot width Tukey-Kramer post-hoc tests. Significance values have been adjusted by the Bonferroni correction for multiple tests, divided by two to result in 1-sided significance. The mean difference is in mm. significantly different pairs are highlighted grey. *: $p < 0.05$, **: $p < 0.005$, ***: $p < 0.0005$.

(I) Group (J) Group	Mean Diff. (I-J)	Std. Error	Sig.	95% Confidence Interval		Effect size d
				Lower Bound	Upper Bound	
3-year-old group- 4-year-old group	-1.917	1.277	0.282	-5.445	1.611	0.530
3-year-old group- 5-year-old group	-5.013	1.290	.000***	-8.576	-1.449	1.260
3-year-old group- 6-year-old group	-7.468	1.266	.000***	-10.965	-3.971	1.830
3-year-old group- 7-year-old group	-8.235	1.384	.000***	-12.058	-4.412	1.920
4-year-old group- 5-year-old group	-3.096	0.903	.004**	-5.592	-0.600	0.880
4-year-old group- 6-year-old group	-5.551	0.868	.000***	-7.950	-3.152	1.540
4-year-old group- 7-year-old group	-6.318	1.033	.000***	-9.172	-3.464	1.660
5-year-old group- 6-year-old group	-2.455	0.887	.025*	-4.907	-0.004	0.620
5-year-old group- 7-year-old group	-3.222	1.049	.011*	-6.121	-0.324	0.790
6-year-old group- 7-year-old group	-0.767	1.019	0.472	-3.583	2.048	0.180

Normalized mid-foot width

The Shapiro-Wilk tests showed that the normalized mid-foot width data of the 6-year-old group was not normally distributed (Shapiro-Wilk statistic=0.945, df=41, p=0.046*), hence median and interquartile range was used to describe the data. Normalized mid-foot width decreased gradually with increasing age from 37% in the youngest group, to 34% in the oldest group, decreasing by 1mm in each subsequent age-group after the age of 4 years amounting to a 3% decrease (Figure 28.). The variability represented by the interquartile range was 2% in each age-group except for the 4-years old group where it was 3%.

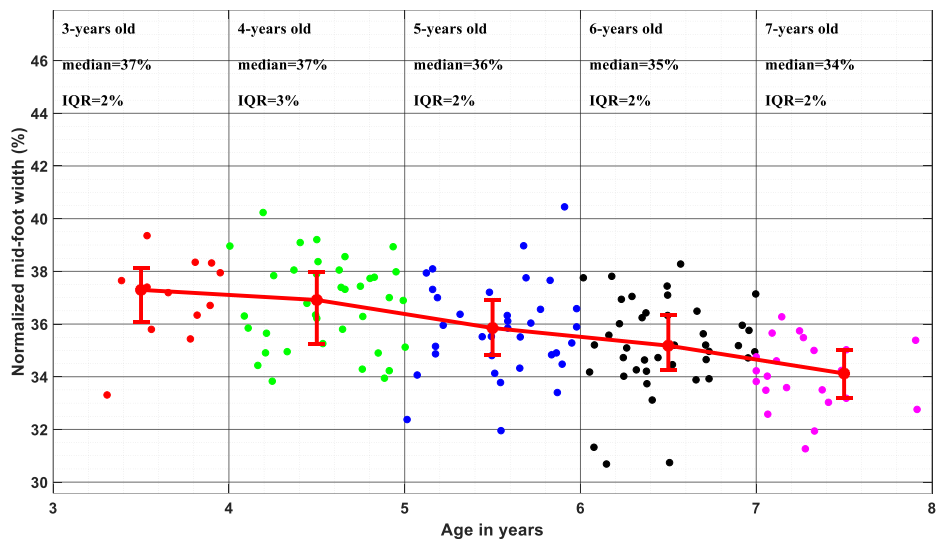


Figure 28.: Normalized mid-foot width scatter plot and error-bars for all age-groups. Error-bar red dots represent the median and caps represent the median ±1 interquartile range (IQR).

The Kruskal-Wallis H test (Table 30.) showed a statistically significant difference between the normalized mid-foot width of different age groups ($\chi^2(2, N = 147) = 38.30, p = 0.000$).

The proportion of variance in the ranked normalized mid-foot width accounted for by the age group variable was 26%.

Table 30.: ANOVA table of Kruskal-Wallis test for normalized mid-foot width comparing the age groups. *: $p < 0.05$, **: $p < 0.005$, ***: $p < 0.0005$

Source	SS	Df	MS	Chi-sq.	Prob>Chi-sq.	Effect size
Groups	70397.617	4.000	17599.404	38.308	0.000***	
Error	199739.383	143.000	1396.779	[]	[]	0.26
Total	270137.000	147.000	[]	[]	[]	

The pairwise Dunn's test results with Bonferroni correction (Table 31.) showed that the normalized mid-foot width of the 3 and 4-year-old groups were significantly different from the 6 and 7-year-old groups and the 5-year-old group was significantly different from the 7-years old group.

Table 31.: Normalized mid-foot width Dunn's post-hoc pairwise comparison tests and effect size. Significance values have been adjusted by the Bonferroni correction for multiple tests, divided by two to result in 1-sided significance. Significantly different pairs of groups are highlighted in grey.¹⁰

Sample 1 Sample 2	Test Statistic	Std. Error	Std. Test Statistic	Sig.	Adj. Sig. ^a	Effect size d
3-year-old group- 4-year-old group	7.487	14.195	.527	.299	1.000	0.14
3-year-old group- 5-year-old group	28.993	14.340	2.022	.022	.220	0.70
3-year-old group- 6-year-old group	41.957	14.070	2.982	.001	.014*	1.09
3-year-old group- 7-year-old group	69.614	15.384	4.525	.000	.000***	2.01
4-year-old group- 5-year-old group	21.506	10.043	2.141	.016	.161	0.56
4-year-old group- 6-year-old group	34.470	9.653	3.571	.000	.002**	0.94
4-year-old group- 7-year-old group	62.127	11.484	5.410	.000	.000***	1.79
5-year-old group- 6-year-old group	12.964	9.865	1.314	.095	0.945	0.36
5-year-old group- 7-year-old group	40.621	11.663	3.483	.000	.002**	1.13
6-year-old group- 7-year-old group	27.656	11.329	2.441	.007	.073	0.72

¹⁰ Sig.: significance. Adj.Sig.: adjusted significance, *: $p < 0.05$, **: $p < 0.005$, ***: $p < 0.0005$

Mid-foot height

All age-group mid-foot height data were normally distributed; hence, mean, and standard deviation were used to describe the data. There was a continuous increase in this measure (Figure 29), and the largest difference in mid-foot height was between the ages of 4 and 5 years (3mm). After the age of 5 years, there was an increase of 1mm only in each subsequent age-group leading to a mid-foot height of 47mm in 7-year-old children. Variability represented by the standard deviation was between 3 and 5mm, the highest variability was in the 3-year-old group (5mm).

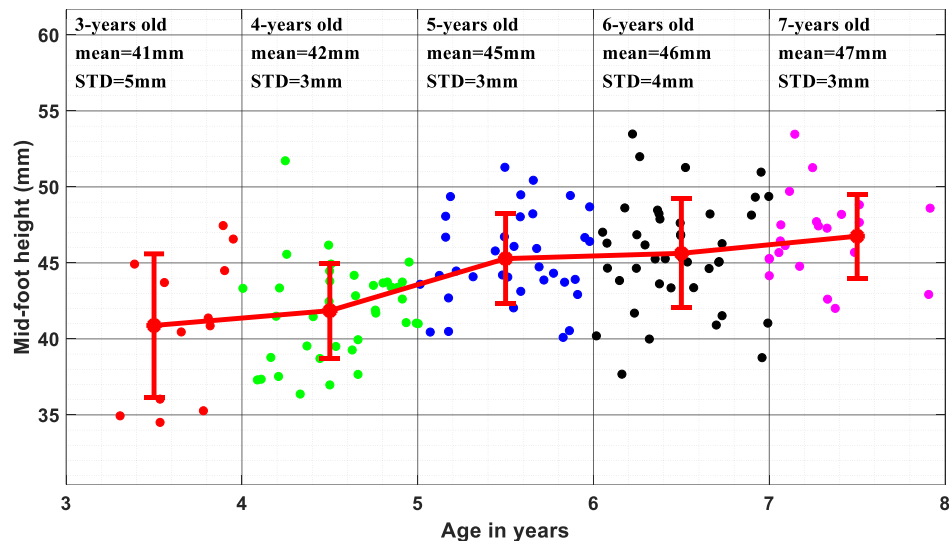


Figure 29.: Mid-foot height scatter plot and error-bars for each age-group. Error-bars' red dot represents the mean of each age-group, caps represent the mean ±1 standard deviation.

The one-way ANOVA (Table 32.) showed differences in the mean of mid-foot height among the age-groups, and the proportion of variance accounted for by the age group variable was ~28%.

Table 32.: ANOVA table of one-way ANOVA test for mid-foot height comparing the age groups. *: p<0.05, **: p<0.005, ***: p<0.0005.

	Sum of Squares	degrees of freedom	Mean Square	F statistics	Sig.	Eta squared
Between Groups	605.462	4	151.366	13.719	.000***	
Within Groups	1577.756	143	11.033			0.28
Total	2183.218	147				

The pairwise Tukey-Kramer results (Table 33.) demonstrated that the mid-foot height of the 3-year-old group was significantly different from that of the 5, 6 and 7-year-old groups. The 4-year-old group was significantly different from the 5, 6 and 7-year-old groups.

Table 33.: Mid-foot height Tukey-Kramer post-hoc tests. Significance values have been adjusted by the Bonferroni correction for multiple tests, divided by two to result in 1-sided significance. The mean difference is in mm. significantly different pairs are highlighted grey. *: $p < 0.05$, **: $p < 0.005$, ***: $p < 0.0005$.

(I) Group (J) Group	Mean Difference (I-J)	Std. Error	Sig.	95% Confidence Interval		Effect size d
				Lower Bound	Upper Bound	
3-year-old group- 4-year-old group	-0.974	1.100	0.451	-4.013	2.065	0.250
3-year-old group- 5-year-old group	-4.400	1.111	.000***	-7.470	-1.330	1.210
3-year-old group- 6-year-old group	-4.747	1.090	.000***	-7.759	-1.735	1.150
3-year-old group- 7-year-old group	-5.874	1.192	.000***	-9.167	-2.581	1.570
4-year-old group- 5-year-old group	-3.426	0.778	.000***	-5.576	-1.276	1.130
4-year-old group- 6-year-old group	-3.773	0.748	.000***	-5.840	-1.707	1.120
4-year-old group- 7-year-old group	-4.900	0.890	.000***	-7.358	-2.441	1.660
5-year-old group- 6-year-old group	-0.347	0.764	0.496	-2.459	1.765	0.110
5-year-old group- 7-year-old group	-1.474	0.904	0.240	-3.971	1.023	0.520
6-year-old group- 7-year-old group	-1.127	0.878	0.351	-3.552	1.299	0.360

Normalized mid-foot height

Since all normalized mid-foot height data were normally distributed, mean, and standard deviation were used to describe the data. Figure 30. demonstrated that normalized mid-foot height decreased from the age of 3 to 4 years from 26% to 25%, and it did not change into the age of five. After the age of five, it decreased to 24% by the age of six and remained the same in the oldest age group. The variability represented by the standard deviation was 2% in each ag-group, except for the 5-year-old groups, where it was 1%.

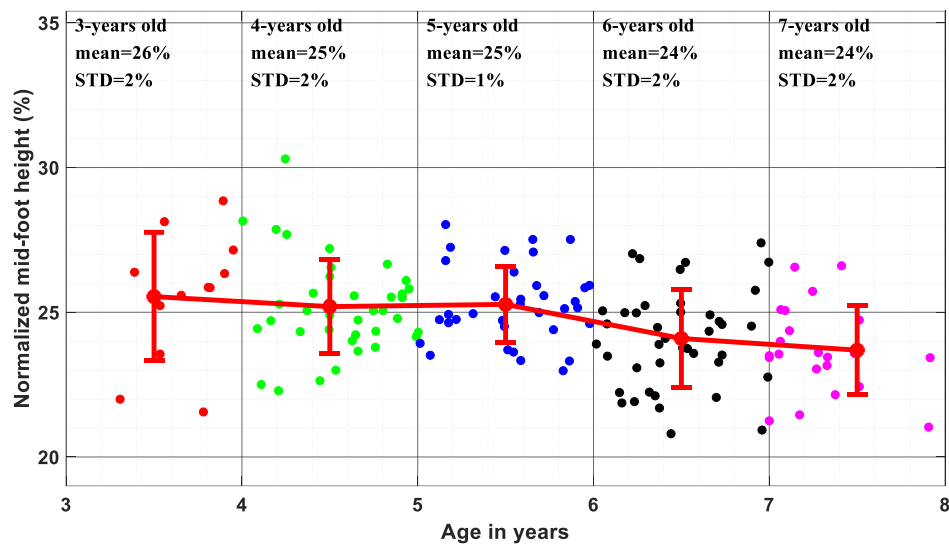


Figure 30.: Normalized mid-foot height scatter plot and error-bars for all age-groups. Error-bar red dots represent the mean and caps represent the mean ± 1 standard deviation.

The one-way ANOVA (Table 34.) showed differences in the mean of normalized mid-foot height among the age-groups, and the proportion of variance accounted for by the age group variable was 13%.

Table 34.: ANOVA table of one-way ANOVA test for normalized mid-foot height comparing the age groups. *: $p < 0.05$, **: $p < 0.005$, ***: $p < 0.0005$.

	Sum of Squares	degrees of freedom	Mean Square	F statistics	Sig.	Eta squared
Between Groups	66.675	4	16.669	6.349	.000***	
Within Groups	375.456	143	2.626			0.13
Total	442.131	147				

The pairwise Tukey-Kramer results (Table 35.) demonstrated that the normalized mid-foot height means of the 3-year-old group was significantly different from the 7-year-old group. The 4-year-old group was significantly different from the 6 and 7-year-old groups, and the 5-year-old group was significantly different from the 6 and 7-year-old groups.

Table 35.: Normalized mid-foot height Tukey-Kramer post-hoc tests. Significance values have been adjusted by the Bonferroni correction for multiple tests, divided by two to result in 1-sided significance. The mean difference is in mm. significantly different pairs are highlighted grey. *: $p < 0.05$, **: $p < 0.005$, ***: $p < 0.0005$.

(I) Group (J) Group	Mean Difference (I-J)	Std. Error	Sig.	95% Confidence Interval		Effect size d
				Lower Bound	Upper Bound	
3-year-old group- 4-year-old group	0.345	0.537	0.484	-1.137	1.828	0.180
3-year-old group- 5-year-old group	0.268	0.542	0.494	-1.230	1.766	0.150
3-year-old group- 6-year-old group	1.447	0.532	.028*	-0.023	2.916	0.740
3-year-old group- 7-year-old group	1.849	0.582	.015*	0.242	3.455	0.990
4-year-old group- 5-year-old group	-0.077	0.380	1.000	-1.126	0.972	0.050
4-year-old group- 6-year-old group	1.101	0.365	.025*	0.093	2.110	0.660
4-year-old group- 7-year-old group	1.504	0.434	.003**	0.304	2.703	0.950
5-year-old group- 6-year-old group	1.179	0.373	.008*	0.148	2.209	0.780
5-year-old group- 7-year-old group	1.581	0.441	.002**	0.363	2.799	1.110
6-year-old group- 7-year-old group	0.402	0.428	0.441	-0.781	1.585	0.250

4.3.2.4. Fore-foot

Fore-foot width

All fore-foot width data were normally distributed; hence, mean, and standard deviation were used to describe the data. Fore-foot width increased from 63mm to 73mm (Figure 31.). Up to the age of 6, there was 3mm increase each year, while it only increased by 1mm between the two oldest age-groups. The variability represented by standard deviation remained the same (4mm) in all age groups.

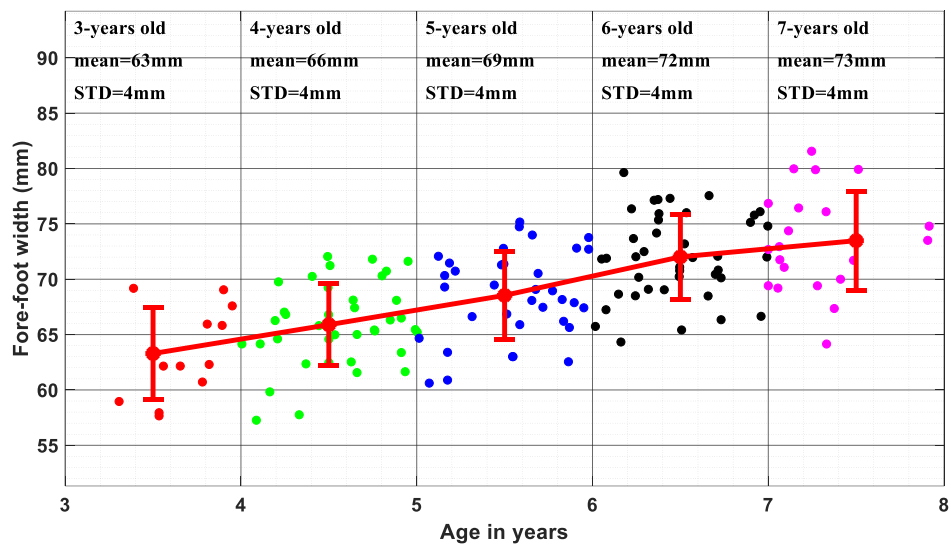


Figure 31.: Fore-foot width scatter plot and error-bars for all age-groups. Error-bar red dots represent the mean and caps represent the mean ± 1 standard deviation.

The one-way ANOVA (Table 36.) showed differences in the mean of fore-foot width among the age-groups and the proportion of variance accounted for by the age group variable was 41%.

Table 36.: ANOVA table of one-way ANOVA test for fore-foot width comparing the age groups. *: $p < 0.05$, **: $p < 0.005$, ***: $p < 0.0005$

	Sum of Squares	degrees of freedom	Mean Square	F statistics	Sig.	Eta squared
Between Groups	1579.174	4	394.793	25.270	.000***	
Within Groups	2234.072	143	15.623			0.41
Total	3813.246	147				

The pairwise Tukey-Kramer test results (Table 37.) demonstrated that the fore-foot width means of all pairs of age-groups were significantly different except for the pairs of 3 and 4; and 6- and 7-years old groups.

Table 37.: Fore-foot width Tukey-Kramer post-hoc tests. Significance values have been adjusted by the Bonferroni correction for multiple tests, divided by two to result in 1-sided significance. The mean difference is in mm. significantly different pairs are highlighted grey. *: $p < 0.05$, **: $p < 0.005$, ***: $p < 0.0005$.

(I) Group (J) Group	Mean Diff. (I-J)	Std. Error	Sig.	95% Confidence Interval		Effect size d
				Lower Bound	Upper Bound	
3-year-old group- 4-year-old group	-2.602	1.309	0.139	-6.218	1.014	0.660
3-year-old group- 5-year-old group	-5.252	1.322	.000***	-8.905	-1.598	1.300
3-year-old group- 6-year-old group	-8.730	1.297	.000***	-12.314	-5.146	2.190
3-year-old group- 7-year-old group	-10.194	1.418	.000***	-14.113	-6.275	2.370
4-year-old group- 5-year-old group	-2.649	0.926	.019*	-5.208	-0.091	0.690
4-year-old group- 6-year-old group	-6.128	0.890	.000***	-8.587	-3.669	1.630
4-year-old group- 7-year-old group	-7.591	1.059	.000***	-10.517	-4.666	1.860
5-year-old group- 6-year-old group	-3.478	0.910	.001*	-5.992	-0.965	0.930
5-year-old group- 7-year-old group	-4.942	1.075	.000***	-7.913	-1.971	1.210
6-year-old group- 7-year-old group	-1.464	1.045	0.314	-4.350	1.423	0.350

Normalized fore-foot width

The Shapiro-Wilk tests showed that the normalized fore-foot width data of the 4-year-old group was not normally distributed (Shapiro-Wilk statistic=0.934, df=38, p=0.027*).

Normalized fore-foot width decreased gradually from the age of 3 years from 40% to 37% in the 7-year-old group by 1% each year, except between the 4 and 5-year-old groups, where there was no change (Figure 32.). Variability represented by the standard deviation stayed between 1 and 3% throughout.

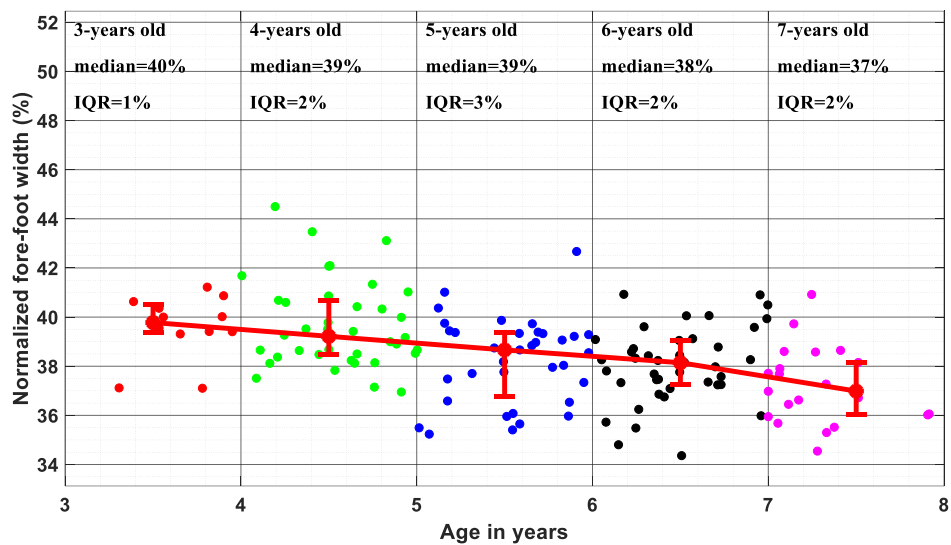


Figure 32.: Normalized fore-foot width scatter plot and error-bars for all age-groups. Error-bar red dots represent the median and caps represent the median ±1 interquartile range (IQR).

The Kruskal-Wallis H test (Table 38.) showed a statistically significant difference between the normalized fore-foot width of different age groups ($\chi^2(2, N = 147) = 33.33, p = 0.000$).

The proportion of variance in the ranked normalized fore-foot width accounted for by the age group variable was ~23%.

Table 38.: ANOVA table of Kruskal-Wallis test for normalized fore-foot width comparing the age groups. SS: The sum of squares due to each source. ¹¹

Source	SS	df	MS	Chi-sq.	Prob>Chi-sq.	Effect size
Groups	61240.50	4.00	15310.13	33.33	0.000***	
Error	208896.50	143.00	1460.81	□	□	0.23
Total	270137.00	147.00	□	□	□	

The pairwise Dunn's test results (Table 39.) with Bonferroni correction showed that the normalized fore-foot width of the 3 and 4-year-old groups was significantly different from the 6 and 7-year-old group and the 4-year-old group was also significantly different from the 5-year-old group.

Table 39.: Normalized fore-foot width Dunn's post-hoc pairwise comparison tests and effect size. Significance values have been adjusted by the Bonferroni correction for multiple tests, divided by two to result in 1-sided significance. Significantly different pairs of groups are highlighted in grey.¹²

Sample 1 Sample 2	Test Statistic	Std. Error	Std. Test Statistic	Sig.	Adj. Sig. ^a	Effect size d
3-year-old group- 4-year-old group	6.373	14.195	.449	.327	1.000	0.05
3-year-old group- 5-year-old group	34.683	14.340	2.419	.008	.078	0.88
3-year-old group- 6-year-old group	41.352	14.070	2.939	.002	.016*	1.09
3-year-old group- 7-year-old group	62.492	15.384	4.062	.000	.000**	1.69
4-year-old group- 5-year-old group	28.311	10.043	2.819	.002	.024*	0.80
4-year-old group- 6-year-old group	34.979	9.653	3.624	.000	.001**	0.99
4-year-old group- 7-year-old group	56.120	11.484	4.887	.000	.000***	1.50
5-year-old group- 6-year-old group	6.668	9.865	.676	.246	1.000	0.14
5-year-old group- 7-year-old group	27.809	11.663	2.384	.009	.085	0.65
6-year-old group- 7-year-old group	21.141	11.329	1.866	.031	.310	0.55

¹¹ Df: Degrees of freedom. MS: The mean squares for each source, which is the ratio SS/df. Chi-sq.: Chi-square statistic. Prob> Chi-sq.: The p-value is the probability that the Chi-square statistic can take a value larger than the computed test-statistic value, derived from the cdf of Chi-square-distribution.

¹² Sig.: significance. Adj.Sig.: adjusted significance, *: p<0.05, **: p<0.005, ***: p<0.0005

Fore-foot height

All age-groups' fore-foot height data were normally distributed; hence mean and the standard deviation were used to describe the data. Fore-foot height increased between the 4- and 5-year-old children from 11mm up to 12mm and remained the same in the older age groups (Figure 33.). The variability represented by the standard deviation was 1mm in all age-groups except for the 6-year-old group where it was 2mm.

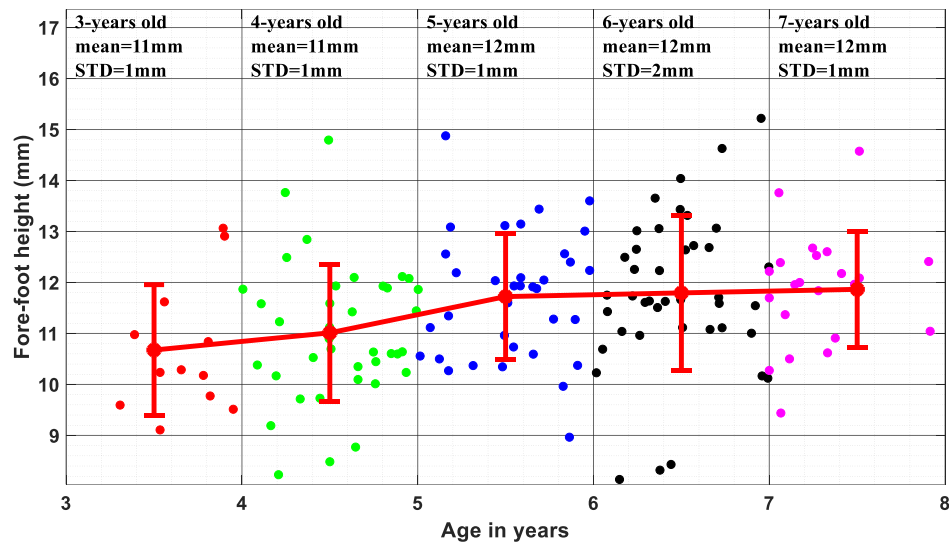


Figure 33.: Fore-foot height scatter plot and error-bars for all age-groups. Error-bar red dots represent the mean and caps represent the mean ± 1 standard deviation.

The one-way ANOVA (Table 40.) showed significant differences in the mean of fore-foot height among the age-groups, and the proportion of variance accounted for by the age group variable was 9%.

Table 40.: ANOVA table of one-way ANOVA test for fore-foot height comparing the age groups. *: $p < 0.05$, **: $p < 0.005$, ***: $p < 0.0005$.

	Sum of Squares	degrees of freedom	Mean Square	F statistics	Sig.	Eta squared
Between Groups	25.458	4	6.364	3.558	.008**	
Within Groups	255.762	143	1.789			0.09
Total	281.220	147				

The Tukey-Kramer post-hoc tests (Table 41.) showed significant differences between the fore-foot height of the 3 and 6 and 4 and 6-year-old groups.

Table 41.: Fore-foot height Tukey-Kramer post-hoc tests. Significance values have been adjusted by the Bonferroni correction for multiple tests, divided by two to result in 1-sided significance. The mean difference is in mm. significantly different pairs are highlighted grey. *: $p < 0.05$, **: $p < 0.005$, ***: $p < 0.0005$.

(I) Group (J) Group	Mean Diff. (I-J)	Std. Error	Sig.	95% Confidence Interval		Effect size d
				Lower Bound	Upper Bound	
3-year-old group- 4-year-old group	-.33743	.44285	.471	-1.5610	.8861	0.26
3-year-old group- 5-year-old group	-1.04801	.44738	.069	-2.2841	.1880	0.84
3-year-old group- 6-year-old group	-1.12061	.43894	.043*	-2.3334	.0921	0.80
3-year-old group- 7-year-old group	-1.19024	.47994	.051	-2.5163	.1358	0.98
4-year-old group- 5-year-old group	-.71058	.31332	.081	-1.5762	.1551	0.55
4-year-old group- 6-year-old group	-.78318	.30115	.038*	-1.6152	.0489	0.55
4-year-old group- 7-year-old group	-.85281	.35828	.064	-1.8427	.1371	0.68
5-year-old group- 6-year-old group	-.07260	.30777	.500	-.9229	.7777	0.05
5-year-old group- 7-year-old group	-.14223	.36387	.498	-1.1476	.8631	0.12
6-year-old group- 7-year-old group	-.06963	.35344	.500	-1.0462	.9069	0.05

Normalized fore-foot height

The Shapiro-Wilk tests showed that the normalized fore-foot height data of the 6-years old group was not normally distributed (Shapiro-Wilk statistic=0.927, df=41, p=0.012*), hence medians and interquartile ranges were used to describe the data. Median normalized fore-foot height was 6-7% in all age groups (Figure 34.). The variability represented by the standard deviation was 1% in all age-groups.

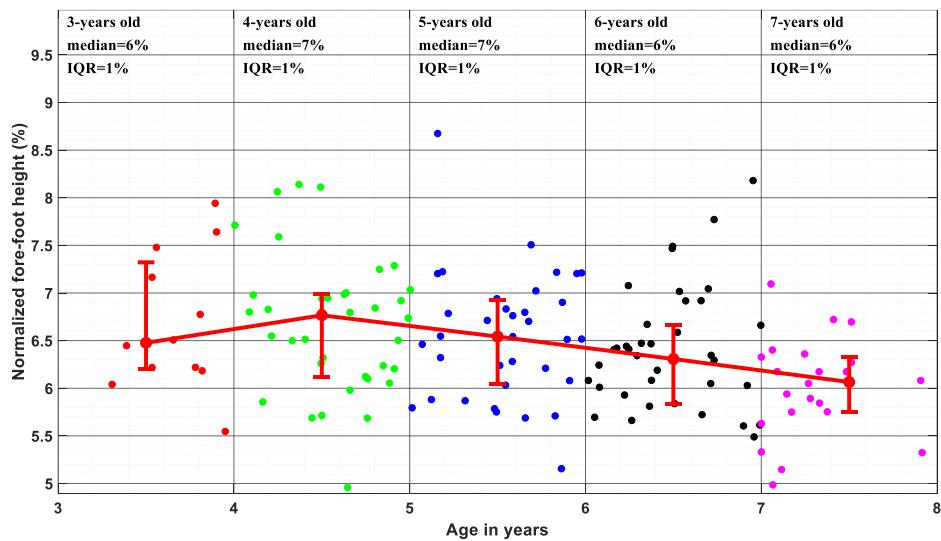


Figure 34.: Normalized fore-foot height scatter plot and error-bars for all age-groups. Error-bar red dots represent the median and caps represent the median ±1 interquartile range.

The Kruskal-Wallis H test (Table 42.) showed a statistically significant difference between the normalized fore-foot height of different age groups ($\chi^2(2, N = 147) = 15.39, p = 0.004$).

The proportion of variance in the ranked foot length accounted for by the age group variable was ~10%.

Table 42.: ANOVA table of Kruskal-Wallis test for normalized fore-foot height comparing the age groups. SS: The sum of squares due to each source. ¹³

Source	SS	df	MS	Chi-sq.	Prob>Chi-sq.	Effect size
Groups	28290.02	4.00	7072.51	15.39	.004**	
Error	241846.98	143.00	1691.24	□	□	0.10
Total	270137.00	147.00	□	□	□	

The pairwise Dunn's test (Table 43.) results with Bonferroni correction showed that the normalized fore-foot height of the 4 and 5-year-old groups were significantly different from the 7-year-old group.

Table 43.: Normalized fore-foot height Dunn's post-hoc pairwise comparison tests and effect size. Significance values have been adjusted by the Bonferroni correction for multiple tests, divided by two to result in 1-sided significance. Significantly different pairs of groups are highlighted in grey. ¹⁴

Pairwise Comparisons of Group							
Sample 1 Sample 2	Test Statistic	Std. Error	Std. Test Statistic	Sig.	Adj. Sig. ^a	Effect size d	
3-year-old group- 4-year-old group	-.693	14.195	-.049	.481	1.000	0.07	
3-year-old group- 5-year-old group	-4.776	14.340	-.333	.370	1.000	0.19	
3-year-old group- 6-year-old group	-20.248	14.070	-1.439	.075	.750	0.55	
3-year-old group- 7-year-old group	-38.833	15.384	-2.524	.006	.058	1.08	
4-year-old group- 5-year-old group	-5.469	10.043	-.545	.293	1.000	0.12	
4-year-old group- 6-year-old group	-20.941	9.653	-2.169	.015	.150	0.48	
4-year-old group- 7-year-old group	-39.526	11.484	-3.442	.000	.003**	0.97	
5-year-old group- 6-year-old group	-15.472	9.865	-1.568	.059	.585	0.39	
5-year-old group- 7-year-old group	-34.057	11.663	-2.920	.002	.018*	0.91	
6-year-old group- 7-year-old group	-18.585	11.329	-1.640	.051	.505	0.34	

¹³ Df: Degrees of freedom. MS: The mean squares for each source, which is the ratio SS/df. Chi-sq.: Chi-square statistic. Prob> Chi-sq.: The p-value is the probability that the Chi-square statistic can take a value larger than the computed test-statistic value, derived from the cdf of Chi-square-distribution.

¹⁴ Sig.: significance. Adj.Sig.: adjusted significance, *: p<0.05, **: p<0.005, ***: p<0.0005

4.4. Discussion of the 2D anthropometric measure results

The purpose of this study was to offer an understanding of 2D anthropometric foot development between the ages of 3 and 7 years, and to provide a contemporary dataset of 2D anthropometric paediatric foot measures. The study employed a hand-held 3D scanner, which has never been used before for this purpose. This technology allows the accurate and relatively fast capturing of children's foot shape in their environment, providing the opportunity to characterize the developmental trajectory of paediatric foot anthropometry. The objectives and research questions were the following.

Objective 1: Characterize the size development of foot regions in children aged 3-7 years.

Research questions:

- How do the dimensions of foot regions change during development?
- Is there a difference in the development of width among the three foot regions between the ages of 3 and 7 years?
- Is there a difference in height development among the three foot regions between the ages of 3 and 7 years?

Objective 2: Characterize the proportional development of foot regions in children aged 3-7 years.

Research questions:

- How do the proportions of foot regions change during development?
- Is there a difference in the development of width proportions among foot regions?
- Is there a difference in the development of height proportions among foot regions?

The study established the differences in 2D measures between age-groups and found differences in the trajectory of development among the three foot regions in width and height that suggested changes in foot shape across age-groups. Furthermore, differences in proportions of the rear-, mid and fore-foot with increasing age were also found. These results will be discussed in the following sections based on the objectives and research questions set out above. Foot length results will be discussed first then width and height measures of each region will be considered in a proximal to distal order, comparing the development of the three regions, answering the first set of research questions. Normalized measures will be considered next to discuss the differences in the three regions' proportional development, answering the second set of research questions.

4.4.1. Foot length

The results have shown that foot length increases by 9-10mm each year between 3 and 7 years of age, with an interquartile range of 10-11mm in each age-group. The statistics demonstrated significant differences between age-groups, except for the two youngest and the two oldest groups. The medians showed that foot length of age-groups was: 159mm, 169mm, 179mm, 188mm and 197mm.

Similar foot length data was shown in a German sample of children by Muller et al. (2012), demonstrating approximately 2mm shorter feet in each age-group, despite the dissimilar sex distribution. The German children had similar height, although their weight in the 4 and 6-year-old groups were slightly higher compared to the current sample. A Spanish sample (Jimenez-Ormeno et al., 2013) of children in the 6 and 7 year-old groups showed similar foot length (187.9mm and 197.8mm respectively), while another Spanish sample (Delgado-Abellán et al., 2014) demonstrated 2-3mm longer feet in the same age-groups. While the former study did not publish weight or height data (indicated normal weight), the latter

sample had higher weight in both age-groups, although their height was very similar. The study of Delgado-Abellán et al. (2014) also had more balanced sex distribution (66 boys and 67 girls in the 6, and 76 boys and 86 girls in the 7-year-old group) and showed 2-3mm longer feet in both age-groups. This could have contributed to the differences in the overall means\medians as the current study had 31 girls and 10 boys in the 6, and 17 girls and 5 boys in the 7-year-old group.

In contrast, the data from the study of Kouchi (1998), although showed similar magnitude of increase in foot length, the Japanese children had on average 6-10mm shorter feet (153.1mm 162.8mm 169.7mm 180.4mm 191.6mm in the respective age-groups). This large difference could be due to ethnic differences. Shorter feet of Asian populations (Jurca et al., 2019) and Japanese and Indonesian samples (Kouchi, 1998) have already been shown, although only in adults, and these differences might start to appear in childhood.

4.4.2. The size development of paediatric foot regions

4.4.2.1. Age-group differences in the width of foot regions

Rear-foot width

The results showed that rear-foot width increased by 1.8-2.3mm each year up to the age of 6 and only 1.6mm into the age of 7. The total increase in rear-foot width was 6mm up to the age of 6, and the statistical results also confirmed the growth trajectory of the rear-foot width. There were significant differences between all age groups except for between the two oldest groups. All effect sizes were at least medium, including the one concerning the non-significant difference. The effect sizes peaked between the ages of 3 and 7 years, but gradually decreased after the age of 4 (the effect sizes for the subsequent age groups are exceptions). The data demonstrated that rear-foot width growth was gradually slowing down with age (2.3mm, 1.9mm, 1.8mm, 1.6mm) up to the age of 7. A similar diminishing trajectory of growth has been shown in a longitudinal study, in a sample of German children (Sacco et al., 2015) with 1mm, 2.8mm, 1.5mm, and 1.4mm growth between subsequent age-groups from 3 to 7 years of age. Spanish children showed a similar increase in rear-foot width compared to the present thesis between 6 and 7 years of age (Delgado-Abellán et al., 2014), while another study reported an increase of only 0.6mm (Jimenez-Ormeno et al., 2013), almost one-third of that in the present study between the same age-groups. While both Spanish studies had large sample sizes and used the same 3D scanner, they reported different results between the 6 and 7-year-old groups. Unfortunately, the study of Jimenez-Ormeno et al. (2013) did not report anthropometric data such as height, weight, or BMI, hence a possible cause of differences between the studies cannot be investigated. Although both studies looked at Spanish children's feet, the regional differences between the samples could be part of the reason for the discrepancies in rear-foot width results. However, while

Jimenez-Ormeno et al. (2013) reported that the participants were from Toledo province, Delgado-Abellán et al. (2014) did not report such information.

In contrast to European samples, Japanese (Kouchi, 1998) and Brazilian (Sacco et al., 2015) children of the same age range were reported to have an accelerating growth of rear-foot width up to the age of 7 years. Ethnicity is likely a factor in the differences between the current and the Japanese children as a wider heel in Asian adult populations compared to European ones has been shown before (Jurca et al., 2019).

Unfortunately, no other researchers measured rear-foot width, although it is an essential measure for proper shoe fit and has also been well established in last construction (Mauch et al., 2009). This parameter can aid in defining the heel contour shape of a foot, hence improving rear-foot fit, so the heel counter can “hold” the foot preventing shape distortion (Luximon et al., 2003).

Mid-foot width

The findings demonstrated that mid-foot width increased considerably until the age of 6 (1.9mm, 3.1mm and 2.5mm increase between age-groups), and the total growth was 7.5mm up to that age, which was followed by a less than 1mm increase between the two oldest age-groups. There were significant changes between subsequent groups occurring between 4 and 5 and also between the 5 and 6-year-old children. However, it was also shown that there were no significant differences between the two youngest and two oldest groups. Based on these results, it can be proposed that most of the growth in mid-foot width takes place between the ages of 4 and 6-years, and growth slows down in the oldest group. This is also supported by the small effect size between the 6 and 7-year-old groups, whereas all other effect sizes were at least medium.

Mid-foot width is usually measured using footprints (Sacco et al., 2015), to estimate MLA width, and hence it does not correspond to the present measure. Although mid-foot width as measured in the current study cannot be compared to the literature, it provides novel and important information on mid-foot development, rather than on the MLA state. By measuring the mid-foot at the widest part, this measure offers crucial information on the morphological changes in the mid-foot structures, without being affected by the height or width of the MLA. This novel measure may also contribute to better shoe design as the appropriate fit in the shoe's mid-foot area is crucial for stabilisation (Mauch et al., 2009).

Fore-foot width

The participants in the current study had a developmental trajectory of fore-foot width that was the steepest out of the three regions (2.6mm, 2.6mm, 3.5mm, 1.5mm growth between subsequent groups) with a total increase of 10.2mm. Despite this, the significant differences occurred between the same age-groups as in the case of mid-foot width. Therefore fore-foot width also increased the most between the ages of 4 and 6 years and the growth slowed down between the two oldest age-groups. This is supported by the effect sizes too, as Cohen's *d* is only 0.35 between the two oldest groups, but all other effect sizes are over 0.66.

Despite the differences in gender distribution between the two study samples, fore-foot width development in the present study was consistent with that of German children (Muller et al., 2012). Their fore-foot width also increased by 2-3mm each year, and the values in all age groups corresponded to the results in the current study. Interesting to note that while Muller et al. (2012) had 48% males and 52% females in their sample, the current thesis had ~30% males and ~70% females, which could have caused differences in mean age-group fore-foot width values. However, the ratio of boys and girls in each age-group has not been reported in Muller et al. (2012); hence its effects on the boys-girls ratio differences between the

studies are not apparent. Another study of European children in a Spanish sample (Jimenez-Ormeno et al., 2013) also demonstrated a similar increase (1.8mm) between the 6 and 7-year-old groups compared to the present data.

In contrast with the previous two studies and the current thesis, a more considerable increase of fore-foot width between 6 and 7 years of age was shown in 94 German (Sacco et al., 2015) and a 295 Spanish (Delgado-Abellán et al., 2014) children: 3.6mm and 3mm respectively. While the German children of the same age had similar weight and height to the present sample, the Spanish children of the same age were generally taller and heavier, which could have caused the larger increase. These studies of European children's feet highlight the differences in measurement technology (three different methods in four studies), sampling techniques (three cross-sectional one longitudinal) and sample size (94-7788). These differences in methods could have been the reason for differing foot measures and underline the importance of standardization.

An Asian, more precisely Japanese sample of 467 children, have been reported to have approximately 1mm wider fore-foot (Kouchi, 1998) up to the age of 6 years than the children in the present thesis. The increases in width were 3.8mm, 2.9mm, 2.8mm up to the age of 6. Although the changes in the first four age-groups were only ~1mm larger than the current results, Japanese children also showed an increase of 3.6mm into the oldest age-group, compared to 1.5mm in the current thesis. Two factors could explain the discrepancies. First, Japanese male adults have been reported to have wider fore-foot (Kouchi, 1998, Jurca et al., 2019), and the development of these differences might start to occur at this age. Second, the 7-year-old group in the present dataset only included 5 boys and 18 girls, while the same group of Japanese children included 56 girls and 56 boys (Kouchi, 1998). Although the present study did not consider differences between sexes, this could have caused the larger

values in the Japanese sample, as by this age, the difference between girls and boys in fore-foot was shown to be statistically significant (Kouchi, 1998, Delgado-Abellán et al., 2014).

4.4.2.2. Differences in the development of width among foot regions

The current data on the three foot regions' width demonstrated differences in the rear-, mid- and fore-foot trajectory. This resulted in the changing shape of the paediatric foot across the age groups. The foot was found to become increasingly wider at the mid and fore-foot compared to the rear-foot until the age of 6. After this age, the mid-foot did not continue to grow as much as the other two sections. The existing literature on this topic only shows data on the rear- and fore-foot. Compared to the children in the present thesis (2.6mm difference in total growth between rear-foot width and fore-foot width), the German (Sacco et al., 2015), Brazilian (Sacco et al., 2015) and Japanese (Kouchi, 1998) children's feet showed a faster change in shape (8.7mm, 6.2mm and 6mm difference in total growth between rear-foot width and fore-foot width respectively) between 3 and 6 years of age. These differences suggest that the fore-foot was becoming wider than the heel faster in these samples. In all of the above studies and in Spanish children (Jimenez-Ormeno et al., 2013, Delgado-Abellán et al., 2014), the shape changes were apparent between the 6 and 7-year-old children too as opposed to the current thesis. Although rear- and fore-foot width have often been reported, mid-foot width as is reported here has rarely been investigated. The missing "link" in the mid-foot has led to incomplete characterisation of foot shape development in terms of width. This thesis for the first time provided this "link" and demonstrated that all three regions' width growth slows down between the last two age-groups, and mid-foot growth is approximately half of the other two regions' growth. This pattern may also be attributable to the decreasing "medial bulging" due to decreasing pronation with increasing age. As the mid-foot area fit of the shoe is important for stability (Mauch et al., 2009), this information

may be crucial in children's footwear last design. Although this is mentioned in Mauch et al. (2009), the authors only used dorsal arch height as a mid-foot measure resulting from a Pearson's correlation coefficient analysis of 15 measures. The 15 parameters used for the analysis are not mentioned; hence, it is unknown whether mid-foot width was part of it. The reduced growth between 6 and 7 years of age probably contributes to the general change in shape resulting in a less robust mid-foot. This will be investigated in more details when the width proportions are considered in section 4.5.3.1-2.

4.4.2.3. Age-group differences in the height of foot regions

Rear-foot height

The results demonstrated that out of the three height measures the rear-foot height had the steepest trajectory with increases of 2.2mm, 5mm, 1.8mm and 2.6mm between age groups up to the age of 7. The total increase was 11.7mm. Significant differences between groups also confirmed the rear-foot height's growth, except for between the two youngest and between the 5 and 6-year-old groups, although the effect sizes were medium in these two comparisons. These results indicated a growth with medium or large effect sizes throughout. While mid- and fore-foot height is often reported in the literature, rear-foot height is novel and has never been investigated in children before. This measure complements the existing ones by providing crucial information on rear-foot development, which can be used in clinical practice and footwear last design. While this measure is directly related to rear-foot development, due to the foot's intrinsic characteristics, the increase in rear-foot height could also be indirectly affected by the decreasing pronation and increase in MLA height occurring in these age-groups.

Mid-foot height

The results showed that the mid-foot height trajectory was less steep than that of the rear-foot height, with increases of 1mm, 3.4mm, 0.3mm, and 1.1mm between subsequent age groups. The total growth was 5.9mm. The statistics showed that significant changes between subsequent groups only occurred between the 4 and 5-years old groups with large effect size. The significant differences between not subsequent age-groups with large effect sizes indicated a constant increase in mid-foot height up to the age of 5 years and suggested that this growth slows down after this age, which is also supported by the decreasing effect sizes. The present data shows 7-8mm smaller mid-foot height in the 6- and 7-year-old groups compared to Spanish children in Jimenez-Ormeno et al. (2013) who reported an increase of 1.8mm, from 53.3mm to 55.1mm between the 6 and 7-year-old groups; and Delgado-Abellán et al. (2014) who reported 53.45mm and 56.1mm in the 6 and 7-years old groups respectively. This is likely due to the different definition of instep\mid-foot height. Jimenez-Ormeno et al. (2013) and Delgado-Abellán et al. (2014) defined the location of the measurement as the point of instep, which is likely to be closer to the ankle compared to the 55% of foot length used in the present thesis. This could have resulted in higher mid-foot in their studies.

Fore-foot height

Fore-foot height only increases by 1mm between the ages of 4 and 5 years, significant differences were found between the 3-6 and 4-6-year-old groups with large and medium effect sizes, respectively. Effect sizes decreased after the age of 5. These findings suggest a slowly increasing fore-foot height, with the most considerable growth between the ages of 4 and 5 years, which slows down after the age of 5.

4.4.2.4. Differences in the development of height among foot regions

Although the magnitude of changes was very different, the developmental trajectory is very similar in all three regions. The most considerable growth in foot height in all regions occurred between the ages of 4 and 5-years, and there was reduced growth in the following two years. The differences in the magnitude of growth suggest a transformation of foot shape with the rear-foot growing to become taller than both the mid and fore-foot. This is novel and crucial information for child footwear last designers that have not been investigated before. The changing trajectory of height growth in the rear- and mid-foot across age groups (and hence foot length and shoe sizes) suggests that the isometric length dimensional grading currently used might not be appropriate. This agrees with Hill et al. (2017), who showed in Caucasian adults that direct arch height measures (navicular height, dorsal arch height: mid-foot height) do not scale isometrically with foot length. This will be explored in more depth when the normalized height measures are considered in section 4.4.3. The results also highlight the importance of regional foot measures, as the magnitude of increase in the height of the rear- and mid-foot are different. As the rear-foot grows faster in height than the mid-foot, this should be reflected in children's footwear to provide a comfortable and stable fit. The faster increase in height in the rear-foot may also be attributable to the decreasing pronation and increasing MLA height. Although mid-foot height has been thought to represent MLA height increase, in the current thesis, rear-foot height increases faster than mid-foot height, indicating that it might be a better representation of MLA height. However, as the absolute rear-foot height is probably a combination of general growth of the foot and the development of foot posture and MLA, normalized rear-foot height may be a more appropriate alternative.

4.4.3. The proportional development of paediatric foot regions

4.4.3.1. Age-group differences in the width proportion of foot regions

Normalized rear-foot width

The findings indicated that normalized rear-foot width changes significantly between the ages of 4 and 6 and 4 and 7 years (23.00%, 23.51%, 22.94%, 22.39% and 22.60% in the five age-groups) with large effect sizes, suggesting, that the rear-foot become slenderer between 4 and 6 years of age but not after. These results are slightly different from Spanish children's data (Delgado-Abellán et al., 2014) who had normalized (to foot length) rear-foot width of 23.35% and 22.9% in the 6 and 7-year-old groups respectively. In another European sample, Mauch et al. (2008), although did not directly report normalized rear-foot width, found more slender type feet in their sample between the ages of 6 and 13 years as age increased. Slender type feet were described as having smaller volume: smaller heel and fore-foot width and smaller dorsal arch height (defined as the height of the dorsum at the medial dorsal junction of the foot and leg). These results agree with the present findings of decreasing normalized rear-foot width but highlight the importance of regional foot shape analysis as the decrease in normalized rear-foot width stops at the age of 6 in the present thesis. Without this information, incorrect data could be derived from cluster analysis approaches, which could undermine the applicability of such datasets in clinical practice or footwear last design. As the heel contour of the shoe is essential in proper footwear fit, the methods used in Mauch et al. (2008) may lead to improper fit due to ignoring the rear-foot width results.

Although normalized rear-foot width has also been reported in German and Brazilian children (Sacco et al., 2015), it was normalized to height; hence the results are not directly comparable.

Normalized mid-foot width

The mid-foot proportional changes were the largest between 4 and 5 years of age, and between 6 and 7 years of age, with a 1% decrease between these age-groups. The total decrease in this measure was 2.9%. The statistics showed that the 3 and 4-year-old groups were significantly different from the 6 and 7-year-old groups, while the 5-year-old group was only significantly different from the 7-year-old group. These results confirm the continuous decrease in normalized mid-foot width from the age of 4 into the age of 7, indicating that the mid-foot became increasingly slender in width after the age of 4 years. The present normalized mid-foot width data agrees with the findings of increasing slenderness in Mauch et al. (2008). While this is the case, normalized mid-foot width was not a variable in defining the slender foot type in Mauch et al. (2008), and it is unknown if it was part of the original 15 measures they used.

The decreasing mid-foot width could be explained by the changes in mid-foot structure and posture resulting from the increasing arch height and the “squashing” of the mid foot bones (cuneiforms, first three metatarsals, and the navicular) up and together. Furthermore, the decrease in normalized mid-foot width also suggests the reduction in “medial bulging” related to a decrease in pronation (Dahle et al., 1991). This suggests that normalized mid-foot width may be an important indicator of changes in mid-foot structure and posture, related to the development of the MLA. This highlights the novelty and importance of the present dataset in providing more detailed measurements about each region and using simple clinical measures that represent structural and postural changes.

Normalized fore-foot width

The results showed that although there was a continuous decrease in normalized fore-foot width (0.5-0.6%), the most considerable change occurred after the age of 6 (-1.2%), with a

total decrease of 2.8%. This suggests that the fore-foot become increasingly slenderer, especially after the age of 6 years. The statistics showed that the 3 and 4-years old groups were significantly different from the 6 and 7-year-old groups and the 4-year-old group was also significantly different from the 5-year-old group. These statistics also indicate a continuous decrease in normalized fore-foot width across the ages; hence increasing slenderness.

The present findings on normalized fore-foot width are consistent with those of German children (Muller et al., 2012). Their results showed that fore-foot width to length ratio decreased by a total of 0.03 arbitrary units (3%) until the age of seven, which corresponds to the current study results. The normalized fore-foot width values in each age-group also corresponded with the current data: 41%, 40%, 39%, 39% and 38%, although approximately 1% higher across all age-groups suggesting a slightly less slender fore-foot shape among the German sample. The present results are also consistent with those of Mauch et al. (2008), who showed increasing slenderness with increasing age, using cluster analysis that included normalized fore-foot width.

In contrast, Japanese children (Kouchi, 1998) have been shown to have higher normalized fore-foot width values and hence less slender feet (defined as foot index: 41.85%, 41.65%, 41.6%, 40.85%, 40.25%). Although there was a decrease in their normalized fore-foot width, the total change was less than 1.6%. This indicates that the Japanese children's fore-foot did not become as slender as those in the present thesis or in Muller et al. (2012) study. These results suggest that Japanese children have wider fore-foot in absolute terms and have more robust feet. Similarly, although Spanish children (Delgado-Abellán et al., 2014) have been reported to have similar slenderness (normalized fore-foot width: 38.9%) to those in the

current thesis at the age of 6, their fore-foot did not become as slender into the age of 7 years (38.35%).

4.4.3.2. Differences in the development of width proportions among foot regions

The results indicated that all regions become increasingly slender, most noticeably between the ages of 4 and 6 years, although normalized rear-foot width decreases much less compared to the other two regions. This difference in magnitude of change is probably due to the development in the posture and structure of the mid- and fore-foot. This development is related to the increasing MLA height and reducing pronation indicated by a reduction in “medial bulging”, which can be quantified by normalized mid-foot width (Menz, 1998, Halabchi et al., 2013, Dahle et al., 1991).

The current results also confirm the findings of existing literature on the slenderness of the foot and add novel and crucial regional information. Consequently, the findings suggest differences in proportional development among the three foot regions due to changes in foot structure and posture, providing new information on children's foot shape development for clinicians. As the three regions' width proportions develop differently due to changes in structure and posture, clinicians may use these measures for the purpose of quick and simple assessment of the paediatric foot. Because the current sample only included healthy feet, the mean and the one or two standard deviation range around the mean may serve as a general guide to for clinicians to assess paediatric foot posture. This new data could also contribute to better footwear last design and fit in children, as along with a piece of general information that the foot becomes slender, this dataset also offers information on how with increasing size, the proportion of each foot region change. The novel normalized width data in the present study suggests that with increasing size (for sizes between the ages of 4 and 7 years:

169-198mm foot length) children's footwear should become slenderer in the mid- and fore-foot up to the age of 7 but only up to the age of 6 years in the rear-foot, to accommodate the changing structure and posture of the paediatric foot.

4.4.3.3. Age-group differences in the height proportion of foot regions

Normalized rear-foot height

Based on this study's results, normalized rear-foot height did not change (no significant differences between age groups), hence its proportion to foot length (~30%) remained the same throughout the age-groups.

Normalized mid-foot height

On the other hand, normalised mid-foot height showed a decreasing pattern, with the most extensive and statistically significant change (-1.17%) between 5 and 6 years of age. The pattern of statistically significant changes (between the ages of 3-6, 3-7, 4-6, 4-7, 5-6, 5-7) indicated that the mid-foot become relatively flatter as age increased, especially between 5 and 6 years of age.

Normalized fore-foot height

The statistical tests of the normalized fore-foot height data indicated a significant decrease between the ages of 4 and 7 and 5 and 7 years. Although the changes were only around 1% between age groups, considering the large effect sizes (0.97,0.91), this could still be considered anatomically significant, suggesting that the fore-foot also becomes relatively flatter with age, from the age of 4 onwards.

4.4.3.4. Differences in the development of height proportions among foot regions

The mid and the fore-foot become relatively flatter between the ages of 4 and 7 years compared to the rear-foot, which grew in proportion with foot length. The results concerning the mid-foot height are in agreement with the findings of Mauch et al. (2008), who included dorsal-arch height in their volume\slenderness cluster, and suggested increased slenderness in the mid-foot. However, rear- and fore-foot height have never been reported before, and these findings indicate that the proportion of the rear-foot is changing differently, and it does not become relatively flatter. This is an important result, as if we only consider the results of Mauch et al. (2008), we might conclude that the whole foot becomes slender with increasing age, which, based on this thesis' results is not correct. The lack of change in normalized rear-foot height suggests that the rear-foot grows in height in proportion with foot length, indicating a decrease in pronation and an increase in the height of the MLA.

We can also infer from the current results that although mid- and fore-foot do become relatively flatter with age, they do so with different magnitude. The mid-foot changes are twice as much as those in the fore-foot between the ages of 5 and 7 years, however normalized mid-foot height actually increases between the ages of 4 and 5 years. This increase may relate to the decrease in normalized mid-foot width between the same age-groups, indicating that mid-foot height increases faster than foot length. These changes are indicative of the increasing arch height and decreasing “medial bulging” as mentioned in the section 4.4.3.2. Similarly to the normalized width data, the normalized rear- and mid-foot height mean and the range of one or two standard deviations around the mean may be a useful characterization of the typical paediatric foot posture.

The findings therefore indicate a change in foot shape during development, suggesting that the mid-foot becomes relatively flatter than the fore-foot and the rear-foot. As the mid-foot

area of a footwear is crucial in stability (Mauch et al., 2009), the lack of higher resolution data resulting from cluster analysis, might lead to inappropriate and unstable footwear.

4.5. Summary and contributions

While the current results are consistent with many studies to a great degree, the full trajectory of the development of the three regions between the 3 and 7-years of age has not been established using a high precision hand-held 3D scanner before. This study also confirmed that differences in foot shape and size development are prevalent between and within countries and continents, highlighting that not all differences can be accounted for by these factors.

4.5.1. Growth trajectory

This thesis indicated that each foot region becomes wider and taller at different ages and rates as age increases. It was shown that all three foot regions had a similar increasing width trajectory with age, but this growth appeared to diminish from the age of 6. The patterns also suggested that by the age of 6, the shape of the foot has changed. The mid-foot grew more in width than the heel, and the fore-foot increased in width more than both the rear- and mid-foot. The increase in width after the age of 6 was smaller in all regions and suggested decreased mid-foot growth compared to the other two regions. Although rear- and fore-foot width measures have been reported, mid-foot width has not been reported before as measured in this thesis. This is novel information regarding the development of the mid-foot and adds to the understanding of foot shape development in children suggesting a gradual proximo-distal increase in the foot's width.

The trajectories of normalized width measures suggested that all regions become increasingly slender after the age of 4, which confirms previous findings that the foot grows

more in length than in width. This process continued into the oldest group of children in the mid- and fore-foot, while the rear-foot grew in proportion with foot length between the two oldest groups. Although similar findings have been reported before, the cluster analysis (Mauch et al., 2009, Mauch et al., 2008) approach used to arrive at these conclusions lacks resolution and may provide incorrect information on foot shape. The foot may become slenderer in all regions up to the age of 6 years, but the current thesis also suggests that it is not the case in the rear-foot, which grows in proportion to foot length after this age.

The examination of the foot regions' height trajectories revealed a common pattern: there was considerable growth in height across the rear- and mid-foot between the ages of 4 and 5-years. However, rear-foot height continued to increase in the older age-groups. Although the mid-foot demonstrated another increase in height between the ages of 6 and 7 years, considering the whole age range, it can also be concluded that the foot becomes taller at the rear-foot compared to the mid- and fore-foot. The normalized height results indicated a change in proportions in the mid- and fore-foot and no changes in the rear-foot. The mid- and fore-foot become relatively flatter between the ages of 4 and 7 years while the rear-foot's relative height remained the same throughout the age-groups.

In summary, the normalized 2D measures indicated that the mid- and forefoot become more slender with age in height and in width. On the other hand, the rear-foot only becomes more slender in width and not in height. Furthermore a pattern was revealed where normalized height measures increased when normalized width measures decreased. This was most noticeable between the ages of 4 and 5 years. These results suggest that there is an increase in the height of all regions (especially the mid-foot) in proportion or faster than foot length. This resulted in the thinning of the foot probably due to the increasing arch height and the "squashing" of the mid foot bones (cuneiforms, first three metatarsals, and the navicular) up

and together. Interesting to note that normalized fore-foot height does not increase between the ages of 4 and 5 years (although it shows minimal decrease), however, the decrease in normalized fore-foot width is the greatest out of the three regions between the same age-groups. This may be because the area between the first and fifth metatarsal heads stays in contact with the ground, while the mid-foot raises up, due to the development of the MLA. Furthermore, as the MLA develops and pushes the mid-foot bones up and together, this also pushes the metatarsals together resulting in the thinning of the forefoot.

Such findings using a hand-held scanner, to the author's knowledge, have not been reported in the literature, and they provide a detailed, higher resolution and accurate dataset on paediatric foot shape development. This dataset not only contributes to the understanding of foot development, but to clinical practice, footwear last design and research too. The implications for these areas will be discussed next.

4.5.2. Contributions to clinical practice

While the 2D anthropometric measures provided an overview of the size and shape development of the paediatric foot, they also provided an insight into how the structure and posture of children's foot change. For this reason, the present results also have implications and contributions to clinical practice. Although there are parameters used by clinicians that aim to quantify or classify the development of the MLA or foot posture, these are mainly foot print measures, looking into the ratios of areas of the plantar surface in contact with the ground (see section 2.1.4. of the literature review). A more comprehensive foot posture measure, the FPI-6 has also been used, however it is somewhat subjective and requires experience.

In comparison, the normalized measures presented here are easy and simple to capture and calculate and based on the results they may help to characterize the development of foot posture and of the MLA. As these measures directly capture changes in the relative width and height of the foot, they are more appropriate for clinical purposes compared to footprint measures. Furthermore, while measuring FPI-6 requires experience, the normalized 2D anthropometric parameters only require the identification of landmarks and are objective. Accordingly, the combination of normalized rear- and mid-foot height and normalized mid- and fore-foot width and their mean ± 1 SD (68% of the sample) may serve as the definition of typical foot posture as well as shape and any children outside of the mean ± 2 SD could be further examined. However, it is important to emphasize that it is the combination of these measures that should be used and not a single parameter on its own. This is due to the 3D multi-planar nature of the foot implying that any change in height proportions will also result in a certain change in width proportions. Additionally, these processes are not limited to one region nor can be quantified using one overarching parameter. Hence a combination of normalized width and height measures from different regions should be used.

Further research could aim to measure these normalized parameters in different samples such as children with symptomatic or asymptomatic flat foot compared to healthy. Such investigation may give an insight into how the proportions of the paediatric foot change in such samples and help clinicians in diagnosis or treatment follow up.

4.5.3. Contributions to footwear design

The differences in 2D measure developmental trajectories across age-groups and among foot regions highlight the need to use foot region specific foot shape and size data in practical applications. In footwear last design and fit, although foot length is an important measure, and is primarily used for grading, a detailed understanding of the size changes in each region allows for a more appropriate design and fit. Shoes that do not fit well can cause long term issues in the development of children's foot and gait, and to design well-fitting shoes, the shape of the footwear must be very similar to that of the foot (Mauch et al., 2008, Mauch et al., 2009). Therefore, the differences in shape between and within foot sizes and different populations should be considered, and the shoes should be designed according to the users' measurements. This way, the adverse effects of inadequate footwear could be reduced (Delgado-Abellán et al., 2014).

Based on the results of the 2D measures in this thesis, children's footwear should allow – with increasing size - for more accelerated growth in the width of the mid- and fore-foot compared to the rear-foot. However, when the normalized measures are considered, it is clear that this growth is not in proportion with foot length. Hence children's footwear should be designed to change shape with increasing size and become slenderer in the mid- and fore-foot, but not so much in the heel. As the changes in the height of foot regions also show a different trajectory, these should also be accounted for. As the current data shows, from the age of 5 years, children's mid- and fore-foot may become relatively flatter (decreasing normalized height measures). This suggests that from this age (approximately 180mm foot length) the range of sizes should include footwear with relatively flatter mid and fore-foot, although this change in relative flatness is far less than the change in relative width (slenderness).

In summary, footwear grading tables for children should consider information from studies like this thesis. Non-linear scaling factors should be used that consider the different developmental trajectories of foot regions and allow for the changing proportions of the foot and foot regions. The grading tables currently in use do not account for the differences in width and height of the developing foot regions, despite the fact, that many problems with shoe fit are related to width because foot grading is usually based on foot length (Delgado-Abellán et al., 2014). As the differences between height and width trajectories in the present study indicate, the scaling factor for height should be lower than that for the width. Another important consideration is that the scaling factor should not be constant across sizes and foot regions, as both width and height measures have different trajectories in different foot regions. As it has already been argued, precise foot width or 3D analysis of foot shape can help alleviate fitting issues (Witana et al., 2004); therefore, the present thesis results are an essential first step towards a better fitting design and manufacturing of footwear.

4.5.4. Contributions to research

The current results and the comparison to the literature also highlighted differences in foot shape among ethnic groups, countries and even between regions within a country. Although some of the discrepancies could be explained by ethnic (Jurca et al., 2019, Kouchi, 1998) or socio-cultural variations (Sacco et al., 2015), the differences in the methods used is also a significant factor. All of the studies that measured the whole age range of this thesis used manual methods: foot-prints, tape measure or scribe, and the definition of the measures were also conflicting (e.g., rear-foot width and mid-foot height measured at different locations). Although these manual methods showed good reliability, they are often under- or overestimated the foot section's actual size due to the equipment used or the measurement's location. As 3D scanning is becoming mainstream and more accessible, its use can provide accurate and reliable measurement at the correct measurement locations. Another advantage of 3D scanning is flexibility: the foot model is saved and can be measured again using different measurement definitions and/or algorithms. This would allow for more opportunities to compare with other research in the future. As 3D scanning is becoming more used, large scale studies in children must use this technology for a more accurate and flexible dataset. Future studies, like the current one, can also create normative datasets for age-groups or foot sizes providing critical information for clinicians and footwear last designers.

4.6. Limitations

The first limitation of the study is the small sample size. The a priori sample size calculation estimated a sample of 20, 35 and 90 needed to correctly reject the null hypothesis in the ANOVA\Kruskal-Wallis tests for foot length, fore-foot width and normalized fore-foot width respectively with a power of 0.95. Although the actual total sample size was well over any of these, the stratification of the age-groups was uneven: 12, 38, 35, 41 and 23 per age-group with increasing age. The estimated samples size to correctly reject the null hypothesis between two subsequent age groups were 14 for foot length (0.97cm mean difference), 36 for fore-foot width (0.25cm mean difference) and 51 for normalized fore-foot width (1% mean difference). Therefore, post-hoc tests for the age-group pairs of the 3 and 4; or the 6 and 7-year-old groups were underpowered for most measures. However, tests between non-subsequent age-groups were only underpowered for the 3-year-old group for absolute and normalized measures except for foot length. A further limitation due to the convenience sampling method is the uneven number of boys and girls in the sample, as there were more than twice as many girls as boys. It has been reported that boys have larger foot measures (Delgado-Abellán et al., 2014) in the older age groups of the age range examined; however, due to the limited sample size, no sex comparisons were performed.

While the validity of the methods was not assessed, similarly to the pilot study, the 2D measures mostly agreed with data in the literature with certain discrepancies, indicating good validity. The discrepancies could be explained by differences in the sample (ethnicity, weight, BMI, or girls-boys' proportions in age-groups) or differences in the measurement techniques used (e.g., calliper vs 3D scanning, or differences in the measurement location). It is also important to note that the validity of the 2D anthropometric measures was not

affected by using a Perspex platform as the part of the foot where these measures were taken was scanned from above the platform.

The study's cross-sectional nature is also a limitation, as this type of data collection is a “snapshot” of the age-group and does not follow individual changes throughout the development. This type of study cannot examine change over time; it can only examine changes between participants of different ages at the same point in time and provide information on age differences. While this is useful data, it cannot describe individual developmental trajectories or cause-and-effect relationships.

4.7. Conclusions

This study aimed to offer an understanding of 2D anthropometric foot development between the ages of 3 and 7 years, and to provide a contemporary dataset of 2D anthropometric paediatric foot measures using the Artec Eva hand-held 3D scanner, and the methods established in the pilot studies. It was found that the three regions of the foot have different developmental trajectories. Rear-foot grows faster in height and in proportion with foot length than the other regions, which become relatively flatter with age, while the mid- and fore-foot grow faster in width, although they become slenderer (relatively less wide) than the rear-foot. The differences between age-groups were more apparent after the age of 4 years, but width growth diminished at the age of 6, while the mid- and fore-foot continued to become slenderer until the age of 7. The most considerable differences in height were between the ages of 4 and 5 years, while the mid- and fore-foot continued to become relatively flatter until the age of 7 years.

Despite the explained limitations, the presented results and discussion imply that foot shape changes during development should not be described and generalized based on a few selected measures. Instead, using the width, height, and normalized counterparts of all three

regions should be considered. More importantly, the results suggested a change in foot posture and the development of the MLA, making these parameters useful in clinical practice for supporting diagnosis or treatment follow up. More specifically, the use of a combination of typical normalized values (mean ± 1 or 2 SD) may be insightful in assessing paediatric foot posture and the MLA. Furthermore, there are implications in footwear last design, as considering the 2D sizes of all three sections will provide a more accurate fit for all sizes. Although there have been studies (Mauch et al., 2008, Mauch et al., 2009) that used the sizes of different regions in their foot shape classification, the measures were not considered separately or compared to one another but used in a cluster analysis to create classes of foot shape such as robust. This approach oversimplifies the shape development of the foot and only provides generalized information. Although these studies intended to provide information for footwear last design, because – as the present data demonstrated – foot regions have different developmental trajectories, their data may be misleading. They may result in the production of ill-fitting shoes and incorrect theory of foot development. In contrast to the existing literature, this thesis provided, for the first time, novel, and detailed information about the developmental trajectory of three foot regions using 2D anthropometric foot measures and a hand-held 3D scanner between the ages of 3 and 7 years.

Although this 2D dataset provides unique and novel information on children's foot growth, it cannot characterize the 3D morphology of the foot surface such as convexity versus concavity or flatness versus curvedness. As an example, this dataset provided age-group information on rear-foot width or rear-foot height, but this type of data cannot describe or quantify the age group differences in concavity in the area under the lateral malleolus, which could be crucial in foot posture assessment in children. The 3D shape of the foot surface could also be important in other areas such as the MLA. This structure is traditionally

measured using height or footprint variables that do not consider the foot's complexity and multi-planar nature (Gill et al., 2016, Uden et al., 2017). These examples highlight the importance of 3D measures in foot shape analysis alongside 2D measures. For these reasons, although the presented dataset provided novel and useful information, further 3D shape analysis was undertaken to characterize differences between age groups and the results will be presented and discussed in the next chapter.

Chapter 5

5. The 3D surface morphology of the paediatric foot

The previous chapter investigated the differences in 2D anthropometric measures and proportions of foot regions among age-groups between the ages of 3 and 7 years. Although they provided a detailed description of age-group differences in each foot region's size and proportion, they cannot fully describe the complex changes occurring on the multi-dimensional foot surface. Similarly, the 2D data in this thesis provides novel information which could inform last design of children's footwear and underpin the theory of foot development; however it is limited in resolution and does not consider 3D shape changes of the foot surface. This is especially true considering the development of the MLA. As discussed in the literature review (section 2.1.4.2.) the development of the MLA is one of the most debated characteristics of the paediatric foot. A range of 2D measures (such as navicular height or footprint measures) exist attempting to quantify the changes taking place in this multiplanar structure, however, these are indirect and consider the height of the navicular tuberosity or the area\width of foot regions touching the ground. Although these measures can estimate the MLA's height, they are indirect and do not capture the 2D\3D changes taking place within the MLA or on its surface. For this reason, they are limited in what they can tell us about the multi-planar changes in this structure (Banwell et al., 2018), such as the convexity or curvedness of the foot surface (Varga et al., 2020).

To date, literature has investigated the foot in higher resolution in adults (Price and Nester, 2016) and in 3D in children (Chang et al., 2014b, Chang et al., 2012). Although the measures used in these studies provided more information than traditional 2D measures, they did not intend to describe the differences in the 3D morphology of the foot surface. More sophisticated 3D foot scan analysis in adults has been carried out using geometric morphometrics (Stanković et al., 2018). Despite the rich resolution of data available from 3D scanning, this study also resulted in a 2D and relatively subjective description (width, length, and height) of foot shape variations. As discussed in the literature review (section 2.2.8.1.), and the pilot study (section 3.7), to allow for a higher resolution and 3D analysis of foot surface morphology, 3D shape descriptors (Koenderink and van Doorn, 1992) can be used (see section 2.2.8.1. for details). These measures can capture the shape of the foot surface at every point of the foot scan, providing a high resolution approach. Although these are used in other research areas such as brain imaging analysis or face recognition (Calignano and Vezzetti, 2011, Vezzetti and Marcolin, 2012), as discussed in the literature review (section 2.3.4.2.) the only study that has applied this method to feet was carried out in adults. This study aimed to locate anatomical landmarks (Liu et al., 2004) and highlighted how the 3D shape descriptors employed can describe the 3D shape of the foot surface.

A pilot study (chapter 3.) was carried out investigating if 3D shape descriptors can be used to identify and locate changes in foot surface morphology during development in childhood. This study described the 3D shape of children's feet in three age groups, two, five and seven years of age. The study confirmed that curvedness and shape-index are useful variables when examining foot shape development in children. Using descriptive methods, these variables could identify and locate changes between age groups, confirming existing knowledge (foot becoming slenderer as age increases) and providing novel information (e.g.

concavity of the MLA). Based on this pilot study and the literature, using 3D shape descriptors, the following phase of work has investigated the differences in 3D foot surface morphology between age-groups of 3, 4, 5, 6 and 7 years. This work adopted statistical parametric mapping (SPM) which provides a framework in which the 3D surface morphology data of the whole foot can be analysed at a vertex level, giving rise to the topological assessment of the foot, identifying, and locating key areas of development. The next section will introduce this method to provide an understanding.

5.1. Introduction to statistical parametric mapping

In phase (b) of the pilot study (section 3.7.) 3D shape descriptor heat maps were used to compare age groups and describe foot surface morphology changes across development. However, comparisons of 3D shape descriptors between groups were based on individual foot data, which is not representative of the whole age-group. A further limitation of this approach was that it was also based on data from different surfaces of the foot separately (such as dorsal, medial, and plantar).

SPM was developed for brain imaging research (Worsley et al., 1992, Worsley et al., 1996, Friston, 1997, Friston et al., 1991). This approach has more recently been applied to pedobarographic research (Pataky and Goulermas, 2008). SPM as an alternative to regional masking of the foot (in the case of this thesis creating surfaces), allows the localization of differences in foot pressure data (Pataky and Goulermas, 2008, Pataky et al., 2008) at a pixel (the smallest unit of an image derived from pressure platforms equal to one pressure sensor) level. Statistical maps represent images of changes in significance rather than changes in magnitude, allowing comparison of regions or pixels based on relative significance (Friston et al., 1991). An alternative way to describe it is that for a given level of significance, they are designed to localize change (Friston et al., 1991). In a statistical parametric map, the value in a pixel, for example in a pressure map image, expresses the evidence against the null hypothesis that there is no change in that pixel induced by the experiment (hence the values are distributed according to a probability density function such as the Student's T or F distributions). SPM is also appropriate for 3D shape data because there is constant intra-subject geometry, varying inter-subject geometry, arbitrary postures, and pixel (vertex) intensity changes. Moreover, these intensity changes represent organ function; in this case, morphological organ development (Pataky and Goulermas, 2008). The formation of such

maps comprises three steps (Friston, 1997). Here, these are described with relevance to brain imaging, and the appropriate steps will be described in the Methods section (section 5.3.) with relation to 3D foot scans.

1. Spatial transformations:

Spatial transformation reduces the variance components of the voxel time-series that are unwanted: (1) Realignment is performed to account for head movement during imaging, (2) spatial normalization to register the mean of the realigned images to a standard template or to register different subjects and (3) smoothing to compensate for variations in gyri. These transformations will reduce the chances that data from a particular voxel derive from other parts of the brain.

2. Construction of an SPM:

A design matrix is used to include the experimental design and a model to test effects or changes. The design matrix is based on the general linear model, consists of effects of interest, confounds of no interest and an error term. This model expresses the observations as a linear combination of expected components and residual error. The estimated contributions are called parameter estimates. The differences amongst these parameter estimates are used to establish regionally specific effects in the brain. These are specified using linear contrasts. For each voxel and each contrast, a t statistic is computed to create an SPMt, and under the null hypothesis, they have a Student's t distribution. The significance of each contrast in each voxel is then assessed.

3. Statistical inferences:

Inferences are made using conventional parametric statistics, which then provide the p-value. Due to the multiple non-independent multiple comparisons, protection against family-wise false-positives is needed. This is achieved using the Gaussian random fields theory (Friston, 1997, Worsley et al., 1996), equivalent to Bonferroni correction for independent data.

The principles of SPM can be applied to 3D data, as shown by Wang et al. (2012), who applied these methods to identify lateral and medial sesamoid bone shape differences between two groups of horses: fractures and controls. Using MATLAB 7.1 (Mathworks Inc., Natick, MA) and Insight Segmentation and Registration Toolkit (ITK; <http://www.itk.org>) the authors created a surface mesh (a surface mesh consists of triangles, where a vertex (plural: vertices) is a point in a triangle) from the computerised tomography (CT) of the sesamoid bones from both groups. This surface mesh is similar to that created by a 3D scanner. The sesamoid bone surfaces were aligned (one specimen's bone overlapping another) to ensure vertices' correspondence across specimens. This ensured that anatomically identical areas of the bones are optimally overlapped. Average sesamoid bone surfaces for each group were calculated by averaging the 3D locations of overlapping vertices in all samples. Statistically significant differences between groups were calculated from the Euclidean distances between overlapping vertices. This technique then produced a distance map, pinpointing statistically significant differences in the distance between vertices (one value of distance for each vertex in the map). A Hotelling's T² test (multivariate t-test at each vertex) was then able to distinguish the statistically significant differences between vertices.

This research revealed morphological differences that were not identified by traditional linear measurements and allowed them to pinpoint the precise location where significant differences in shape occurred. This method also helped them determine where the differences were in terms of the linear measurements, as linear parameters only give one value, e.g. for a circumference measure. In contrast, SPM can localize where the difference is along the path of the measurement. This method provided a more robust statistical approach reflecting the entire surface of the bone.

In summary, SPM was first used in brain imaging analysis to identify areas of the brain where significant effects occurred; however, it can and has been used in other research areas such as plantar pressure analysis. SPM can identify and locate pixels in plantar pressure images where significant differences are, for example, between two groups of participants. Furthermore, due to the intrinsic nature of 3D foot scans, SPM can also be applied to this type of data giving rise to high-resolution topological analysis of 3D foot shape.

5.2. Aims

This chapter aims to advance the understanding of 3D foot surface morphology development between the ages of 3 and 7 years and identify 2D measures that may predict the identified developmental changes.

Objective 1: Determine and locate differences in 3D foot surface morphology between the ages of 3 and 7 years.

Research questions

- What is the average 3D foot surface morphology in each age-group based on curvedness and shape-index?
- What are the differences between age-groups in curvedness, and how do these relate to differences in foot posture and underlying structure?
- What are the differences between age-groups in shape-index, and how do these relate to differences in foot posture and underlying structure?

Objective 2: Determine 2D predictors of 3D surface morphology changes across age-groups

Research question

- What are the best predictors of the identified 3D foot surface morphology differences?

5.3. Methods

This chapter of the thesis utilized the same 3D scans from the same participants as the previous chapter; hence the participants, data capture and part of the scan post-processing were identical to these in Chapter 4. Therefore, only the post-processing that differed from the previous chapter will be described.

5.3.1. Post-processing of scans

A 3D model was created from each foot scan to calculate 3D shape descriptors (Figure 35.). This procedure followed the same process as in the pilot study (see section 3.2.5.), up to the point of small object filter and hole filling. After this, the following steps were taken:

1. **Isotropic remeshing** was performed using a resolution of 1.5 to reduce the number of vertices by approximately half the original numbers. This was necessary to limit file sizes and avoid memory overload in MATLAB processing and statistics.
2. **Smoothing** was performed with a factor of one to remove skin artefacts (creases or folds of the skin) that would affect 3D shape descriptor calculations. This factor was identified arbitrarily by the researcher.
3. **Coordinate system alignment:** The Brannock axis was aligned with the x-axis of the software, the y-axis was aligned with the mediolateral direction, while the z-axis represented the vertical direction. The origin of the coordinate system was at the most posterior point of the heel.
4. These models were exported into MATLAB as .stl files.

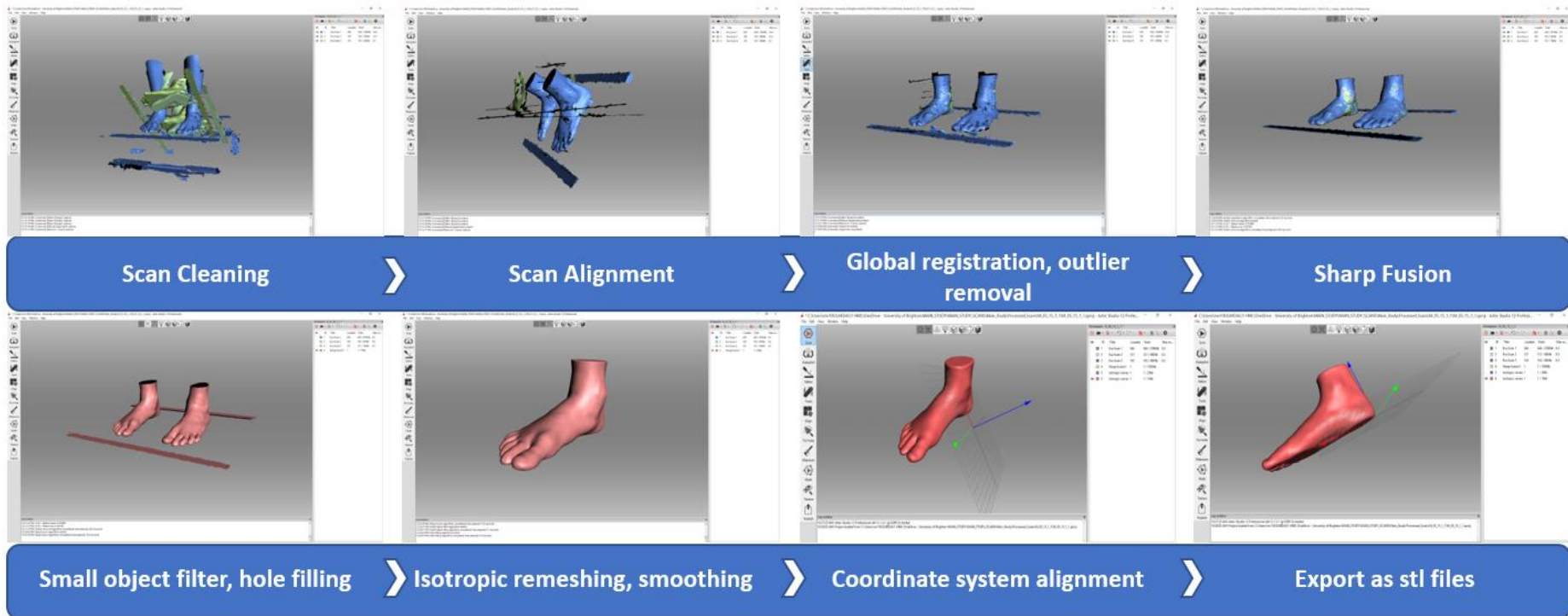


Figure 35.: Post-processing steps in Artec Studio 12.

5.3.2. Calculating 3D shape descriptors

The 3D shape descriptors (shape-index and curvedness) and their calculations were identical to the ones used in the pilot study (section 3.3.6.) to have curvedness and shape-index for each point on each foot

5.3.3. 3D registration of foot scans

As mentioned in the introduction to statistical parametric mapping section (section 5.1.), the first step in SPM is the spatial transformation to align the data of different subjects, so that anatomically corresponding vertices optimally overlap. In brain imaging studies, this is performed using a template brain image; however, such a template does not exist for 3D foot scans. For this reason, a template from within the sample was chosen. Because such template choice has never been undertaken in this research area, a method used in pedobarographic research was adopted (Pataky et al., 2011). As a preliminary template, the foot scan with foot length and width closest to the whole dataset's mean foot length and width was chosen as described in Pataky et al. (2011). All foot scans from 148 participants were then scaled to the preliminary template's size in all three dimensions. Following the scaling, a rigid six parameters (translation and rotation) registration was performed using a MATLAB built-in function specifically for point clouds based on an iterative closest point method. This function calculates the root mean squared error after each iteration of registration. The rigid registration allowed the spatial alignment of scaled foot scans without changing their shape or the number of points in the point-clouds.

After all 148 scans were registered, the mean of all point clouds was calculated. This was performed by finding the corresponding points (nearest neighbours using a built-function of MATLAB) to each point in the template in each foot scan, calculating the average 3D coordinates and using these creating a new mean point cloud. All registered foot scans were

then re-registered (rigid six parameter registration) to this mean point cloud. Finally, corresponding points were found using the nearest neighbour method via MATLAB's built-function. Having corresponding points allowed the calculation of the mean of 3D shape descriptors and statistical analysis.

5.3.4. Statistical analysis

The methods described in the previous section allowed the calculation of mean 3D shape descriptor maps for each age group. These maps help to describe age group characteristics in terms of the 3D surface shape. When considering curvedness, the maps were divided into low curvedness (0~0.0069) areas marked by blue, medium curvedness (~0.007~0.0129) areas marked by green and high curvedness (~0.013-∞) areas marked by red (highest curvedness is orange) for interpretation. This classification was arbitrary and based on a qualitative assessment of the heat maps to identify areas of differing curvedness. Flat areas: areas where the surface is slightly curved possibly due to adipose tissue or shallow valleys around landmarks; and areas of higher curvedness possibly marking other soft tissue or anatomical landmarks and more profound valleys around anatomical landmarks. Although many of the curved areas are protruding (convex), there are areas where the curvedness marks indentations or valleys (concave areas). This difference can be investigated using the shape-index mean maps. Shape-index maps show seven different shapes (see Figure 1 in section 2.2.8.1.), (a) concave shapes (indentations) such as a cup, trough, rut, saddle and (b) convex (anatomical landmarks that protrude.) shapes such as a ridge, dome and cap (Koenderink and van Doorn, 1992). Although Koenderink and van Doorn (1992) defined nine shapes, this was reduced to seven for more straightforward interpretation, leaving out the two different saddle shapes, concave and convex.

5.3.4.1. Non-parametric SPM1D ANOVA

The MATLAB toolbox `spm1d` (<http://www.spm1d.org>) used to perform the SPM on the present type of data is restricted to non-parametric statistics; hence, the assumption of normal distribution did not have to be met. A one-way ANOVA test (the non-parametric SPM1D test for comparing multiple groups) was completed in a pointwise manner to assess if there are differences between the age groups in terms of curvedness and shape-index using the SPM1D software in MATLAB (MATLAB, 2020. 9.9.0.1538559 (R2020b), Natick, Massachusetts: The MathWorks Inc.). Although mean shape-index heat maps identified seven different shapes, for statistical purposes, shape-index will be considered as a continuous variable. This will help in interpreting the result and to identify areas that change shape to become more concave or convex. The alpha level was set to 0.05 with an iteration of 1000. The ANOVA tests yielded F distributions for the foot, and since F is both parametric and point-specific, it is called a ‘statistical parametric map’ (Penny et al., 2011). The resulting SPMs were projected back onto the template foot scan point-cloud, each point having an F value. In the visual representation of the ANOVA SPMs (heat maps), the value of F was marked by a range of grey colours. As the points change from dark to light grey (increasing F values), the differences among the groups grow larger and red clusters indicate significantly different ($p < 0.05$) areas. The threshold in non-parametric SPM1D is calculated using a non-parametric inference, namely the multiple comparison (due to the multiple points in the foot scan) permutation test (Nichols and Holmes, 2002), which rather than using a normal distribution, it uses the data to find the distribution of the statistic under the null hypothesis.

Post-hoc independent non-parametric SPM1D t-tests were performed to establish the differences between each age-group, with Bonferroni correction for ten tests; hence the corrected alpha level for each independent t-test was 0.005. These tests yielded a t-

distribution (t-map) for each pair of groups mapped onto the foot surface. The same non-parametric multiple comparison permutation test is used for the calculation of the t-threshold as in the case of the ANOVA. However, because this approach is very conservative (due to the Bonferroni correction), the t-maps, t values represented by colours, were also considered when describing the differences between age-groups (Phethean et al., 2014). As each point's colour on the foot surface is now defined by the t-value, the colours can help locate differences (albeit not necessarily significant) in the 3D shape descriptors on the foot. This approach has been used in Phethean et al. (2014) when interpreting regression between age and plantar pressure in a cross-sectional study of children aged 4 to 7 years. The colour bar on these figures will be set from the negative to the positive t-threshold, allowing the directional analysis of the 3D shape descriptors' differences. Larger positive or larger negative t values suggest more considerable differences in the 3D shape descriptors in either direction, while t values closer to zero represent small differences. Dark to light blue colours indicate a decrease in the 3D shape descriptor from the younger to the older age-group, while dark red through orange to yellow colours suggest an increase. As the colours become lighter, the differences between the groups grow larger, white areas mark significantly different, so-called supra-threshold clusters at an alpha level of 0.005 (after Bonferroni correction). The presented post-hoc comparison figures will contain all post-hoc pairwise comparisons: columns will be the younger age-groups and rows will be the older groups, to which the younger groups are compared using the independent t-tests.

5.3.4.2. Non-parametric SPM1D Regression

Similarly, to the ANOVA and T-tests, the non-parametric simple linear regression was also performed in a pointwise manner resulting in a linear correlation (r) coefficient distribution for the foot. This r distribution was then transformed into a t-distribution using the identity:

Equation 2.: Equation for transforming the r distribution into t distribution.

$$t = r(n - 2)^{0.5} (1 - r^2)^{-0.5}$$

where n is the number of subjects and t has the Student's t distribution with $(n - 2)$ degrees of freedom. This t distribution is then used the same way as in the independent t -tests to identify suprathreshold points using the non-parametric multiple comparison permutation test. However, the interpretation of the colours is different. Negative values (blue regions) represent negative correlation of the 3D shape descriptor with the independent variable (age or 2D measure), and positive values (red, orange, and yellow) represent positive correlations. The lighter the colour, the stronger the correlation. Significantly correlated (supra-threshold) clusters ($p < 0.05$) are represented by white colour.

The simple linear regressions were performed to establish whether age or any normalized 2D linear measures predict the 3D shape differences identified by the T -tests. Only normalized measures were used, as absolute measures do not consider foot length; hence their practical application would be limited. Age and each normalized 2D measure were regressed separately with both 3D shape descriptors as no multiple regression options were available in the `spm1d` software. Although age and all normalized 2D measures were regressed with the 3D shape descriptors (see Appendix 4.), only the ones with strong predictive power for the particular areas were selected for presentation. These were chosen based on the t values (calculated from the r values) in the areas of 3D shape differences identified using the T tests. Higher absolute t values (lighter blue and lighter red vertices) in the identified areas indicated stronger correlation, hence stronger predictive power. Furthermore, age as a possible predictor of 3D shape differences was compared to the selected normalized 2D measures. The age regression heat map was presented if (1) there were normalized 2D measures that had strong predictive power, for comparison purposes or

if (2) age was the only strong predictor of that particular 3D shape difference. If neither age nor any normalized 2D measures were strong predictors, no heat maps were presented. This section of the results will be organized based on the 3D shape differences identified in the T-tests. Each figure will present the selected regression heat maps with strong predictive power for the identified 3D shape difference.

The results of the 3D shape analysis will be presented the following way. First the results of age-group comparisons will be shown in three main sections: (1) analysis of the dorsolateral aspect, (2) the medial aspect and (3) the plantar aspect. Within these sections, curvedness and shape-index will be investigated separately regarding the research questions in the following order: (a) what is the average 3D shape of that surface in each age-group? (mean age-group heat-maps of curvedness and shape-index) and (b) what are the differences between age-groups on that surface (SPM1D ANOVA, SPM1D independent t-tests). These results will then be discussed and areas of 3D foot surface morphology differences between age-groups will be highlighted for further investigation using simple linear regression to identify predictors (age and normalized 2D measures) of these differences.

The results of simple linear regressions will then be presented as described in the methods section (section 5.3.4.2.) based on the 3D shape differences identified in the previous three sections. This will be followed by a discussion of the regression results, and finally, a summary and contributions section will close this chapter.

5.4. Results: The 3D surface morphology development of the paediatric foot

5.4.1. The 3D surface morphology development of the dorsolateral aspect

5.4.1.1. Age-group average 3D surface morphology of the dorsolateral aspect

Curvedness

Mean curvedness heat-maps for the dorsolateral aspect are shown in Figure 36., and the below description refers to this Figure throughout. The mean heat-maps of the age-groups look similar with the highest curvedness around the lateral border of the foot and the toes. Other areas of high curvedness can be found on the lateral malleolus (LM); inferior and anterior to the LM; and the instep. Low curvedness areas are visible on the anterior surface of the dorsum over the metatarsals and above the lateral edge of the rear- and mid-foot.

As age increases, the area of the LM marked by high curvedness reduces, and there is a decrease of high curvedness into medium curvedness inferior to the LM by the age of 5. A reduction in curvedness is apparent at the instep (reduction in orange and red areas) throughout the age-groups, and there is an increase in low curvedness on the posterior part of the dorsum (increasing blue areas).

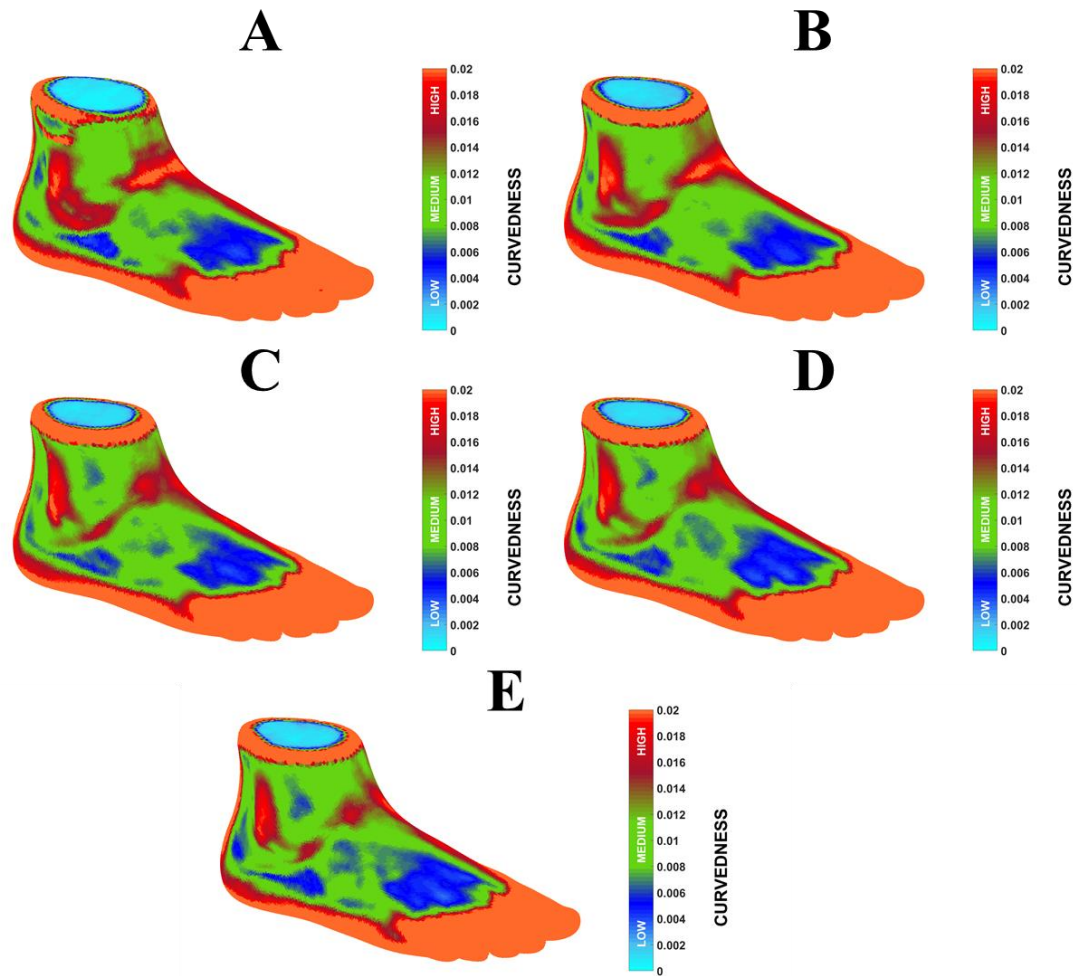


Figure 36.: Mean curvedness maps for each age-group, dorsolateral view: A: 3-year-old mean, B: 4-year-old mean, C: 5-year-old mean, D: 6-year-old mean and E: 7-year-old mean curvedness map.

Shape-index

The mean shape-index heat maps of each age-group's dorsolateral aspect are shown in Figure 37. and will be referred to throughout. High convexity areas (dome: orange regions) can be found at the distal end of the toes, the lateral heel and the LM, which are also high curvedness areas. Areas of convexity (rut and trough: blue and cyan regions) are found around the LM, the lateral part of the instep and between the toes. Saddle-shaped areas (black regions) are found around the concave regions and on the dorsum's lateral side.

The differences between age-groups are less apparent compared to the curvedness results. The only area of trough shape (the most concave area on this surface) appears on the lateral

side of the Achilles-tendon posterior to the LM at the age of 4. There is also an area on the lateral side of the posterior dorsum (marked by an ellipse) that changes from saddle shape (black) in the 3-year-old group to ridge shape (yellow) in the 4, 5 and 6-year-old group and finally to dome shape (orange) in the 7-year-old group.

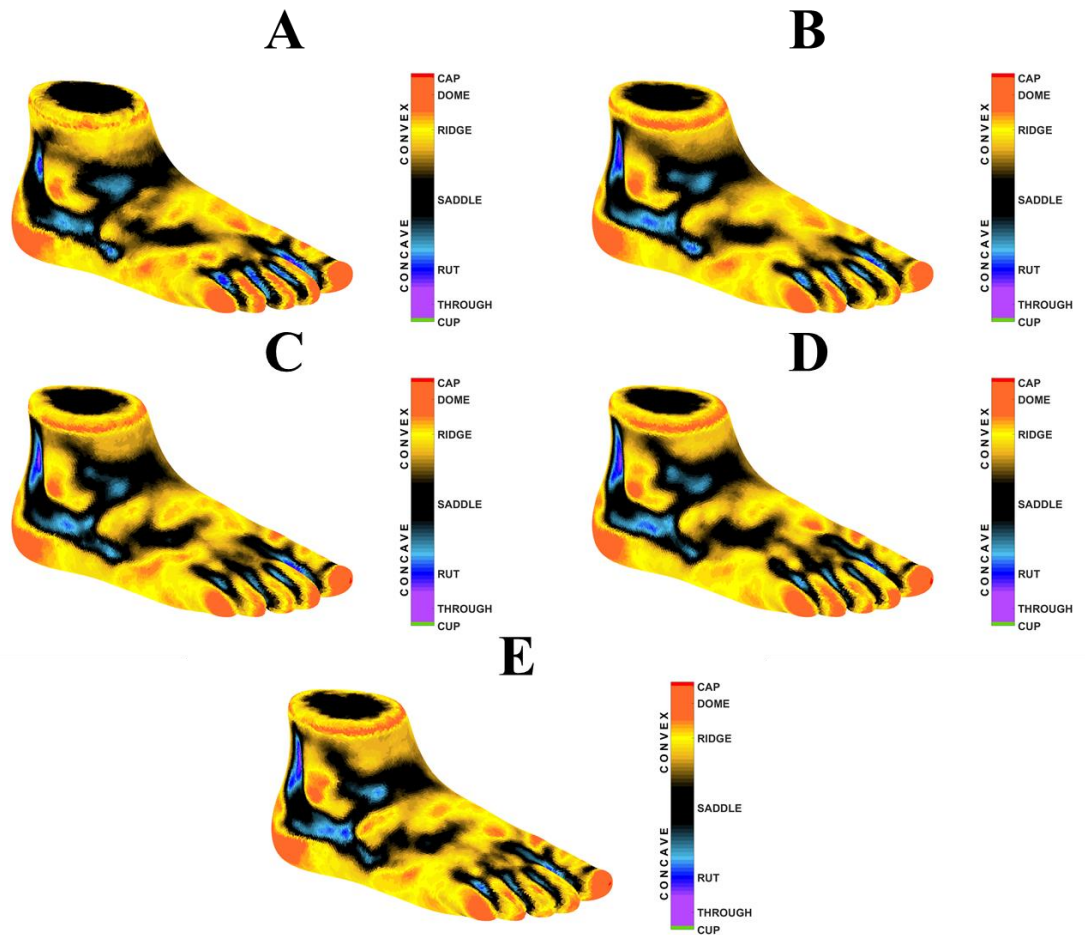


Figure 37.: Mean shape-index maps for each age-group, dorsolateral view: A: 3-year-old mean, B: 4-year-old mean, C: 5-year-old mean, D: 6-year-old mean and E: 7-year-old mean shape-index map.

5.4.1.2. Age-group differences in 3D surface morphology of the dorsolateral aspect

Curvedness

Curvedness

This paragraph will describe the results of the SPM1D ANOVA of curvedness among the five age-groups on the dorsolateral aspect, referring to Figure 38. The two clusters marking significant differences among age-groups (red regions) on the F statistics heat-map are superior to the lateral malleolus and on the instep. Although the number and size of significant clusters are limited, the F statistics can help identify tendencies of curvedness differences. The F values increase as the points' colour becomes lighter, indicating more considerable (although not significant) differences among groups. The main areas of higher F values are found (1) inferior, superior and anterior to the LM, (2) on the instep, (3) in smaller clusters spread out on the dorsum and finally (4) on the lateral side of the dorsum.



Figure 38.: SPM1D ANOVA test results of curvedness among age-groups from the dorsolateral view. The colour bar represents the F statistics, with the threshold marked by red. Red points mark significant (at the $\alpha=0.05$ level) differences among age-groups. Dark to light grey colours indicate increasing F statistics, hence increasing differences among groups. The direction of change is not specified.

The post-hoc comparisons in Table 44. are consistent with the descriptive and ANOVA results and mostly indicate decreasing curvedness (light blue areas) as age increases. The following paragraphs refer to Table 44.

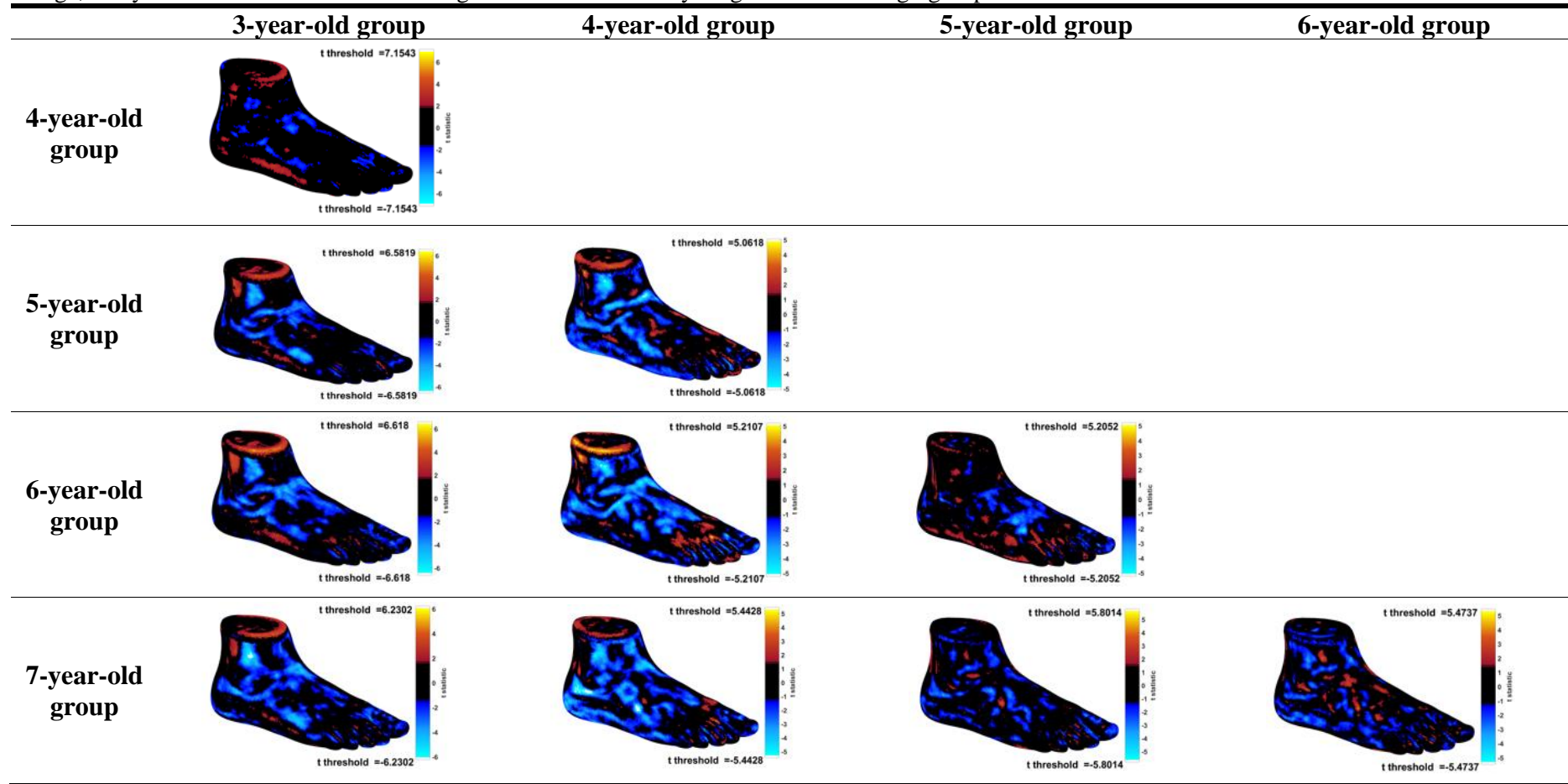
When the 3-year-old group was compared to the 4-year-old group, very few light blue and red areas are visible, suggesting that there were no considerable differences between these age-groups in curvedness on the dorsolateral aspect. As the 3-year-old group was compared to older age-groups, light blue areas appeared marking a decrease in curvedness in the following areas. (1) around the LM, (2) the instep and (3) the lateral side of the dorsum; when compared to the 6 and 7-year-old groups, there were additional clusters of decreasing curvedness on the dorsum.

Most of the larger t values (lighter blue areas); hence differences between subsequent age-groups were found between the ages of 4 and 5. These all indicated decreasing curvedness as age increased and occurred in the following areas (1) around the LM, (2) on the instep, (3) on the lateral part of the dorsum and (4) on the lateral border of the foot. When the 4-year-old group was compared to the 6 and 7-year-old groups, the areas of reducing curvedness (light blue regions) increased to include a large part of the dorsum.

There were light blue areas on the dorsum between the ages of 5 and 6, indicating a decreasing curvedness. When the 5-year-old group was compared to the 7-year-old group, there was no clear pattern to the differences.

Between the ages of 6 and 7 separated small clusters of red areas were present, marking an increase in curvedness on the dorsum's lateral and posterior parts.

Table 44.: Post-hoc SPM1D two-tailed independent t-test results of curvedness projected onto heatmaps. The colour bars represent the t statistics, with the t threshold at each end. White points mark significant differences between age-groups. Dark to light blue colours indicates decreasing curvedness, while red, orange, and yellow colours indicate increasing curvedness from the younger to the older age-groups.



Shape-index

The ANOVA results for shape-index of the dorsolateral aspect are reported in Figure 39. This heat map indicates no large clusters of significant differences among age-groups. As before, to identify qualitative trends, the F-values were considered. Light grey areas marking non-significant differences are situated (1) on and around the lateral malleolus, (2) on the instep and (3) the anterior and postero-lateral dorsal aspect and (4) on the metatarsal heads. As the ANOVA cannot indicate the direction of differences, the post-hoc t-tests will be considered now.



Figure 39.: SPM1D ANOVA test results of shape-index among age-groups from the dorsolateral view. The colour bar represents the F statistics, with the threshold marked by red. Red points mark significant (at the $\alpha=0.05$ level) differences among age-groups. Dark to light grey colours indicate increasing F statistics, hence increasing differences among groups. The direction of differences is not specified.

The post-hoc comparisons in Table 45. are consistent with the descriptive and ANOVA results in Figure 39. and indicate various differences in shape-index between age-groups. The following paragraphs refer to Table 45. The most considerable differences between subsequent age-groups occur between the ages of 4 and 5, and 6 and 7 years.

The comparison of the two youngest age-groups suggests that the shape-index of the dorsolateral aspect did not change considerably (no light blue and red areas are visible). As the youngest group is compared to the older age-groups, differences appear. Between the ages of 3 and 6 and 3 and 7 (1) the lateral malleolus and the lateral side of the posterior dorsum become more convex, while the (2) dorsum of the metatarsal heads become more concave.

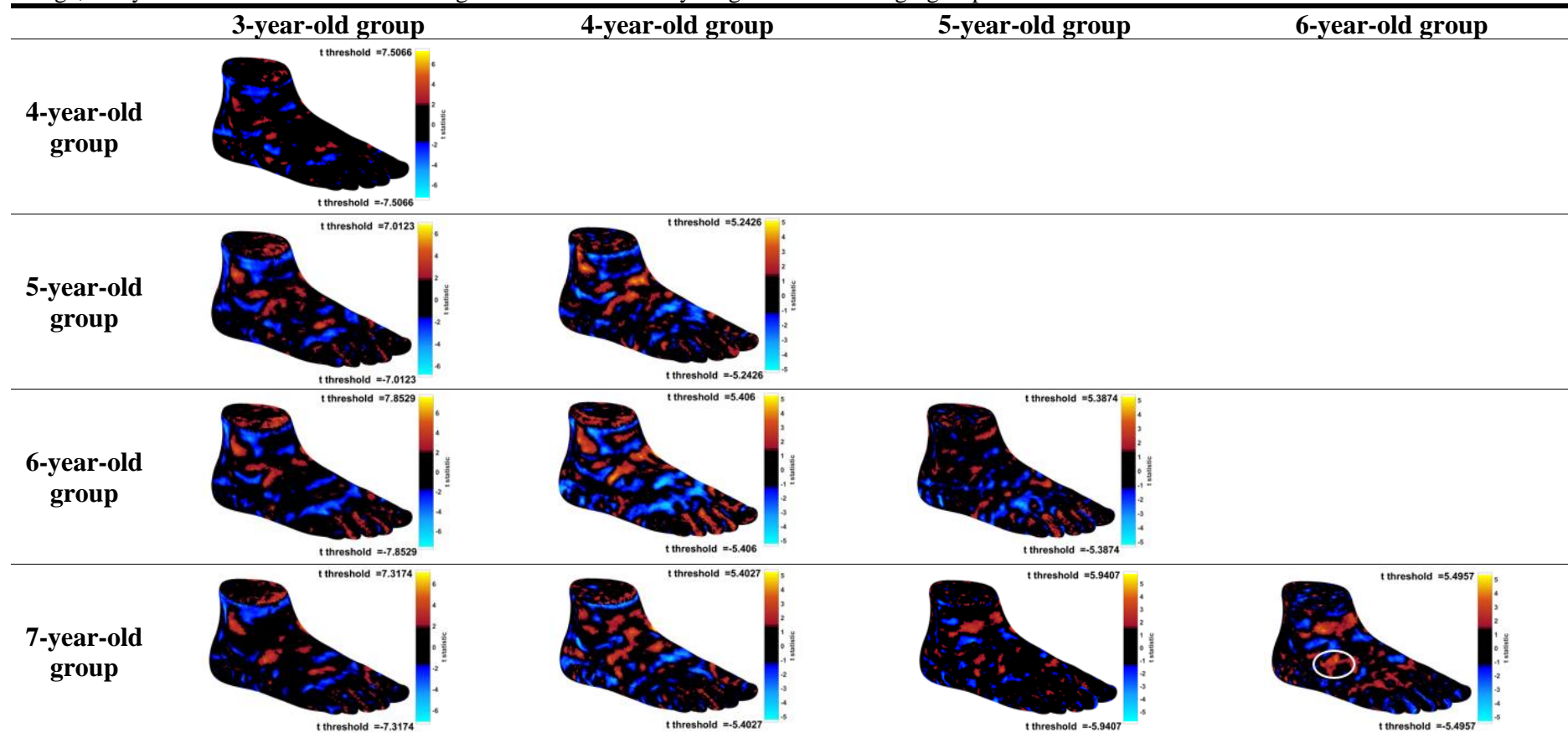
Between the ages of 4 and 5, the areas that become more concave are under the lateral malleolus, and on the anterior dorsum. Areas that become more convex between these two age-groups are found (1) anterior to and on the lateral malleolus, (2) on the instep and (3) on the lateral side of the posterior dorsum.

When the 4-year-old group is compared to the 6-year-old group, the previously mentioned differences become more apparent and more extensive, while the toes' superior side also becomes more convex. Compared to the oldest age-group, the differences are mainly a shift towards convexity on the lateral side of the posterior dorsum and on the anterior ankle.

As the 5-year-old group is compared to the 6 and 7-year-old groups, there are no clear patterns of differences.

Comparing the two oldest age-groups reveals that the foot becomes more convex (1) on the anterior and lateral side of the ankle, (2) the lateral side of the posterior dorsum (marked by a circle) and (3) over the dorsum of the metatarsal heads. Some smaller clusters indicating a shift towards concavity are present anterior to the lateral malleolus and on the instep.

Table 45.: Post-hoc SPM1D two-tailed independent t-test results of shape-index projected onto heatmaps. The colour bars represent the t statistics, with the t threshold at each end. White points mark significant differences between age-groups. Dark to light blue colours indicates decreasing curvedness, while red, orange, and yellow colours indicate increasing curvedness from the younger to the older age-groups.



5.4.2. The 3D surface morphology development of the medial aspect

5.4.2.1. Age-group average 3D surface morphology of the medial aspect

Curvedness

The mean curvedness heat maps of the medial aspect can be seen in Figure 40, and the next paragraphs refer to this Figure throughout.

Although the medial side's prevailing shape is medium curvedness (green), there are clear landmarks and areas of lower and higher curvedness. The mean heat maps show high curvedness (orange and red regions) in (1) the toes area, (2) the dorsum, (3) on the medial aspect of the fore-foot, (4) the inferior medial part of the mid-foot, (5) the medial heel and (6) on the medial malleolus. Low curvedness (blue regions) areas are found (1) posterior and inferior to the medial malleolus, (2) above the medial heel and (3) on the medial mid-foot.

As age increases the high curvedness on the medial malleolus becomes smaller in area, but higher in curvedness. The high curvedness area on the mid-foot dorsum recedes towards the dorsum as age increases. The thick line of high curvedness region on the inferior part of the mid-foot becomes thicker and shorter and completely disconnected from the high curvedness area on the medial heel. At the age of 3, this region is almost connected to the high curvedness on the medial heel, while by the age of 7, these two areas are clearly separated.

The low curvedness areas posterior and inferior to the medial malleolus separate by the age of 4, and at the age of 5 another area of low curvedness appears above the medial heel. There is also a line of low curvedness appearing in the centre of the medial mid-foot above the thick line of high curvedness with increasing age.

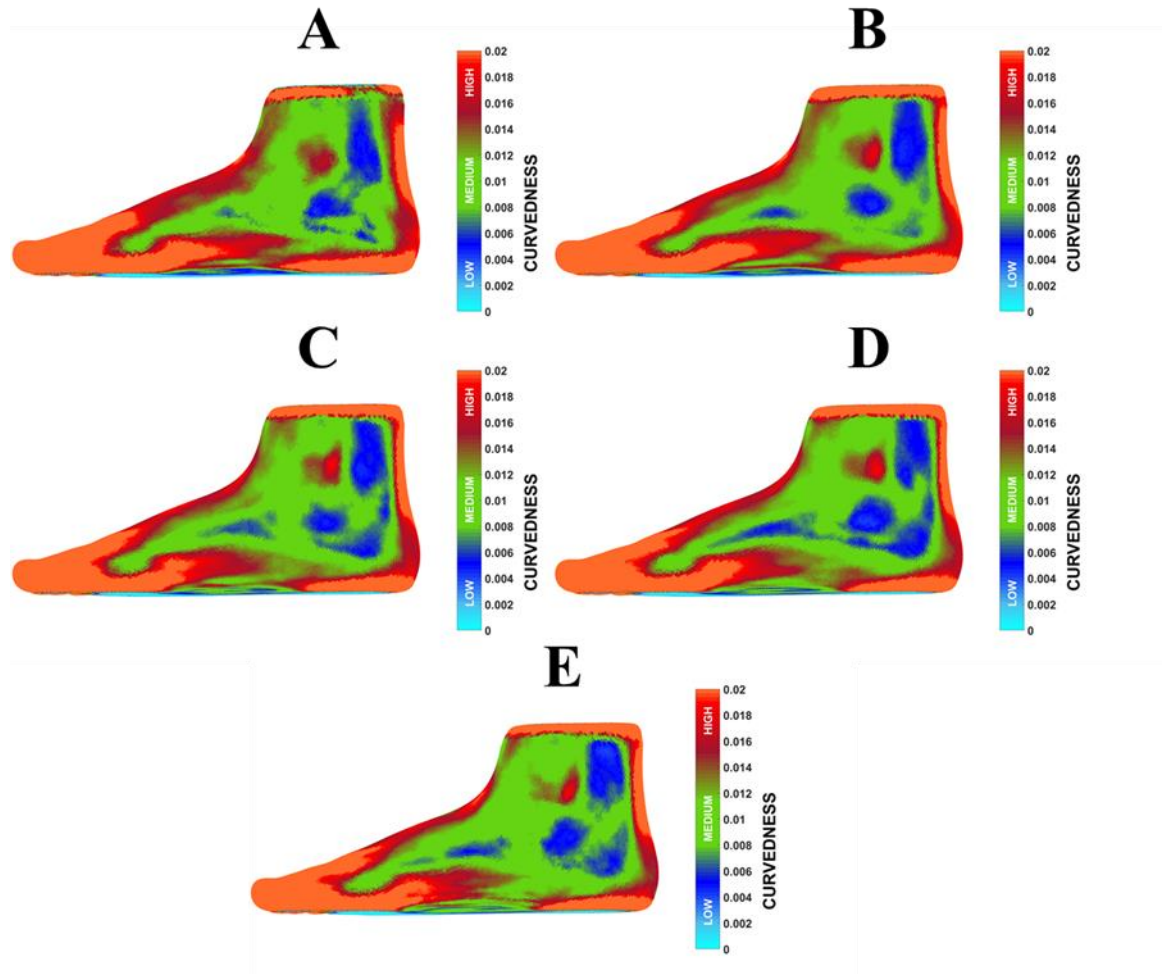


Figure 40.: Mean curvedness maps for each age-group, medial view: A: 3-year-old mean, B: 4-year-old mean, C: 5-year-old mean, D: 6-year-old mean and E: 7-year-old mean curvedness map

Shape-index

Mean shape-index heat-maps are shown in Figure 41, and this Figure will be referred to throughout the next paragraphs.

The medial aspect is dominated by ridge-shaped areas (yellow); however, there are distinct concave and convex regions that will be reviewed. There is high convexity (dome: orange regions) areas (1) on the medial malleolus, (2) posterior and inferior to the medial malleolus (marked by a rectangle), (2) the medial heel, (3) the navicular tuberosity (marked by a circle), (4) the hallux and (5) in an almost vertical line on the medial side of the first metatarsal head. Saddle (black regions) shaped areas are (1) between the medial malleolus and the Achilles-

tendon, (2) above the medial heel and (3) anterior to the navicular tuberosity on the medial aspect of the mid-foot. Concave (rut: blue regions, cyan: trough regions) areas only appear within the first two saddle-shaped regions mentioned previously.

As age increases, the dome shaped (orange region) area on the navicular tuberosity (marked by a circle), although does not change 3D shape, it becomes larger and elongated. The dome shaped (orange region) area posterior and inferior to the medial malleolus (marked by a rectangle) decreases in size and convexity during development from 3 to 7 years of age. On the other hand, the vertical dome shaped area on metatarsal head one increases in width.

As age increases the saddle-shaped regions (black) between the medial malleolus and the Achilles-tendon become larger and more prominent. The concavity (rut shape: blue regions) within this saddle-shaped region appears at the age of 4 and becomes more extensive. With age, this area becomes more concave, and a trough-shaped centre develops within it. A saddle-shaped line (black) is also developing from the navicular tuberosity to the metatarsal head one.

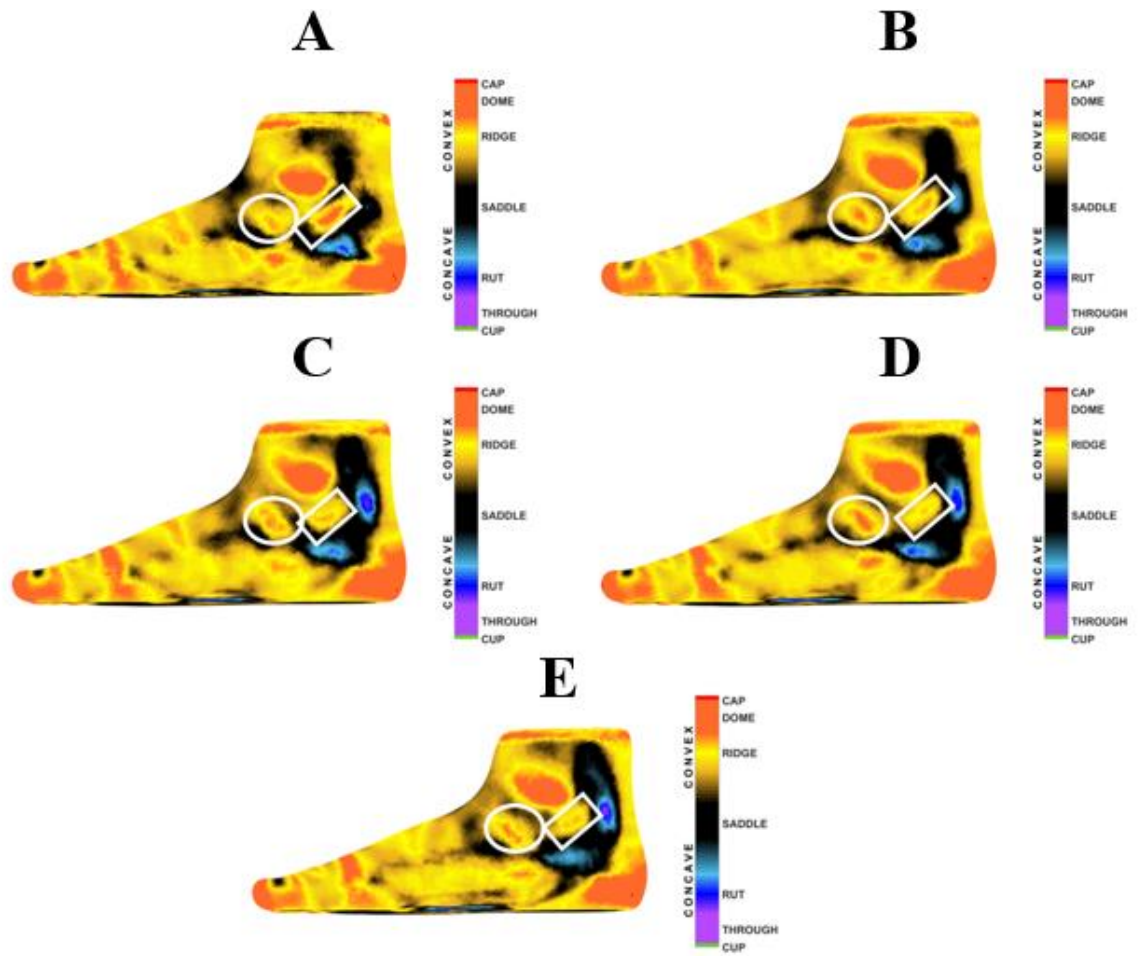


Figure 41.: Mean shape-index maps for each age-group, medial view: A: 3-year-old mean, B: 4-year-old mean, C: 5-year-old mean, D: 6-year-old mean and E: 7-year-old mean shape-index map.

5.4.2.2. Age-group differences in 3D surface morphology of the medial aspect

Curvedness

Figure 42. shows the results of the one-way ANOVA test of curvedness on the medial aspect. Red regions mark the significant clusters (1) between the medial malleolus and the Achilles-tendon, (2) superior to the medial heel, (3) on the medial side of the instep, (4) on the posterior side of the heel and (5) on the first metatarsal head. Further non-significant differences are marked by light grey areas (high F-values). These are apparent (1) in a vertical line on the medial side of the Achilles-tendon, (2) on and inferior to the medial malleolus, (3) in a diagonal line running from the anterior aspect of the ankle through the instep, onto the medial edge of the dorsum, the first metatarsal head and the hallux. There is also a horizontal line of higher F values along the mid- and rear-foot medial border.

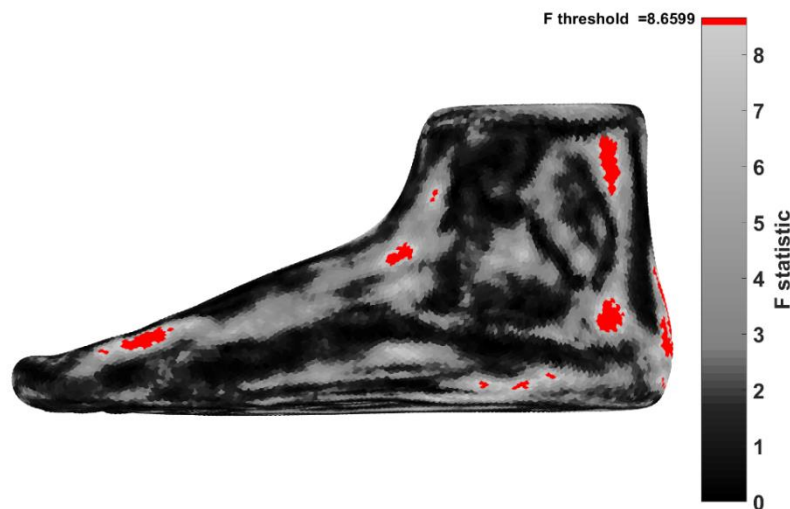


Figure 42.: SPM1D ANOVA test results of curvedness among age-groups from the medial view.

The post-hoc t-tests of curvedness for the medial aspect are shown in Table 46., which will be referred to in the next paragraphs.

The least number of differences occur between the two youngest age-groups. Only two areas of possible differences appear, one in a vertical line on the medial side of the Achilles-

tendon, and another one in the centre of the rear-foot. As the youngest group is compared to the older age-groups, the differences identified are the following. Decreasing curvedness (1) on the medial side of the Achilles-tendon, (2) superior to the medial heel, (3) on the medial border of the rear- and mid-foot and in a diagonal line from the anterior ankle to the hallux (marked by a circle). The largest differences are apparent on the medial side of the Achilles-tendon and on the medial instep.

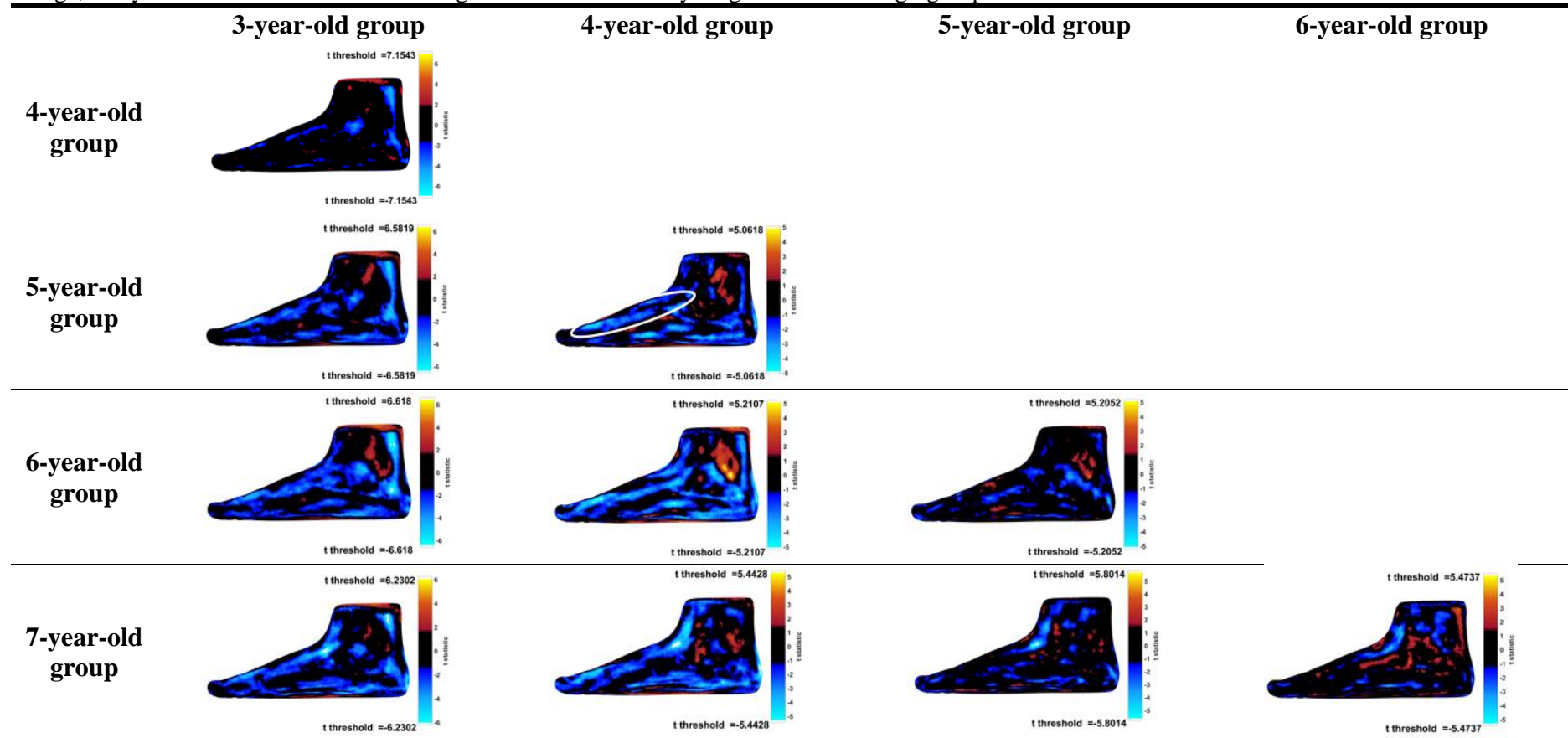
The most considerable differences between subsequent age-groups are between the 4 and 5-year-old groups indicating decreasing curvedness in the areas described in the previous paragraph. Increasing curvedness can only be found posterior to the medial malleolus.

As the 4-year-old group is compared to the 6 and 7-year-old groups, the previous differences magnify. The largest increase in curvedness among all age-group pairs occur between the ages of 4 and 6 years, on the posterior facet of the medial malleolus.

The differences between the 5 and 6-year-old groups are more scarce and less clear. There is increasing curvedness posterior to the medial malleolus and a diagonal line of decreasing curvedness running from inferior to the medial malleolus to the medial heel. When the 5-year-old group is compared to the 7-year-old group, the only difference is a decreasing curvedness on the medial instep.

When the 6 and 7-year-old groups are compared, the changes are also not evident, although there is decreasing curvedness on the medial side of the instep and ankle and increasing curvedness on the Achilles-tendon.

Table 46.: Post-hoc SPM1D two-tailed independent t-test results of curvedness projected onto heatmaps. The colour bars represent the t statistics, with the t threshold at each end. White points mark significant differences between age-groups. Dark to light blue colours indicates decreasing curvedness, while red, orange, and yellow colours indicate increasing curvedness from the younger to the older age-groups.



Shape-index

The ANOVA results for shape-index on the medial aspect are shown in Figure 43. The heat-map shows a small significant cluster on the instep and larger areas of non-significant differences. These are (1) around the significant cluster on the instep, (2) on and around the medial malleolus and (3) on the medial side of the Achilles-tendon.



Figure 43.: SPM1D ANOVA test results of shape-index among age-groups from the medial view.

The post-hoc t-tests are shown in Table 47., which will be referred to throughout the next paragraphs.

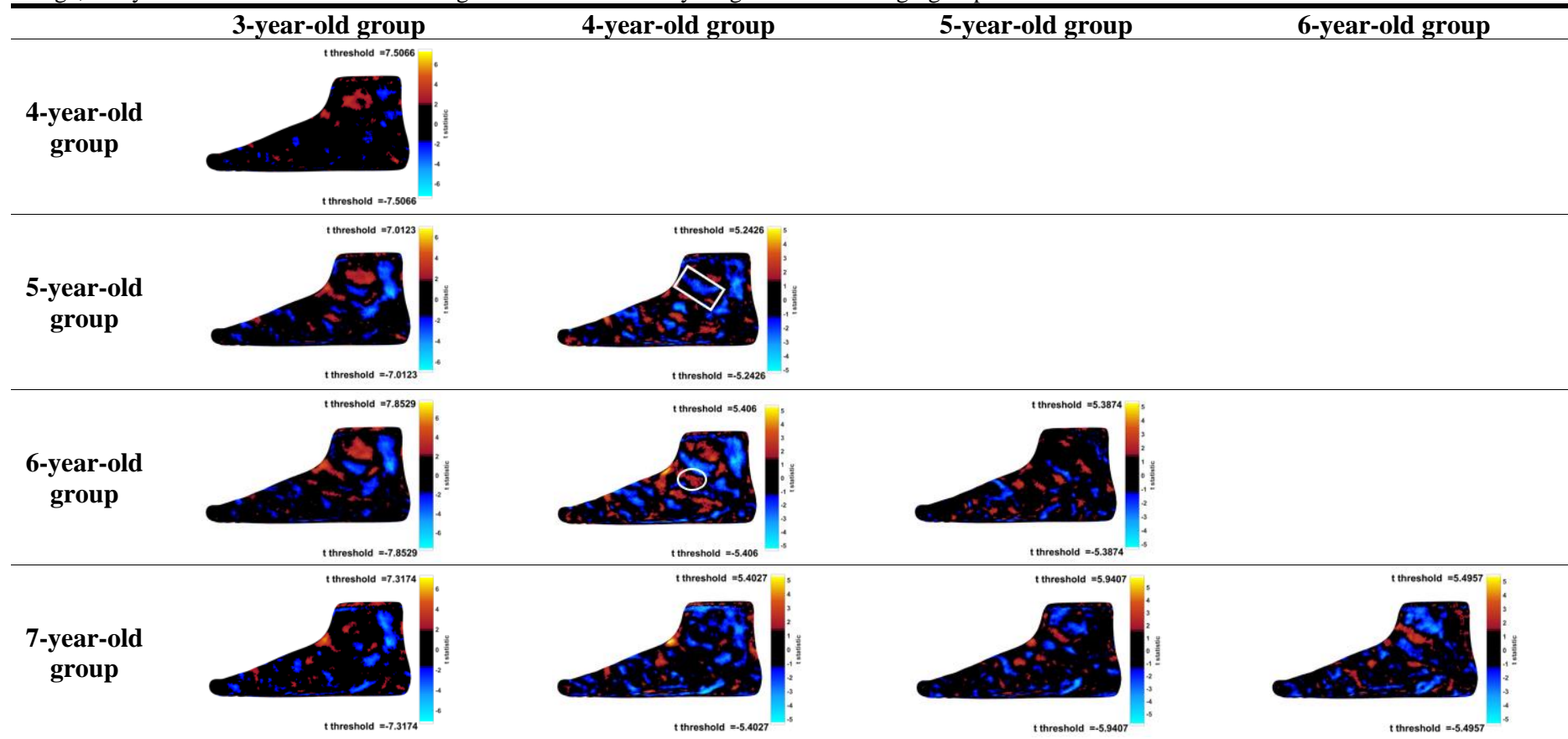
There are no major differences between the 3 and 4-year-old groups. Differences become apparent compared to the 5 and 6-year-old groups. Increasing convexity occur on the medial malleolus and the instep while increasing concavity appears (1) on the medial side of the Achilles-tendon, (2) inferior to the medial malleolus and (3) superior to the medial heel. Compared to the oldest age-group, the same differences are present except for the increasing convexity on the medial malleolus.

Similar to the dorsolateral aspect, the most considerable differences on the medial aspect are between the 4 and 5 and 6 and 7-year-old groups, and the smallest differences are between the two youngest groups. When the 4 and 5-year-old groups are compared, increasing concavity (blue regions) is apparent anterior and inferior to the medial malleolus (marked by a rectangle) and between the Achilles-tendon and the medial malleolus. There are also smaller areas of increasing concavity and convexity spread out on the medial aspect and a small area of increasing convexity on the first metatarsal head. As the 4-year-old group is compared to the 6-year-old group, the differences identified between the ages of 4 and 5 become larger and more defined. Larger areas of increasing convexity also appear on the medial malleolus and the instep. Compared to the oldest age-group, the differences are less prominent, although they are still present as increasing convexity on the instep and increasing concavity on the medial side of the Achilles-tendon.

When the 5-year-old group is compared to the two oldest groups, only small patches of differences can be found.

When the 6 and 7-year-old groups are compared, there is a large area of increasing concavity on and anterior the medial malleolus and an increasing convexity inferior to this area, followed by a smaller increasing concavity inferior to that one.

Table 47.: Post-hoc SPM1D two-tailed independent t-test results of shape-index projected onto heatmaps. The colour bars represent the t statistics, with the t threshold at each end. White points mark significant differences between age-groups. Dark to light blue colours indicates decreasing curvedness, while red, orange, and yellow colours indicate increasing curvedness from the younger to the older age-groups.



5.4.3. The 3D surface morphology development of the plantar aspect

5.4.3.1. Age-group average 3D surface morphology of the plantar aspect

Curvedness

The mean curvedness heat maps of each age-group's plantar aspect can be found in Figure 44., which will be referred to throughout the next paragraphs.

The main characteristics of the plantar aspect in terms of curvedness are (1) a ring of high and medium curvedness on all borders of the foot, (2) a flat area corresponding to the weight-bearing surface and (3) an area of low-medium curvedness on the medial mid-foot extending laterally into the flat area.

The main difference between age-groups occurs in the medial mid-foot, although there is a widening of medium curvedness (green) area in the lateral mid-foot. The only visible difference between the two youngest age-groups is a widening medium curvedness (green) area on the medial mid-foot. After the age of 4, the medium curvedness (green) area in the medial mid-foot extends laterally, and there is a green medium curvedness line moving anteriorly from the posterior edge of the medial mid-foot. Alongside these changes, the medium curvedness area on the medial mid-foot also increases in size. By the age of 7, the medial mid-foot almost only contains medium curvedness points and is connected to the foot's lateral edge by light blue lines of low curvedness.

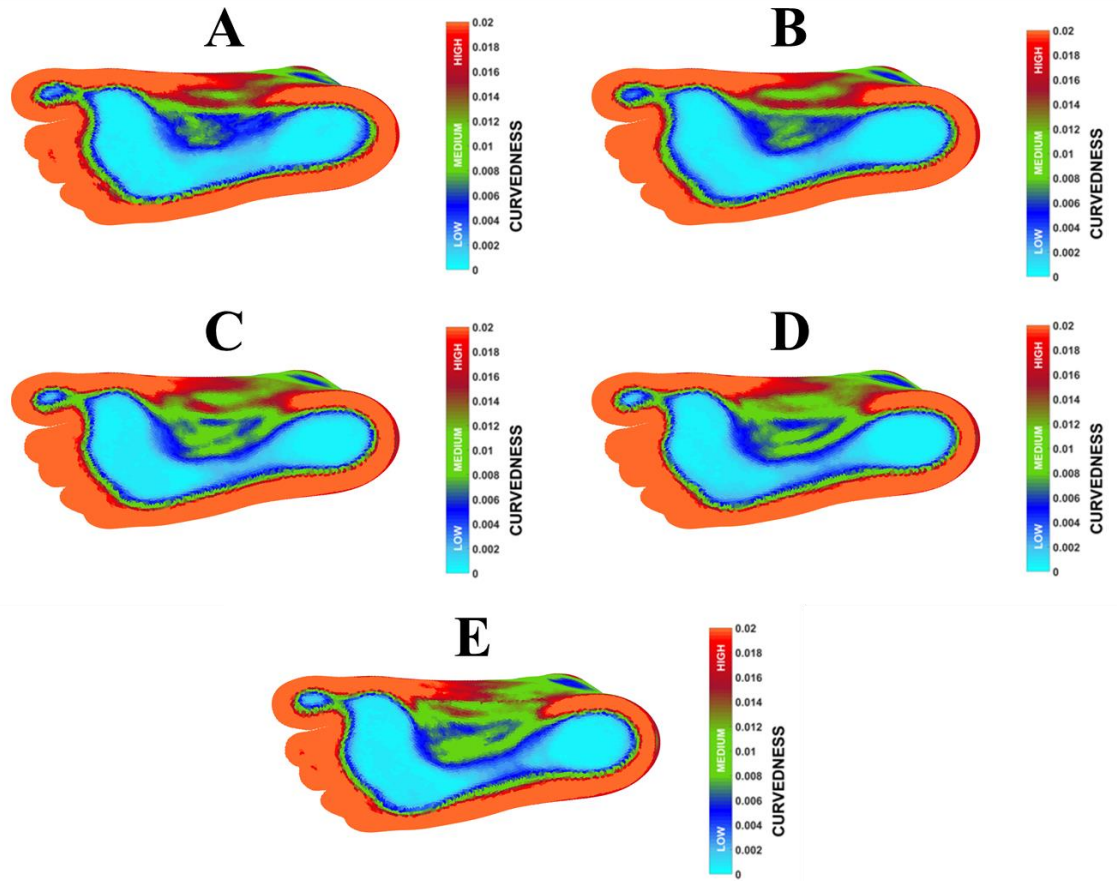


Figure 44.: Mean curvedness heat-maps for each age-group, plantar view: A: 3-year-old mean, B: 4-year-old mean, C: 5-year-old mean, D: 6-year-old mean and E: 7-year-old mean curvedness

Shape-index

The mean shape-index heat-maps for each age-group are shown in Figure 45.

The 3D shape of the plantar aspect is characterised by (1) dome and cap-shaped (orange) hallux and lesser toes, (2) ridge-shaped (yellow) foot borders, (3) dome and cap-shaped (orange) posterior heel border, (4) a flat (black) weight-bearing area and a (4) rut\trough-shaped (blue\cyan) landmark enclosed by a (5) ridge-shaped (yellow) border on the medial mid-foot.

The heat maps show an increase in the size of the rut-shaped (concave) area within the medial mid-foot, with some trough areas appearing in the 5 and 7-year-old groups. The ridge-shaped line enclosing this concavity becomes more defined and extends towards the lateral edge of the plantar aspect as age increases.

The dome\cap-shaped area on the posterior border of the heel becomes thinner as age increases.

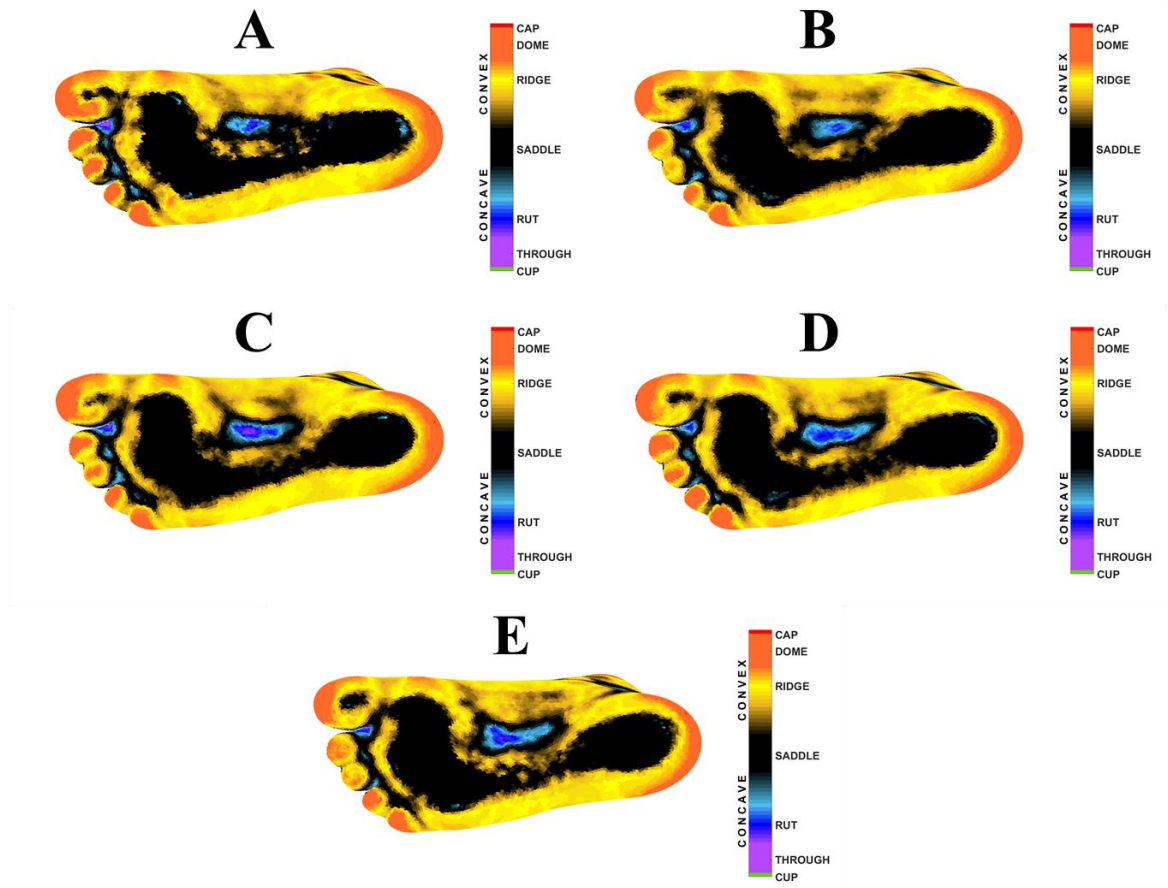


Figure 45.: Mean shape-index maps for each age-group, plantar view A: 3-year-old mean, B: 4-year-old mean, C: 5-year-old mean, D: 6-year-old mean and E: 7-year-old mean curvedness map.

5.4.3.2. Age-group differences in 3D surface morphology of the plantar aspect

Curvedness

The ANOVA results of curvedness for the plantar aspect are shown in Figure 46. Although there is only a small number of significant clusters, the light grey areas highlight parts of the plantar aspect where non-significant differences exist. These are (1) on the posterior border of the heel, (2) a narrow line on the lateral edge of the mid-foot, (3) the medial border of the mid-foot and (4) a line from the medial heel running into the centre of the mid-foot.

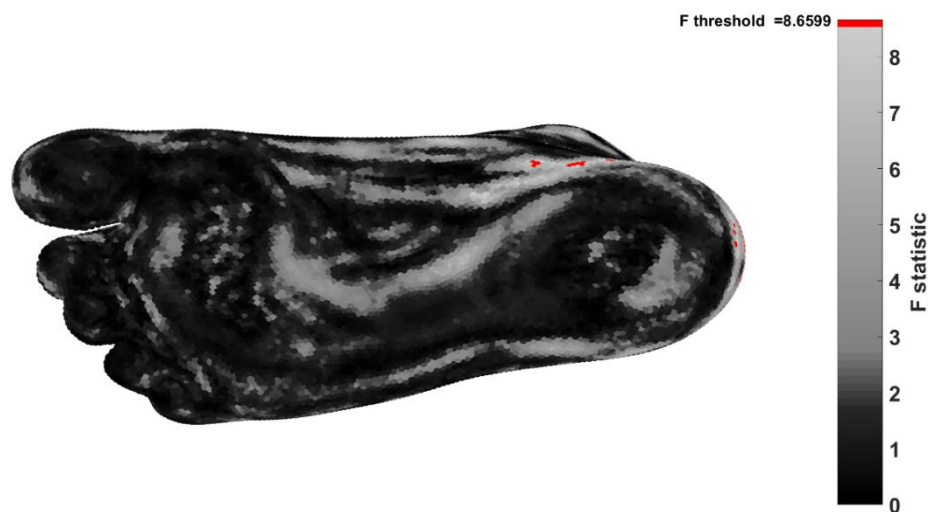


Figure 46.: SPM1D ANOVA test results of curvedness among age-groups from the plantar view.

Table 48. shows the results of the ten independent t-tests of curvedness between age-groups with Bonferroni corrections.

There were no differences between the two youngest groups. As the 3-year-old-group is compared to the older groups, the differences become more apparent on all borders of the foot (decreasing curvedness) and in the centre of the mid-foot (increasing curvedness). As the youngest group is compared to the 6 and 7-year-old groups, (1) decreasing curvedness areas appear anterior to the metatarsal heads and (2) an area of increasing curvedness also appears on the lateral mid-foot.

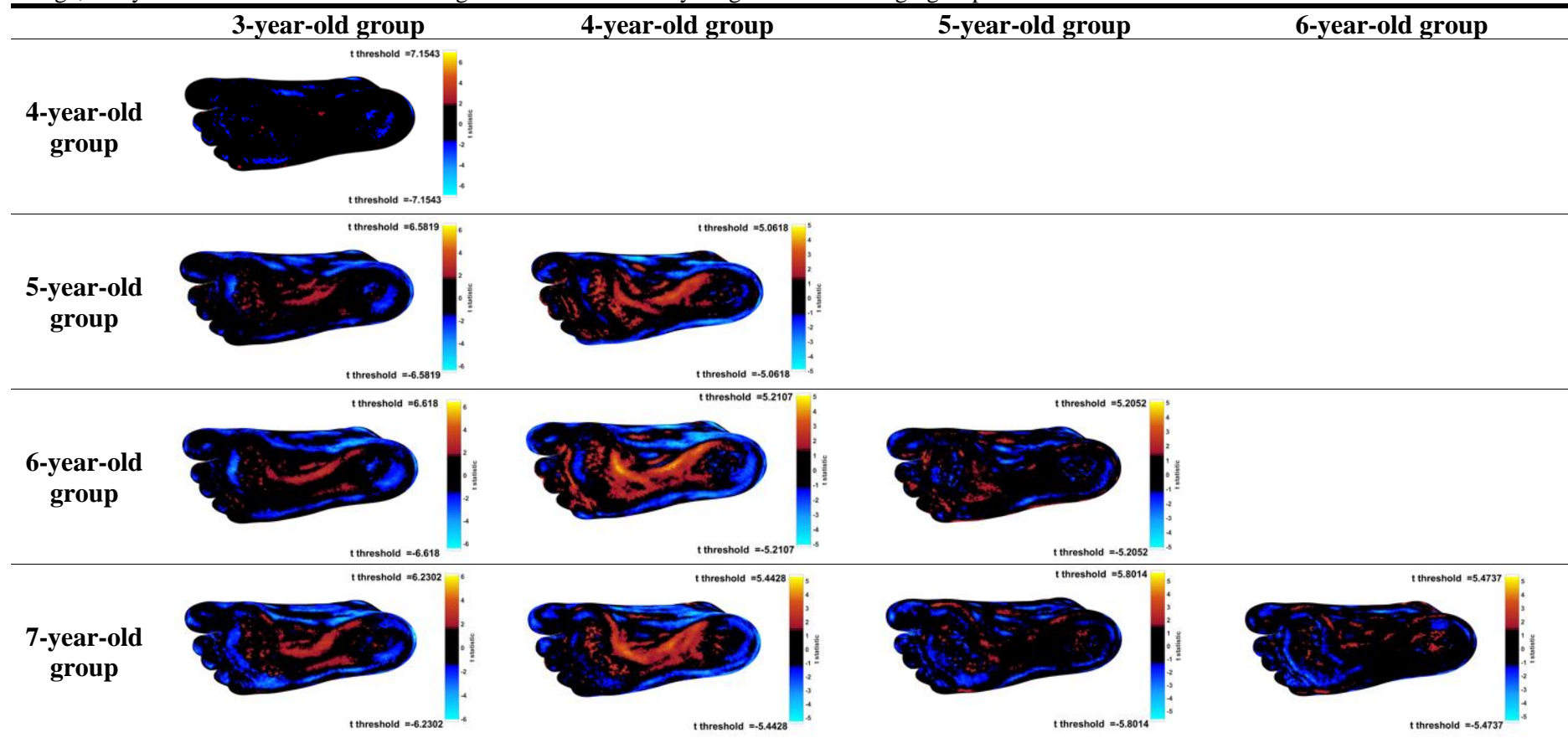
The most considerable differences in curvedness between subsequent age-groups occur between the 4 and 5-year-old groups. These changes are a (1) decreasing curvedness on the border of most of the plantar aspect and (2) increasing curvedness in a line from the medial heel to the centre of the mid-foot. As the 4-year-old group is compared to the two oldest groups, the differences identified before become larger. The line of increasing curvedness in the mid-foot centre becomes more prominent and extends laterally until finally arching back medially to the posterior edge of the first two metatarsal heads. The line of decreasing curvedness on the lateral border bends medially.

The differences between the ages of 5 and 6 were negligible and when the 5-year-old group is compared to the two oldest groups, very few differences occur.

The differences between the ages of 6 and 7 mark a decreasing curvedness around the metatarsal heads' plantar aspect.

Considering the increasing curvedness in the mid-foot centre, there is a pattern of changes as age increases. Comparing the 3 and 4-year-old groups to the older age-groups shows that this increasing curvedness emerges posteriorly from the medial heel and extends anteriorly and laterally before extending medially again towards the posterior edge of the first metatarsal head.

Table 48.: Post-hoc SPM1D two-tailed independent t-test results of curvedness projected onto heatmaps. The colour bars represent the t statistics, with the t threshold at each end. White points mark significant differences between age-groups. Dark to light blue colours indicates decreasing curvedness, while red, orange, and yellow colours indicate increasing curvedness from the younger to the older age-groups.



Shape-index

Figure 47. shows the ANOVA results for shape-index on the plantar aspect. Although there are no significant differences on the plantar aspect, there is a line of light grey area around the lateral edge of the medial mid-foot. These suggest a non-significant change in shape index.

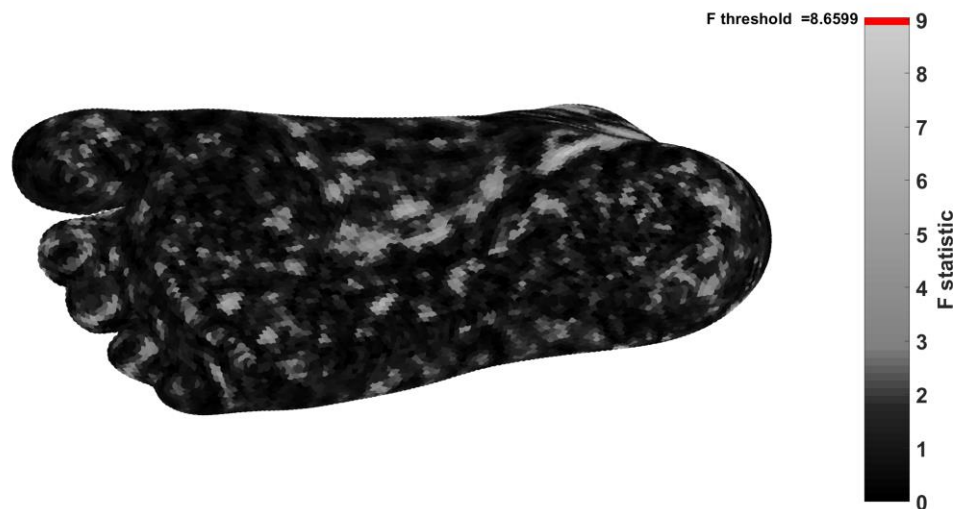


Figure 47.: SPM1D ANOVA test results of shape-index among age-groups from the plantar view.

The post-hoc independent t-test results for shape-index are shown in Table 49. This will be referred to throughout the next paragraphs.

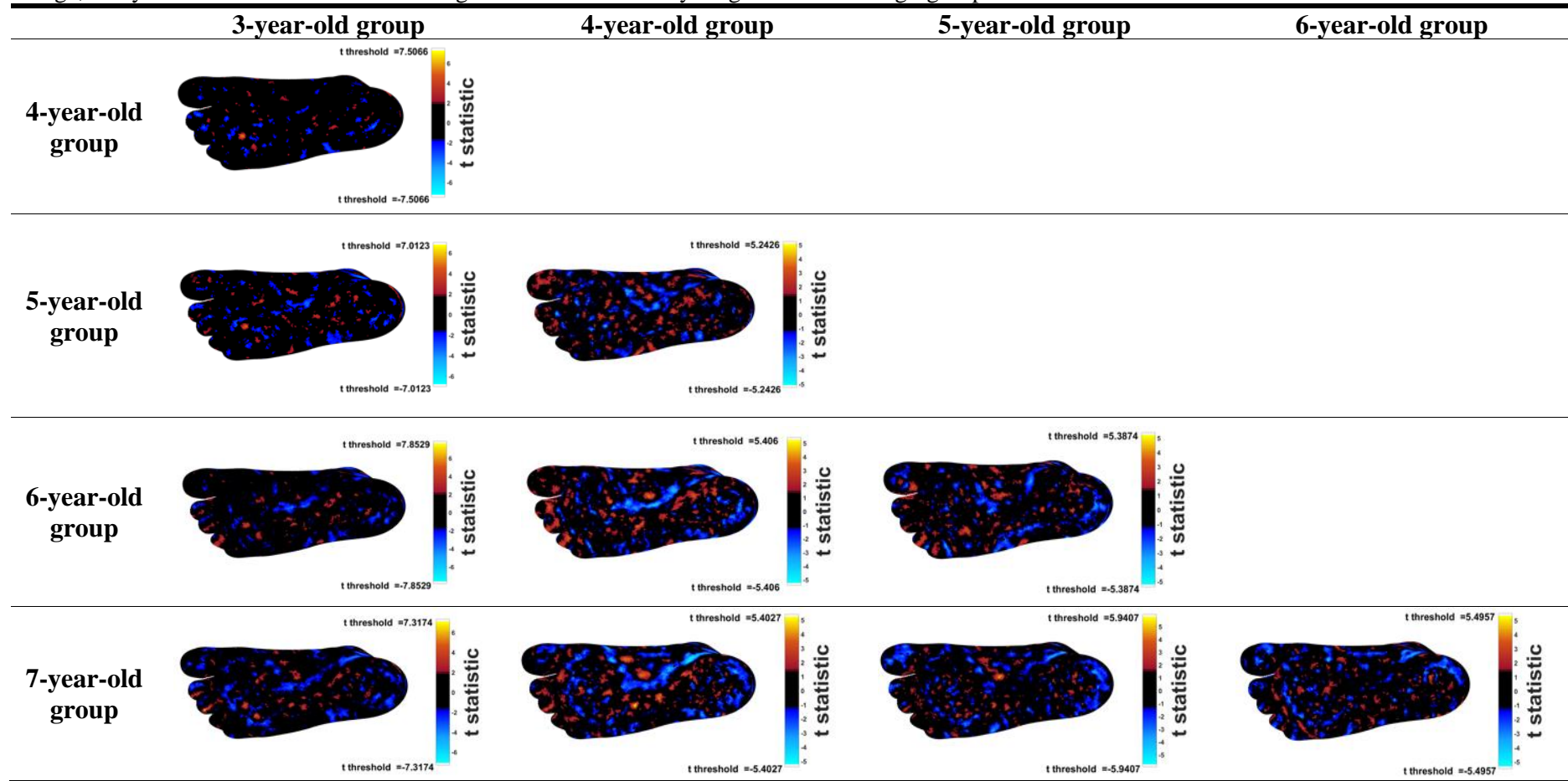
Comparing the two youngest groups did not show any differences, while the comparison of the two oldest groups showed small randomly arranged red and blue clusters, except for a larger cluster of increasing concavity on the medial heel.

When considering differences between subsequent age-groups, the most noticeable differences were between the ages of 4 and 5 and between the ages of 5 and 6. Although most of the red and blue areas seem to be arranged randomly, there was a line of increasing concavity on the posterior and lateral side of the medial mid-foot

As the 3 and 4-year-old groups are compared to older age-groups, the line of increasing concavity on the lateral edge of the medial-mid-foot becomes more prominent and follows the same pattern as the increasing curvedness described in the previous section.

There were no apparent differences between the 5 and 7-year-old groups except for the increasing concavity on the medial heel.

Table 49.: Post-hoc SPM1D two-tailed independent t-test results of curvedness projected onto heatmaps. The colour bars represent the t statistics, with the t threshold at each end. White points mark significant differences between age-groups. Dark to light blue colours indicates decreasing curvedness, while red, orange, and yellow colours indicate increasing curvedness from the younger to the older age-groups.



5.5. Discussion of the 3D surface morphology development of the paediatric foot

The aim of this chapter was to provide an advanced understanding of the development of 3D surface morphology of the paediatric foot. It was demonstrated that 3D shape descriptors (curvedness and shape-index) could offer an advanced understanding of 3D surface morphology development in children and provide a relevant and novel description of the paediatric foot trajectory. These parameters could contribute information about the changes in the underlying structures without the use of more expensive imaging methods and help clinicians in decision making or shoe manufacturers in footwear last design

5.5.1. The 3D surface morphology development of the dorsolateral aspect

The primary results on the dorsolateral aspect suggested two main postural\structural changes: increased 3D slenderness and a reduction in rear-foot eversion. Secondary findings indicated the increased prominence of anatomical landmarks

The differences in curvedness and shape-index between age-groups indicate that the surface of the dorsum becomes flatter between the ages of 4 and 6 years. This suggests that the surface morphology of the foot changes to a slenderer shape between the ages of 4 and 6 years. Related results have also been shown in the literature (Mauch et al., 2008) using a group of normalized 2D anthropometric measures. The 2D results of this thesis have also shown that both the normalized fore-foot and mid-foot height decreases (section 4.4.2.3 and 4.4.2.4.), suggesting that the height of the fore- and mid-foot does not grow in proportion with foot length. Although the two types of data show similar changes, the 3D shape descriptors indicate an increase in 3D slenderness in terms of local 3D surface morphology,

while the 2D anthropometric measures suggest an increase in 2D slenderness in terms of global 2D foot shape.

Furthermore, the increasing 3D slenderness is carried on into the age of 7 years. These results also agree with the pilot study's findings (sections 3.7-3.9.) that suggested these changes are markers of adipose tissue reduction (Varga et al., 2020). On the other hand, although the amount of adipose tissue might not change, it might be spread out more evenly, reducing local adipose tissue thickness, therefore the curvedness of the surface. This hypothesis may be confirmed by the changes in BMI and fat percentage of the reference children in Fomon et al. (1982). These two measures decreased up to the age of 6 years in boys and 7 years in girls. These conclusions are also supported by Weber et al. (2012) and, more recently, by Wells et al. (2020) using fat mass index (kg/m^2). Wells et al. (2020) used percentiles to present changes in fat mass index between the ages of 6 weeks and 5 years and found that fat mass index decreased from the age of one continuously, although suggest that fat was gained in proportion with height after 2 years of age.

The decrease in curvedness inferior to the lateral malleolus between the ages of 4 and 5 years and after the age of 6 years could be a sign of decreasing calcaneus or rear-foot angle (the angle between the Achilles and the line of the calf). The curves of this area is also an item in the Foot posture index (FPI-6) (Redmond et al., 2006a). It has been shown by Martínez-Nova et al. (2018) in Spanish children that this item significantly reduced from the initial (5-11-year-old) to the repeat (8-14-year-old) measurement after three years (curves at the malleolus item (initial)=0.50, repeat=0.46, $p=0.038$). However, the current thesis only showed a reduction in curvedness between the ages of 4 and 5 years and after the age of 6. As the repeat measurement in Martínez-Nova et al. (2018) occurred three years after the initial one, the year by year differences cannot be distinguished, and it could be the case that

there were no reductions in this item between 5 and 6 years of age. While their study confirmed a change in curves around the lateral malleolus after the age of 5, the present thesis showed that these changes start earlier, at the age of 4 years. Although this is only one item in the FPI-6 index and hence cannot capture the changes in foot pronation, it may be an indicator of calcaneus\rear-foot angle reduction. This can also be considered as a representation of the resting calcaneal stance position (RCSP) or the rear-foot angle (Langley et al., 2016). Both of these capture the same angle: the angle between the perpendicular line to the ground and the bisector of the calcaneus (Žukauskas et al., 2021, Cho et al., 2019). This parameter is commonly used in diagnosing flatfoot and was shown to have moderate correlation with FPI-6 in 8 to 13-year-old children (Cho et al., 2019), and moderate agreement with FPI-6 in adults (Langley et al., 2016). However, it was also shown, that although RCSP correlated moderately with FPI-6 in children aged 5 to 8, when all other measurements were also considered in a multiple linear regression, it did not predict FPI-6 (Žukauskas et al., 2021). Further work will be required to establish the relationship between the changes in 3D surface morphology related to rear-foot posture and FPI-6. Therefore, using the curvedness changes around the lateral malleolus from 3D scans of children's feet may be a tool to assess rear-foot posture and a more objective alternative to capture this item in FPI-6.

Although the curvedness inferior to the lateral malleolus decreases in the current study, the shape-index seems to be shifting towards concavity (but not significantly) superior to the same area. When considering the average shape-index heat maps, this shift towards concavity could result from the widening gap between the lateral heel and the lateral malleolus due to the raising of the malleolus, rather than the change in rear-foot angle.

The following secondary results suggest the increasing prominence of anatomical landmarks: (1) a reduction of high curvedness around the lateral malleolus, (2) a shift towards convexity on the lateral malleolus, (3) a shift towards convexity on the lateral side of the posterior dorsum between the ages of 3 and 5 years (extensor digitorum brevis muscle), (4) a shift towards convexity over the metatarsal heads between the ages of 6 and 7 years and finally (5) a shift towards convexity and reducing curvedness on the instep between the ages of 4 and 5 years. This final finding could be related to the changing proportions of the foot and the strengthening of the extensor and tibialis anterior muscles. These muscles and respective tendons become stronger with age, their cross-section increases, causing them to become more prominent, reducing concavity in the instep.

In summary, the main changes in 3D surface morphology on the dorsolateral aspect are twofold. First, there is a reduction in curvedness and shift towards concavity on the dorsum between the ages of 4 and 6 years, suggesting an increase in foot 3D slenderness and possibly a reduction in adipose tissue thickness related to increasing 2D slenderness (normalized width measures). Second, the reduction in curvedness under the lateral malleolus between the ages of 4 and 5 years and after 6 years of age suggests a reduction in rear-foot angle, indicating a change in rear-foot posture towards a more inverted one. The findings of the changing curves inferior to the lateral malleolus could also be a more objective alternative to the same item in FPI-6.

The secondary findings indicated the increasing prominence of anatomical landmarks due to bony development and increase in muscle cross section.

5.5.2. The 3D surface morphology development of the medial aspect

The primary findings on the medial aspect indicated changes in rear-foot posture, while secondary findings indicated the increased prominence of the medial malleolus.

One of the major changes in 3D foot surface morphology on the medial aspect is the shift towards concavity on the medial side of the Achilles-tendon between the 4 and 5-year-old groups, coupled with increasing curvedness on the posterior facet of the medial malleolus between the 4 and 6-year-old groups. These differences could be attributed to (1) the changing proportions of the rear-foot, (2) the decreasing thickness of adipose tissue and the (3) emergence of the Achilles-tendon and (4) the medial malleolus. These differences in shape-index and curvedness occur between the ages of 4 and 6 years. Although curvedness also decreases in this area, this reduction seems to be concentrated in a thin line just medial of the Achilles-tendon. When comparing these differences to the lateral side of the Achilles-tendon on the dorsolateral aspect (section 5.6.4.), there are stark differences. On the lateral side of the Achilles-tendon, there are no large areas of shift towards concavity except for a thin line just lateral to the tendon, and curvedness does not change in this area. This suggests that the medial side of the Achilles-tendon becomes more concave and curved than the lateral one, which could indicate a decrease in the rear-foot angle\RCSP as age increases.

A further main change in 3D surface morphology is related to the muscles (tibialis posterior, flexor digitorum longus and flexor hallucis longus) running inferior and posterior to the medial malleolus and are marked by an orange cluster of points suggesting a dome or cap-shaped area. The average heat maps indicate that this dome\cap shape (red area), after 4 years of age, changes into a ridge shape (yellow area), which is also supported by the t-test results, demonstrating a reduced convexity in the same location. These findings may suggest that the area where these muscles run becomes less prominent as age increases, especially

from 4 years of age. This decrease in prominence could be associated with reducing rear-foot angle, suggesting a change in rear-foot posture.

The secondary findings suggested that the navicular tuberosity can be identified by a dome or cap shape (orange cluster) anterior and inferior to the medial malleolus. The talonavicular joint's concavity or convexity, hence the navicular tuberosity, is an item in the FPI-6 (Redmond et al., 2006a) and the landmark's prominence; hence convexity contributes towards a total score marking a more pronated rear-foot posture. While it has been shown that the FPI-6 reduces significantly between the ages of 5 and 14 years (Martínez-Nova et al., 2018), when the talonavicular joint prominence index was separately investigated, no significant differences (mean FPI (initial)=0.54 vs. FPI (repeat)=0.53, $p=0.841$) could be found between the initial and the repeat measurement after three years. This agrees with the current thesis results confirming the validity of this FPI-6 item and suggesting that the current methods may be an objective alternative to capture this item.

The medial malleolus could also be identified on the mean shape-index heat-maps by the large orange cluster on the ankle's medial side, indicating a dome-shaped landmark. This landmark becomes more convex as age increases suggesting the increasing prominence of this bony structure. This is in accordance with the findings of LaMont et al. (2015), who confirmed four stages of ossification of the medial malleolus between the ages of 4 and 12, with secondary ossification centres being more common in girls aged 6 to 9 and boys aged 8 to 11 years.

In summary, the primary findings suggested a decrease in rear-foot eversion. This was based on the increasing concavity on the medial aspect of the Achilles-tendon and over the tarsal tunnel's location between the ages of 4 and 5 years. These results, together with the results

of the previous section (decreasing rear-foot eversion assumed based on the changes under the lateral malleolus), suggest that the 3D surface morphology of the paediatric foot is a useful tool to investigate the posture of the rear-foot. Once the typical 3D surface morphology of the related areas is established throughout development, the individual morphological foot maps can be used to help with diagnoses of pathologies related to rear-foot eversion. Furthermore, the 3D morphology data in these areas may also support the assessment of flat foot as increased rear-foot eversion is a sign of flat foot. In addition, the same data may also be captured during the Jack's test, to establish the presence of rigid flat foot. Although this may require a faster 3D scanning technology as children may not be able to stand on tiptoes for a long period of time.

Secondary results indicated the increased prominence of the medial malleolus with age and that although there were no differences in 3D shape between age-groups in the navicular tuberosity, the fact that it could be identified may prove useful as a more objective alternative to the talonavicular joint prominence item of FPI-6.

5.5.3. The 3D surface morphology development of the plantar aspect

The primary findings on the plantar aspect are related to the emergence of the MLA based on the 3D surface morphology of the mid-foot.

The results suggest that most of the 3D plantar aspect morphology changes occurred between the 4 and 5-year-old groups with little to no changes between any other subsequent age-groups. The increasing curvedness between the ages of 4 and 5 years running in the centre of the mid-foot suggests the raising of the arch's surface, indicating the development of the MLA. The average curvedness heat maps also suggest an increase in medium curvedness within the MLA, although the t-tests do not support this.

Although there are no visible differences between older subsequent age-groups, further developments can be noticed when the 4-year-old group is compared to older groups. The MLA, marked by the increasing curvedness, becomes more defined and extends laterally and eventually reaches the metatarsal heads' posterior edge. The increased curvedness posterior to metatarsal heads may indicate the development of the transverse arch from the age of 5 years.

Although curvedness increases between the ages of 4 and 5 years, the shape-index changes occur more gradually up to the age of 6 years. This comprises a shift towards concavity surrounding the MLA, marking the inside of the arch's edge. These findings suggest that the medial side of the MLA edge is becoming more concave from the age of 4 years up to the age of 6 years. The curvedness and shape-index results combined may indicate that the edge of the MLA develops by the age of 5 years, and further increases in arch height up to the age of 6 years result in the shift towards concavity on the inside edge of the MLA edge. The average shape-index heat maps indicate that although there is a slight shift towards concavity

(not seen on the t-tests), the main difference between age-groups is the increasing size of the concave area as it becomes longer and broader.

In contrast with this are reports in the literature (Muller et al., 2012, Bosch et al., 2010b, Sacco et al., 2015) that the MLA continued to develop after the age of 6 years. However, these findings are based on the area under the MLA (AI, footprints) and not on MLA surface height or curvedness. Although the 3D shape descriptors in the current study are also not direct representations of MLA height, the combined changes in 3D surface shape around the MLA are markers of increasing height in its centre. These present results combined with the literature may suggest that the MLA, although it may increase in area beyond the age of 6, may not increase in surface height. The current findings corroborate the results of Chang et al. (2012), who measured the 3D volume of the MLA and suggested that the MLA not only increases in height but in 3D volume too up to the age of 6 years. They also argued that although navicular height has a higher discrimination rate between age-groups, it may not represent the complete 3D development of the MLA due to its 2D nature. While these results may show changes in the overall MLA volume, the methods in the current thesis can also locate where these changes within the MLA occur, providing a morphological map of MLA development.

On the other hand, Chang et al. (2012) did not show significant differences between the navicular height or arch volume of 4 and 5-year-old children but found significant differences between 3 and 4 years of age. This contrasts with the current findings, although the sample size in Chang et al. (2012) was limited to 36 children in the four age-groups from 3 to 6 years of age.

The lack of changes between the two youngest groups may seem to contradict studies in the existing literature, which suggest the continuous raising of the MLA from or even before the age of 3 years (Muller et al., 2012, Bosch et al., 2010b, Sacco et al., 2015, Chang et al., 2012). Although the t-tests do not show a difference in 3D surface morphology in the MLA between the two youngest groups, the arch's presence is observable in the average curvedness and shape-index heat maps in the 3-year-old group. This suggests that the reason for the lack of differences between the two youngest age-groups could be the small sample size in the 3-year-old group (12).

The patterns described in the previous paragraphs suggest a distal to proximal development of the MLA until the age of 5. After this, a proximo-distal development occurs along with the development of the transverse arch. Gill et al. (2016) have also identified similar patterns using footprint measures regressed with gait parameters such as step length. They argued that MLA height might increase first to support longer steps, while the lower transverse arch may help with stability, developing later. However, this study used a measure called the Keimig Index, which quantifies the whole missing area of a footprint relative to the size of a toeless footprint. This parameter cannot locate where the changes in missing footprint areas are, while the current thesis methods can pinpoint curvedness changes. As a result of this high resolution, it was found that the increased curvedness posterior to the metatarsal heads indicate that the foot surface becomes less flat; hence it is not entirely in contact with the ground, indicating the development of the transverse arch. To the author's knowledge, the present thesis is the first study to identify these patterns in the development of the arches with exact locations of the changes occurring.

In summary, based on the results, the development of the plantar aspect is characterized by several factors. Firstly, an existing MLA at the age of 3 years is visible in the anterior part

of the medial mid-foot. This is indicated by mostly low curvedness, rut shape in the centre, and small ridge shape areas on the edges of the MLA. Secondly, the changes in 3D surface morphology on the edges of and within the MLA between the ages of 4 and 6 years indicate the raising of the plantar aspect within the arch. Thirdly, the patterns of 3D surface shape differences between age-groups suggest that the MLA develops first until the age of 6, supporting longer steps, and the transverse arch starts to develop later to provide stability before raising up. The results may also suggest that the MLA only increases in height up to the age of 6 years, and from then on, it only increases in area.

The following section will present the results of simple linear regression of the normalized 2D anthropometric measures with the 3D surface shape descriptors, focusing on the changes identified in the previous sections.

5.6. Results: Predictors of paediatric 3D foot surface morphology

The main 3D surface morphology changes and proposed postural and structural changes were threefold.

First, decreasing rear-foot eversion was indicated by (a) reduced curvedness inferior to the lateral malleolus, (b) increased concavity on the medial side of the Achilles-tendon and (c) increased concavity over the tarsal canal.

Second, an increase in arch height was demonstrated by (1) an increased curvedness (a) on the lateral edge of the MLA, (b) on the transverse arch and (c) the lateral longitudinal arch; and by (2) an increased concavity (a) on the medial and posterior aspects of the lateral edge of the MLA and (b) within the transverse arch.

Third, there was an increasing slenderness of the foot (a) on the dorsum, (b) around the malleoli and (c) on the instep (reduced curvedness or increased concavity).

The 2D anthropometric predictors of these changes will be presented next.

5.6.1. Predictors of decreasing rear-foot eversion

Considering the decreasing rear-foot eversion, (1) age, (2) normalized mid-foot width, (3) normalized rear-foot height and (4) normalized fore-foot width were selected as the strongest predictors of the corresponding curvedness and shape-index differences (see Table 50. for SPM1D simple linear regression heat maps) identified by the post-hoc t-tests. This Table will be referred to in the next paragraphs.

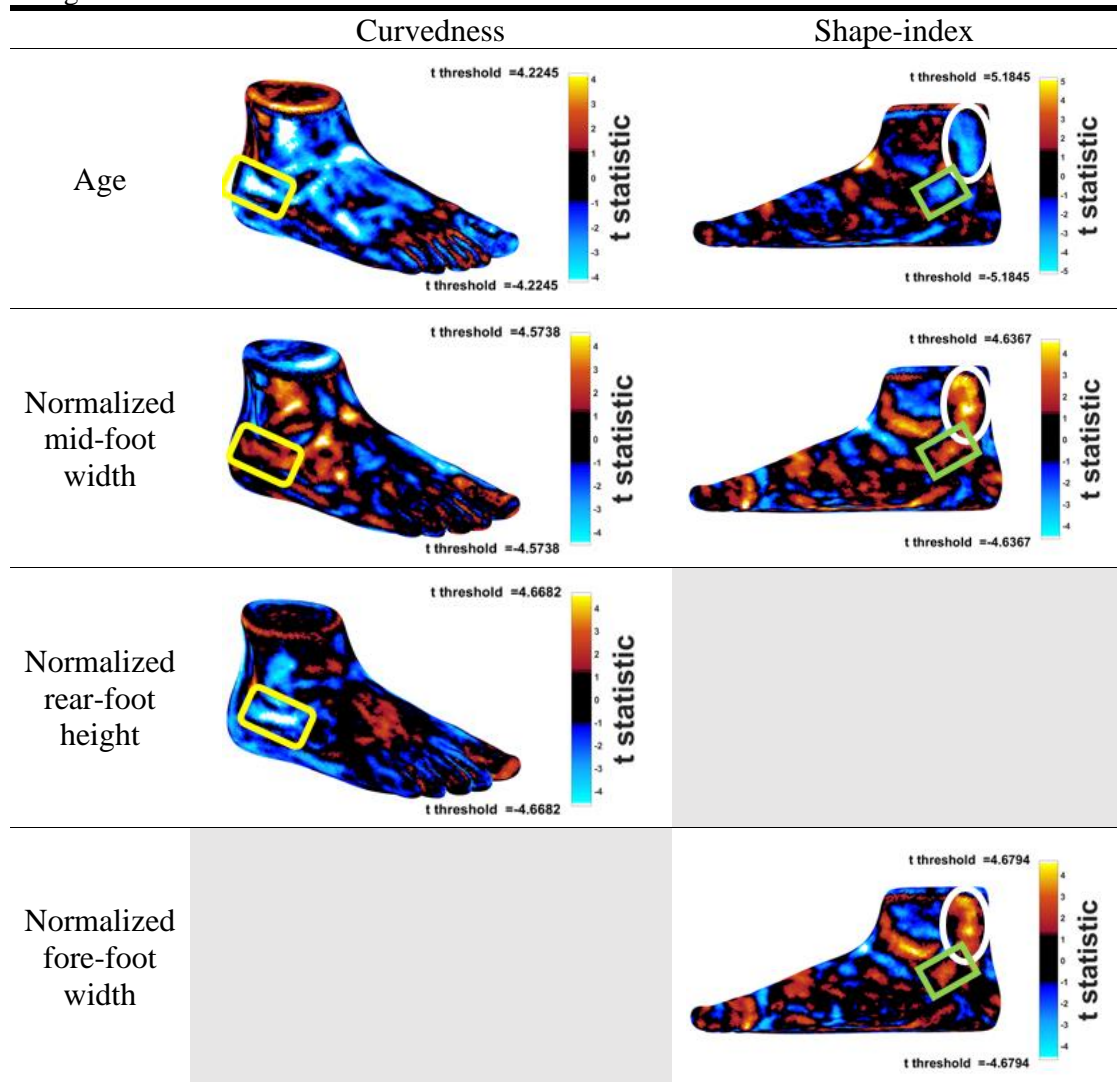
The main areas of concern are the following. (1) Inferior to the lateral malleolus marked by yellow rectangles: age vs. curvedness, blue clusters indicating decreasing curvedness, normalized mid-foot width vs. curvedness, red clusters indicating decreasing curvedness and normalized rear-foot height vs. curvedness, blue clusters indicating decreasing curvedness. (2) On the medial aspect of the Achilles-tendon marked by white circles: age vs. shape-index, blue clusters indicating increasing concavity; normalized mid-foot width vs. curvedness and normalized fore-foot width vs. curvedness, red clusters indicating increasing concavity. Finally, (3) over the tarsal canal marked by green rectangles: age vs. shape-index), blue clusters indicating decreasing convexity and normalized mid-foot width vs. shape-index and normalized fore-foot width vs. shape-index, red clusters indicating decreasing convexity.

Based on curvedness inferior to the lateral malleolus, age and normalized rear-foot height are stronger predictor of decreasing rear-foot eversion than normalized mid-foot width.

Based on shape index on the medial aspect of the Achilles-tendon (white circles), normalized mid-foot width and normalized fore-foot width are stronger predictors of decreasing rear-foot eversion than age. Finally, regarding the area over the tarsal canal (green rectangles)

age, normalized mid-foot width and normalized fore-foot width are similarly strong predictors of decreasing rear-foot eversion.

Table 50.: SPM1D simple linear regressions: Each cell contains a heat map with regression results between the variable at the beginning of the row and the 3D shape descriptor at the top of the column. Markings are referred to in the text.



5.6.2. Predictors of increasing arch height

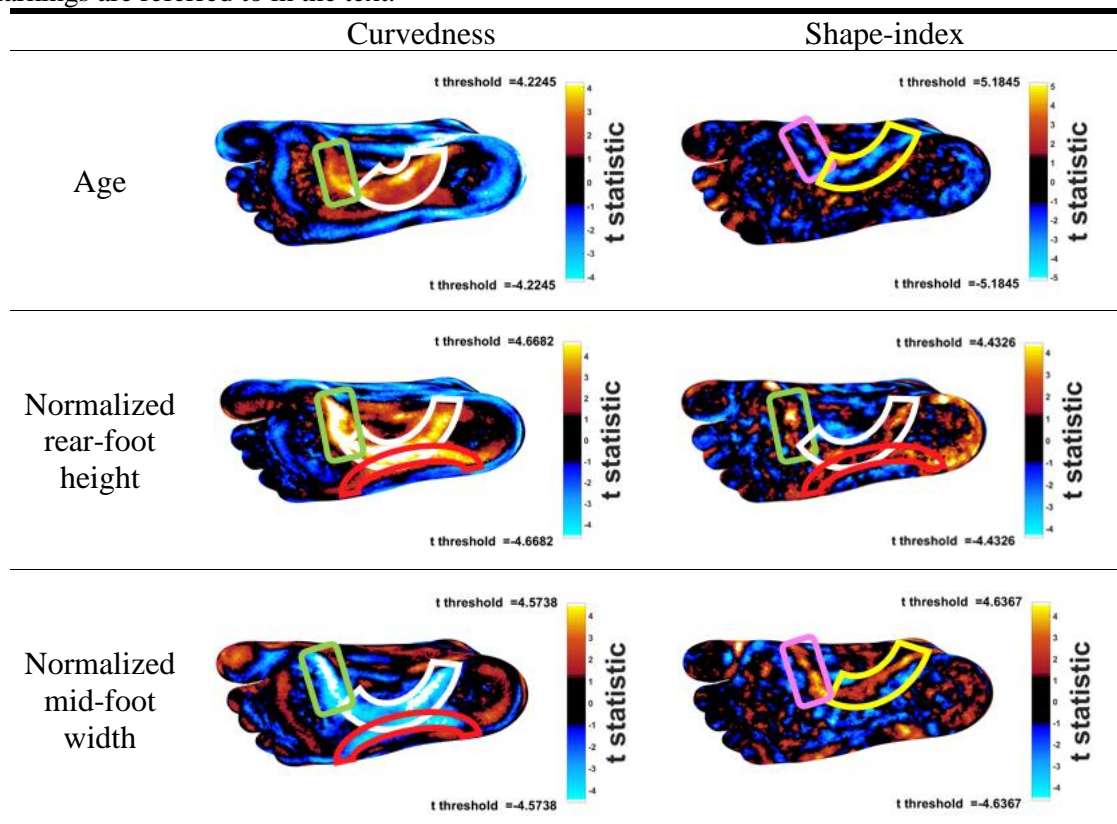
Considering the increasing height of the foot arches (1) age, (2) normalized rear-foot height and (2) normalized mid-foot width were selected as the strongest predictors of the corresponding curvedness and shape-index differences (see Table 51. for SPM1D simple linear regression heat maps) identified by the post-hoc t-tests. This Table will be referred to in the next paragraphs.

The main areas of concern are (1) the lateral and posterior edge of the MLA marked by white arches (age and normalized rear-foot height vs. curvedness: red clusters indicating increasing curvedness, normalized mid-foot width vs curvedness: blue clusters indicating increasing curvedness, normalized rear-foot height vs. shape-index: red clusters indicating increasing convexity), (2) medial aspect of the lateral and posterior edge of the MLA marked by yellow arches (age vs. shape-index: blue clusters indicating increasing concavity and normalized mi-foot width vs. shape-index: red clusters indicating increasing concavity), (3) the transverse arch marked by green rectangles (age and normalized rear-foot height vs. curvedness: red clusters indicating increasing curvedness, normalized mid-foot width vs. curvedness: blue clusters indicating increasing curvedness, normalized rear-foot height vs. shape-index: red clusters indicating increasing convexity), (4) the posterior aspect of the transverse arch marked by purple rectangles (age vs. shape-index: blue clusters indicating increasing concavity and normalized mid-foot width vs. shape-index: red clusters indicating increasing concavity) and (5) the lateral longitudinal arch marked by red arches (normalized rear-foot height vs. curvedness: red clusters indicating increasing curvedness and normalized mid-foot width vs. curvedness: blue clusters indicating increasing curvedness, normalized rear-foot height vs. shape-index: red clusters indicating increasing convexity).

Based on curvedness on all aspects of all arches, normalized rear-foot height and normalized mid-foot width are stronger predictors of increasing arch heights (MLA, transverse, and lateral longitudinal arch) than age. Furthermore, normalized rear-foot height is a stronger predictor of the above differences than normalized mid-foot width.

Based on shape-index on the medial aspect of the lateral edge of the MLA (yellow arches) age and normalized mid-foot width heat map are similarly strong predictors of increasing arch heights). Considering the shape-index on the posterior aspect of the transverse arch (purple rectangle), normalized mid-foot width is a stronger predictor of arch height than age. Considering the shape-index on all the edges of the MLA, on the lateral arch and on the transverse arch normalized rear-foot height is a predictor of arch height.

Table 51.: SPM1D simple linear regressions: Each cell contains a heat map with regression results between the variable at the beginning of the row and the 3D shape descriptor at the top of the column. Markings are referred to in the text.



5.6.3. Predictors of 3D Slenderness

Considering the increased slenderness of the foot, (1) age, (2) normalized mid-foot width, (3) normalized fore-foot width and (4) normalized mid-foot height were selected as the strongest predictors of the corresponding curvedness and shape-index differences identified by the post-hoc t-tests. See Table 52. for SPM1D simple linear regression heat maps, this Table will be referred to in the next paragraphs.

The main areas of correlation are the (1) dorsum, marked by red rectangles, (2) the instep, marked by white circles, and (3) around both malleoli marked by yellow rectangles.

The heat-maps in Table 52. demonstrating predictive power on the dorsum marked by red rectangles are: (1) age vs. curvedness, blue clusters indicating reducing curvedness with increasing age, (2) age vs. shape-index, blue clusters indicating increasing concavity with age and (3) normalized mid-foot height vs. curvedness, red clusters indicating reducing curvedness with reducing normalized mid-foot height.

The heat-maps in Table 52. demonstrating the predictive power on the instep marked by white circles are: (1) age vs. curvedness, blue clusters indicating reducing curvedness with increasing age, (2) normalized mid-foot width vs. curvedness, red cluster indicating reducing curvedness with reducing normalized mid-foot width, (3) normalized fore-foot width vs. curvedness red cluster indicating reducing curvedness with reducing normalized mid-foot width, (4) age vs. shape-index, red clusters indicating increasing convexity with increasing age and (5) normalized mid-foot width vs. shape-index, blue clusters indicating increasing convexity with decreasing normalized mid-foot width.

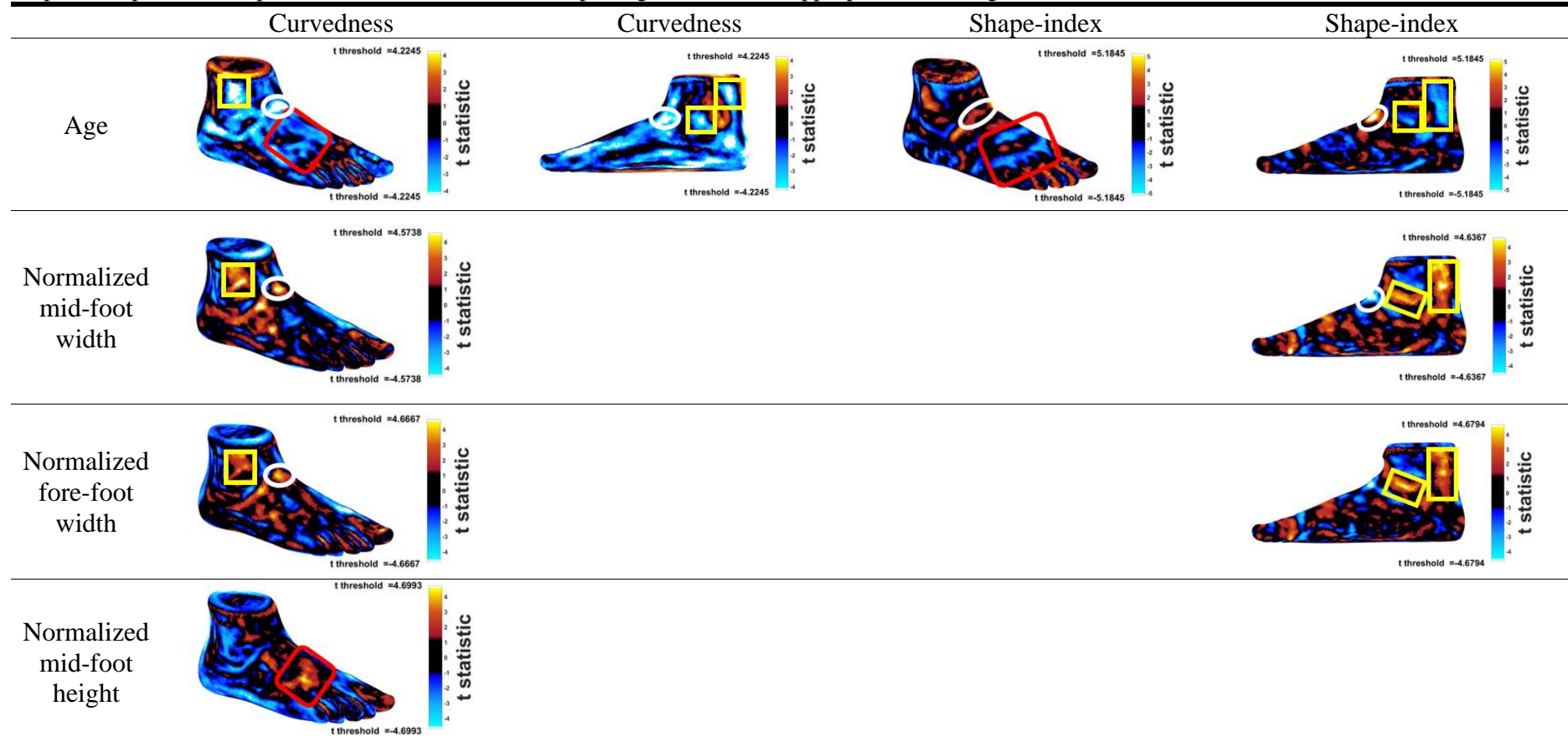
The heat-maps in Table 52. demonstrating the predictive power around both malleoli marked by yellow rectangles are (1) age vs. curvedness, blue clusters indicating reducing curvedness

with increasing age, (2) normalized mid-foot width vs. curvedness, red clusters indicating reducing curvedness with reducing normalized mid-foot width, (3) normalized fore-foot width vs. curvedness, red clusters indicating reducing curvedness with reducing normalized mid-foot width, (4) age vs. shape-index, blue clusters indicating increased concavity, (5) normalized mid-foot width vs. shape-index and normalized fore-foot width vs. shape-index, red clusters indicating increased concavity with decreasing normalized mid-foot width and decreasing normalized fore-foot width respectively.

Based on curvedness, age is a stronger predictor (light blue clusters) of slenderness on the dorsum (red rectangles), the instep (white circles) and around the medial malleolus (yellow rectangles) compared to any 2D measures.

Considering the shape-index, on the dorsum (red rectangle) age is a stronger predictor than any normalized 2D measures. On the instep (white circles), age and normalized mid-foot width are similarly strong predictors of 3D shape change. In the case of the areas around the medial malleolus (yellow rectangles), age is a weaker predictor of slenderness than normalized mid- and fore-foot width.

Table 52.: SPM1D simple linear regressions: Each cell contains a heat map with regression results between the variable at the beginning of the row and the 3D shape descriptor at the top of the column, with two views per regression where appropriate. Markings are referred to in the text.



The strongest predictors of 3D shape and the identified structural and postural differences are shown in Table 53.: (1) age, (2) normalized mid-foot width, (3) normalized fore-foot width and (4) normalized rear-foot height.

Table 53.: Predictors of the identified structural and postural differences.¹⁵

Curvedness			
Foot area	Increasing arch height	Decreasing rear-foot eversion	Increasing slenderness
Dorsum			AGE
Instep			AGE
Malleoli			AGE
Inf. to LM	AGE+NRFH		
MLA	NMFW+NRFH		
TA	NMFW+NRFH		
LLA	NMFW+NRFH		
Shape-index			
Foot area	Increasing arch height	Decreasing rear-foot eversion	Increasing slenderness
Dorsum			AGE
Instep			AGE+NMFW
Malleoli			NMFW+NFFW
MAA	NMFW+NFFW		
Tarsal canal	AGE+NMFW+NFFW		
MLA	AGE+NMFW+NRFH		
TA	NMFW+NRFH		
LLA	NRFH		

Age is the most common predictor of differences in curvedness associated with the identified structural and postural changes, except for the increasing arch heights, where normalized rear-foot height and normalized mid-foot width are the strongest predictors. When the shape-index is considered, normalized mid- and fore-foot width are the most common predictors, although they often predict the 3D shape changes with the same strength as age.

¹⁵ Abbreviations: Inf to LM: Inferior to lateral malleolus. MAA: medial aspect of the Achilles-tendon. MLA: medial longitudinal arch. TA: transverse arch. LLA: lateral longitudinal arch. NMFW: normalized mid-foot width. NFFW: normalized fore-foot width. NRFH: normalized rear-foot height. +: variables are similar in predictive power.

5.7. Discussion of the paediatric 3D foot surface morphology predictors

5.7.1. Predictors of decreasing rear-foot eversion

The simple linear regressions have shown that the strongest predictors of decreasing rear-foot eversion are age, normalized rear-foot height, normalized mid-foot width and normalized fore-foot width. The sites at which these changes occur are inferior to the lateral malleolus, on the medial aspect of the Achilles-tendon and over the tarsal canal.

Although age is among the predictors, the 2D measures predict this process in more areas, suggesting that the decreasing rear-foot eversion may not be best predicted by the general development of the child, but by foot specific processes. The strong predictive power of normalized fore-foot width indicates that the global 2D slenderness of the foot can help in predicting the decreasing rear-foot eversion.

Normalized rear-foot height has been shown to be a strong predictor of rear-foot eversion in the area inferior to the lateral malleolus. This is probably due to the fact that this measure is representative of the height of the malleoli, which is affected by the changing rear-foot angle. As this parameter is measured as the mid-height between the medial and lateral malleoli, the increasing height of the medial malleoli possibly caused by reducing pronation is also a contributing factor.

The strong predictive power of normalized mid-foot width, while still a marker of 2D slenderness, indicates that the changes in the structure of the mid-foot may also help in predicting the decreasing rear-foot eversion. These structural changes are related to the development of the MLA and foot posture as the arch height increases and the foot becomes less pronated, reducing the “medial bulging” hence decreasing its normalized width. Menz

(1998) and Halabchi et al. (2013) suggested that the clinically observed “medial bulging”, which is associated with pronated foot posture (Dahle et al., 1991), may be quantifiably indicated by the medial drift of the navicular during a transition from subtalar neutral position to a resting calcaneal position. Kothari et al. (2014) have also suggested that the medial navicular drift is a composite measure of fore-foot abduction and rear-foot valgus (eversion). While navicular drift has been used to assess transverse plane mid-foot mobility (Menz, 1998, Vinicombe et al., 2001), McPoil et al. (2011) and McPoil et al. (2009) suggested the use of mid-foot width as an alternative measure of medio-lateral mobility of the mid-foot in adults. Although in the current thesis foot mobility was not measured, normalized mid-foot width measured statically in this thesis is related to medial bulging and it was measured similarly in McPoil et al. (2011) and McPoil et al. (2009), although they used 50% of foot length as opposed to 55% in the present study. Hence, the strong predictive power of normalized mid-foot width on decreasing rear-foot eversion may be explained by the fact that rear-foot eversion is a component of pronation (Dahle et al., 1991).

In summary, both normalized fore- and mid-foot width are strong predictors of rear-foot eversion on the medial aspect of the Achilles-tendon and over the tarsal canal, while age is a strong predictor inferior to the lateral malleolus and over the tarsal canal and normalized rear-foot height is a predictor of changes inferior to the lateral malleolus only. These results suggest that rear-foot eversion can be predicted more based on foot specific processes compared to slenderness. Furthermore, as medial bulging is considered being associated with foot pronation and normalized mid-foot width is associated with the medial bulging, normalized mid-foot width may be a predictor of pronation. However, in the current section only rear-foot eversion was considered.

5.7.2. Predictors of increasing arch height

The simple linear regressions have shown that the strongest predictors of increasing arch height are age, normalized mid-foot width and normalized rear-foot height.

The strongest predictor of MLA surface morphology is normalized rear-foot height. This is demonstrated by the significant positive correlations with curvedness and shape-index around the edges of the MLA and on the lateral aspect of the plantar mid-foot. This relationship might be explained by the increasing height of the malleoli due to the decreasing pronation and increasing arch heights. Interesting to note that there were no significant differences among the age-groups in normalized rear-foot height (see section 4.4.2.3.), which also supports the claim in the previous paragraph. This indicates that children of different ages have similar normalized rear-foot heights predicting similar surface morphology of the MLA. On the other hand, if the children are ranked in ascending order based on normalized rear-foot height (Figure 48.), the first and the last children are both in the 7-year-old group, suggesting high intra-age-group variability of the 2D measure, as well as that of the 3D surface morphology of the MLA.

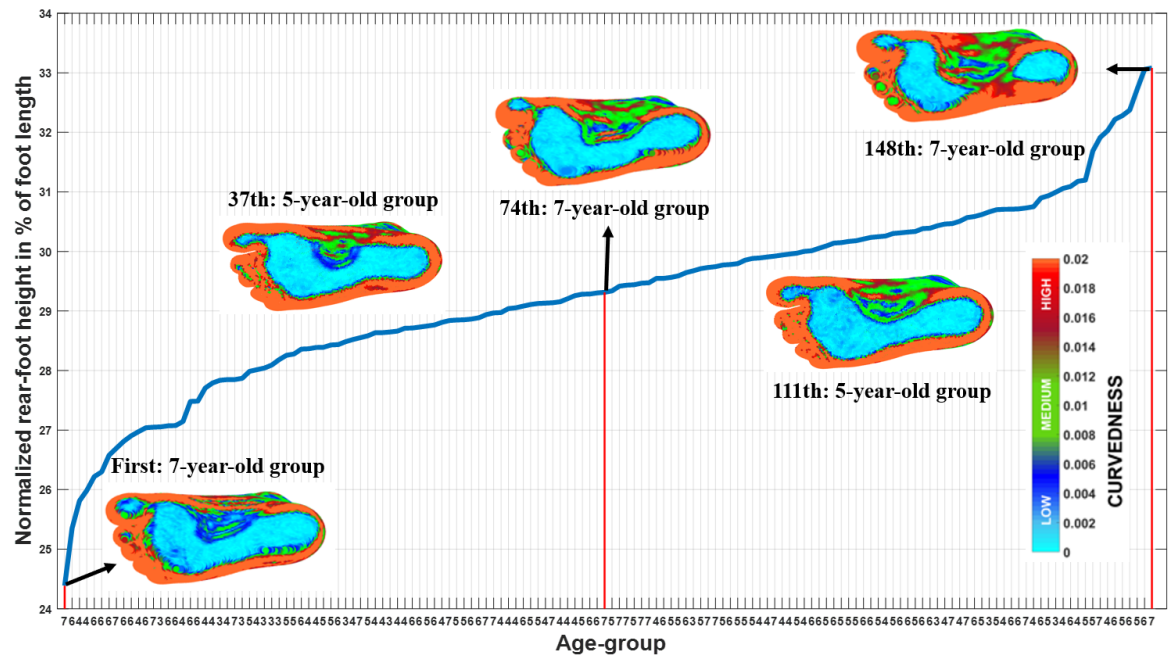


Figure 48.: Normalized rear-foot height in ascending order and curvedness heat maps of the first, 37th, middle (74th), 111th and last (148th) participant in this order. Red lines indicate the first, middle and last participants.

The high intra-age-group variability demonstrated in Figure 48. confirms previous findings by Gijon-Nogueron et al. (2019) who highlight the broad range of FPI-6 values: -1 to +11 at the age of 3 years and -4 to +12 at the age of 7 years. Although FPI-6 is a measure of whole foot pronation, it is related to the development of the MLA. Figure 48. also suggests that the increase in MLA curvedness may be less related to age, and more related to rear-foot posture. Furthermore, the figure demonstrates the results of the simple linear regression, indicating an increasing curvedness on the edges of the MLA, suggesting an increase in MLA height with increasing normalized rear-foot height. These results may suggest that there is a typical range for normalized rear-foot height that predicts a typical MLA 3D surface morphology. This range, based on the mean (29.27%) and one standard deviation (1.52%) of the whole sample, may be from ~27% to 31% (this range then contains 68% of the children)

The shape-index regression indicates similar relationship between normalized rear-foot height and MLA surface morphology. There are clusters of increasing convexity with increasing normalized rear-foot height suggesting that the edges of the MLA become more

convex, hence the MLA height increases. There is also a cluster of increasing concavity within the MLA, indicating the increasing height of the arch.

This has never been reported before, as this rear-foot measure is rarely used. However, due to its strong predictive power, the typical range defined above can be a useful parameter in the clinics, as it is easy to measure and calculate, and the landmarks (both malleoli) that need palpating are relatively easy to locate. Although it might not replace direct arch measures such as normalized navicular height, it can be a confirmatory variable when the navicular is difficult to palpate due to the adiposity of the foot. While normalized rear-foot height is a strong predictor of the arch heights, it is a simple height measure and as such cannot represent the multi-planar 3D surface morphology of the MLA. The use of 3D measures (sections 5.4. and 5.5.) complements height measures and provide a detailed characterization of the morphology of the MLA with high resolution.

The negative correlation of curvedness and positive correlation of shape-index with normalized mid-foot width around the edges of the MLA suggest that the increasing mid-foot 2D slenderness is a predictor of the changes in MLA surface morphology. As it was suggested in the previous section, normalized mid-foot width is related to medial bulging and predicts rear-foot eversion. In addition to this, a decrease in normalized mid-foot width predicts the increasing curvedness and convexity on the edges of the MLA, hence its height. These three components, medial bulging, rear-foot eversion and the height of the MLA are indicative of foot pronation (Dahle et al., 1991). For these reasons, the results of the previous and the current section indicate that normalized mid-foot width may be a predictor of foot pronation in children aged three to seven years. This finding confirms previous literature that suggested an association between medial bulging and foot pronation (Menz, 1998, Halabchi

et al., 2013). For this reason, the simple measure of normalized mid-foot width may serve as a quick and easy assessment of rear-foot eversion, MLA height and foot pronation.

On the other hand, there is only a very small area of non-significant positive correlation of normalized mid-foot width with curvedness within the MLA, indicating that mid-foot 2D slenderness and the extent of the medial bulging is not a predictor of curvedness within the MLA. Furthermore, normalized rear-foot height also has not shown strong correlation within the MLA. These results indicate that the main surface morphological changes occur on the edges of the MLA rather than within it.

The results of the regression of curvedness with age demonstrate similar but weaker correlations compared to the regression with normalized mid-foot width or normalized rear-foot height. Furthermore, as age only appears once as a predictor of arch height, it can be assumed that more foot specific processes – such as changes in rear- and mid-foot posture - predict the surface morphology of the MLA as opposed to general development represented by age. Although the post-hoc t-tests in the previous chapter (5.4.3.2.) showed an increasing trend in curvedness around the edges of the MLA between the ages of 4 and 5, no other or significant differences were found. The lack of strong predictive power of age confirms the inconclusiveness of the literature around the development of the MLA (see section 2.1.4.2.), which usually links this to age.

5.7.3. Predictors of 3D slenderness

As indicated in the results, the strongest predictors of increasing 3D slenderness on the dorsum, instep and around the malleoli are age, normalized mid-foot width and normalized fore-foot width. It has been shown before that 2D slenderness (decrease in normalized width or height measures) is linked to increasing age (Mauch et al., 2008, Mauch et al., 2009, Kouchi, 1998, Bosch et al., 2007, Muller et al., 2012). In these studies, 2D slenderness was based mostly on fore-foot width, rear-foot width and dorsal arch height. In the current thesis although normalized mid-foot height (comparable to dorsal arch height) was among the selected measures for regression, it was not chosen as the strongest predictor of any slenderness areas. The above studies used the rear and fore-foot regions to define slenderness while in the current thesis normalized mid- and fore-foot width were the strongest predictors of 3D slenderness (besides age), although their predictive power was limited to the instep, the medial aspect of the Achilles-tendon and to the areas around the malleoli. Although normalized mid- and fore-foot width showed high correlation with shape-index on the medial aspect of the Achilles-tendon, similar correlations were not detected on the lateral aspect. This may indicate that the increasing concavity on the medial aspect is not a predictor of increasing slenderness, but of decreasing rear-foot eversion. If it was indeed a marker of slenderness, the same would be detected on the lateral aspect. The prediction of decreasing rear-foot eversion is discussed in section 5.7.1..

In summary, although normalized mid- and fore-foot width are strong predictors of increasing slenderness on the instep and around the malleoli, age is the main predictor of overall increasing 3D slenderness. While in the literature slenderness is defined globally in 2D (normalized width or height of a foot region), which represents bony structures, in the present chapter slenderness is defined locally in 3D. This 3D definition is based on local

changes in curvedness and shape-index, which is presumed to represent changes in local soft tissue structures that cannot be assessed using 2D measures. The findings of this section suggest that 3D slenderness of the foot is somewhat independent of 2D slenderness, and it characterizes a different and novel aspect of foot surface morphology development related to local soft tissue changes.

5.8. Summary

5.8.1. The 3D surface morphology development of the paediatric foot

5.8.1.1. Dorsolateral and medial aspects

The 3D shape descriptor analysis of the 3 to 7-year-old children's feet may detect three main developmental processes on the dorsolateral and medial aspects.

First, it is proposed that due to proportional changes in the foot between the ages of 3 and 6 years (Mauch et al., 2008), there might be a reduction in adipose tissue thickness. As children gain fat in proportion to height after the age of 2 years (Wells et al., 2020), and the foot becomes longer and slenderer in 2D, the existing and gained fat is not sufficient to maintain the adipose tissue thickness in the foot. This proposed decrease in fat tissue thickness was located (1) on the dorsum, (2) over the metatarsal heads, (3) on the instep, (4) around both malleoli and (5) on the medial side of the Achilles tendon between the ages of 4 and 6 years. These were identified based on curvedness reduction or increased concavity\reduction in convexity (except the instep, where it is a shift towards convexity), suggesting that these surfaces become flatter increasing 3D slenderness. Further research is required to identify direct links between 3D foot surface shape and soft tissue thickness.

Second, a change in rear-foot angle\posture towards a more inverted one was proposed to be identified through a series of 3D surface morphology changes in different areas of the paediatric foot between the ages of 4 and 6 years. These are (1) a reduction in curvedness inferior to the lateral malleolus (related to a similar item in the FPI-6), (2) increased concavity on the medial side of the Achilles-tendon and (3) a shift towards concavity over the tarsal canal indicating a reduction in its prominence. Although these proposed processes are not substantial enough to indicate a decreased pronation as suggested in the literature

(Martínez-Nova et al., 2018, Gijon-Nogueron et al., 2019), they are proposed to suggest a decrease in calcaneal\rear-foot angle, therefore a reduction in eversion in the rear-foot mainly between the ages of 4 and 6 years.

Secondary findings between the ages of 4 and 7 years indicated the increasing prominence of bony and muscle landmarks characterised by increased curvedness and/or a shift towards convexity. These landmarks are (1) both malleoli, (2) metatarsal head one, (3) dorsal aspect of metatarsal heads and (4) muscles on the lateral part of the posterior dorsum. Although no change was identified on the navicular tuberosity, it could be identified using the mean age-group shape-index heat-maps. This increase in prominence of landmarks is proposed to be the result of multiple processes, such as (1) changes in the proportion of the foot reducing the thickness of soft tissues, (2) the increase in muscle cross-section due to strengthening and (3) ossification of the bones.

5.8.1.2. Plantar aspect

The 3D plantar aspect shape trajectory investigated indicates the development of the MLA.

The 3D shape descriptors identified a proposed trajectory of MLA development. In this trajectory, the MLA at the age of 3 years consists of a small concave area in the anterior medial mid-foot surrounded by low curvedness. Age-group comparisons suggested that the MLA then develops from distal to proximal and lateral, increasing in size and height, supporting longer step length in the age-groups of 4-5 years. After this age, the curvedness changes also indicate the development of the transverse arch, including in the 7-year-old group. The combination and timings of these events are supported by Gill et al. (2016), who argued that the delayed development of the transverse arch allows it to provide stability as step length increases. Although Gill et al. (2016) proposed these explanations for the

footprint patterns identified, the measures they used could not identify the exact locations of the changes. For these reasons, the explanations they provided were based on interpretations and may not have been accurate. Similarly, although Chang et al. (2012) measured the 3D volume of the MLA, they could not locate where the changes in volume occurred. In contrast, the current results – for the first time – located changes in the 3D surface shape of the MLA and the transverse arch providing a map of morphological development.

5.8.2. Predictors of paediatric 3D foot surface morphology

This chapter investigated how the 2D measures in Chapter 4. may predict the 3D surface morphology changes identified in sections 5.4.-5.5. These changes were (1) decreased rear-foot eversion, (2) increased MLA height and (3) increased 3D slenderness. The analysis was performed using simple linear regression of all normalized width and height measures of foot regions with curvedness and shape-index, however only the ones with strong predictive power were selected for further examination. Table 52. has summarized which 2D measures predicted the postural\structural changes on different areas of the foot. The strongest predictors of 3D foot surface morphology are (1) age, (2) normalized mid-foot width, (3) normalized fore-foot width and (4) normalized rear-foot height. The most common predictor is normalized mid-foot width, which predicts all four identified morphological changes in multiple areas. Although age is present as a predictor in all four cases too, it has the strongest predictive power for slenderness. Normalized fore-foot width is also a common predictor, except for in the MLA, where normalized rear-foot height and normalized mid-foot width are the strongest ones.

These findings have shown that the identified 2D normalized measures are useful predictors of 3D surface morphology. Hence, they may be used in the clinics for diagnostic purposes, post-treatment or surgery follow up assessments. It was also shown that with the exception of slenderness, all identified changes are best predicted by the normalized 2D measures and not age. This suggests that the decreasing eversion and increasing curvedness of the MLA edge are less dependent on the general growth of the child. This indicates that environmental factors, footwear choice, benign joint hypermobility (El et al., 2006) or activity levels may have a stronger effect on these surface morphology changes.

Rear-foot eversion, as a component of foot pronation can be predicted using age, normalized rear-foot height, normalized mid- and fore-foot width. Normalized mid-foot width is a strong predictor as it is also a measure of medial bulging, which is associated with foot pronation and hence rear-foot eversion. Although rear-foot eversion can be measured in the clinics using resting calcaneal stance position or rear-foot angle, normalized mid-foot width is a simpler measure providing wider predictive power and hence may be an alternative to the traditional parameters. While normalized mid- and fore-foot width have a wide predictive power, normalized rear-foot height only predicts rear-foot eversion and the 3D surface morphology of the MLA.

Age is a much weaker predictor of arch height compared to the normalized 2D measures. This is a novel finding and suggests that there is high variability of arch surface morphology within and between age-groups. This was further confirmed by Figure 48. demonstrating the spread of ages with the increasing normalized rear-foot height. Although based on the literature the percentage of children with low arch reduces with age (Chen et al., 2009), this was mainly shown using footprint measures such as AI. While footprint measures may indicate the changes in the width of the MLA, they cannot quantify the height or the shape of this multi-planar 3D structure. In contrast, the current thesis used novel and direct 3D surface morphology measures, which could be predicted by normalized 2D measures.

As a consequence, clinicians should not only rely on age-group norms when making diagnostic decisions regarding MLA development. Although mid- and rear-foot height are strong predictors of MLA 3D surface morphology (see Appendix 4.), they are absolute measures, hence do not account for the general growth of the foot and may lead to misinterpretation. On the other hand, normalized measures provide an indicator of relative changes in foot dimensions, differentiating between general growth and local changes in foot

posture. This thesis has shown that normalized mid-foot width and normalized rear-foot height strongly predict the surface morphology of the MLA and might be used independent of age. As the strongest predictor is normalized rear-foot height, its percentiles (in bipedal stance) of the whole dataset may provide guidance in establishing the developmentally appropriate morphology of the MLA. This may also suggest that there is a typical range of normalized rear-foot height for children between the ages of 3 and 7 years, which maybe between 27 and 31%. Additionally, normalized mid-foot width may be used as one of the indicators of foot pronation, as it is a strong predictor of not only MLA surface morphology but also of rear-foot eversion as well as capturing medial bulging.

As increased 3D slenderness was not strongly predicted by the normalized 2D measures, which represent 2D slenderness, it can be suggested that these are two different processes. 3D slenderness may indicate changes in local soft tissue structures, while 2D slenderness may imply changes in global foot shape affected mainly by bony structures and foot posture.

5.9. Contributions

5.9.1. Contributions to footwear design

Although 3D surface morphology data cannot contribute to size information for footwear last design, it can provide shape information, which can be used to design the shape of the internal surface of children's footwear. This information can be crucial when designing footwear shape and material for these age-groups so that the shoe's internal shape matches the shape of the paediatric foot (Mauch et al., 2009, Mauch et al., 2008). Changes in foot proportions not only cause changes in 2D measures but also in the 3D surface morphology, reducing overall curvedness and convexity on the medial and dorsolateral aspects. These 3D changes were identified and located -for the first time – and provide information for appropriate footwear shape.

Other changes during this age, such as changing instep shape or more prominent bony landmarks, could also affect footwear fit. Unless the instep's reducing concavity or the increasing convexity of the metatarsal heads or malleoli is considered, the footwear will be uncomfortable and could even cause injury to the foot. The adjustable laces or Velcro are also essential to adapt to variations and fast changes in 3D surface morphology.

The 3D shape changes identified in the rear-foot can also be useful information for footwear last design. Although 2D measures of the rear-foot can provide information in the lateral and medial malleolus area, these cannot describe how the 3D shape changes around these landmarks. The concavity and curvedness assessment not only allows estimates of rear-foot posture; they also provide information for footwear last design. The decreasing curvedness below the lateral malleolus or the shift towards concavity posterior to the medial malleolus

could be considered in the design of the rear part of the last to allow for a more supporting fit in the rear-foot.

An essential aspect of each footwear is its insole and how it supports the MLA. While 2D measures contribute towards quality insole design, the current 3D data, although it does not provide height information on the MLA, allows the characterisation of the 3D shape of the arch. This could be crucial information for footwear insole design, as it allows the matching of the shape of the insole to the shape of the plantar aspect, hence providing a better fit and support. A crucial aspect of the MLA's 3D shape is its concavity, position, and size. The current data suggest that this concave area expands posteriorly as age increases, which could be used to design quality supporting insoles to avoid injury to the foot, such as calluses. Another aspect is the curvedness of the MLA edge, which increases with age. While it is crucial that the insole mirrors the MLA in size (lateral expansion), the curvedness of the edge is also important, so the foot is not just supported at the right place but at the right degree too.

5.9.2. Contributions to research

The measures and analysis methods used in this chapter have never been used before for the assessment of paediatric foot development. While there have been attempts to characterize the 3D shape of the foot in different populations, the surface morphology of the foot has only been investigated once, in adults with the purpose of identifying anatomical landmarks (Liu et al., 2004). The authors of this study argued that shape-index and curvedness are useful variables in locating landmarks. The current thesis employed the same 3D shape descriptors and SPM to quantify and visualize the changes in foot surface morphology between age-groups and provided information about the development of children's feet that has never been shown before. These measures may complement 2D anthropometric measures in the assessment of the foot, uncovering details about the changing 3D surface morphology. While 2D measures relate to the global shape and proportions of the foot, the 3D measures relate to local surface shape in the neighbourhood of each point of the foot. For this reason, the two types of measures capture different characteristics of foot morphology with very different resolution. While 2D measures are taken between two points, 3D measures are calculated on each point of the foot (22498 points in this case). For this reason, the 3D measures allow a much higher resolution and localised analysis of foot surface morphology, although for the same reasons these measures will not allow the direct analysis of foot proportions.

Once established, 3D surface morphology measures such as curvedness and shape-index may replace or complement 2D anthropometric measures when investigating the MLA. While footprint or height measures provide information about the MLA in a single plane, 3D shape descriptors can describe and quantify the multi-planar 3D changes occurring on the surface of the MLA. The characteristics captured by these measures are directly related

to the structure of the MLA hence are better suited to assess it. Similarly, the links between other identified surface morphology changes and proposed structural changes may be used in the clinics and research.

The regression results suggest that certain 3D surface morphology characteristics may be predicted using 2D anthropometric measures. This allows researchers without 3D scanning facilities to estimate and relate their 2D results to 3D surface morphology changes.

5.9.3. Contributions to clinical practice

One of the aims of this chapter was to provide information on the 3D surface morphology changes during the development of the paediatric foot between the ages of 3 and 7 years. While the direct application of this data in the clinics is currently difficult, in the future they may be used similarly to growth charts, where the typically developing foot surface morphology is established, and a child's foot can be compared to it. Furthermore, typical foot surface morphology could be established for pathologic presentations, which may aid diagnosis. In addition, if the surface morphology of the foot is captured before treatment (surgery or otherwise), it can be compared to the surface morphology during and after treatment, providing visual and quantitative information about the success of the treatment. Visual information may come in the form of heat-maps, similarly to the average shape descriptor heat maps in section 5.5. This may also help explanation of the original pathology and the success of treatment to parents. On the other hand, quantitative differences can be demonstrated by calculating the mesh deviations (distance of corresponding points on the foot surface) or shape descriptor differences between corresponding points between the two scans. Similar calculations (mesh deviations and shape descriptor RMSE) were performed in section 3.4.2. when assessing the reliability of the methods.

Another aim of the chapter was to identify predictors of 3D surface morphology changes. As three measures and age were identified as predictors of all the changes, these may be useful in the clinical practice too. All three measures (normalized mid- and fore-foot width and normalized rear-foot height) can be easily measured by a clinician, and together with age these can predict the surface morphology without the use of expensive 3D scanner. Although further investigation is needed in larger sample, these measures may be useful to offer a quick assessment of the developmental state of the foot in terms of foot posture and

3D slenderness. A further implication of the regression results is that the development of the MLA surface morphology and rear-foot posture can be better predicted using normalized 2D measures rather than age. This indicates that although normative datasets\growth charts of normalized mid- and fore-foot width may be useful in terms of 3D slenderness (this was also strongly predicted by age), when the MLA is considered there may be an optimum range of normalized rear-foot height which applies to all age-groups. This may be between 27 and 31% between the ages of 3 and 7 years as demonstrated in Figure 26.

This requires the establishment of normative dataset and\or growth charts of these measures, so the values for typically developing children can be generated. The fact that three measures and age predicted rear-foot eversion and the changes in the MLA, highlights the need to use more than one measure (such as a single footprint measure) for the assessment of foot posture in children. While FPI-6 is a composite measure for this purpose, it is subjective and there are currently no normative datasets for this age-group. On the other hand, the measures established in the current study are objective and can be measured and calculated quickly and, as the regression results show, represent similar characteristics of paediatric foot posture.

Chapter 6

6. Thesis summary

The literature review in Chapter 2, section 2.2. has shown that the size and shape development of children's feet is poorly understood. Although research have been conducted, utilising mostly manual methods, these studies provided limited information through 2D measures, and there is very little agreement on which ones to use for what purpose. While literature to date provided basic foot size and proportion information; there remain three main concerns.

First, the present review of the literature (Chapter 2) exposed the lack of consensus on standardized parameters to describe typical foot development. Therefore, several 2D measures are used in attempts to define the changes occurring in different parts of the foot, or certain distinct measures are used to describe the whole foot. This makes it difficult to merge the findings and incorporate them into a unified understanding of foot development and into practical applications.

Second, while certain foot measures were commonly reported from studies using manual methods, a detailed analysis of the dimensions and proportions of foot regions using current technology is missing from the literature. To the author's knowledge, there is no current data available in the 3 to 7-year-old age range, that was captured with a 3D scanner.

Finally, the 2D measures used are low in resolution and are not able to characterize the multi-planar, 3D changes occurring during development. Although FPI-6 is used to assess foot posture, it is an inherently subjective measure. For these reasons, currently there is no studies looking at the structural, postural, and local morphological changes without the use of a subjective measure or more invasive and expensive methods such as x-ray.

Therefore, this research was undertaken to attempt to fill these gaps. It was conducted to provide an understanding of 2D, and 3D size and morphology development of the paediatric foot. Furthermore, it also aimed to provide methods, measures, and data for the analysis of the anthropometric and 3D surface morphology development of the paediatric foot. This Chapter summarises the key contributions of the research carried out, providing details of the study limitations, and recommendations for future research in this field.

6.1. Summary of the findings

6.1.1. Measuring the paediatric foot using a hand-held 3D scanner

The aim of this chapter was to establish protocols and 3D measures for describing 2D and 3D foot development trajectory. Phase (a) examined the reliability and validity of capturing 2D and 3D foot measures in children aged 2 to 7 years using a hand-held 3D scanner. Phase (b) investigated whether 3D shape descriptors can help characterise and quantify differences in 3D foot surface morphology between the age groups of 2, 5 and 7 years. This is the first time a structured light hand-held scanner, a custom-built stand and platform and 3D shape-descriptors have been used in the measurement of children's feet.

The comparison of the current results with existing literature showed that the methods used captured valid 2D foot anthropometric data in all age-groups and the discrepancies compared to literature are due to ethnic and methods differences. Considering reliability, the 2 year-old children had the lowest reliability in (1) most 2D measures, (2) in both 3D shape descriptors and (3) spatial agreement between 3D models of the same foot. These reliability issues were proposed to be due to certain behavioural, neuromuscular, and soft tissue properties of this age-group as opposed to the functional capacity of the scanner or the setup. Although the 2-year-olds had the lowest reliability, the higher mesh deviations did not directly translate into considerable 3D surface morphology differences. For this reason, the 3D shape descriptors were still used in phase (b) of the pilot study. Furthermore, based on the researcher's experience when scanning this age-group, the children who were closer to the age of three, were more likely to be able to stand still during scanning and have a more consistent stance throughout the scans. Therefore, the lowest age in the main study was increased to three years of age. These findings should also serve as warnings for researchers using 3D scanning in young children, so they are aware of the possible reliability issues.

The review of the literature using 3D foot scanning (Chapter 2, section 2.2.3.) indicated that researchers adapted this technology to provide a time efficient and accurate way of capturing 2D foot measures, without providing 3D surface morphology information. For this reason, to date the 3D surface morphology of the developing foot has never been examined. Therefore, the research in Chapter 3, sections 7, 8 and 9 investigated whether 3D shape descriptors are appropriate for characterising differences in 3D foot surface shape between age-groups. This is the first time that 3D shape descriptors have been used from 3D scans of paediatric feet, resulting in new knowledge about the development of the 3D surface morphology of the paediatric foot.

The findings of this phase of work demonstrated that the use of 3D shape descriptors derived from 3D foot scans can contribute to identifying, locating, and characterising changes in foot surface morphology during development. Furthermore, the results confirmed previous findings in the literature (e.g., the foot becomes slenderer with increasing age, the area of the MLA increases), but more importantly offered new insights into the 3D surface shape development (e.g., the MLA becomes more concave with increasing age, emergence of bony landmarks, reduction in adipose tissue) through the use of high resolution 3D surface morphological heat maps. This study is a novel attempt to translate 3D shape descriptor research into 3D foot measures which can be interpreted in an applied clinical setting (Varga et al., 2020). Importantly, the results of this study also validated the use of 3D shape descriptors in Chapter 5.

6.1.3. The 2D anthropometry of the paediatric foot

Following the reliability analysis, the aim of chapter 4 was to offer an understanding of 2D anthropometric foot development between the ages of 3 and 7 years, and to provide a contemporary dataset of 2D anthropometric paediatric foot measures. 2D measures for the rear-, mid- and fore-foot were captured and analysed in 148 children using the Artec Eva hand-held scanner. The changes in height, width and proportions of the foot regions were successfully evaluated to establish a developmental trajectory of the paediatric foot and to characterize differences in development among foot regions.

The three foot regions were found to have different developmental trajectories especially after the age of 4 years. Rear-foot was shown to grow faster in height but in proportion with foot length compared to the other regions, which become relatively flatter with age until the age of 7 years. It was also demonstrated that the mid- and fore-foot grows faster in width, although they become slenderer than the rear-foot up to the age of 7 years suggesting that the development of paediatric foot shape should not be described and generalized based on a few selected measures. Instead, using the width, height, and their normalized counterparts of all three regions should at least be considered. Furthermore, the results indicated an intense development of foot posture and the MLA between the ages of 4 and 5 years and suggested that the typical normalized parameters have practical value for clinicians in assessing the paediatric foot posture.

6.1.4. The 3D surface morphology of the paediatric foot

This chapter aimed to advance the understanding of 3D foot surface morphology development between the ages of 2 and 7 years. Its tasks were to describe the average 3D surface morphology of each age-group and to identify the differences in 3D surface morphology among age-groups. Furthermore, the second objective was to determine 2D measures that can predict the 3D surface morphology changes identified. This thesis is the first to study 3D shape descriptors in a relatively large sample of children, using an advanced statistical method: statistical parametric mapping.

The ANOVA and post-hoc t-tests performed in the SPM framework on curvedness and shape-index among the five age-groups identified three main developmental processes in the paediatric foot.

First, it was proposed that the 3D surface morphology differences between age-groups on the medial aspect of the Achilles-tendon, inferior to the lateral malleolus and over the tarsal canal suggested a decrease in rear-foot eversion between the ages of 4 and 5 years.

Second, on the plantar aspect, the 3D surface morphology differences indicated an increase in the height of the MLA between the ages of 4 and 6 years marked by the increasing curvedness on its lateral edge. Further development of the MLA was indicated by the increasing concavity on the medial aspect of the MLA edge after the age of 6 years. It was also established, that an MLA existed in the youngest age-group and that its development is distal to proximal until the age of 5, after which it is proximo-distal. A novel result demonstrated that a considerable size development of the MLA is observable up to the age of 6, and transverse arch develops later.

Finally, an increased 3D slenderness of the foot related to local soft tissue changes on the dorsum, around the malleoli and on the instep was proposed, based on the 3D surface morphology differences between the ages of 4 and 6 years.

This is the first time that 3D shape-descriptors have been used to describe the development of 3D foot surface morphology in children, and this data can characterize structural\postural changes, which could not be identified using 2D data. For these reasons, although further research is required, the methods and the results of this chapter are unique and crucial steps towards an optimal quantification and description of paediatric foot development.

6.1.5. Predictors of paediatric 3D foot surface morphology

The objective of this part of chapter 5., utilising the results from Chapter 4 and section 5.4. was to investigate how the 3D surface morphology of the paediatric foot may be predicted using normalized 2D anthropometric foot measures.

The results of this chapter have shown that with the exception of the increasing 3D slenderness, age is not the strongest predictor of 3D surface morphology changes in the paediatric foot.

The decreasing rear-foot eversion was mainly predicted by normalized mid- and fore-foot width, while the increasing arch heights were mainly predicted by normalized mid-foot width and normalized rear-foot height. On the other hand, 3D slenderness was strongly predicted by age and less so by the normalized 2D measures, indicating that 2D and 3D slenderness are two distinct phenomena. While 2D slenderness relates to the global shape of the foot mainly affected by bony structures and foot posture, 3D slenderness is defined by surface morphology affected by local soft tissue changes. Based on the analysis, it is also proposed that the 3D slenderness of the foot can be predicted by the general development of the child (such as height and weight).

The most common predictor of 3D surface morphology changes was normalized mid-foot width, which was proposed to predict three components of foot pronation: rear-foot eversion, MLA height and medial bulging (as itself measures this). These properties make this measure a robust and useful parameter to employ in clinical practice for diagnostic or treatment follow up purposes. On the other hand, normalized rear-foot height predicted rear-foot eversion and MLA height. It was also suggested that there may be an optimal range of normalized rear-foot height that indicates optimal MLA 3D surface morphology, which is between ~27% and ~31% containing 68% of children.

6.2. Contributions

6.2.1. Contributions to footwear industry

The findings of Chapter 4 and 5 also have contributions for the footwear industry. Ill-fitting shoes may cause long term problems in the development of children's foot and gait. To design shoes that fit well, the shape of the footwear must be very similar to that of the foot (Mauch et al., 2008, Mauch et al., 2009a). In footwear last design and fit, although foot length is an important measure, a detailed understanding of the developmental trajectory of each foot region, and the 3D shape of the foot allows a more appropriate design and fit reducing the negative effects of inadequate footwear (Delgado-Abellán et al., 2014).

The results of Chapter 4 indicated that to allow for the changing size and proportions, and different developmental trajectories of the foot and foot regions, non-linear scaling factors are suggested to be used. Due to the different trajectories of width and height measures in the rear-, mid- and fore-foot, the scaling factor should not be constant across sizes and foot regions. As it has already been argued, precise foot width or 3D analysis of foot shape can help alleviate fitting issues (Witana et al., 2004), therefore, the results of the present thesis are an important step towards a better fitting design and manufacturing of footwear.

The results of Chapter 5 have also provided implications for the footwear industry. The changing 3D foot surface morphology throughout the age-groups suggests that not only the size, but the shape of footwear should also be changing. First, there is an increased 3D slenderness between the ages of 4 and 7 years, and the footwear should adapt to that. With increasing size, its shape needs to become flatter on the dorsal aspect but also allow for bony landmarks to develop. These adaptations have already been addressed in the footwear industry by the use of Velcro or laces to also allow for variations within the same size.

Second, the inversion gradually occurring in the rear-foot within this age-range should be considered in footwear design, to account for a reducing medial mid-foot bulging, and changes in concavity around both malleoli. Finally, the results also suggest that the insoles of children's footwear with increasing size, should account for an increased curvedness around the MLA, an increased area of concavity, and a posterior shift of this concavity.

6.2.2. Contributions to research

While the findings of Chapter 4. compared to the literature demonstrated that there are differences in foot region developmental trajectories among ethnic groups or countries, the same could not be shown in Chapter 5. due to the lack of 3D surface morphology literature in children's foot development. Similarly, the differences in the methods used could also have caused some of the discrepancies between the literature and the 2D results of the current thesis, while no 3D surface morphology data about children's feet exists. The literature that studied the same age-range used manual methods and inconsistent measurement definitions (Kouchi, 1998, Forriol et al., 1990, Gilmour and Burns, 2001, El et al., 2006, Chen et al., 2011, Muller et al., 2012, Sacco et al., 2015, Sobel et al., 1999, Redmond et al., 2008, Sadeghi-Demneh et al., 2015, Gijon-Nogueron et al., 2019, Martínez-Nova et al., 2018, Gijon-Nogueron et al., 2017, Gijon-Nogueron et al., 2016a), hence the comparison to the current thesis is difficult. The contribution of this thesis to foot developmental research is threefold. First, this unique dataset provides an up to date description of the trajectory of foot development in (1) 2D, utilising a specific three region size and proportional analysis and in (2) 3D, utilising – for the first time – 3D surface morphology data (curvedness and shape-index). Second, the methods of this thesis offer novel approaches to foot scanning and foot shape analysis. The hand-held scanning technology used allows the scanning to take place in the children's own environment making it easier to scan younger participants. Furthermore, the use of curvedness and shape-index along with SPM offers a unique, relevant, and comprehensive 3D surface morphology analysis and provides a high resolution 3D morphological map of the foot. Future studies could utilise these methods to create normative datasets for age-groups or foot sizes providing key information for clinicians and footwear last designers. Finally, the analysis of curvedness and shape-index on the MLA could offer new insights and methods for the research of this highly debated topic. A

combination of degree of concavity and the percentage of concave area of the plantar aspect could provide a more relevant measure of the developmental state of the MLA.

6.2.3. Contributions to clinical practice

The understanding of paediatric foot development is crucial in clinical practice, and while there have been studies investigating it, this thesis is the first to offer a detailed analysis of size and shape development in three regions of the foot. Hence, the results of chapter 4. (the 2D anthropometry of the paediatric foot) provide an up to date, comprehensive dataset about the typically developing foot between the ages of 3 and 7 years. This may also aid clinicians in diagnosis and in the assessment of children's foot posture, identifying children with non-typical presentations. Furthermore, the trajectory of foot region development is novel information, which may be important in the education of clinicians.

While chapter 4. provided a 2D foot anthropometric dataset on paediatric foot development, chapter 5. offered a novel, high resolution 3D surface morphology dataset. The direct application of this dataset is currently difficult; however, they can help do develop a dataset of typically developing foot surface morphology, and children's feet can be compared to this. The methods used can also help in diagnosing, visualizing and quantifying foot deformities and pathologies. Furthermore, the method may also provide a tool for assessing treatment outcome visually and quantitatively using heat-maps and mesh deviation measurements.

The second part of chapter 5. demonstrated that three normalized 2D measures can predict 3D surface morphology changes of the paediatric foot. All three measures are easy to capture in the clinics and hence can be used as a quick assessment of children's feet in terms of 3D slenderness, rear-foot posture and MLA surface morphology. Furthermore, the use of normalized rear-foot height may be suggested as a marker of MLA height, with an optimum range between ~27% and ~31%. This provides a quick assessment of the MLA, and along

with normalized mid- and fore-foot width they may be able to evaluate the paediatric foot posture.

6.3. Limitations

6.3.1. Measuring the paediatric foot using a hand-held 3D scanner

6.3.1.2. Reliability of capturing 2D and 3D measures of the paediatric foot using the Artec-Eva hand-held 3D scanner

This study investigated the reliability of capturing 2D and 3D measures of children's feet using the Artec Eva hand-held scanner. Although all data was successfully captured and analysed, due to the limited number of similar studies in the literature, the evaluation of the reliability parameters is limited. The two available similar studies investigating the reliability of 2D measures by Mauch et al. (2008) and Mauch et al. (2009) showed RMSE values between 0.5 and 2mm. As there is no standard cut-off value for 2D measure reliability, the decision to exclude the youngest age-group from the main study was partly subjective, based on the fact that in eight out of the 11 measures, the 2 years old children had the largest RMSE. The limitations regarding the 3D measure reliability are similar. There are no studies assessing these in children, hence the conclusion to exclude the youngest group from the main study based on vertex deviations and shape descriptor RMSE was partly subjective. Furthermore, both of the results were supported by the experience of the investigator scanning the children's feet, arguing that 3 year-olds were much more able to stand still during scanning compared to 2 years old children, therefore producing higher quality and more reliable results.

An important consideration in every study using novel methods is the validity of the technology. In this study, although the validity of Artec Eva was not directly assessed, this has already been examined in previous research (Koban et al., 2020, Seminati et al., 2017)

looking at comparing it to reference scanners. Investigating residual limb models or faces of volunteers, it was found that the RMSE between the reference scanners and the Artec Eva was under 1mm suggesting high validity of the Artec Eva scanner. Furthermore, as mentioned in the limitations section of chapter 3, the 2D data resulted from the pilot study agreed with data in the literature (table 13.), also suggesting validity of the current methods. In addition, the upper part of the foot, where all 2D measures were measured from, was scanned similarly to other scanning techniques, hence the use of the Perspex platform did not affect validity of the anthropometric measures. Further research is required to directly assess the validity of Artec Eva in scanning children's feet with regards to the 3D measures captured through the Perspex platform. For this reason, a technical validation of the protocols may be necessary to eliminate or control the effects of light refraction of the Perspex platform. Anwer et al. (2017) argued that depending on the thickness of the platform, the distance of each point measured in the scan from the scanner maybe different from the real distance. This could cause inaccuracies in the 3D model. The validation may have to be done using a known sized object at a known distance from the scanner, that is scanned through the Perspex platform and without the Perspex platform and/or through refraction correction and adjusting time of flight values as detailed in Anwer et al. (2017).

6.3.1.1. Three-dimensional foot shape analysis in children: a pilot analysis using three-dimensional shape descriptors

In phase (b) of the pilot study, a 3D shape descriptor based approach successfully showed that heat-maps and histograms are appropriate to identify differences in 3D foot shape between age-groups. However, the small sample size, the subjective choice of the representative foot, and the lack of statistical analysis limited the scope of this study. These

issues were addressed in the main study, where the same measures were examined in a larger sample, using SPM.

6.3.2. The 2D anthropometry of the paediatric foot

Chapter 4 explored the trajectory of foot development using 2D measures resulting from 3D scanning. However, the findings from this research were limited by the number of participants involved in each age-group, and therefore caution must be applied in the interpretation of the results. Based on the a-priory sample size calculation, post-hoc tests for the age-group pairs of the 3 and 4; or the 6 and 7 year-old groups were underpowered for most measures. On the other hand, the tests between non subsequent age-groups were only underpowered for the 3-year-old group for absolute and normalized measures except for foot length.

A further limitation due to the convenience sampling method is the uneven number of boys and girls in the sample, as there were more than twice as many girls as boys. It has been reported before that boys have larger foot measures (Delgado-Abellán et al., 2014) in the older age groups of the age range examined. For this reason, in the two older age groups, the 2D measures could have been underestimated and no meaningful comparison of genders could be performed.

A further limitation is the lack of validity assessment of the methods. Although no such assessment was performed, the validity of the 2D anthropometric measures is acceptable as most measures agree with data in the literature apart from differences resulting from discrepancies in the sample or data capture and measurement techniques. Furthermore, the scanning technique (bipedal stance on a Perspex platform) did not affect validity as all measures were captured from the dorsal part of the foot, which was scanned above the platform.

An inherent limitation of this research is its cross-sectional nature. For this reason, the interpretation of the result has to be careful and not rely on cause and effect or change, as this cannot be deduced from this type of study.

6.3.3. The 3D surface morphology of the paediatric foot

Similar limitations are present in the study looking at the 3D measures, due to the fact that it used the same sample, although a-priori sample size estimation was not available in the software. Further research with larger sample size in each age-group is required to confirm and support the 3D surface morphology results of the current thesis.

Another limitation is concerning the SPM method. An inherent feature of the non-parametric 1D SPM tests performed on the current data is the lack of exact p-values. Although significant clusters with $p < 0.05$ can be identified, the exact p-value is unknown, hence the t-value maps had to be used in the analysis. While the t-value considers the mean, standard deviation and sample size, exact likelihood information cannot be calculated. This is a limitation of the software and not how it was used in this particular study.

Further limitations include the methods used during the pre-processing and registration of the foot scans. These resulted in a loss of resolution, data loss, and duplicates in the corresponding points, possibly altering the actual results. However, due to the still high resolution of the point clouds, these problems are unlikely to significantly change the results and their interpretation. While these are important limitations, the current methods have never been utilised in this type of data before, hence further research is required to establish more effective and accurate pre-processing and registration algorithms.

6.3.4. Predictors of 3D surface morphology of the paediatric foot

The limitations of chapter 6 are fourfold. First, there was no available sample size estimation option in SPM within the software, which undermines the statistical interpretation of the results. Although this was the case, the interpretation did not rely on significant results, but on the magnitude of the t-values derived from the r values indicating tendencies in the data. Second, as currently there is no non-parametric multiple regression option in SPM, the analysis relied on using a series of non-parametric simple linear regressions of the normalized 2D measures. These were chosen against the absolute measures to account for foot length within the sample. Third, the normalized 2D measures for further analysis were chosen in a partly subjective way. This was based on considering the size of the clusters and the magnitude of the t-values within these clusters that were thought to be related to a particular 3D surface morphology change. Finally, the contribution of each normalized 2D measure to predicting the 3D changes could not be quantified, and again, the t-values and the size of the clusters were used to estimate this.

6.4. Future directions

This thesis has made several noteworthy contributions to suggest how the developmental trajectory of the paediatric foot should be captured and analysed, along with a dataset of this trajectory between the ages of 3 and 7 years. However, the methods used still need further validation to justify the incorporation into research or practical applications. Testing of different scanning strategies to automate pre-processing and marker identification would provide valuable methodological information to researchers and clinicians alike.

In addition to addressing the limitations discussed in all the chapters, a number of studies can be undertaken to provide further insight into the understanding of paediatric foot shape development. Although the direct application of the current data in clinical practice is currently difficult, in the future they may be used similarly to growth charts, where the typically developing foot surface morphology is established, and a child's foot can be compared to it. In addition, typical foot surface morphology could be established for pathologic presentations such as clubfoot or bunions, which may aid diagnosis.

Furthermore, once the surface morphology of the foot is captured before treatment (such as in the case of clubfoot), it can be used as a baseline to compare it to the surface morphology during and after treatment. This can offer qualitative (visual) and quantitative assessment of treatment success. Visual assessment may be performed using heat-maps, similarly to the average shape descriptor heat maps in section 5.5. This approach may aid explanation of the original pathology and the success of treatment to parents. Additionally, the differences before and after treatment can be demonstrated quantitatively by calculating the mesh deviations (distance of corresponding points on the foot surface) or shape descriptor differences between corresponding points between the two scans. Similar calculations (mesh

deviations and shape descriptor RMSE) were performed in section 3.4.2. when assessing the reliability of the methods.

The present study dealt with the visible presentation of the foot and the estimation of structure and posture from 3D measures. However, the links between measures and structure and posture are not direct. Therefore, further research should explore these links by utilising direct measures of these changes along with 2D and 3D parameters. This could also include studies looking into the relationship between FPI-6 and its items and 3D surface morphology during the development of the paediatric foot or between healthy controls and pathological presentations. Furthermore, a study looking into the changes in 3D surface morphology during the hallux dorsiflexion test or the Jack's test could validate the use of these parameters in the clinics to support the diagnosis of rigid flat foot. Subsequently, once the relationship between 2D and 3D shape and posture and structure are established, further investigations should aim to assess the links between 2D, and 3D shape and function. These studies could look into how the morphology of the foot changes during dynamic tasks such as gait or balancing and how morphological parameters maybe related to kinematic, kinetic or muscle activity parameters. This could be achieved using 3D motion analysis with reflective markers synchronized with 4D scanning (dynamic scanning over time).

Two 3D shape descriptors were tested and used to characterize 3D surface morphology changes in the foot in Chapter 5. Curvedness and shape-index were selected due to their intuitive nature and straight forward interpretation. However, future studies should explore different derivatives of these two measures or other 3D measures of surfaces such as Gaussian-curvature, principal curvatures, and mean curvature. Such studies could help in the automatic identification of anatomical landmarks or further description of 3D surface

morphology changes in the foot. The use of 3D shape-descriptors may also contribute to the development of better fitting footwear for children or personalized orthotics.

Finally, the research of 2D and 3D parameters should also focus on gathering information relevant to specific pathology under interest and its treatment. Once the links between 3D measures and foot posture and structure are established, the new 3D parameters could be used instead of subjective and/or expensive methods. They may also allow faster diagnosis and follow up assessments after or between treatments.

7. References

- ABOELNASR, E. A., HEGAZY, F. A., ZAGHLOUL, A. A., EL-TALAWY, H. A. & ABDELAZIM, F. H. 2018. Validation of normalized truncated navicular height as a clinical assessment measure of static foot posture to determine flatfoot in children and adolescents: A cross sectional study. *The Foot*, 37, 85-90.
- AHN, S. Y., BOK, S. K., KIM, B. O. & PARK, I. S. 2017. The Effects of Talus Control Foot Orthoses in Children with Flexible Flatfoot. *Journal of the American Podiatric Medical Association*, 107, 46-53.
- ALLARD, T., SITCHON, M., SAWATZKY, R. & HOPPA, R. 2005. Use of Hand-held Laser Scanning and 3D Printing for Creation of a Museum Exhibit. *The 6th International Symposium on Virtual Reality, Archaeology and Cultural Heritage VAST*. Pisa, Italy.
- ALLIEZ, P., COHEN-STEINER, D., DEVILLERS, O., L, B., #233, VY & DESBRUN, M. 2003. Anisotropic polygonal remeshing. *ACM SIGGRAPH 2003 Papers*. San Diego, California: ACM.
- ALVAREZ, C., DE VERA, M., CHHINA, H. & BLACK, A. 2008. Normative data for the dynamic pedobarographic profiles of children. *Gait & Posture*, 28, 309-315.
- ANDERSON, M., BLAIS, M. & GREEN, W. T. 1956a. Growth of the normal foot during childhood and adolescence; length of the foot and interrelations of foot, stature, and lower extremity as seen in serial records of children between 1-18 years of age. *Am J Phys Anthropol*, 14, 287-308.

- ANDERSON, M., BLAIS, M. M. & GREEN, W. T. 1956b. Lengths of the growing foot. *J Bone Joint Surg Am*, 38-A, 998-1000.
- ANWER, A., ALI, S. S. A., KHAN, A. & MÉRIAUDEAU, F. 2017. Underwater 3-D Scene Reconstruction Using Kinect v2 Based on Physical Models for Refraction and Time of Flight Correction. *IEEE Access*, 5, 15960-15970.
- ARMITAGE, L., KWAH, L. K. & KARK, L. 2019. Reliability and validity of the iSense optical scanner for measuring volume of transtibial residual limb models. *Prosthetics and Orthotics International*, 43, 213-220.
- ASHER, C. 1975. *Postural variations in childhood*, London, England, Butterworth-Heinemann.
- AZERNIKOV, S. & FISCHER, A. 2008. Emerging non-contact 3D measurement technologies for shape retrieval and processing. *Virtual and Physical Prototyping*, 3, 85-91.
- BANWELL, H. A., PARIS, M. E., MACKINTOSH, S. & WILLIAMS, C. M. 2018. Paediatric flexible flat foot: how are we measuring it and are we getting it right? A systematic review. *Journal of Foot and Ankle Research*, 11, 21.
- BEESON, P. 1999. Frontal plane configuration of the knee in children. *Foot (Edinburgh, Scotland)*, 9, 18-26.
- BERNHARDT, D. B. 1988. Prenatal and postnatal growth and development of the foot and ankle. *Physical therapy*, 68, 1831.

- BERTSCH, C., UNGER, H., WINKELMANN, W. & ROSENBAUM, D. 2004. Evaluation of early walking patterns from plantar pressure distribution measurements. First year results of 42 children. *Gait Posture*, 19, 235-42.
- BESL, P. J. & MCKAY, N. D. 1992. A method for registration of 3-D shapes. *IEEE Transactions on Pattern Analysis and Machine Intelligence*, 14, 239-256.
- BLAND, J. M. & ALTMAN, D. G. 1996. Statistics notes .21. Measurement error (vol 312, pg 1654, 1996). *British Medical Journal*, 313, 744-744.
- BOOKSTEIN, F. L. 1992. *Morphometric Tools for Landmark Data: Geometry and Biology*, Cambridge, Cambridge University Press.
- BOSCH, K., GERSS, J. & ROSENBAUM, D. 2007. Preliminary normative values for foot loading parameters of the developing child. *Gait & Posture*, 26, 238-247.
- BOSCH, K., GERSS, J. & ROSENBAUM, D. 2010a. Development of healthy children's feet-Nine-year results of a longitudinal investigation of plantar loading patterns. *Gait & Posture*, 32, 564-571.
- BOSCH, K., GERSS, J. & ROSENBAUM, D. 2010b. Development of healthy children's feet--nine-year results of a longitudinal investigation of plantar loading patterns. *Gait Posture*, 32.
- BOSCH, K., NAGEL, A., WEIGEND, L. & ROSENBAUM, D. 2008. From "first" to "last" steps in life – pressure patterns of three generations. *Journal of Foot and Ankle Research*, 1.

- CALIGNANO, F. & VEZZETTI, E. 2011. A Morphological Methodology for Three-dimensional Human Face Soft-tissue Landmarks Extraction: A Preliminary Study. *Aesthetic Plastic Surgery*, 35, 289-302.
- CAVANAGH, P. R. & RODGERS, M. M. 1987. The arch index: A useful measure from footprints. *Journal of Biomechanics*, 20, 547-551.
- CHANG, C.-C., LI, Z., CAI, X. & DEMPSEY, P. 2007. Error control and calibration in three-dimensional anthropometric measurement of the hand by laser scanning with glass support. *Measurement*, 40, 21-27.
- CHANG, C. H., CHEN, Y. C., YANG, W. T., HO, P. C., HWANG, A. W., CHEN, C. H., CHANG, J. H. & CHANG, L. W. 2014a. Flatfoot diagnosis by a unique bimodal distribution of footprint index in children. *PLoS One*, 9, e115808.
- CHANG, H. W., CHIEH, H. F., LIN, C. J., SU, F. C. & TSAI, M. J. 2014b. The Relationships between Foot Arch Volumes and Dynamic Plantar Pressure during Midstance of Walking in Preschool Children. *Plos One*, 9.
- CHANG, H. W., LIN, C. J., KUO, L. C., TSAI, M. J., CHIEH, H. F. & SU, F. C. 2012. Three-dimensional measurement of foot arch in preschool children. *Biomedical Engineering Online*, 11.
- CHEN, J.-P., CHUNG, M.-J. & WANG, M.-J. 2009. Flatfoot Prevalence and Foot Dimensions of 5– to 13-Year-Old Children in Taiwan. *Foot & Ankle International*, 30, 326-332.
- CHEN, K.-C., CHEN, K.-C., TUNG, L.-C., TUNG, L.-C., YEH, C.-J., YEH, C.-J., YANG, J.-F., YANG, J.-F., KUO, J.-F., KUO, J.-F., WANG, C.-H. & WANG, C.-

- H. 2013a. Change in flatfoot of preschool-aged children: a 1-year follow-up study. *European journal of pediatrics*, 172, 255-260.
- CHEN, K.-C., TUNG, L.-C., TUNG, C.-H., YEH, C.-J., YANG, J.-F. & WANG, C.-H. 2014. An investigation of the factors affecting flatfoot in children with delayed motor development. *Research in Developmental Disabilities*, 35, 639-645.
- CHEN, K. C., TUNG, L. C., YEH, C. J., YANG, J. F., KUO, J. F. & WANG, C. H. 2013b. Change in flatfoot of preschool-aged children: a 1-year follow-up study. *Eur J Pediatr*, 172, 255-60.
- CHEN, K. C., YEH, C. J., KUO, J. F., HSIEH, C. L., YANG, S. F. & WANG, C. H. 2011. Footprint analysis of flatfoot in preschool-aged children. *Eur J Pediatr*, 170, 611-7.
- CHEN, Y. & MEDIONI, G. 1992. Object modelling by registration of multiple range images. *Image and Vision Computing*, 10, 145-155.
- CHENG, J. C., CHAN, P. S., CHIANG, S. C. & HUI, P. W. 1991. Angular and rotational profile of the lower limb in 2,630 Chinese children. *Journal of pediatric orthopaedics*, 11, 154.
- CHENG, J. C., LEUNG, S. S., LEUNG, A. K., GUO, X., SHER, A. & MAK, A. F. 1997a. Change of foot size with weightbearing. A study of 2829 children 3 to 18 years of age. *Clin Orthop Relat Res*, 123-31.
- CHENG, J. C., LEUNG, S. S., LEUNG, A. K., GUO, X., SHER, A. & MAK, A. F. 1997b. Change of foot size with weightbearing. A study of 2829 children 3 to 18 years of age. *Clinical orthopaedics and related research*, 123-131.

- CHO, Y., PARK, J.-W. & NAM, K. 2019. The relationship between foot posture index and resting calcaneal stance position in elementary school students. *Gait & Posture*, 74, 142-147.
- COHEN-SOBEL, E. & LEVITZ, S. J. 1991. Torsional development of the lower extremity. Implications for in-toe and out-toe treatment. *Journal of the American Podiatric Medical Association*, 81, 344.
- COLE, T. J., BELLIZZI, M. C., FLEGAL, K. M. & DIETZ, W. H. 2000. Establishing a standard definition for child overweight and obesity worldwide: international survey. *BMJ*, 320, 1240-1243.
- COLTMAN, C. E., MCGHEE, D. E. & STEELE, J. R. 2017. Three-dimensional scanning in women with large, ptotic breasts: implications for bra cup sizing and design. *Ergonomics*, 60, 439-445.
- CUTTER, J. R., STYLES, I. B., LEONARDIS, A. & DEHGhani, H. 2016. Image-based Registration for a Neurosurgical Robot: Comparison Using Iterative Closest Point and Coherent Point Drift Algorithms. *Procedia Computer Science*, 90, 28-34.
- DAANEN, H. A. M. & TER HAAR, F. B. 2013. 3D whole body scanners revisited. *Displays*, 34, 270-275.
- DAHLE, L. K., MUELLER, M., DELITTO, A. & DIAMOND, J. E. 1991. Visual Assessment of Foot Type and Relationship of Foot Type to Lower Extremity Injury. *Journal of Orthopaedic & Sports Physical Therapy*, 14, 70-74.

- DE MITS, S., COOREVITS, P., DE CLERCQ, D., ELEWAUT, D., WOODBURN, J. & ROOSEN, P. 2010. Reliability and validity of the Infoot 3D foot digitizer for normal healthy adults. *Footwear Science*, 2, 65-75.
- DELGADO-ABELLÁN, L., AGUADO, X., JIMÉNEZ-ORMEÑO, E., MECERREYES, L. & ALEGRE, L. M. 2014. Foot morphology in Spanish school children according to sex and age. *Ergonomics*, 57, 787-797.
- DESSERTY, Y. & PALLARI, J. 2018. Measurements agreement between low-cost and high-level handheld 3D scanners to scan the knee for designing a 3D printed knee brace. *PLOS ONE*, 13(1), e0190585.
- DINNO, A. 2018. Nonparametric Pairwise Multiple Comparisons in Independent Groups using Dunn's Test. *The Stata journal*, 15, 292-300.
- DOMJANIC, J., FIEDER, M., SEIDLER, H. & MITTEROECKER, P. 2013. Geometric morphometric footprint analysis of young women. *Journal of Foot and Ankle Research*, 6, 27.
- DOMJANIC, J., SEIDLER, H. & MITTEROECKER, P. 2015. A combined morphometric analysis of foot form and its association with sex, stature, and body mass. *American journal of physical anthropology*, 157, 582-591.
- DORAI, C. & JAIN, A. K. 1997. COSMOS-A representation scheme for 3D free-form objects. *IEEE Transactions on Pattern Analysis and Machine Intelligence*, 19, 1115-1130.

- DRERUP, B. & HIERHOLZER, E. 1985. Objective determination of anatomical landmarks on the body surface: measurement of the vertebra prominens from surface curvature. *J Biomech*, 18, 467-74.
- DRYDEN, I. L. & MARDIA, K. V. 1998. *Statistical shape analysis*, Chichester, Wiley.
- EL, O., AKCALI, O., KOSAY, C., KANER, B., ARSLAN, Y., SAGOL, E., SOYLEV, S., IYIDOGAN, D., CINAR, N. & PEKER, O. 2006. Flexible flatfoot and related factors in primary school children: a report of a screening study. *Rheumatology International*, 26, 1050-3.
- ENGEL, G. M. & STAHELI, L. T. 1974. The natural history of torsion and other factors influencing gait in childhood. A study of the angle of gait, tibial torsion, knee angle, hip rotation, and development of the arch in normal children. *Clinical orthopaedics and related research*, 12-7.
- EVANS, A. 2010. *Paediatrics*, Edinburgh, Churchill Livingstone.
- FOMON, S. J., HASCHKE, F., ZIEGLER, E. E. & NELSON, S. E. 1982. Body composition of reference children from birth to age 10 years. *The American journal of clinical nutrition*, 35, 1169.
- FORRIOL, F., FORRIOL, F., PASCUAL, J. & PASCUAL, J. 1990. Footprint analysis between three and seventeen years of age. *Foot and Ankle*, 11, 101-104.
- FRANCO DE SÁ GOMES, C., LIBDY, M. R. & NORMANDO, D. 2019. Scan time, reliability and accuracy of craniofacial measurements using a 3D light scanner. *Journal of oral biology and craniofacial research*, 9, 331-335.

- FRISTON, K. J. 1997. Testing for anatomically specified regional effects. *Human brain mapping*, 5, 133-136.
- FRISTON, K. J., FRITH, C. D., LIDDLE, P. F. & FRACKOWIAK, R. S. 1991. Comparing functional (PET) images: the assessment of significant change. *J Cereb Blood Flow Metab*, 11, 690-9.
- FROBIN, W. & HIERHOLZER, E. 1982. Analysis of human back shape using surface curvatures. *Journal of Biomechanics*, 15, 379-390.
- FROWEN, P., NEALE, D. & DAWSONERA 2010. *Neale's disorders of the foot*, Edinburgh, Churchill Livingstone.
- GANAPATHI, I. I. & PRAKASH, S. 2018. 3D ear recognition using global and local features. *IET Biometrics*, 7, 232-241.
- GANESAN, B., LUXIMON, A., AL-JUMAILY, A. A., YIP, J., GIBBONS, P. J. & CHIVERS, A. 2017. Developing a Three-Dimensional (3D) Assessment Method for Clubfoot-A Study Protocol. *Front Physiol*, 8, 1098.
- GHASEMI, A. & ZAHEDIASL, S. 2012. Normality tests for statistical analysis: a guide for non-statisticians. *International journal of endocrinology and metabolism*, 10, 486-489.
- GIJON-NOGUERON, G., MARTINEZ-NOVA, A., ALFAGEME-GARCIA, P., MONTES-ALGUACIL, J. & EVANS, A. M. 2019. International normative data for paediatric foot posture assessment: a cross-sectional investigation. *BMJ Open*, 9, e023341.

- GIJON-NOGUERON, G., MONTES-ALGUACIL, J., ALFAGEME-GARCIA, P.,
CERVERA-MARIN, J. A., MORALES-ASENCIO, J. M. & MARTINEZ-NOVA,
A. 2016a. Establishing normative foot posture index values for the paediatric
population: a cross-sectional study. *Journal of foot and ankle research*, 9, 24-24.
- GIJON-NOGUERON, G., MONTES-ALGUACIL, J., ALFAGEME-GARCIA, P.,
CERVERA-MARIN, J. A., MORALES-ASENCIO, J. M. & MARTINEZ-NOVA,
A. 2016b. Establishing normative foot posture index values for the paediatric
population: a cross-sectional study. *Journal of Foot and Ankle Research*, 9, 24.
- GIJON-NOGUERON, G., MONTES-ALGUACIL, J., MARTINEZ-NOVA, A.,
ALFAGEME-GARCIA, P., CERVERA-MARIN, J. A. & MORALES-ASENCIO,
J. M. 2017. Overweight, obesity and foot posture in children: A cross-sectional
study. *J Paediatr Child Health*, 53, 33-37.
- GILL, S. V., KEIMIG, S., KELTY-STEPHEN, D., HUNG, Y.-C. & DESILVA, J. M.
2016. The relationship between foot arch measurements and walking parameters in
children. *BMC Pediatrics*, 16, 16:15.
- GILMOUR, J. C. & BURNS, Y. 2001. The measurement of the medial longitudinal arch in
children. *Foot & Ankle International*, 22, 493-498.
- GOONETILLEKE, R. S. 2012. *The Science of footwear*, Boca Raton, CRC Press.
- GOULD, N., MORELAND, M., TREVINO, S., ALVAREZ, R., FENWICK, J. & BACH,
N. 1990. Foot growth in children age one to five years. *Foot Ankle*, 10, 211-3.

- HALABCHI, F., MAZAHERI, R., MIRSHAHI, M. & ABBASIAN, L. 2013. Pediatric flexible flatfoot; clinical aspects and algorithmic approach. *Iranian journal of pediatrics*, 23, 247-260.
- HAWES, M. R., SOVAK, D., MIYASHITA, M., KANG, S. J., YOSHIHUKU, Y. & TANAKA, S. 1994. Ethnic differences in forefoot shape and the determination of shoe comfort. *Ergonomics*, 37, 187-196.
- HE, Y., LIANG, B., YANG, J., LI, S. & HE, J. 2017. An Iterative Closest Points Algorithm for Registration of 3D Laser Scanner Point Clouds with Geometric Features. *Sensors (Basel)*, 17, 1862.
- HEATH, C. H. & STAHELI, L. T. 1993. Normal limits of knee angle in white children-- genu varum and genu valgum. *Journal of pediatric orthopaedics*, 13, 259.
- HEBAL, F., PORT, E., HUNTER, C. J., MALAS, B., GREEN, J. & REYNOLDS, M. 2019. A novel technique to measure severity of pediatric pectus excavatum using white light scanning. *Journal of Pediatric Surgery*, 54, 656-662.
- HEGAZY, F. A., ABOELNASR, E. A., SALEM, Y. & ZAGHLOUL, A. A. 2020. Validity and diagnostic accuracy of foot posture Index-6 using radiographic findings as the gold standard to determine paediatric flexible flatfoot between ages of 6–18 years: A cross-sectional study. *Musculoskeletal Science and Practice*, 46, 102107.
- HENNESSY, R. J. & MOSS, J. P. 2001. Facial growth: separating shape from size. *Eur J Orthod*, 23, 275-85.
- HENNIG, E. M. & ROSENBAUM, D. 1991. Pressure distribution patterns under the feet of children in comparison with adults. *Foot & ankle*, 11, 306.

- HILL, M., NAEMI, R., BRANTHWAITE, H. & CHOCKALINGAM, N. 2017. The relationship between arch height and foot length: Implications for size grading. *Applied Ergonomics*, 59, 243-250.
- HO, H. T. & GIBBINS, D. 2009. Curvature-based approach for multi-scale feature extraction from 3D meshes and unstructured point clouds. *IET Computer Vision* [Online], 3. Available: <https://digital-library.theiet.org/content/journals/10.1049/iet-cvi.2009.0044>.
- HONG, Y., WANG, L., XU, D. Q. & LI, J. X. 2011. Gender differences in foot shape: a study of Chinese young adults. *Sports Biomechanics*, 10, 85-97.
- HORVAT, V., MISIGOJ-DURAKOVIĆ, M. & PRSKALO, I. 2009. Body size and body composition change trends in preschool children over a period of five years. *Collegium antropologicum*, 33, 99.
- IALONGO, C. 2016. Understanding the effect size and its measures. *Biochemia medica*, 26, 150-163.
- INAN, T. & HALICI, U. 2012. 3-D Face Recognition With Local Shape Descriptors. *IEEE Transactions on Information Forensics and Security*, 7, 577-587.
- JACKSON-LEACH, R. & LOBSTEIN, T. 2006. Estimated burden of paediatric obesity and co-morbidities in Europe. Part 1. The increase in the prevalence of child obesity in Europe is itself increasing. *International Journal of Pediatric Obesity*, 1, 26-32.

- JANKOWICZ-SZYMANSKA, A. & MIKOLAJCZYK, E. 2015. Effect of excessive body weight on foot arch changes in preschoolers a 2-year follow-up study. *Journal of the American Podiatric Medical Association* 105, 313-319.
- JAY, R. M., SCHOENHAUS, H. D., SEYMOUR, C. & GAMBLE, S. 1995. The dynamic stabilizing innersole system (DSIS): The management of hyperpronation in children. *The Journal of foot and ankle surgery*, 34, 124-131.
- JIMENEZ-ORMENO, E., AGUADO, X., DELGADO-ABELLAN, L., MECERREYES, L. & ALEGRE, L. M. 2013. Foot morphology in normal-weight, overweight, and obese schoolchildren. *European Journal of Pediatrics*, 172, 645-652.
- JURCA, A., ŽABKAR, J. & DŽEROSKI, S. 2019. Analysis of 1.2 million foot scans from North America, Europe and Asia. *Scientific Reports*, 9, 19155.
- KIRBY, K. & GREEN, D. 1992. Evaluation and Non-Operative Management of Pes Valgus Deformity. *In book: Foot and Ankle Disorders in Children*. Churchill-Livingstone.
- KOBAN, K. C., PERKO, P., ETZEL, L., LI, Z., SCHENCK, T. L. & GIUNTA, R. E. 2020. Validation of two handheld devices against a non-portable three-dimensional surface scanner and assessment of potential use for intraoperative facial imaging. *Journal of Plastic, Reconstructive & Aesthetic Surgery*, 73, 141-148.
- KOENDERINK, J. J. & VAN DOORN, A. J. 1992. Surface shape and curvature scales. *Image and Vision Computing*, 10, 557-564.
- KOTHARI, A., DIXON, P. C., STEBBINS, J., ZAVATSKY, A. B. & THEOLOGIS, T. 2014. Motion Analysis to Track Navicular Displacements in the Pediatric Foot:

- Relationship With Foot Posture, Body Mass Index, and Flexibility. *Foot & Ankle International*, 35, 929-937.
- KOUCHI, M. 1998. Foot Dimensions and Foot Shape: Differences Due to Growth, Generation and Ethnic Origin. *Anthropological Science*, 106, 161-188.
- KRAUSS, I., GRAU, S., MAUCH, M., MAIWALD, C. & HORSTMANN, T. 2008. Sex-related differences in foot shape. *Ergonomics*, 51, 1693-709.
- KRAUSS, I., VALIANT, G., HORSTMANN, T. & GRAU, S. 2010. Comparison of Female Foot Morphology and Last Design in Athletic Footwear-Are Men's Lasts Appropriate for Women? *Research in Sports Medicine*, 18, 140-156.
- LAKENS, D. 2013. Calculating and reporting effect sizes to facilitate cumulative science: a practical primer for t-tests and ANOVAs. *Frontiers in Psychology*, 4, 1-12.
- LAMONT, L., LADENHAUF, H. N., EDOBOR-OSULA, F., BOGNER, E., DO, H. T. & GREEN, D. W. 2015. Secondary ossification centers in the development of the medial malleolus. *J Pediatr Orthop*, 35, 314-7.
- LANGLEY, B., CRAMP, M. & MORRISON, S. C. 2016. Clinical measures of static foot posture do not agree. *Journal of Foot and Ankle Research*, 9, 45.
- LEE, J. S., KIM, K. B., JEONG, J. O., KWON, N. Y. & JEONG, S. M. 2015. Correlation of Foot Posture Index With Plantar Pressure and Radiographic Measurements in Pediatric Flatfoot. *Ann Rehabil Med*, 39, 10-17.
- LEE, S. & LEE, D. K. 2018. What is the proper way to apply the multiple comparison test? *Korean journal of anesthesiology*, 71, 353-360.

- LEE, Y. C., LIN, G. & WANG, M. J. J. 2014. Comparing 3D foot scanning with conventional measurement methods. *Journal of Foot and Ankle Research*, 7, 44.
- LEUNG, A. K. L., CHENG, J. C. Y. & MAK, A. F. T. 2005. A cross-sectional study on the development of foot arch function of 2715 Chinese children. *Prosthetics and orthotics international*, 29, 241-253.
- LI, Z., CHANG, C.-C., DEMPSEY, P. G. & CAI, X. 2008a. Refraction effect analysis of using a hand-held laser scanner with glass support for 3D anthropometric measurement of the hand: A theoretical study. *Measurement*, 41, 842-850.
- LI, Z., CHANG, C.-C., DEMPSEY, P. G., OUYANG, L. & DUAN, J. 2008b. Validation of a three-dimensional hand scanning and dimension extraction method with dimension data. *Ergonomics*, 51, 1672-1692.
- LIU, K., SHINODA, K., AKIYOSHI, T. & WATANABE, H. 1998. Longitudinal Analysis of Adolescent Growth of Foot Length and Stature of Children Living in Ogi Area of Japan: A 12 Years Data. *Zeitschrift für Morphologie und Anthropologie*, 82, 87-101.
- LIU, X., KIM, W. & DRERUP, B. 2004. 3D characterization and localization of anatomical landmarks of the foot by FastSCAN. *Real-Time Imaging*, 10, 217-228.
- LIU, X., KIM, W., DRERUP, B. & MAHADEV, A. 2005. Tibial torsion measurement by surface curvature. *Clinical Biomechanics*, 20, 443-450.
- LOBSTEIN, T., BAUR, L. & UAUY, R. 2004. Obesity in children and young people: a crisis in public health. *Obesity Reviews*, 5, 4-85.

- LOBSTEIN, T. J., JAMES, W. P. T. & COLE, T. J. 2003. Increasing levels of excess weight among children in England. *International Journal of Obesity*, 27, 1136-1138.
- LUNDEEN, R. O. 1985. The Smith STA-peg operation for hypermobile pes planovalgus in children. *Journal of the American Podiatric Medical Association*, 75, 177-183.
- LUXIMON, A., GOONETILLEKE, R. & TSUI, K. 2003. Foot landmarking for footwear customization. *Ergonomics*, 46, 364-383.
- MACRON, A., PILLET, H., DORIDAM, J., VERNEY, A. & ROHAN, P.-Y. 2018. Development and evaluation of a new methodology for the fast generation of patient-specific Finite Element models of the buttock for sitting-acquired deep tissue injury prevention. *Journal of Biomechanics*, 79, 173-180.
- MAGNUSSON, M. 2009. *The three-dimensional normal-distributions transform an efficient representation for registration, surface analysis, and loop detection*, Örebro, Sweden, Örebro University.
- MARTÍNEZ-NOVA, A., GIJÓN-NOGUERÓN, G., ALFAGEME-GARCÍA, P., MONTES-ALGUACIL, J. & EVANS, A. M. 2018. Foot posture development in children aged 5 to 11 years: A three-year prospective study. *Gait & Posture*, 62, 280-284.
- MAUCH, M., GRAU, S., KRAUSS, I., MAIWALD, C. & HORSTMANN, T. 2008. Foot morphology of normal, underweight and overweight children. *International Journal of Obesity*, 32, 1068-1075.

- MAUCH, M., GRAU, S., KRAUSS, I., MAIWALD, C. & HORSTMANN, T. 2009. A new approach to children's footwear based on foot type classification. *Ergonomics*, 52, 999-1008.
- MCCARTHY, J. J. & DRENNAN, J. C. 2009. *Drennan's The child's foot and ankle*, London;Philadelphia, Pa;, Lippincott Williams & Wilkins.
- MCPOIL, T. G., VICENZINO, B., CORNWALL, M. W., COLLINS, N. & WARREN, M. 2009. Reliability and normative values for the foot mobility magnitude: a composite measure of vertical and medial-lateral mobility of the midfoot. *Journal of Foot and Ankle Research*, 2, 6.
- MCPOIL, T. G., WARREN, M., VICENZINO, B. & CORNWALL, M. W. 2011. Variations in Foot Posture and Mobility Between Individuals with Patellofemoral Pain and Those in a Control Group. *Journal of the American Podiatric Medical Association*, 101, 289-296.
- MENZ, H. B. 1998. Alternative techniques for the clinical assessment of foot pronation. *Journal of the American Podiatric Medical Association*, 88, 119-129.
- MENZ, H. B. 2004. Two feet, or one person? Problems associated with statistical analysis of paired data in foot and ankle medicine. *The Foot*, 14, 2-5.
- MODABBER, A., PETERS, F., KNIHA, K., GOLOBORODKO, E., GHASSEMI, A., LETHAUS, B., HÖLZLE, F. & MÖHLHENRICH, S. C. 2016. Evaluation of the accuracy of a mobile and a stationary system for three-dimensional facial scanning. *Journal of Cranio-Maxillofacial Surgery*, 44, 1719-1724.

- MORRISON, S. C. & FERRARI, J. 2009. Inter-rater reliability of the Foot Posture Index (FPI-6) in the assessment of the paediatric foot. *Journal of Foot and Ankle Research*, 2, 26.
- MORRISON, S. C., MCCARTHY, D. & MAHAFFEY, R. 2018. Associations Between Obesity and Pediatric Foot Dimensions. *Journal of the American Podiatric Medical Association*, 108, 383-389.
- MORRISON, S. C., MCCLYMONT, J., PRICE, C. & NESTER, C. 2017. Time to revise our dialogue : how flat is the paediatric flatfoot ? *Journal of foot and ankle research*, 10, 50-50.
- MORRISON, S. C., TAIT, M., BONG, E., KANE, K. J. & NESTER, C. 2020. Symptomatic pes planus in children: a synthesis of allied health professional practices. *Journal of Foot and Ankle Research*, 13, 5.
- MULLER, S., CARLSOHN, A., MULLER, J., BAUR, H. & MAYER, F. 2012. Static and dynamic foot characteristics in children aged 1-13 years: A cross-sectional study. *Gait & Posture*, 35, 389-394.
- MYRONENKO, A. & SONG, X. 2010. Point Set Registration: Coherent Point Drift. *IEEE Transactions on Pattern Analysis and Machine Intelligence*, 32, 2262-2275.
- NELSON, A. E., GOLIGHTLY, Y. M., LATEEF, S., RENNER, J. B., JORDAN, J. M., ASPDEN, R. M., HILLSTROM, H. & GREGORY, J. S. 2017. Cross-sectional associations between variations in ankle shape by statistical shape modeling, injury history, and race: the Johnston County Osteoarthritis Project. *Journal of Foot and Ankle Research*, 10, 34.

- NICHOLS, T. E. & HOLMES, A. P. 2002. Nonparametric permutation tests for functional neuroimaging: a primer with examples. *Human brain mapping*, 15, 1-25.
- NIELSEN, R. G., RATHLEFF, M., KERSTING, U. G., SIMONSEN, O., MOELGAARD, C., JENSEN, K., OLESEN, C. G., LUNDBYE-CHRISTENSEN, S. & KAALUND, S. 2008. The predictive value of the foot posture index on dynamic function. *Journal of Foot and Ankle Research*, 1, O37-O37.
- NIKOLAIDOU, M. E. & BOUDOLOS, K. D. 2006. A footprint-based approach for the rational classification of foot types in young schoolchildren. *Foot (Edinburgh, Scotland)*, 16, 82-90.
- O'MEARA, D., VANWANSEELE, B., HUNT, A. & SMITH, R. 2010. The reliability and validity of a three-camera foot image system for obtaining foot anthropometrics. *Journal of Applied Biomechanics*, 26, 349-356.
- ONODERA, A. N., SACCO, I. C. N., MORIOKA, E. H., SOUZA, P. S., SÁ, M. R. D. & AMADIO, A. C. 2008. What is the best method for child longitudinal plantar arch assessment and when does arch maturation occur? *Foot (Edinburgh, Scotland)*, 18, 142-149.
- OZSOY, U., SEKERCI, R. & OGUT, E. 2015. Effect of sitting, standing, and supine body positions on facial soft tissue: detailed 3D analysis. *International Journal of Oral and Maxillofacial Surgery*, 44, 1309-1316.
- PARK, H. J., LEE, J. D., CHUN, J. W., SEOK, J. H., YUN, M. J., OH, M. K. & KIM, J. J. 2006. Cortical surface-based analysis of 18F-FDG PET: Measured metabolic

abnormalities in schizophrenia are affected by cortical structural abnormalities.

Neuroimage, 31, 1434-1444.

PATAKY, T. C., BOSCH, K., MU, T., KEIJSERS, N. L., SEGERS, V., ROSENBAUM, D. & GOULERMAS, J. Y. 2011. An anatomically unbiased foot template for inter-subject plantar pressure evaluation. *Gait Posture*, 33, 418-22.

PATAKY, T. C., CARAVAGGI, P., SAVAGE, R., PARKER, D., GOULERMAS, J. Y., SELLERS, W. I. & CROMPTON, R. H. 2008. New insights into the plantar pressure correlates of walking speed using pedobarographic statistical parametric mapping (pSPM). *J Biomech*, 41, 1987-94.

PATAKY, T. C. & GOULERMAS, J. Y. 2008. Pedobarographic statistical parametric mapping (pSPM): A pixel-level approach to foot pressure image analysis. *Journal of Biomechanics*, 41, 2136-2143.

PAYNE, V. G. & ISAACS, L. D. 2016. *Human motor development: a lifespan approach*, Scottsdale, Arizona, Holcomb Hathaway, Publishers.

PENNY, W. D., FRISTON, K. J., ASHBURNER, J. T., KIEBEL, S. J. & NICHOLS, T. E. 2011. *Statistical parametric mapping: the analysis of functional brain images*, Elsevier.

PETERS, F., MÖHLHENRICH, S. C., AYOUB, N., GOLOBORODKO, E., GHASSEMI, A., LETHAUS, B., HÖLZLE, F. & MODABBER, A. 2016. The use of mobile 3D scanners in maxillofacial surgery. *Int J Comput Dent*, 19, 217-30.

PEYRE, G. 2007. Toolbox Graph. *MATLAB Central File Exchange*.

- PFEIFFER, M., KOTZ, R., LEDL, T., HAUSER, G. & SLUGA, M. 2006. Prevalence of flat foot in preschool-aged children and its relationship with BMI. *Pediatrics*, 118, 634-639.
- PHETHEAN, J., PATAKY, T. C., NESTER, C. J. & FINDLOW, A. H. 2014. A cross-sectional study of age-related changes in plantar pressure distribution between 4 and 7 years: a comparison of regional and pixel-level analyses. *Gait Posture*, 39, 154-60.
- PRICE, C. & NESTER, C. 2016. Foot dimensions and morphology in healthy weight, overweight and obese males. *Clinical Biomechanics*, 37, 125-130.
- PSIKUTA, A., FRACKIEWICZ-KACZMAREK, J., MERT, E., BUENO, M.-A. & ROSSI, R. M. 2015. Validation of a novel 3D scanning method for determination of the air gap in clothing. *Measurement*, 67, 61-70.
- RAZALI, N. M. & WAH, Y. B. 2011. Power comparisons of Shapiro-Wilk , Kolmogorov-Smirnov , Lilliefors and Anderson-Darling tests. *J. Stat. Model. Analytics.*, 21-33.
- RAZEGHI, M. & BATT, M. E. 2002. Foot type classification: a critical review of current methods. *Gait & Posture*, 15, 282-291.
- REDMOND, A. C., CRANE, Y. Z. & MENZ, H. B. 2008. Normative values for the Foot Posture Index. *Journal of Foot and Ankle Research*, 1, 6.
- REDMOND, A. C., CROSBIE, J. & OUVRIER, R. A. 2006a. Development and validation of a novel rating system for scoring standing foot posture: the Foot Posture Index. *Clin Biomech (Bristol, Avon)*, 21, 89-98.

- REDMOND, A. C., CROSBIE, J. & OUVRIER, R. A. 2006b. Development and validation of a novel rating system for scoring standing foot posture: The Foot Posture Index. *Clinical Biomechanics*, 21, 89-98.
- ROBLING, A. G. & TURNER, C. H. 2009. Mechanical signaling for bone modeling and remodeling. *Critical reviews in eukaryotic gene expression*, 19, 319.
- ROOT, M., ORIEN, W. P., WEED, J. H. & HUGHES, R. J. 1971. *Biomechanical examination of the foot, Volume 1*, Los Angeles, Clinical Biomechanics Corporation.
- SACCO, I. C. N., ONODERA, A. N., BOSCH, K. & ROSENBAUM, D. 2015. Comparisons of foot anthropometry and plantar arch indices between German and Brazilian children. *Bmc Pediatrics*, 15:4.
- SADEGHI-DEMNEH, E., JAFARIAN, F., MELVIN, J. M. A., AZADINIA, F., SHAMSI, F. & JAFARPISHE, M. 2015. Flatfoot in School-Age Children: Prevalence and Associated Factors. *Foot and ankle specialist*, 8, 186-193.
- SALENIUS, P. & VANKKA, E. 1975. The development of the tibiofemoral angle in children. *Journal of bone and joint surgery. American volume*, 57, 259.
- SAWH-MARTINEZ, R. & STEINBACHER, D. M. 2018. Commentary on: Three-Dimensional Imaging of the Face: A Comparison Between Three Different Imaging Modalities. *Aesthetic Surgery Journal*, 38, 586-589.
- SEMINATI, E., CANEPA TALAMAS, D., YOUNG, M., TWISTE, M., DHOKIA, V. & BILZON, J. L. J. 2017. Validity and reliability of a novel 3D scanner for

assessment of the shape and volume of amputees' residual limb models. *PLoS One*, 12, e0184498.

SHEPHERD, R. B. 1995. *Physiotherapy in paediatrics*, Oxford, Butterworth Heinemann.

SOBEL, E., LEVITZ, S. J., CASELLI, M. A., TRAN, M., LEPORE, F., LILJA, E., SINAIE, M. & WAIN, E. 1999. Reevaluation of the relaxed calcaneal stance position. Reliability and normal values in children and adults. *Journal of the American Podiatric Medical Association*, 89, 258-264.

STAHELI, L. T., CHEW, D. E. & CORBETT, M. 1987. The longitudinal arch. A survey of eight hundred and eighty-two feet in normal children and adults. *Journal of bone and joint surgery. American volume*, 69, 426.

STANKOVIĆ, K., BOOTH, B. G., DANCKAERS, F., BURG, F., VERMAELEN, P., DUERINCK, S., SIJBERS, J. & HUYSMANS, T. 2018. Three-dimensional quantitative analysis of healthy foot shape: a proof of concept study. *Journal of Foot and Ankle Research*, 11, 8.

STEWART, A., LEDINGHAM, R., FURNACE, G. & NEVILL, A. 2015. Body size and ability to pass through a restricted space: Observations from 3D scanning of 210 male UK offshore workers. *Applied Ergonomics*, 51, 358-362.

STEWART, A., LEDINGHAM, R., FURNACE, G., SCHRANZ, N. & NEVILL, A. 2016. The ability of UK offshore workers of different body size and shape to egress through a restricted window space. *Applied Ergonomics*, 55, 226-233.

- SUBBURAJ, K., RAVI, B. & AGARWAL, M. 2009. Automated identification of anatomical landmarks on 3D bone models reconstructed from CT scan images. *Comput Med Imaging Graph*, 33, 359-68.
- TACHDJIAN, M. O. 1985. *The child's foot*, London;Philadelphia;, Saunders.
- TAX, H. R. 1985. *Podopediatrics*, Baltimore;London, Williams & Wilkins.
- TELFER, S. & WOODBURN, J. 2010. The use of 3D surface scanning for the measurement and assessment of the human foot. *Journal of Foot and Ankle Research*, 3 (19).
- TOMCZAK, M. & TOMCZAK, E. 2014. The need to report effect size estimates revisited. An overview of some recommended measures of effect size. *TRENDS in Sport Sciences*, 1(21), 19-25.
- UDEN, H., SCHARFBILLIG, R. & CAUSBY, R. 2017. The typically developing paediatric foot: how flat should it be? A systematic review. *Journal of Foot and Ankle Research*, 10:37.
- VARGA, M., PRICE, C. & MORRISON, S. C. 2019. Reliability of Measuring Morphology of the Paediatric Foot Using the Artec Eva Hand Held Scanner. 10th International Conference and Exhibition on 3D Body Scanning and Processing Technologies, 2019 Lugano, Switzerland. 236-243.
- VARGA, M., PRICE, C. & MORRISON, S. C. 2020. Three-dimensional foot shape analysis in children: a pilot analysis using three-dimensional shape descriptors. *Journal of Foot and Ankle Research*, 13, 6.

- VEZZETTI, E. & MARCOLIN, F. 2012. Geometrical descriptors for human face morphological analysis and recognition. *Robotics and Autonomous Systems*, 60, 928-939.
- VEZZETTI, E., MARCOLIN, F. & FRACASTORO, G. 2014. 3D face recognition: An automatic strategy based on geometrical descriptors and landmarks. *Robotics and Autonomous Systems*, 62, 1768-1776.
- VINICOMBE, A., RASPOVIC, A. & MENZ, H. B. 2001. Reliability of Navicular Displacement Measurement as a Clinical Indicator of Foot Posture. *Journal of the American Podiatric Medical Association*, 91, 262-268.
- WAN, F. K. W., YICK, K.-L. & YU, W. W. M. 2017. Validation of a 3D foot scanning system for evaluation of forefoot shape with elevated heels. *Measurement*, 99, 134-144.
- WANG, D. F., SHI, L., GRIFFITH, J. F., QIN, L., YEW, D. T. W. & RIGGS, C. M. 2012. Comprehensive surface-based morphometry reveals the association of fracture risk and bone geometry. *Journal of Orthopaedic Research*, 30, 1277-1284.
- WASEDA, A., SUDA, Y., INOKUCHI, S., NISHIWAKI, Y. & TOYAMA, Y. 2014. Standard growth of the foot arch in childhood and adolescence--derived from the measurement results of 10,155 children. *Foot Ankle Surg*, 20, 208-14.
- WEBER, D. R., LEONARD, M. B. & ZEMEL, B. S. 2012. Body composition analysis in the pediatric population. *Pediatric endocrinology reviews : PER*, 10, 130-139.
- WELLS, J. C. K., DAVIES, P. S. W., FEWTRELL, M. S. & COLE, T. J. 2020. Body composition reference charts for UK infants and children aged 6 weeks to 5 years

- based on measurement of total body water by isotope dilution. *European Journal of Clinical Nutrition*, 74, 141-148.
- WILLIAMS, D. S. & MCCLAY, I. S. 2000. Measurements Used to Characterize the Foot and the Medial Longitudinal Arch: Reliability and Validity. *Physical Therapy*, 80, 864-871.
- WITANA, C. P., FENG, J. & GOONETILLEKE, R. S. 2004. Dimensional differences for evaluating the quality of footwear fit. *Ergonomics*, 47, 1301-1317.
- WITANA, C. P., XIONG, S. P., ZHAO, J. H. & GOONETILLEKE, R. S. 2006. Foot measurements from three-dimensional scans: A comparison and evaluation of different methods. *International Journal of Industrial Ergonomics*, 36, 789-807.
- WORSLEY, K. J., EVANS, A. C., MARRETT, S. & NEELIN, P. 1992. A three-dimensional statistical analysis for CBF activation studies in human brain. *J Cereb Blood Flow Metab*, 12, 900-18.
- WORSLEY, K. J., MARRETT, S., NEELIN, P., VANDAL, A. C., FRISTON, K. J. & EVANS, A. C. 1996. A unified statistical approach for determining significant signals in images of cerebral activation. *Hum Brain Mapp*, 4, 58-73.
- XIONG, S. P., GOONETILLEKE, R. S., ZHAO, J. H., LI, W. Y. & WITANA, C. P. 2009. Foot deformations under different load-bearing conditions and their relationships to stature and body weight. *Anthropological Science*, 117, 77-88.
- YAMAMOTO, S., MIYACHI, H., FUJII, H., OCHIAI, S., WATANABE, S. & SHIMOZATO, K. 2016. Intuitive Facial Imaging Method for Evaluation of Postoperative Swelling: A Combination of 3-Dimensional Computed Tomography

and Laser Surface Scanning in Orthognathic Surgery. *J Oral Maxillofac Surg*, 74, 2506.e1-2506.e10.

YAN, L. & SHAH, P. 2017. B2-1 Effect of the accuracy of 3D head scanners in product design development. *The Japanese Journal of Ergonomics*, 53, S372-S375.


ŽUKAUSKAS, S., BARAUSKAS, V. & ČEKANAUSKAS, E. 2021. Comparison of multiple flatfoot indicators in 5–8-year-old children. *Open Medicine*, 16, 246-256.

8. Appendices

Appendix 1. Main study information sheets

Information sheet for recruitment in schools, nurseries, and sport centres

PIS_GFLFS_V1



Appendix 3: Participant Information Sheet for Parents

Participant information sheet

Summary and what is the purpose of the project?
I (Matyas Varga) am a PhD student at the University of Brighton and this project is part of my PhD study and is looking to understand how children's foot shape and size change as they develop and learn to walk, run, jump and skip.

Why have I been invited to participate?
You have been invited because your child is in the age group we would like to examine, and in this project, we will invite 300 children to take part. Children who have a diagnosis (or may be under medical investigation for a diagnosis) of epilepsy or similar light sensitive conditions cannot take part in the study. Also, if your child suffers from any skin disorders affecting the foot such as dermatitis, psoriasis or any skin abrasions they will not be able to participate.

Do I have to take part?
It is your choice to decide whether you are happy for your child to take part in this project, as it is voluntary, and you are providing consent on their behalf. You might want to explain this to your child and we have provided a booklet that includes a series of photos about what is going to happen. We will then ask you to sign a consent form to show you agree for them to take part.

What can I expect?
In this project, we are looking to capture the shape of your child's feet. This will be achieved using a specialist equipment (a 3D scanner) and will be done when your child is standing barefoot, with socks and shoes removed. I will hold the 3d scanner and move it around your child's foot, which is completely pain free and does not cause any irritation or damage. This will take 2-3 minutes.

Where will it take place?
We will carry out the test at your child's school/nursery/sport centre (name to be inserted once confirmed) during school/nursery times or before/after sport activity at the sport centre. You do not need to be present during scanning, however you are more than welcome to do so.

How can I find out more information?
The following information will ensure that you understand everything about taking part in the project, and what it will involve. Contact details are provided at the end of this document if you have any further questions.

What is the purpose of the study?
This study aims to describe and quantify the trajectory (and typical variation) of children's foot development. This project will allow the researchers to take a small step toward providing seminal large scale and in-depth information to the greater public.

What will happen if we take part?

We will be doing this study in your child's school/nursery/sport centre. This has been approved by *** [head teacher or centre manager or equivalent] and we will attend your child's school/nursery/sport centre on an agreed date. We will ensure that your child's participation in this study has minimal disruption on their time at school/nursery/sport centre.



Capturing a scan of your child's feet is achieved with a 3-D scanner (pictured above). This involves moving the scanner around your child's feet for 1.5-2 minutes. The scanner will record the dimensions of your child's feet and we will then use a software to build-up a reconstruction of your child's foot. Prior to participation, your child's foot will be cleaned with an antibacterial skin wipe. We will also clean the surface that they will be standing on (before and after each child has taken part). The child will always be kept safe standing on the platform by an adult (school teacher, nursery nurse or yourself) **known to the child.**

The researchers undertaking this study are not qualified medical doctors or health professionals and are not in a position to screen your child's foot development.

What will we need to do or bring?

For the day of the testing please *refrain from applying skin preparations (oils, talcs, creams) the evening before and the morning of testing*, unless you have been instructed to do so by a medical professional.

What are the possible disadvantages and risks of taking part?

We anticipate no specific risk of injury during the testing any more than your child would experience during a normal school/nursery/sport centre day. If your child becomes uncomfortable or distressed, then the testing will be stopped. The testing will be unusual for your child, but the researchers and the assistant will do their best to make the testing as comfortable as possible and have undertaken specific training and have experience with children in similar scenarios.

What are the possible benefits of taking part?

The study has no immediate benefits for the volunteers or their families, but it is hoped that this study and the following research study will help us to better understand the developing feet of children.

Will my taking part in the study be kept confidential?

Your child's participation in the study will remain confidential with only the primary researcher having access to your (and your child's) full name, address, and personal data. Data will be coded and saved on a secure drive with password protected access. A master list will also be saved in a secured drive accessible only by the primary researcher. All data will be completely anonymized by removing all coding once I have finished post-processing the captured data, which is likely to be maximum 1 week after data collection. Anonymized data will be retained for 10 years following data collection, in line with University of Brighton's data collection and storage ethics and guidelines. **Please find the web address to the University's Research Privacy Notice here: <https://staff.brighton.ac.uk/ease/ro/CREC%20Published%20Documents/Data%20Management%20Policy%20Final%20May%202018.pdf>.**

What will happen if I don't want to carry on with the study?

You are free to withdraw them at any time, without giving a reason to the research team. If this is the case, the information we have already collected about your child's feet, may still be used within the research and within resulting publications unless you explicitly tell us not to do so.

What will happen to the results of the research study?

The results of this study will be used to describe and quantify how the foot shape develops in children and will be part of the primary researcher's PhD dissertation. As anonymized data sets they will also be fed back to the grant funder and may also be published in journals and presented at conferences. Study results will be summarized and available on the project website (please see below).

Who is organizing or sponsoring the research?

The research is being undertaken collaboratively as part of a 5-year project with the University of Salford funded by the William M. Scholl Endowment Fund. The research has been approved by the Research Ethics Committee of the University of Brighton.

What if there is a problem?

If you have a concern about any aspect of this study, you should ask to speak to the researchers who will do their best to answer your questions and resolve any problems (please see below). If you remain unhappy and wish to complain formally, or wish to speak to someone else, you can do this through the University Complaints Procedure:

Name: Prof Kate Galvin

Title: Deputy Head of School, School of Health Sciences, Head of the Centre of Health Research

Address: University of Brighton, Aldro Building, 49 Darley Road, Eastbourne, BN20 7UR

Telephone: +44 (0) 1273 643 578

Email: K.Galvin@brighton.ac.uk

Further information and contact details:

Contact details of primary researcher:

PhD student: Matyas Varga MPEd

Email: m.varga@brighton.ac.uk

Phone: 01273 644 166







Project Lead: Dr. Stewart Morrison
Email: S.C.Morrison@brighton.ac.uk
Phone : 01273 643 675



Research Fellow: Dr. Carina Price
Email: C.L.Price@salford.ac.uk
Phone: 0161 295 6883

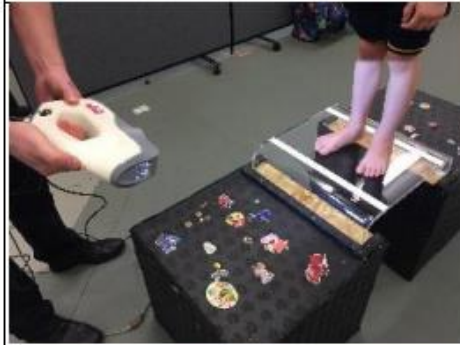
Project website: www.greatfoundations.org.uk

Participant Information Sheet for children

	<ul style="list-style-type: none">• I will chat to you and your mom about my research and you can ask me questions if you wish.
	<ul style="list-style-type: none">• If you change your mind and don't want to take part at any time, that is OK too.• You don't have to tell me why.
	<ul style="list-style-type: none">• You will sit down• Your mom/dad will take off your shoes and your socks.• and will clean your feet.
	<p>Mom/dad will help you to get on the platform and roll your trousers up to your knees.</p>



I will draw some points on your foot.



I will take special photos of your feet, with a special camera, and you will not feel a thing.



Once finished, you can choose a sticker, and have a look at the special photos of your feet.



Appendix 6: Participant Information Sheet for Parents

Participant information sheet

Summary and what is the purpose of the project?

I (Matyas Varga) am a PhD student at the University of Brighton and this project is part of my PhD study and is looking to understand how children's foot shape and size change as they develop and learn to walk, run, jump and skip.

Why have I been invited to participate?

You have been invited because your child is in the age group we would like to examine, and in this project, we will invite 300 children to take part. Children who have a diagnosis (or may be under medical investigation for a diagnosis) of epilepsy or similar light sensitive conditions cannot take part in the study. Also, if your child suffers from any skin disorders affecting the foot such as dermatitis, psoriasis or any skin abrasions they will not be able to participate.

Do I have to take part?

It is your choice to decide whether you are happy for your child to take part in this project, as it is voluntary, and you are providing consent on their behalf. You might want to explain this to your child and we have provided a booklet that includes a series of photos about what is going to happen. We will then ask you to sign a consent form to show you agree for them to take part.

What can I expect?

In this project, we are looking to capture the shape of your child's feet. This will be achieved using a specialist equipment (a 3D scanner) and will be done when your child is standing barefoot, with socks and shoes removed. I will hold the 3d scanner and move it around your child's foot, which is completely pain free and does not cause any irritation or damage. This will take 2-3 minutes.

Where will it take place?

We will carry out the test at the Human Motion Laboratory, Robert Dodds, Annexe 1, University of Brighton, 49 Darley Road, BN20 7UR.

How can I find out more information?

The following information will ensure that you understand everything about taking part in the project, and what it will involve. Contact details are provided at the end of this document if you have any further questions.

What is the purpose of the study?

This study aims to describe and quantify the trajectory (and typical variation) of children's foot development. This project will allow the researchers to take a small step toward providing seminal large scale and in-depth information to the greater public.

What will happen if we take part?

We will be doing this study at the University of Brighton. The study has been approved by the University's ethical committee.



Capturing a scan of your child's feet is achieved with a 3-D scanner (pictured above). This involves moving the scanner around your child's feet for 2-3 minutes. The scanner will record the dimensions of your child's feet and we will then use a software to build-up a reconstruction of your child's foot. Prior to participation, your child's foot will be cleaned with an antibacterial skin wipe. We will also clean the surface that they will be standing on (before and after each child has taken part). The child will always be kept safe standing on the platform by an adult (an assistant or the accompanying adult).

The researchers undertaking this study are not qualified medical doctors or health professionals and are not in a position to screen your child's foot development.

What will we need to do or bring?

For the day of the testing please *refrain from applying skin preparations (oils, talcs, creams) the evening before and the morning of testing*, unless you have been instructed to do so by a medical professional.

What are the possible disadvantages and risks of taking part?

We anticipate no specific risk of injury during the testing any more than your child would experience during a normal day. If your child becomes uncomfortable or distressed, then the testing will be stopped. The testing will be unusual for your child, but the researchers and the assistant will do their best to make the testing as comfortable as possible and have undertaken specific training and have experience with children in similar scenarios.

What are the possible benefits of taking part?

The study has no immediate benefits for the volunteers or their families, but it is hoped that this study and the following research study will help us to better understand the developing feet of children.

Will my taking part in the study be kept confidential?

Your child's participation in the study will remain confidential and anonymous with only the primary researcher having access to your (and your child's) full name, address, and personal data. Data will be coded and saved on a secure drive with password protected access. A master list will also be saved in a secured drive accessible only by the primary researcher. All data will be completely anonymized by removing all coding once post-processing the captured data is finished, which is likely to be maximum 1 week after data collection. Anonymized data will be retained for 10 years following data collection, in line with University of Brighton's data collection and storage ethics and guidelines. Please find the web address to the University's Research Privacy Notice here: <https://staff.brighton.ac.uk/ease/ro/CREC%20Published%20Documents/Data%20Management%20Policy%20Final%20May%202018.pdf>.

What will happen if I don't want to carry on with the study?

You are free to withdraw them at any time, without giving a reason to the research team. If this is the case, the information we have already collected about your child's feet, may still be used within the research and within resulting publications unless you explicitly tell us not to do so.

What will happen to the results of the research study?

The results of this study will be used to describe and quantify how the foot shape develops in children and will be part of the primary researcher's PhD dissertation. As anonymized data sets they will also be fed back to the grant funder and may also be published in journals and presented at conferences. Study results will be summarized and available on the project website (please see below).

Who is organizing or sponsoring the research?

The research is being undertaken collaboratively as part of a 5-year project with the University of Salford funded by the William M. Scholl Endowment Fund. The research has been approved by the Research Ethics Committee of the University of Brighton.

What if there is a problem?

If you have a concern about any aspect of this study, you should ask to speak to the researchers who will do their best to answer your questions and resolve any problems (please see below). If you remain unhappy and wish to complain formally, or wish to speak to someone else, you can do this through the University Complaints Procedure:

Name: Prof Kate Galvin

Title: Deputy Head of School, School of Health Sciences, Head of the Centre of Health Research

Address: University of Brighton, Aldro Building, 49 Darley Road, Eastbourne, BN20 7UR

Telephone: +44 (0) 1273 643 578

Email: K.Galvin@brighton.ac.uk

Further information and contact details:

Contact details of primary researcher:

PhD student: Matyas Varga MPEd

Email: m.varga@brighton.ac.uk

Phone: 01273 644 166



Project Lead: Dr. Stewart Morrison
Email: S.C.Morrison@brighton.ac.uk
Phone : 01273 643 675



Research Fellow: Dr. Carina Price
Email: C.L.Price@salford.ac.uk
Phone: 0161 295 6883

Project website: www.greatfoundations.org.uk

Appendix 2. Informed consent forms and demographic data collection sheet

Main study consent form



Participant Consent Form, GFLFS_V1

Appendix 1: Participant Consent Form

Project Title – Little Foot Shapes: the development of children's feet

Please read the statements below and confirm that you understand the aspects to the study by circling the appropriate YES/NO answer. If consented please insert your child's date of birth, gender and ethnicity within the spaces below.

I confirm that I have read and understood the information sheet and I understand the principles, procedures and possible risks involved, for the above study and that I have had the opportunity to ask questions and consider the information provided and I agree to take part in this research.	YES	NO
I understand that the data collected within this study will be utilized by the researchers for publications, including as a secondary data set for joining researchers, in the future for conferences or journal papers. It has been explained to me that all data presented will be anonymous.	YES	NO
I understand that anonymous data will be stored for a minimum of 10 years.	YES	NO
I understand that I am providing consent on behalf of my child, our participation is voluntary and that at any time we can withdraw from the study, our data will be destroyed, and I do not have to give a reason.	YES	NO
I give consent for my child to participate in the LITTLE FOOT SHAPES main study.	YES	NO
My child is typically developing.	YES	NO
My child is able to stand barefoot for 5 minutes	YES	NO
My child is free from any skin disorders affecting the foot such as dermatitis, psoriasis or any skin abrasions.	YES	NO
My child is free from epilepsy or light sensitive conditions.	YES	NO
My child is free from any foot deformity.	YES	NO

SIGNATURE OF PERSON GIVING CONSENT

Name of Parent or Guardian Relationship to Participant

Signature of Participant Parent or guardian Date

NAME OF PARTICIPANT **PARTICIPANT CODE**

SIGNATURE OF PERSON OBTAINING CONSENT

Name of person obtaining consent Participant code

Signature of person obtaining consent Date

Main study Participant data collection sheet



Participant Consent Form, GFLFS_V1

Appendix 4: Participant data collection sheet

Project Title – Little Foot Shapes: the development of children's feet

Please read the statements below and confirm that you understand the aspects to the study by circling the appropriate YES/NO answer. If consented please insert your child's date of birth, gender and ethnicity within the spaces below.

I give consent for my child's gender to be used for research anonymously: The gender of my child is: Male, female Other, please specify:	YES	NO
I give consent for my child's date of birth to be used for research anonymously. The date of birth (month and year) of my child is:	YES	NO
I give consent for my child's ethnicity to be used for research anonymously. The ethnicity of my child is (please circle): Black, Chinese, Indian, Mixed, Pakistani, White British, White other Other, please specify:	YES	NO

Weight:

Height:

_____ Participant code

Appendix 3. Shapiro-Wilk tests of normality for 2D

anthropometric measures per age-group

Table 54.: Normality test for foot length for each age-group. Sig.: significance, df.: degrees of freedom. *: p<0.05, ***: p<0.001

Group	Shapiro-Wilk		
	Statistic	df	Sig.
3 years old group	.937	12	.457
4 years old group	.932	38	.023*
5 years old group	.972	35	.500
6 years old group	.989	41	.965
7 years old group	.964	22	.579

Table 55.: Normality tests for rear-foot width for each age-group. Sig.: significance, df.: degrees of freedom. *: p<0.05, ***: p<0.001

Group	Shapiro-Wilk		
	Statistic	df	Sig.
3 years old group	.951	12	.654
4 years old group	.983	38	.808
5 years old group	.953	35	.143
6 years old group	.987	41	.921
7 years old group	.904	22	.035*

Table 56.: Normality tests for normalized rear-foot width for each age-group. Sig.: significance, df.: degrees of freedom. *: p<0.05, ***: p<0.001

Group	Shapiro-Wilk		
	Statistic	df	Sig.
3 years old group	.944	12	.552
4 years old group	.973	38	.471
5 years old group	.965	35	.325
6 years old group	.971	41	.381
7 years old group	.743	22	.000***

Table 57.: Normality tests for rear-foot height for each age-group. Sig.: significance, df.: degrees of freedom. *: p<0.05, ***: p<0.001

Group	Shapiro-Wilk		
	Statistic	df	Sig.
3 years old group	.971	12	.918
4 years old group	.953	38	.113
5 years old group	.976	35	.615
6 years old group	.991	41	.980
7 years old group	.952	22	.342

Table 58.: Normality tests for normalized rear-foot height for each age-group. Sig.: significance, df.: degrees of freedom. *: p<0.05, ***: p<0.001

Group	Shapiro-Wilk		
	Statistic	df	Sig.
3 years old group	.891	12	.120
4 years old group	.981	38	.763
5 years old group	.958	35	.201
6 years old group	.972	41	.386
7 years old group	.932	22	.135

Table 59.: Normality tests for mid-foot width for each age-group. Sig.: significance, df.: degrees of freedom. *: p<0.05, ***: p<0.001

Group	Shapiro-Wilk		
	Statistic	df	Sig.
3 years old group	.942	12	.530
4 years old group	.962	38	.221
5 years old group	.949	35	.103
6 years old group	.971	41	.370
7 years old group	.950	22	.311

Table 60.: Normality tests for normalized mid-foot width for each age-group. Sig.: significance, df.: degrees of freedom. *: p<0.05, ***: p<0.001

Group	Shapiro-Wilk		
	Statistic	df	Sig.
3 years old group	.950	12	.642
4 years old group	.972	38	.439
5 years old group	.990	35	.980
6 years old group	.945	41	.046*
7 years old group	.982	22	.938

Table 61.: Normality tests for mid-foot height for each age-group. Sig.: significance, df.: degrees of freedom. *: p<0.05, ***: p<0.001

Group	Shapiro-Wilk		
	Statistic	df	Sig.
3 years old group	.906	12	.192
4 years old group	.947	38	.074
5 years old group	.967	35	.371
6 years old group	.987	41	.907
7 years old group	.975	22	.816

Table 62.: Normality tests for normalized mid-foot height for each age-group. Sig.: significance, df.: degrees of freedom. *: p<0.05, ***: p<0.001

Group	Shapiro-Wilk		
	Statistic	df	Sig.
3 years old group	.937	12	.454
4 years old group	.952	38	.106
5 years old group	.964	35	.294
6 years old group	.975	41	.510
7 years old group	.958	22	.448

Table 63.: Normality tests for fore-foot width for each age-group. Sig.: significance, df.: degrees of freedom. *: p<0.05, ***: p<0.001

Group	Shapiro-Wilk		
	Statistic	df	Sig.
3 years old group	.922	12	.299
4 years old group	.970	38	.390
5 years old group	.971	35	.480
6 years old group	.976	41	.535
7 years old group	.975	22	.827

Table 64.: Normality tests for normalized fore-foot width for each age-group. Sig.: significance, df.: degrees of freedom. *: p<0.05, ***: p<0.001

Group	Shapiro-Wilk		
	Statistic	df	Sig.
3 years old group	.866	12	.059
4 years old group	.934	38	.027*
5 years old group	.954	35	.152
6 years old group	.983	41	.771
7 years old group	.973	22	.788

Table 65.: Normality tests for fore-foot height for each age-group. Sig.: significance, df.: degrees of freedom. *: p<0.05, ***: p<0.001

Group	Shapiro-Wilk		
	Statistic	df	Sig.
3-years old group	.895	12	.138
4-years old group	.973	38	.483
5-years old group	.983	35	.848
6-years old group	.962	41	.189
7-years old group	.963	22	.556

Table 66.: Normality tests for normalized fore-foot height for each age-group. Sig.: significance, df.: degrees of freedom. *: p<0.05, ***: p<0.001

Group	Shapiro-Wilk		
	Statistic	df	Sig.
3 years old group	.945	12	.567
4 years old group	.972	38	.450
5 years old group	.956	35	.173
6 years old group	.927	41	.012*
7 years old group	.982	22	.942

Appendix 4. Curvedness and shape-index regressions with normalized 2D anthropometric measures.

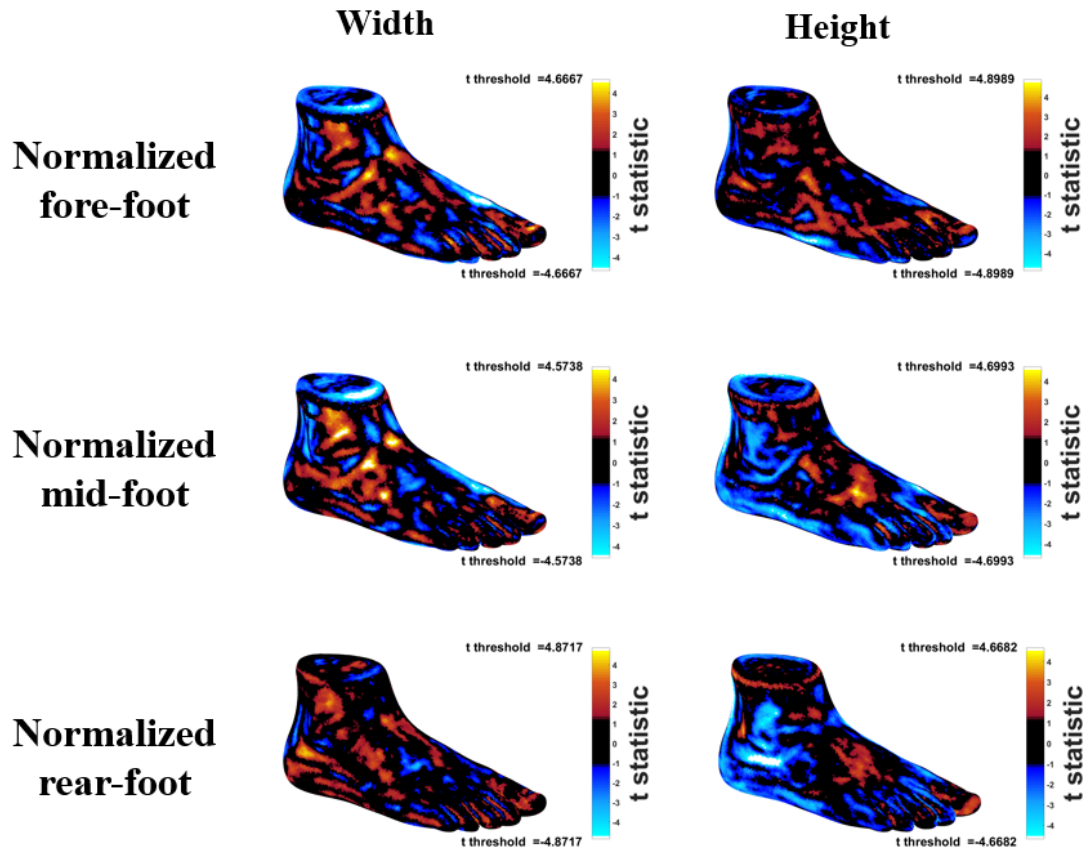


Figure 49.: SPM1D regression of curvedness with normalized 2D measures, dorsolateral view. The colour bar represents the t statistics, with the threshold at each end (alpha level of 0.05). White points mark significant correlation. Dark to light blue colours indicate increasing negative correlation, red, orange, and yellow colours indicate increasing positive correlation.

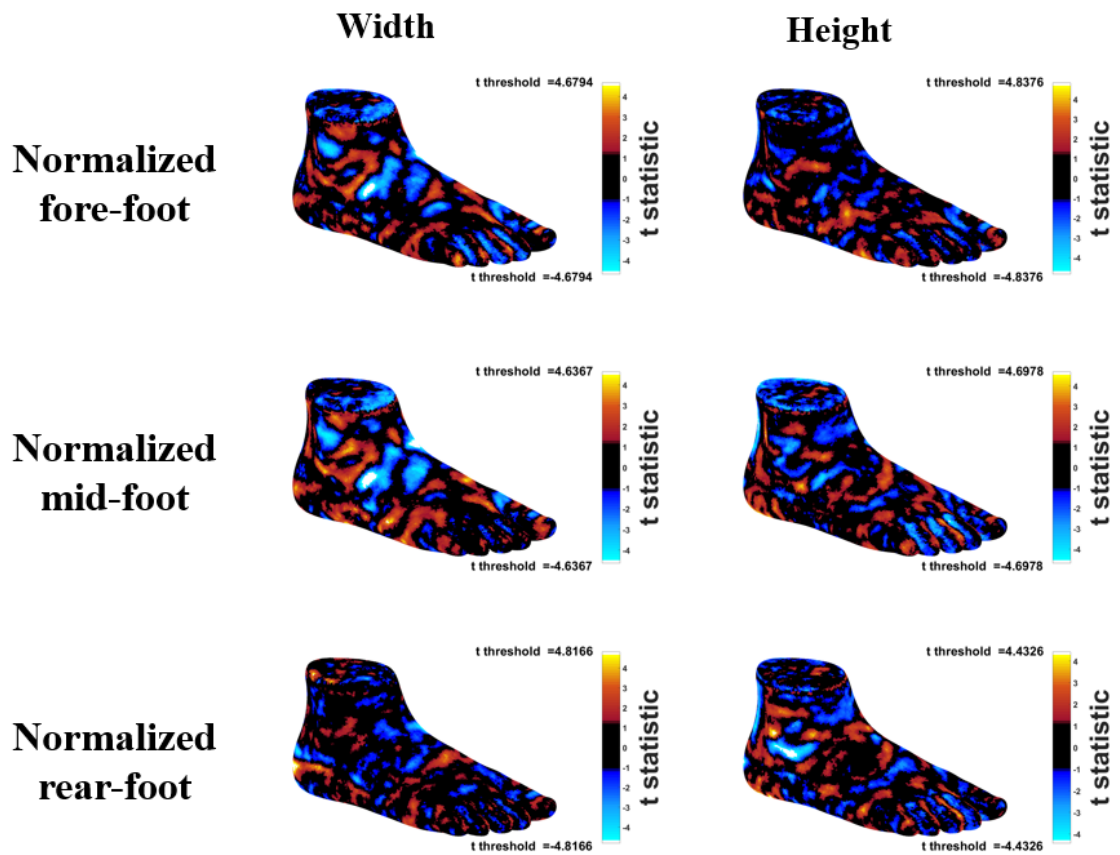


Figure 50.: SPM1D regression of shape-index with normalized 2D measures, dorsolateral view. The colour bar represents the t statistics, with the threshold at each end (alpha level of 0.05). White points mark significant correlation. Dark to light blue colours indicate increasing negative correlation, red, orange, and yellow colours indicate increasing positive correlation.

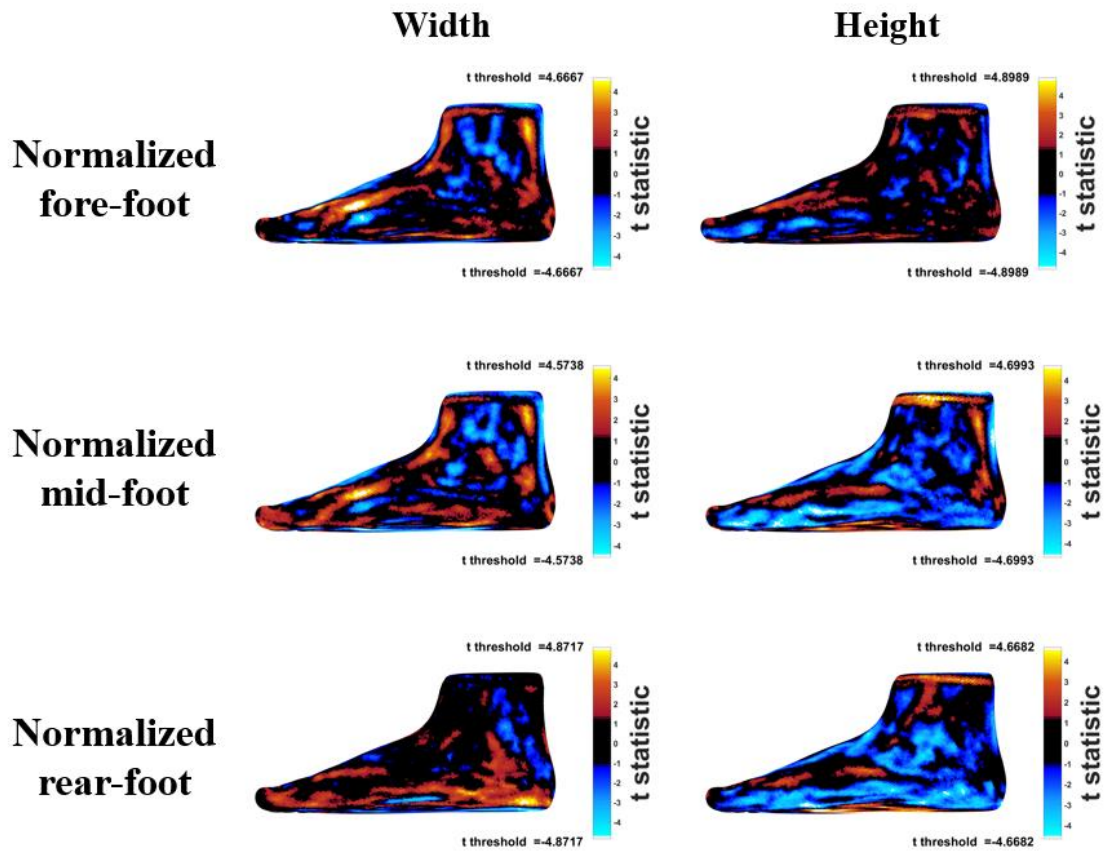


Figure 51.: SPM1D regression of curvedness with normalized 2D measures, medial view. The colour bar represents the t statistics, with the threshold at each end (alpha level of 0.05). White points mark significant correlation. Dark to light blue colours indicate increasing negative correlation, red, orange, and yellow colours indicate increasing positive correlation.

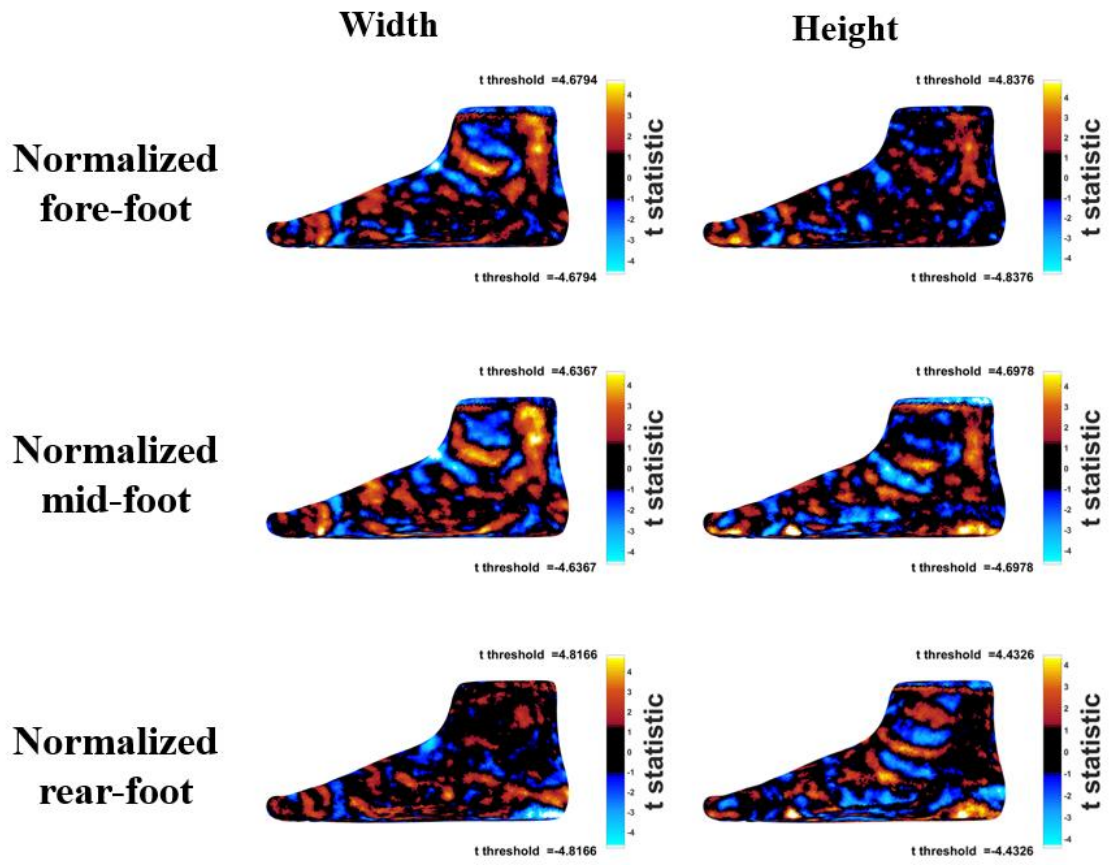


Figure 52.: SPM1D regression of shape-index with normalized 2D measures, medial view. The colour bar represents the t statistics, with the threshold at each end (alpha level of 0.05). White points mark significant correlation. Dark to light blue colours indicate increasing negative correlation, red, orange, and yellow colours indicate increasing positive correlation.

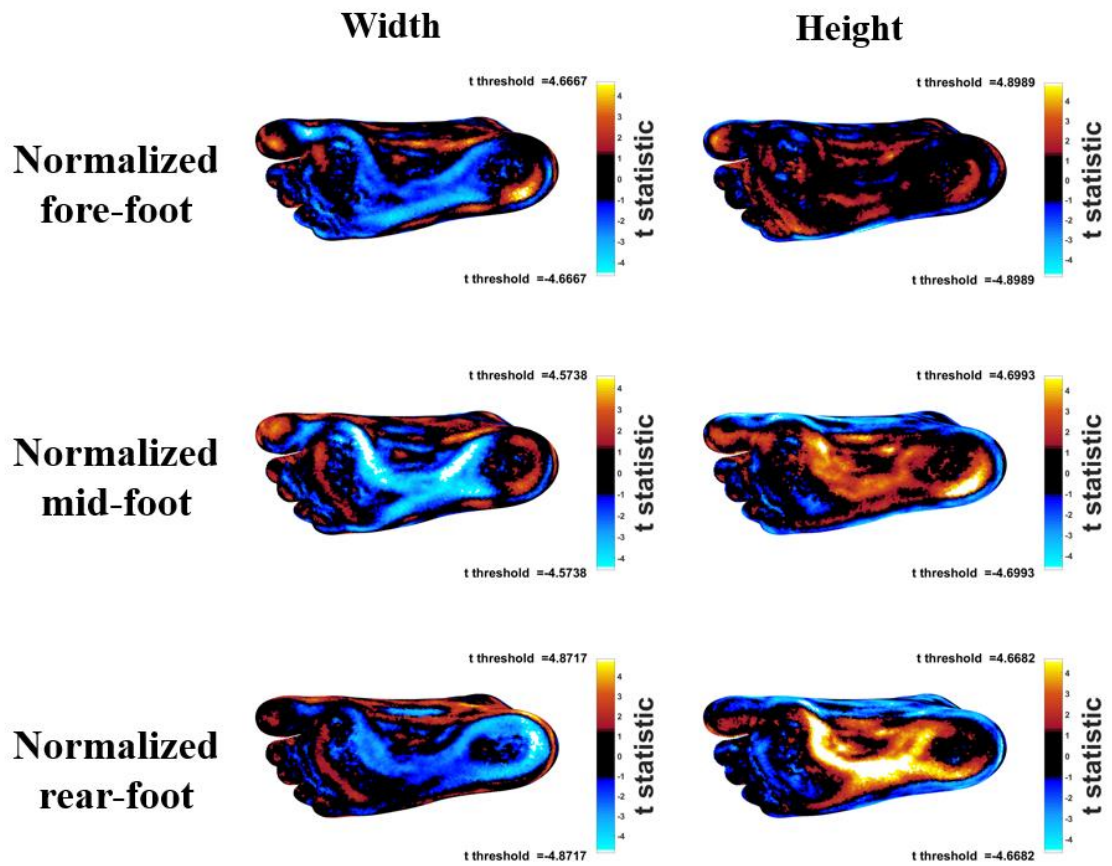


Figure 53.: SPM1D regression of curvedness with normalized 2D measures, plantar view. The colour bar represents the t statistics, with the threshold at each end (alpha level of 0.05). White points mark significant correlation. Dark to light blue colours indicate increasing negative correlation, red, orange, and yellow colours indicate increasing positive correlation.

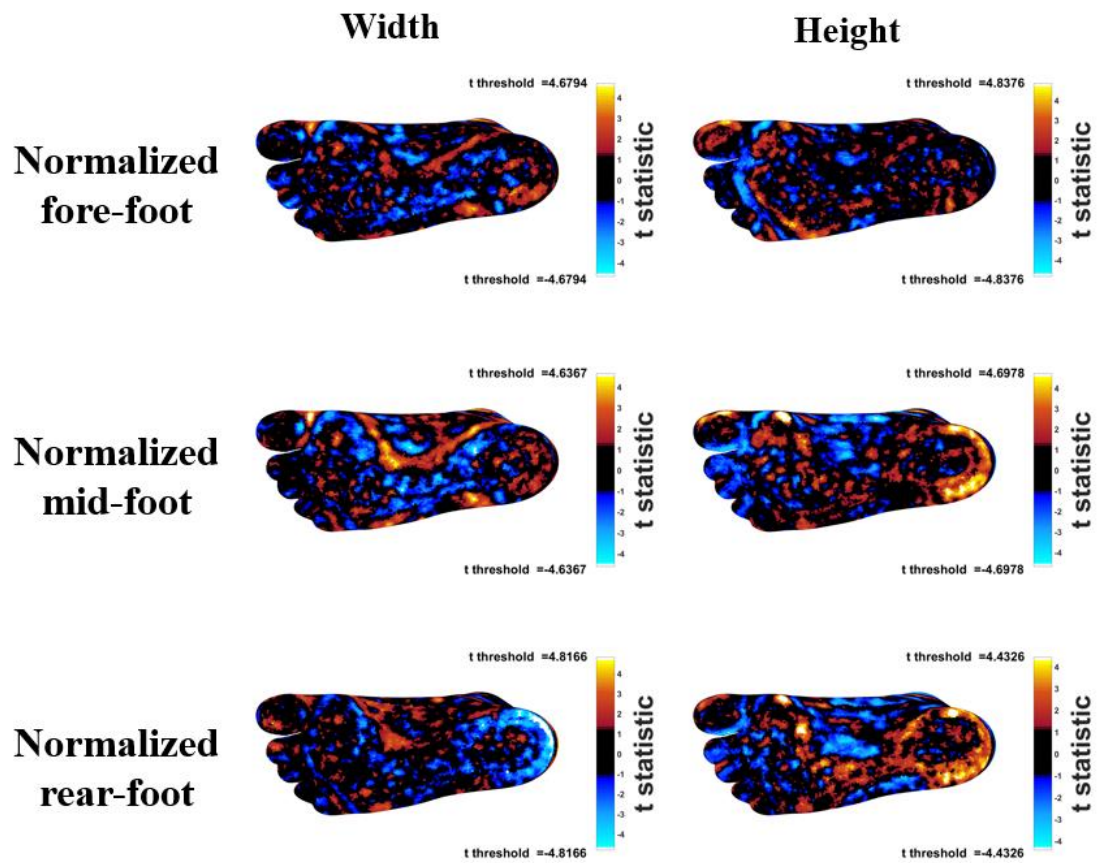


Figure 54.: SPM1D regression of shape-index with normalized 2D measures, plantar view. The colour bar represents the t statistics, with the threshold at each end (alpha level of 0.05). White points mark significant correlation. Dark to light blue colours indicate increasing negative correlation, red, orange, and yellow colours indicate increasing positive correlation.